IMMUOCYTOCHEMICAL AND ULTRASTRUCTURAL STUDIES OF LYMPHOID TISSUE OF SCRAPIE INFECTED MICE AND SHEEP

Gillian McGovern

Thesis submitted for the degree of
Doctor of Philosophy

THE UNIVERSITY OF EDINBURGH

2004

CONTENTS

2.2. Experimental techniques

Chapter 3. Results

Chapter 6. Appendices

List of Abbreviations

ABC: Avidin biotin complex

ANS: Autonomic Nervous System

APC: Antigen Presenting Cell

ATC: Antigen Transporting Cell

BSE: Bovine Spongiform Encephalopathy

CJD: Creutzfeldt-Jacob Disease

CNS: Central Nervous System

CSF: cerebrospinal fluid

CWD: Chronic Wasting Disease

DAB: Diamiobenzidine Tetra-hydrochloride

DPI: days post infection

EM: Electron Microscope

ENS: Enteric Nervous System

FDC: Follicular Dendritic Cell

FFI: Fatal Familial Insomnia

FH: Fibrohistocytoid Cell

FSE: Feline Spongiform Encephalopathy

GSS: Gerstmann Sträussler Scheinker Syndrome

HIV: Human Immunodeficiency Virus

HRP: Horseradish peroxidase

huTNFR:Fc: human Tumor necrosis factor fusion protein

hu-Ig: human immunoglobulin

i.c.: Intracerebral

IL: Interleukin

i.p.: Intraperitoneal

IHC: Immunohistochemistry

LM: Light Microscope

LRS: Lymphoreticular System

LTβR: Lymphotoxin beta-receptor

MHC: Major Histocompatibility Complex

MLN: Mesenteric lymph node

PALS: Periarteriolar Lymphoid Sheath

PK: Proteinase K

PNS: Peripheral Nervous System

PrP: Prion Protein

PrP^{d}: Disease specific Prion Protein

PrP^{sc}: Scrapie specific Prion Protein

PrP^{c}: Normal Cellular form of the Prion Protein

PrP^{sen}: Protease sensitive form of the Prion Protein

RER: Rough Endoplasmic Reticulum

RML: Rocky Mountain Laboratory

Sinc: scrapie incubation

SCID: Severe Combined Immunodeficiency

SRBC: Sheep red blood cell

TBM: Tingible Body Macrophage

TCR: T Cell Antigen Receptor

TME: Transmissible Mink Encephalopathy

TNF: Tumour Necrosis Factor

TSE: Transmissible Spongiform Encephalopathy

UV: Ultra Violet

vCJD: variant Creutzfeldt-Jacob Disease

List of Figures Page

List of Tables Page

Acknowledgements

I would like to thank the following people, whose assistance and support has been greatly appreciated.

Firstly, VLA for allowing me the time and flexibility to undertake this project, my colleagues at VLA Lasswade for their technical assistance, and for accepting the slightly off centre work practices required to produce this thesis, and also my supervisor, John Hopkins for invaluable assistance in producing the final piece of work.

I am extremely grateful to Moira Bruce, Neil Mabbott, Karen Brown and others at the Institute of Animal Health, Neuropathogenesis Unit in Edinburgh for providing me with tissues from experimentally inoculated mice, and for allowing me access to mice within ongoing experiments.

I would also like to thank my family for their continual, yet subtle interest in my progress, and Carole Helfter for her proof reading skills and heartfelt encouragement.

Finally, I would like to express my gratitude to my supervisor at VLA Lasswade, Martin Jeffrey, for spending so many sunny weekends reading the continual barrage of re-written chapters. Without his tireless moral and academic support, this PhD would not have been possible.

Declaration

I certify that this thesis, submitted for the degree of Doctorate of Philosophy represents my own work. All material in this thesis that is not my own work has been identified.

This thesis has not been previously submitted for any degree, diploma or other qualification.

The work presented in this thesis was carried out at VLA Lasswade. All murine experiments were performed at IAH - NPU in Edinburgh.

Abstract

The transmissible spongiform encephalopathies (TSEs) are a group of progressive neurological diseases of unknown cause. Infection is associated with an abnormal form of a host protein designated 'prion protein'. Previous studies have shown that lymphoid tissues are involved in the peripheral pathogenesis of TSEs prior to neuroinvasion. Using immunoelectron microscopy, disease specific PrP (PrP^d) accumulation was demonstrated within the spleens of scrapie-infected mice where it was found in association with the plasmalemma and extracellular space around follicular dendritic cell (FDC) processes (dendrites), and in the lysosomes of tingible body macrophages (TBMs). In light zones of secondary follicles, almost all FDCs at the terminal stages of disease form hypertrophic labyrinthine glomerular complexes. Within these labyrinthine complexes PrP^d is consistently seen on the plasmalemma of adjacent dendritic profiles and in association with abundant electron dense material held between dendrites. The latter was interpreted as excess trapped antigen-antibody complexes. Contrary to previous dogma, these results show that a pathological response within the immune system follows murine scrapie infection. The nature of these changes is similar irrespective of the strain of agent used. To help determine the significance of these changes, scrapie-infected mice were inoculated with cytokines that alter the biology of secondary follicles. Tumour necrosis factor receptor fusion protein (Hu-TNFR:Fc) or Lymphotoxin β receptor fusion protein (LTβR:Fc), have been reported to induce de-differentiation of FDCs and heighten B cell apoptosis. However, in this study, mature FDCs were present 3 and 35 days after treatment with LTβR:Fc and retained PrP^d accumulation. The mechanisms by which

these cytokines modulate incubation period were not determined. To ensure that the pathology of experimental disease is similar to that occurring in natural disease, ovine scrapie tissue samples were examined. The results presented suggest that natural scrapie is closely similar to that of experimental murine scrapie. Further technique refinement is still necessary to give comparable levels of sensitivity and tissue preservation in ovine tissue.

1. INTRODUCTION

1.1. Scrapie and other TSEs

Scrapie, a disease that has been present naturally in British sheep and goats for many centuries, belongs to a group of neurodegenerative diseases known as the transmissible spongiform encephalopathies (TSEs) or prion diseases, and following its experimental transmission to rodents is the most extensively studied of the group. The disease is now endemic to many other countries throughout the world and its control and potential eradication poses a problem worldwide.

1.1.1. Animal and human TSEs

TSEs affect both animals and humans and are invariably fatal. Bovine Spongiform Encephalopathy (BSE) of cattle and exotic ungulates was first identified in a Nyala (Jeffrey & Wells 1988), and subsequently in cattle (Wells et al. 1987)[1]. It is considered to have arisen as a result of scrapie agent contamination of inadequately rendered scrapie-infected sheep offal. The TSE agent contaminated meat and bone meal produced by the rendering process was then used as a nutritional supplement in cattle feed with subsequent mutation or amplification of the BSE agent (Wilesmith et al. 1988; Wilesmith et al. 1991). Other TSE infections related to BSE include: Feline Spongiform Encephalopathy (FSE), which is thought to have emerged as a result of similar dietary exposure to contaminated food supplements, Transmissible Mink

[1] Published out of sequence relating to case occurrence.

Encephalopathy (TME), a disease of captive mink in the United States which is thought to have originated from the consumption of scrapie affected sheep carcasses, and chronic wasting disease or CWD, a scrapie like disease of mule deer and elk, the origins of is completely unknown (Williams et al. 2002).

Human forms of the disease exist as infectious, inherited or sporadic disorders. Creutzfeldt-Jacob disease (CJD) and Kuru are infectious forms of the disease and can occur through horizontal transmission. Iatrogenic transmission of CJD occurs rarely, for example through intake of contaminated growth hormone or neurosurgery using non-sterile instruments (Brown 1998; Blattler 2002). Kuru has been attributed to ritualistic cannibalism and is restricted to the Fore tribe in Papua New Guinea. It is thought to have arisen from a single case of sporadic CJD (Knight & Collins 2001). Fatal Familial Insomnia (FFI), familial CJD and Gertsman-Sträussler-Scheinker syndrome (GSS) are inherited disorders in which there are germ line mutations in the protein-coding region of the prion protein gene. The causative agent of sporadic human TSEs remains unknown, however, it has been hypothesised that the disease may occur as a result of spontaneous conversion of the normal prion to the infectious agent, or that a somatic mutation may arise in the protein coding gene (Gajdusek 1977; Prusiner 1989). More recently, variant CJD has been diagnosed, presumptively a result of transmission of BSE to humans by the consumption of brain or spinal cord of BSE infected cattle (Ironside 1996; Will et al. 1996; Bruce et al. 1997).

1.1.2. Experimental TSEs

In the 1930s, experimental sheep to sheep scrapie transmission was achieved by Cuille and Chelle, demonstrating the infectious nature of the agent (Cuille & Chelle 1936). This was further shown by the infection of 10% of a sheep flock with scrapie as a result of total flock vaccination with a scrapie contaminated louping ill vaccine (original report: Gordon et al. (Gordon 1946)). However, much of the current information concerning scrapie is derived from rodent experimental models, first transmitted successfully from homogenised sheep brain in 1961 (Chandler 1961). Subsequent studies have characterised many different murine scrapie strains based on neuropathological changes and incubation period (Fraser & Dickinson 1973; Dickinson 1976). Primarily the murine *Sinc* gene, short for scrapie incubation, which encodes a specific PrP sequence, determines incubation period. The difference between s7 and p7 *Sinc* genes lies in the amino acid sequence at two positions in the protein; if it has leucine at position 108 and threonine at 189 it is designated *Sinc* s7, whereas if it has proline at position 108 and valine at 189, it is *Sinc* p7 (Bostock, 2000). This difference in amino acid sequence exerts consistently different scrapie incubation periods between the 2 genotypes, and the s7 or p7 sequences determine whether a short or prolonged incubation period occurs respectively (Westaway et al. 1987; Hunter et al. 1992). These alleles can alter incubation period of a specific scrapie strain by up to 400 days (Dickinson et al. 1968). Route of infection is also known to regulate incubation period. The most efficient route of transmission is via intracerebral (i.c.) inoculation, although alternative routes such as intraperitoneal (i.p.), intravascular, oral, intraneural, subcutaneous and intraoccular inoculation have

also proved efficient (Kimberlin & Walker 1979a; Bruce & Fraser 1981; Kimberlin & Walker 1986). The species barrier is an important factor in disease transmission with interspecies transmission being considerably less efficient than transmission within the same species. However, those animals that do develop disease following interspecies transmission are readily able to transmit disease within their own species (Scott et al. 2000).

The introduction of transgenic mouse models led to the discovery that the species barrier was regulated by amino acid differences between the donor and host prion protein (Prusiner et al. 1990). Introduction of a donor prion gene to the host species greatly increased the likelihood of developing the disease from the donor species, and also reduced the incubation period. These results suggest that PrP^{d} replication occurs optimally if both the inoculated PrP^{d} and PrP^{c} of the recipient animal share the same primary structure.

1.1.3. TSE pathology and the molecular properties of PrP^{c} / PrP^{d}

Prion diseases are generally characterised in the later stages of disease by the development of lesions within the central nervous system (CNS). Vacuoles develop within regions of the CNS, astrocytes become hypertrophic, while neurones degenerate (Fraser 1993). These CNS changes co-localise with the accumulation of the abnormal disease-specific form of a cell surface glycoprotein, designated PrP^{d} or PrP^{res}. When compared with the normal form of PrP found at the cell surface of neurons, the abnormal form of PrP is partially protease-resistant in nature. This abnormal form of PrP also accumulates in the peripheral nervous system and

lymphoreticular tissues of some naturally occurring diseases and many animal experimental models. The normal cellular form of this protein (PrP^c or PrP^{sen}) is sensitive to protease digestion and is expressed abundantly at the membrane of many CNS cells (Manson et al. 1992; Ford et al. 2002), but also at lower levels in many peripheral tissues (Oesch et al. 1985). However, it was noted that TSE pathology could be present without the detection of protease-resistant PrP (Collinge et al. 1995). Similarly, protease-resistant PrP can be detected in the absence of infectivity (Riesner et al. 1996) suggesting there may be a variety of forms of PrP associated with infection that differ from PrP^c or PrP^{sen}. As a result of this ambiguity, the term PrP^c will be used to indicate the normal form of the prion protein in the absence of pathology. Similarly, the use of PrP^{res} implies the molecule has been tested for Proteinase K (PK) sensitivity. This test is not possible using resin post embedding methods, however, it is impossible to visualise PrP^c in normal resin embedded tissues, which would imply that the harsh processing involved in preparation of tissues for ultrastructural study renders the normal form of PrP unobtainable. PK treatment prior to immunohistochemical labelling of paraffin embedded TSE infected tissues can determine whether the PrP present is sensitive or resistant to PK digestion (Stack et al. 1996). The term "PrP^{sc}" has also been used to describe disease-specific PrP, which has been tested for PK sensitivity and the presence of β pleated sheet. In this thesis PrP^d will be used to indicate a form of the molecule that has not been PK tested but coincides with infection.

Whether abnormal PrP is the causative agent of the TSEs or whether it is a by-product of an unconventional viral infection is still a contentious issue. Early studies demonstrated that the TSE agents were highly resistant to UV radiation, which may

therefore imply that they are devoid of nucleic acid (Alper et al. 1967). In addition, no viral-like agent containing a nucleic acid genome has been discovered. However, the interpretation of the original UV inactivation data has now been shown to be erroneous (Rohwer 1991; Somerville 2002). If nucleic acids are present in infectious extracts, they may be small, present in small amounts, and well protected by protein. The "protein only" hypothesis initially proposed by Griffith (Griffith 1967), and later updated (Prusiner 1989) was therefore advanced to explain this absence of nucleic acid. The "protein only", or prion hypothesis has continued to gain ground over recent years. In this hypothesis it is suggested that the causative agent is the altered form of the normal cellular PrP protein. Infection is thought to occur as a result of introduction of a conformationally modified form (the disease-specific form) of PrP into the organism, inducing the additional formation of the same conformer of the protein from the normal cellular precursor protein. The exact mechanism for this conversion remains unclear, however, PrP^c has been shown to be rich in α helices while virtually devoid of β pleated sheets (Pan et al. 1993). In contrast, both Pan et al. and Caughey et al. (Caughey et al. 1991) demonstrated that PrP^d has a high β sheet content and a low α helix content, suggesting the conversion of normal PrP into an abnormal disease-specific form appears to involve unfolding of the molecule and refolding into β pleated sheets.

Normal prion protein function is unknown (Bueler et al. 1992; Sakaguchi et al. 1996; Aguzzi & Weissman 1997; Ford et al. 2002); however, its location on the cell surface indicates a role in signalling, cell adhesion or transport functions (Rieger et al. 1997). Mice devoid of PrP develop and reproduce normally. It has however been suggested that this may be due to the organisms compensation for the loss of the gene by over

expression of others, or manipulation of alternative developmental pathways (Bueler et al. 1992; Manson et al. 1994). More recently, Long-term Potentiation (LTP) of the synapses of neurones within the CA1 region of the hippocampus was found to be inhibited in mice devoid of PrP (Collinge et al. 1994), while altered circadian rhythms (Tobler et al. 1996) and defects in copper metabolism have also been identified in these mice (Brown et al.1997).

PrP-knockout mice do not develop experimental prion disease (Bueler et al. 1993), demonstrating that the normal PrP molecule is necessary for infection to take place. In addition, heterozygous mice carrying a single copy of the PrP gene are only partially susceptible to disease with a considerably longer incubation period than wild type mice, indicating availability of PrP^c may be a rate-limiting factor in disease progression (Manson 1996). Subsequent investigations involving neurografts in transgenic and knockout mice further demonstrate the necessity for PrP^c in prion propagation within the CNS (Brandner et al. 1996 and reviewed by Aguzzi & Weissman 1997). A similar study involving reconstitution of PrP-null ($PrP^{-/-}$ or $PrP^{0/0}$) mice with wild type lymphohaemopoietic cells resulted in wild type levels of prion titre within the spleen following scrapie inoculation, but no scrapie pathology within the PrP expressing neurograft, again indicating PrP^c is also required for neuroinvasion (Blattler et al. 1997).

1.2. Peripheral stages of infection.

Peripheral infection of the lymphoreticular system (LRS) and Enteric Nervous System (ENS) occurs in some TSEs. For example, the emergence of variant CJD

(vCJD), presumably from the oral uptake of BSE contaminated foodstuffs, results in infection of the PNS and ENS. The infectious agent although ultimately targeting cells of the CNS, may initially infect peripheral organs in some forms of TSEs.

1.2.1. Lymphoreticular system involvement and neuroinvasion.

Bioassays of rodents and sheep experimentally infected by the peripheral route, show initial infectivity is detected in tissues of the LRS, (Fraser & Dickinson 1970; Kimberlin & Walker 1979; Bueler et al. 1993). In murine models of scrapie initial neuroinvasion occurs via the splanchnic nerves that innervate the spleen (Kimberlin & Walker 1988). Intragastric inoculation of 139A in mice leads to initial accumulation of the infectious agent in intestinal Peyer's patches (Kimberlin & Walker 1988), with CNS neuroinvasion occurring at two sites, one via the splanchnic nerve and the other via the vagus (McBride et al. 2001). In naturally occurring sheep scrapie, initial infection may be detected in the Peyer's patches, but initial sites of replication can also be detected in the tonsils, retropharyngeal lymph nodes and the spleen (Jeffrey et al. 2001b). Abnormal forms of PrP detected by immunohistochemistry (IHC) can be identified in the peripheral nervous system in both naturally affected (Van Keulen et al. 2000) and intraperitoneally inoculated sheep scrapie (Groschup et al. 2000). Studies of natural sheep scrapie indicated more specifically that sympathetic noradrenergic fibres might be responsible for the transport of infectivity from the spleen to the CNS (Bencsik et al. 2001). However, as not all sheep infected with TSE show evidence of peripheral PrP^d accumulation, it

is possible that other routes may be involved . This will be discussed later in section 3.2.4.

1.2.2. Scrapie-specific cellular targeting within the lymphoreticular system

Many studies have indicated the importance of the LRS in TSE pathogenesis. Those TSEs known to have a peripheral phase will show PrP^d accumulation in LRS components at an early stage of infection, however, until recently, accumulation seemed to occur in the absence of an integrated immune response, with no recognition of antigens by specific antibodies or previously sensitized lymphocytes. As PrP^d is a conformationally altered form of the normal cell surface protein, this is not particularly surprising (Porter et al. 1973). It was considered likely that although PrP antibodies are able to recognise conformational determinants of self-proteins, the protein may be altered in such a way as to mask the abnormal part of the molecule, or, alternatively, the abnormal form may be similar to another self-protein. Following immunisation with purified protein, Prusiner at al. synthesised polyclonal antibodies against prion protein in PrP-null mice (Prusiner et al. 1993), while more recently, PrP-null mice were used to generate monoclonal antibodies against prion proteins (Krasemann et al. 1996; Krasemann et al. 1999).

I.p. inoculation allows early detection of the infectious agent in the LRS

Subsequently, this route has been studied extensively in transmission experiments of rodent scrapie. For many years, investigators have attempted to identify the cells necessary for prion propagation within the LRS. Genetic asplenia, or surgical splenectomy shortly before of after peripheral challenge increases the incubation

period of TSE models, while genetic athymia or surgical thymectomy have no effect (Fraser & Dickinson 1978). Whole body gamma irradiation before or after infection also failed to alter scrapie incubation periods (Fraser & Farquhar 1987). Cell fractionation techniques have demonstrated that, when separated into pulp and stroma, a greater concentration of infectivity was observed in the stromal fraction (Clarke & Kimberlin 1984). Taken together, these studies indicate a population of radio-resistant cells, present in the splenic stromal fraction and not derived from the thymus or bone marrow, are responsible for scrapie replication in the LRS. Based on these findings, follicular dendritic cells (FDCs) have been proposed as the cells necessary for prion propagation within the LRS (Fraser & Farquhar 1987). Using immunohistochemical techniques, it was demonstrated cells morphologically similar to FDCs with an immune trapping function also immunolabelled with antibodies to PrP (McBride et al. 1992).

Studies involving severe combined immunodeficient (SCID) mice have further indicated an important role for FDCs in LRS prion replication. These mice are resistant to both i.c. and peripheral scrapie infection and have no functional B or T-lymphocytes to influence the maturation of FDCs. This defect can be reversed by reconstitution with immunocompetent bone marrow (Kapasi et al. 1993). In this study, no PrP^d accumulations were associated with FDCs in SCID mice, which remained resistant to infection via peripheral inoculation. Similarly, SCID mice are resistant to the ME7 strain of scrapie following peripheral infection with a moderate dose of scrapie brain homogenate (10^{-2} or 10^{-3}) (Fraser et al. 1996). However, peripheral infection with a highly concentrated dose results in a 100% disease incidence rate. It is likely that infection of peripheral nerves occurs directly without

LRS involvement at high concentrations (Kimberlin & Walker 1988a). Direct i.c. inoculation with either CJD or scrapie results in levels of i.c. infection in SCID mice similar to that found in the brain of comparable immunocompetent mice, while immunocompetent bone marrow reconstitution of SCID mice also gives scrapie incubation periods similar to that of immunocompetent control mice (Fraser et al. 1996).

In contrast to the above studies that implicate FDCs in peripheral infection and replication of TSE agents, Klein et al. (Klein et al. 1997) suggested B cells play a primary role in neuroinvasion of scrapie. Using a series of immunodeficient mice lacking T cells, B and T cells, and B cells only, i.c. inoculation with the Rocky Mountain Laboratory (RML) scrapie isolate resulted in the development of clinical scrapie with similar incubation periods to that of immunocompetent controls. I.p. inoculation only caused clinical scrapie in those mouse models that did not have B-lymphocyte disruption. As no mature FDCs are present in B cell deficient models (Klein et al. 1997), further investigation to demonstrate whether the resistance of B cell deficient mouse models to peripherally inoculated scrapie is due to the lack of B cells or mature FDCs, was necessary.

Although PrP^c expression is necessary for the neuroinvasion of infectivity (Blattler et al. 1997), it was later shown that B cells which lack PrP^c do not impair scrapie neuroinvasion in reconstituted SCID mice (Klein et al. 1998). This indicates that B cells are not directly responsible for accumulation and transport of infectivity.

FDC maturation is dependent on cytokine signalling from B cells (Chaplin & Fu 1998). Tumor Necrosis Factor α (TNFα) and Lymphotoxin α (LTα) are structurally related, secreted proteins, and can each interact and activate two defined TNF

receptors, designated TNFRI and TNFRII. Lymphotoxin β (LTβ) was later discovered and exists in a membrane bound hetrotrimeric formation with one LTα chain (LTα / β). This molecule does not show an affinity for TNF receptors but binds through the LT β receptor (LTβR) (Fu et al. 1999). If the gene for TNFα or LTα is deleted, follicles do not develop and FDC are absent (Pasperakis et al.1996; Matsumoto et al 1997). Similar results are obtained if TNFRI is deleted, and in addition, the defect cannot be corrected by reconstitution with wild type bone marrow (Matsumoto et al 1997). In contrast, if TNFRII is deleted, FDCs and follicles mature normally (Le Hir et al.1996). Deletion of the gene for LTβ leads to partial follicular alterations, while deletion of the LTβR has a similar affect to that of LTα deletion (Rennert et al.1997).

When TNFα null (or $TNF\alpha^{-/-}$) mice and interleukin 6-null ($IL6^{-/-}$) mice were i.p. challenged with the ME7 strain of scrapie, most $TNF\alpha^{-/-}$ mice failed to develop scrapie up to 503 days post scrapie injection, while all $IL\text{-}6^{-/-}$ mice succumbed to disease at the same timepoint as wild type mice. High levels of PrP^d were also detected in association with FDCs in the spleens of $IL6^{-/-}$ mice, while $TNF\alpha^{-/-}$ mice showed no PrP^d accumulation. The authors concluded that mature FDCs are essential for replication of the scrapie agent in lymphoid tissues and that in their absence, neuroinvasion following peripheral challenge is impaired (Mabbott et al. 2000a). FDC maturation can also be inhibited by lack of signal or by blocking the FDC signal receptor. In the TNFα R1-deficient model, B and T cells remain fully mature. Clinical scrapie has been observed in RML inoculated TNFα R1-deficient mice, with an incubation period similar to that of wild type control mice, following peripheral inoculation with this strain of agent (Klein et al. 1997; Prinz et al. 2002). The authors

of these studies suggested that B cells or macrophages and not FDCs as previously suggested, play a pivotal role in scrapie pathogenesis. However, as splenic infectivity titre was not measured in the TNFαR1-deficient mice, it cannot be excluded that due to the high titres of infectivity used in the inoculum, disease entered the PNS, and subsequently the CNS, without a LRS replication phase. Following treatment with LTβR:Ig, which is known to inhibit FDC development in a similar way to that of TNF, neuroinvasion of the RML scrapie isolate after i.p. inoculation was impaired (Montrasio et al. 2000; Prinz et al. 2002). However, it was demonstrated that lymph node development was more severely impaired in LT than in TNF deficient mice, which may imply the effect of TNF depletion is more easily overridden by a high scrapie dosage than LT depletion (Fu & Chaplin 1999).

In addition to FDCs, macrophages of the LRS have been identified as reservoirs of the TSE infectious agent. In some studies these cells have been shown to retain more infectivity than lymphoid cells (Carp et al. 1994). In an in vitro system, mouse peritoneal macrophages exposed to scrapie infection for prolonged periods were demonstrated to produce longer disease incubation periods following re-inoculation into indicator mice when compared to those cells exposed to infectious agent for a shorter time period (Carp & Callahan 1982). In the early stages of scrapie pathogenesis in the spleen, studies indicated that macrophages play the role of scavenger cells. Using a cell suicide technique to transiently deplete all splenic macrophage populations, the author's demonstrated accelerated replication of the scrapie agent in the early stages of scrapie pathogenesis (Beringue et al. 2000). Both studies indicate macrophages participate in the clearance of scrapie inoculum.

1.2.3. Follicular Dendritic Cell involvement in scrapie pathogenesis.

To clarify the role of FDCs and B-lymphocytes in scrapie pathogenesis, Brown et al. produced chimaeric mice by crossing SCID with PrP-knockout (SCID / $PrP^{0/0}$) or PrP wild type (SCID / $PrP^{+/+}$) mice (Brown et al. 1999). The two models were reconstituted with bone marrow from $PrP^{+/+}$ or $PrP^{0/0}$ mice respectively. Bone marrow grafting is known to replace only B and T cells from the graft tissue itself, while the presence of mature B cells allows host-derived immature FDCs to develop normally (Brown et al. 1999). Subsequently, SCID / $PrP^{+/+}$ mice reconstituted with $PrP^{0/0}$ bone marrow will express PrP on FDCs but not B or T cells, while SCID / $PrP^{0/0}$ mice reconstituted with bone marrow from wild type mice will express PrP on B and T cells but not FDCs. Following peripheral infection with the ME7 strain of mouse scrapie, SCID / $PrP^{+/+}$ mice reconstituted with $PrP^{0/0}$ or $PrP^{+/+}$ bone marrow had high splenic levels of infectivity. Infectivity was not detectable in the spleens of SCID / $PrP^{0/0}$ reconstituted with $PrP^{+/+}$ bone marrow, thus indicating LRS involvement in scrapie pathogenesis is directly dependent on PrP expressing FDCs, and indirectly upon B cells which are required for FDC maturation.
Further investigation using the RML scrapie isolate as inoculum, has demonstrated that reconstitution of $PrP^{0/0}$ mice with $PrP^{+/+}$ bone marrow results in high levels of infectivity within the spleen, indicating replication of the RML scrapie isolate is dependent on haemopoietic derived cells (Klein et al. 1998). This finding again implies that different scrapie strains target different cells in the LRS, as occurs in the CNS (Fraser 1976).

The exact mechanism by which infection reaches lymphoid follicles and FDCs remains unclear. However, as will be discussed in section 1.3.2.3, FDCs are responsible for the trapping and retention of antigens in association with antibodies on their cell surface. This trapping is initiated by the interactions of complement and cellular complement receptors (Nielsen et al. 2000). A prolonged incubation period of ME7 scrapie following peripheral infection in mice deficient in complement components C3 or C1q, which are known to be critical for complex retention by FDCs (Nielsen et al. 2000), was demonstrated (Mabbott et al. 2001). This suggests that the complement system is involved in the initial trapping of the infectious agent in lymphoid follicles.

1.2.4. Scrapie pathogenesis of sheep.

Although the TSEs have been extensively studied in rodent models, studies of TSEs within sheep flocks remain at an early stage, with the pathogenesis of the natural disease remaining relatively unclear.

Initial problems with studying the disease in sheep included difficulty in identifying preclinical cases and the laborious nature of scrapie infectivity detection methods. Sheep genotype was also identified as an important factor in susceptibility and disease progression. Many of the early studies of natural disease were performed without the knowledge of the PrP genotype of affected and exposed sheep (e.g. (Hadlow et al. 1982).

However, in the mid 1990's, the study of ovine TSEs intensified. An immunohistochemical method for the preclinical detection of PrP^d in the tonsil of

scrapie-infected sheep was identified (Schreuder et al. 1998; Van Keulen et al. 2000), while studies of the effects of PrP genotype on scrapie susceptibility and incubation period were being undertaken by a number of groups (Belt et al. 1995; Bossers et al. 1996; Elsen et al. 1996; Hunter 1996a).

More recently, immunoblotting techniques have become commonly used for large-scale TSE surveillance and diagnosis. This technique detects the presence of a protease-resistant form of PrP, which is present only in diseased animals (Katz et al. 1992; Beekes et al. 1995; Schaller et al. 1999). Nevertheless, immunohistochemical methods remain a useful method for the detection of a range of different forms of disease-specific PrP present in the tissues of infected animals. In particular, immunohistochemical techniques have the added advantage of allowing accurate cellular localisation of the agent (Gonzalez et al. 2003; Jeffrey et al. 2003).

Following ovine necropsy, immunohistochemical studies have shown that PrP^d accumulation occurs in the CNS and all lymph nodes of clinically affected animals (Van Keulen et al. 1996). Histopathological studies have shown some variation in intensity of neuropathological vacuolation, with the dorsal motor nucleus of the vagus and the thalamic nuclei most commonly affected (Begara-McGorum et al. 2002; Ligios et al. 2002). Recognised PrP^d labelling patterns within the brain included intraneuronal, perivascular and neuropil associated, the profile or patterns of which are scrapie strain specific (Gonzalez et al. 2002). The study also confirms previous findings which suggested PrP genotype and sheep breed influenced the susceptibility to disease and rate of PrP^d accumulation within the brain (Bossers et al. 1996; Hunter 1996b; Hunter et al. 1997).

The route of transmission of natural scrapie remains unknown to date; however, extensive studies involving natural and experimentally infected flocks have postulated many possible routes. The apparent early involvement of the alimentary tract in some breeds of sheep has made the oral route a likely candidate (Jeffrey et al. 2001c).

Using a sheep genotype known to be highly susceptible to natural scrapie, it was demonstrated that scrapie infection of the CNS occurs following initial PrP^d detection in the ENS. Histopathology results from sequential necropsies indicate that the ENS acts as the initial entry point for disease to neural tissues, followed by spread through the autonomic nervous system (ANS) firstly to the spinal cord and then to the medulla oblongata (Van Keulen et al. 2000).

This study does not eliminate the possibility that other routes of CNS infection follow natural scrapie infection, for example, a sympathetic noradrenergic involvement following splenic PrP^d accumulation (Bencsik et al. 2001). Lymphoid tissues are infected at an early stage of disease and may act as an initial entry site for infection to the CNS. However, a lymphoreticular phase of infection is not common to all sheep genotypes (Van Keulen et al. 1995; Van Keulen et al. 1996).

Within lymph nodes of scrapie susceptible sheep, virtually all secondary follicles showed PrP^d accumulation. Labelling of CD21, which is known to be expressed on FDC membrane surface and on B cells (Zabel & Weis 2001), co-localised with PrP^d immunolabelling only on cells morphologically similar to FDCs. This FDC pattern of labelling was found in the light zone of the secondary follicle, while Tingible Body Macrophage (TBM) type labelling was observed in the light, dark, mantle and paracortical zone (Jeffrey et al. 2001b). PrP^d labelling has also been detected within

mononuclear cells of the periarteriolar lymphoid sheath (PALS) and within the marginal zone (Heggebo et al. 2002). Although cell types involved in PrP^d accumulation have tentatively been identified as both TBMs and FDCs, ultrastructural study is required in order to conclusively verify the association between the disease-specific form of the protein and these cell populations.

1.3. The secondary lymphoid tissues

The secondary lymphoid organs are located at strategic sites within the body where foreign antigens can be intercepted. Antigens in the blood are intercepted by the spleen but localised antigenic challenges arising from individual tissues and external sources are usually first dealt with in lymph nodes. Although lymph nodes and the spleen are morphologically dissimilar, they share some common features that provide the necessary microenvironment for the cellular interactions needed to remove unwanted pathogens efficiently, and the subsequent development of immune responses.

In this section, the spleen will primarily be discussed, with particular reference to rodent spleen, as LRS involvement in scrapie pathogenesis has been most extensively studied in this model.

1.3.1. Structure of the spleen.

The spleen, one of the largest lymphoid organs in mammals, is separated into two major components, the red and white pulp, and is enclosed by a capsule of

connective tissue. The red pulp consists of sinuses and cords and areas of capillaries, venules and connective tissue. Sinusoids are lined by endothelial cells, supported by reticulin fibres and separated by cords of Billiroth. The function of the cords is to provide a blood supply to the sinuses from terminal arteries. Circulating monocytes that differentiate into macrophages are also located within the cords. In addition, these cords contain many transitory cells such as red blood cells, plasma cells, and $CD8^+$ T cells, which are randomly scattered amongst macrophages (Weiss 1983; Wilkins 1997).

The white pulp is organised around branches of the splenic artery and consists of three highly organised compartments: the marginal zone, PALS, and the follicles (van Ewijk et al. 1977). The marginal zone separates the red pulp from the PALS and follicles, and is readily apparent due to the numerous, large memory B-lymphocytes that have a distinctive open nuclei with little chromatin (Steiniger & Barth 2000). It is also the pathway for B and T cell entry into the white pulp. This cellular region is characterised by memory B cells expressing high levels of IgM and low levels of IgD on the cell surface (Liu et al. 1988). The PALS region primarily contains $CD4^+$ T cells and some interdigitating dendritic cells, and forms a cylinder that encapsulates the secondary follicle (Wilkins 1997). T cells can be morphologically identified as small densely packed cells with little cytoplasm and small, very dark nuclei. This T cell dominant area can be immunohistochemically detected by applying antibodies against T-lymphocyte cell surface proteins such as alpha/beta T cell antigen receptor (TCR) or CD5. Interdigitating cells are of a similar size, while the nuclei contain less chromatin and are therefore less dark in routine histological preparations. They are

characterised by their high levels of MHC class II antigen expression (Steiniger & Barth 2000).

Primary follicles are small groups of B-lymphocytes within a meshwork of immature FDCs, and are usually attached to one side of the PALS region. Immature FDCs, or their precursors, have no cytoplasmic extensions, while the cytoplasm is limited and contains few organelles (Rademakers 1992). Upon antigenic stimulation, their capacity to produce matrix elements is lost, while adhesion molecules, complement and specific surface antigens, are created in turn (Heinen et al. 1995). Primary follicular B-lymphocytes are characterised by their simultaneous expression of both IgM and IgD, and by their expression of the high molecular weight form of leukocyte common antigen (CD45R) (Steiniger & Barth 2000).

Immune stimulation of primary follicles leads to the development of germinal centre-containing secondary follicles, as a result of the deposition of antigen / antibody complexes on the surface of FDCs (Thorbecke et al. 1994). The function of these germinal centres is B cell proliferation, selection and heavy chain switch. Germinal centres consist of a light and dark zone; the dark zone of the follicle is adjacent to the T cell compartment. It is populated by predominantly round, large, tightly packed B blast cells with an irregular nucleus, which may contain up to three peripheral nucleoli, while the cell cytoplasm contains large amounts of polyribosomes and scarce cell organelles. These cells are known as centroblasts, and undergo extensive mitosis. Non-differentiating centrocytes are the primary cell type in the light zone of the follicle, and are less densely packed (Thorbecke et al. 1994). They are irregularly shaped and have a small ring of cytoplasm containing free ribosomes, coated vesicles and mitochondria, surrounding an indented nucleus.

Centrocyte nuclei contain heavy marginal chromatin, an inconspicuous nucleolus and occasional nuclear pockets (Rademakers 1992). An area rich in FDCs expressing high levels of immune complexes supports this zone. FDC networks spread throughout the germinal centre but are much denser in the light zone than in the dark zone. Surrounding the germinal centre is the mantle zone that consists of small re-circulating B cells.

1.3.2. Lymphocyte circulation within the spleen.

The passage of lymphocytes through the spleen is essential to allow antigenic surveillance, optimal cellular interactions within the spleen, and to maintain whole body immunity. Unlike most other lymphoid tissues, the spleen lymphocyte entry and exit is blood-borne and does not involve the lymphatic vessels. In rodents, circulating lymphocytes initially enter the white pulp via the marginal zone (van Ewijk et al. 1977). They arrive in the marginal zone either via the marginal sinus or from capillaries (Weiss 1983; van Ewijk & Nieuwenhuis 1985). B-lymphocytes move into the secondary follicle from the marginal zone, while T cells move into the PALS. To leave the white pulp, both B and T cells can enter a side branch of the central arteriole known as a marginal zone bridging channel which crosses the marginal zone, and enter the red pulp (Liu & Banchereau 1996). The precise exit route from the white pulp via these bridging channels has yet to be investigated. Although lymphocyte recirculation within the white pulp of rodent spleen has been extensively categorised, that of the exit route of lymphocytes from the white pulp and subsequent red pulp recirculation remains equivocal (Steiniger & Barth 2000).

1.3.3. Splenic function

Again, knowledge concerning both immunological and blood related functions of the spleen have been acquired almost entirely from studies of rodents. Immunological reactions including antibody production have been thoroughly studied, while the spleen has been found to play an essential role in blood circulation and processing.

1.3.3.1. Red pulp

The red pulp is essentially a filtration unit for the blood but contains both filtering and non-filtering areas. Blood from the splenic artery reaches the sinuses either directly from the finest splenic arterioles, or indirectly from arterioles via splenic cords. These two routes constitute the "closed" and "open" parts of splenic circulation respectively.

The main filtration function of the spleen occurs within the cords which are composed of reticular fibres, and are associated with many cell types; the most important of these cells are macrophages which are thought to be responsible for the removal of unwanted debris and effete red blood cells (erythrophagocytosis). The walls of the sinuses themselves are also thought to have a filtering function (Steiniger & Barth 2000). Antibody synthesis by plasma cells also occurs primarily within the splenic cords that also contain large numbers of T-lymphocytes.

1.3.3.2. The white pulp and immunological response to antigenic challenge.

Production of antibody can be induced in the spleen as a result of exposure to "T cell independent "and "T cell dependent" antigens. Antigens which are composed of glycoproteins, glycolipids and polymeric polysaccharides, such as are found on viruses or bacterial capsules, are processed by T cell independent pathways (Humphrey 1985; Mond et al. 1995). The antibody response by marginal zone B cells to T independent antigens can occur in the absence of germinal centres and memory cells, with non-T cell signals decisive in promoting antibody production. However, studies have shown that under certain circumstances, specific memory cells of the marginal zone can be provoked. This finding correlates with the fact that T cell help during the antibody response to T independent antigens is reduced, but not totally lacking (Mond et al. 1995). The mechanism of marginal zone B cell stimulation by T cell independent antigens remains unclear. It has been suggested that they may be stimulated directly by the T independent antigen via immune complexes and / or complement receptors (van den Eertwegh et al. 1992). Alternatively, some authors suggest marginal zone macrophages that accumulate antigen play an important role marginal zone B cell stimulation (Humphrey 1981). The T cell dependent pathway processes antigens rich in protein. The primary role of white pulp of the spleen is in B cell reactions against protein antigens. These cellular responses occur in different white pulp compartments and occur sequentially. During the immunological response to antigenic challenge, the function and morphology of germinal centres change markedly. Primary follicles are areas of the white pulp that serve as recirculation sites for B-lymphocytes to survey FDC for

specific attached antigen. If their cognate antigen is encountered, the B-lymphocyte will remain in the follicle, proliferate and hypermutate. The life span of a germinal centre depends on the amount of antigen present.

The first stage of a primary germinal centre reaction involves the activation of naïve $CD4^+$ T helper cells in the T cell zone by antigen presenting cells (APCs), which express antigenic peptide in association with MHC class II molecules (Figure 1.1).

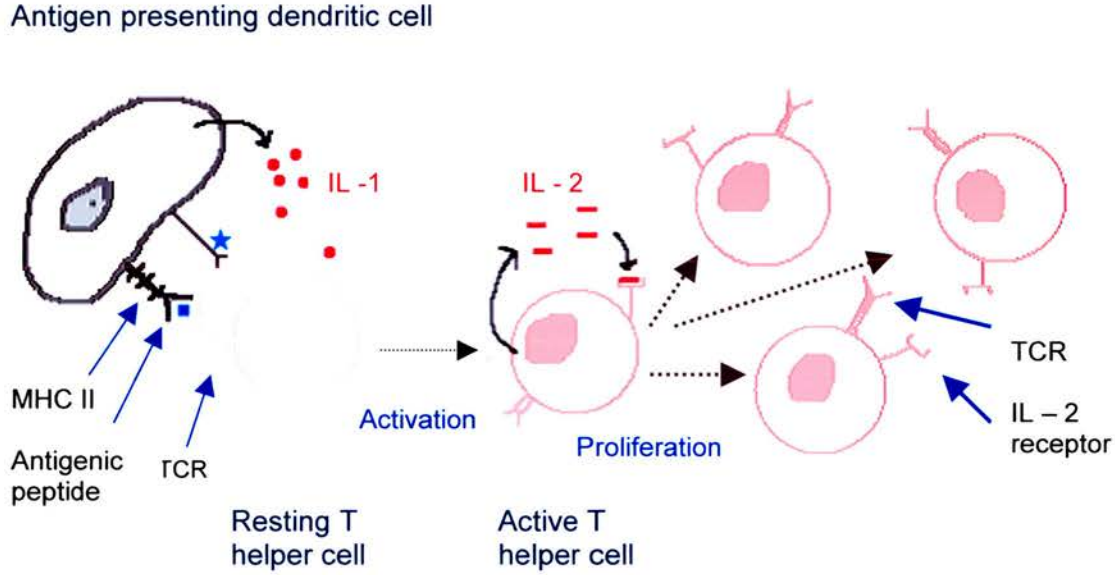

Figure 1.1. Diagrammatic representation of the sequence of events leading to the activation and proliferation of T helper cells.
★ Following MHC-II / antigen binding to the TCR molecule, co–stimulation of the naive T cell by CD28 / B7, and CD40 / CD40 ligand molecules occurs.

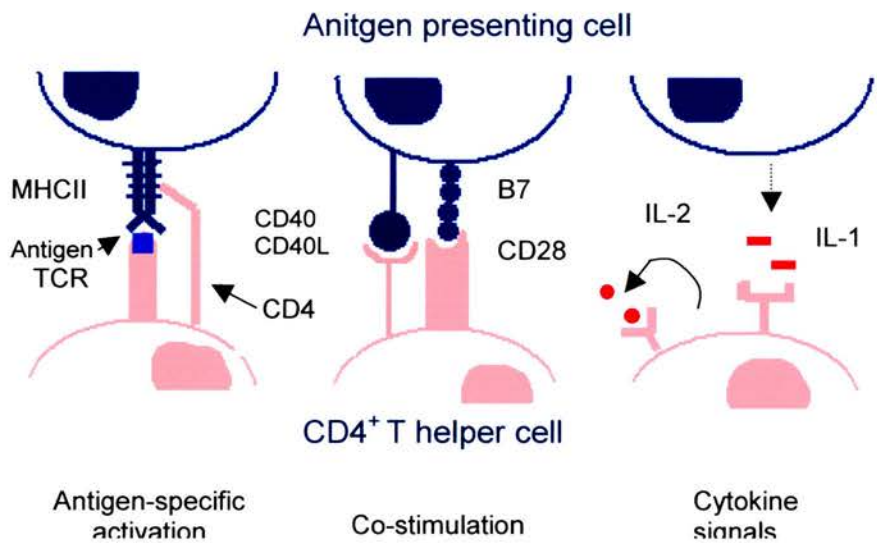

Figure 1.2. Steps in $CD4^+$ T helper cell activation

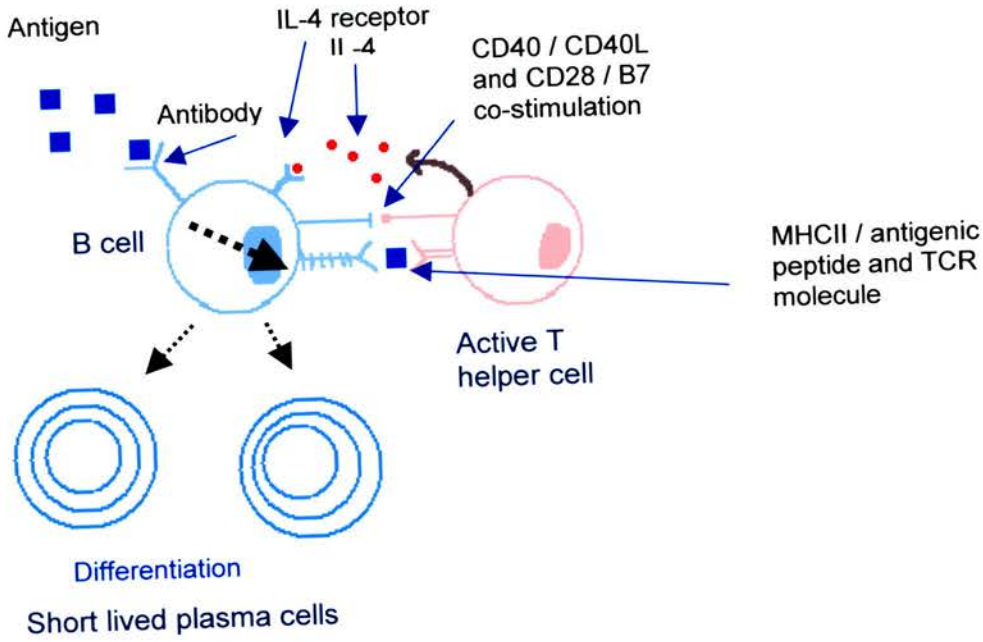

Figure 1.3. Diagrammatic representation of the signals involved in the initial stages of B cell activation

The attachment of the antigen peptide, in association with the MHC class II molecule to the T helper cell receptor molecules (TCR), initiates activation of the naïve T helper cell. In addition, the T cell CD4 molecule binds to the α and β chains of the MHC class II molecule on the APC. The most important molecules for co-stimulation of T cells by APCs, are two membranes receptor ligand pairs: the CD28 molecule on T cells which binds to the B7 ligands on the APC, and the CD40 ligand on T cells which binds to the CD40 molecule on the APC (Steiniger & Barth, 2000). Interleukin-1 (IL-1) receptor on the T cell also receives stimulation in the form of IL-1 from APCs. Finally, IL-2 receptor is induced on stimulated T cells, and IL-2 signals serve to self-stimulate and induce T cell proliferation (Figure 1.2). In the outer PALS region, the primed T helper cells meet antigen specific B cells. These B cells have bound and internalised their specific antigen through cell surface immunoglobulin receptors, and presented it together with MHC class II molecules on the B cell surface. Antigen presented in this way is able to induce primed T cell help in the form of CD40 ligand interaction, B cell B7 molecule and T cell CD28 molecule interaction, and IL secretion by B cells, while they pass through the outer PALS region. The interaction of the B cell CD40 molecule and CD40 ligand on the T helper cell, signal the B cell to activate transcription factor NFκB, and increase surface expression of intracellular adhesion molecule 1 (ICAM-1). Thus, the bonds between B cells and T helper cells are strengthened. A signal produced in the T helper cell causes the secretion of cytokines including IL-4, which is essential for B cell proliferation. T cell stimulation induces B cells to differentiate into short-lived plasma cells that migrate to the cords of the red pulp (Figure 1.3). As these plasma cells have not passed through a germinal centre, secreted immunoglobulin will be of

low affinity (Ford 1975). If the antibody secreted by these cells then encounters its specific antigen, immune complexes form, which localise on the FDC cell surface attached to Fc or complement receptors (Tew et al. 1997). Subsequently, B cells move into the primary follicle still attached to their cognate $CD4^+$ T helper cells, which are also essential fro the formation of the germinal centre. As they divide, they become large, metabolically active centroblasts, which become increasingly close packed and form the dark zone of the follicle. The germinal centre or secondary follicle reaction contains morphologically distinct light and dark zones constituting the centrocyte and centroblast rich areas of the germinal centres, respectively. As a result of T cell cytokine stimulation, centroblasts within the germinal centre hypermutate to form non-dividing centrocytes with mutated surface immunoglobulin within the light zone of the follicle. After hypermutation, the surface immunoglobulin expressed by an individual centrocyte can have an affinity for its specific antigen that is higher or lower that the un-mutated immunoglobulin. Thus, the population of centrocytes in a germinal centre express immunoglobulins with a range of affinities for a specific antigen. Survival of these centrocytes depends on whether their surface immunoglobulin is bound to antigen retained by FDCs, i.e. those centrocytes with high antigen affinity will preferentially bind antigen. These antigens, in the form of immune complexes, are shed by FDCs and taken up by centrocytes via their cell surface immunoglobulin. Antigenic peptides, derived from the internalised immune complex, are presented on the centrocytes in association with MHC class II molecules, and are then presented to primed T helper cells. Subsequently, T cell CD40 ligand interaction occurs. (Figure 1.4). This induces the centrocyte to express the Bcl-x_L protein, which prevents apoptosis. If this process

does not occur, centrocytes are programmed to die by apoptosis. T helper cells are then stimulated to proliferate in the germinal centre, and can transmit signals in the form of direct cell surface interactions or of cytokines, to the specific centrocyte sub-population, allowing them to survive and switch expression of the low affinity IgM to IgG by a process of somatic hypermutation. The particular isotype to which the immunoglobulin switch is made depends on the cytokines secreted by the T helper cell. Predominantly, IL-4, IL-5 and TGF–β are secreted. Somatic hypermutation is the process by which DNA base changes occur during the lifetime of a B cell. Immunoglobulin polypeptide mutations occur as a result of the recombination of the variable (V) regions of the immunoglobulin gene. The mutated surface immunoglobulin has an affinity for its specific antigen, and those centrocytes that express immunoglobulin of low affinity are prone to apoptosis (Steiniger & Barth, 2000). Centrocytes with the greatest specific IgG survive longest in the germinal centre. As the amount of antigen on FDCs decreases during the course of an immune reaction, competition amongst centrocytes for this antigen increases. Only centrocytes with a high expression of antigen will be "helped" by T cells. Centrocytes that do not receive adequate T helper stimulation will eventually die close to the dark zone. Centrocytes / FDC interactions are also necessary for centrocyte survival (see section 1.3.3.3).

Surviving centrocytes then perform a number of different tasks. Centrocytes can leave the germinal centre and redistribute around the body to locally differentiate into plasma cells. Other centrocytes can develop into memory B cells to spread specific immunity around the body. In this way the affinity of antibodies for a

specific antigen increases during the course of an immune response and in subsequent exposures to the same antigen.

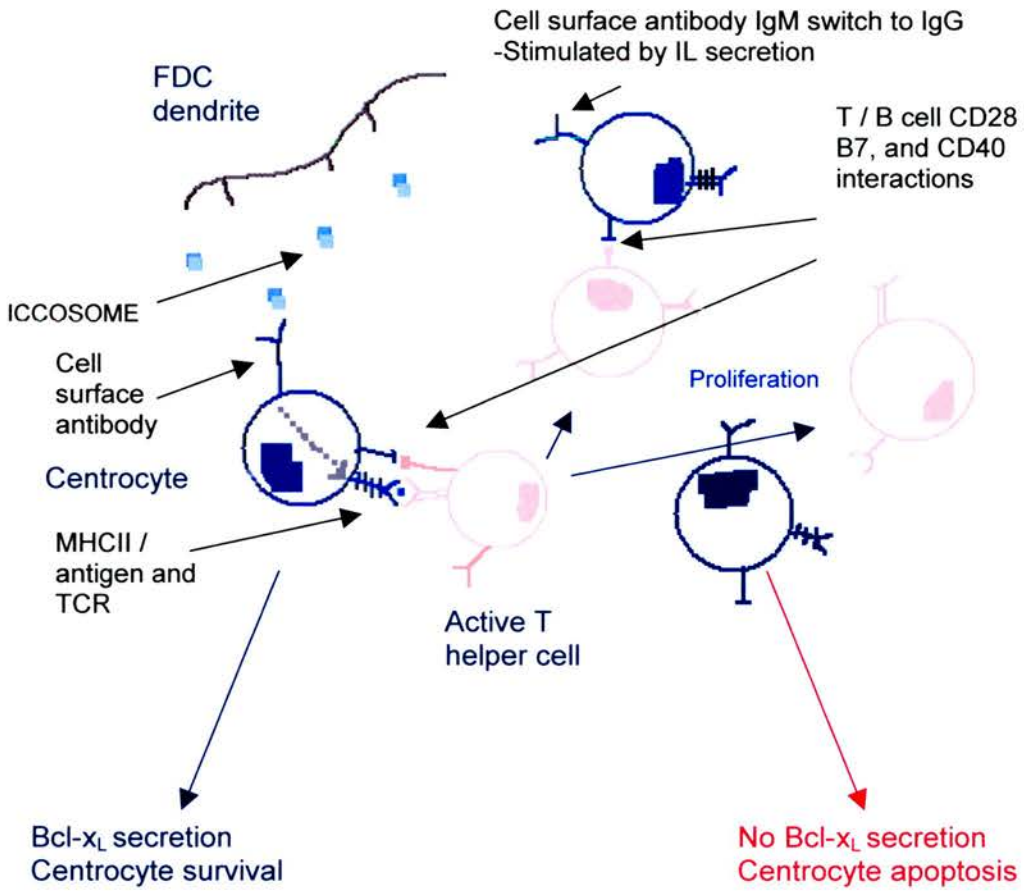

Figure 1.4. Diagrammatic representation of the signals and cellular interactions involved in the proliferation and immunoglobulin class switch of centrocytes in the secondary follicle.

It has further been speculated that centrocytes can move to the dark zone to revert to centroblasts (MacLennan et al. 1997). The mechanism for differentiation of a centrocyte into a memory B cell remains unclear. However, the B cell surface receptor CD40 must react with the T helper ligand CD40, in order for this differentiation to occur. In the absence of this CD40 interaction (Liu & Banchereau 1997), it has been shown that centrocytes maintained *in vitro,* terminally differentiate into antibody-secreting plasma cells. There is generally a lack of consensus relating to whether antibody-secreting cells are located at extrafollicular or germinal centre sites. However, plasma cells may persist in the follicle under certain conditions such as pre existing memory B cells or an excess of antigen (Steiniger & Barth 2000). Unlike other lymphoid organs, splenic white pulp contains the marginal zone that selectively retains IgM-positive memory B cells for certain types of T cell independent antigens. In addition, the marginal zone also contains memory B-lymphocytes to T cell dependent antigens. The marginal zone therefore plays a vital role in the initial response to infection by some viral or bacterial pathogens.

1.3.3.3. Origin, function and morphology of FDCs

The exact origin of FDCs has yet to be established. Several studies on the ontogeny of FDCs have indicated that they may be derived from the bone marrow, while others suggest a stromal-derived origin (Heinen et al. 1995). Following the study of antigen transport and bone marrow chimeras in SCID mouse models, it was concluded that FDCs were of a bone marrow origin, hypothesising that Antigen Transporting Cells (ATCs) are the precursor of FDCs (Kapasi et al. 1994; Yoshida et al. 1994; Kapasi et

al. 1995). The location of ATCs within the lymph node indicated an origin outwith the node itself. These cells appeared monocytic in morphology. Investigators also noted that ATCs seemed to alter in morphology as they travelled along the pathway from subcapsular sinus to the follicle, ultimately closely resembling the FDC (Kapasi et al. 1994). Parallel *in situ* antigenic phenotyping demonstrated both cell types had a similar phenotype, further supporting the conclusion that ATCs are the FDC precursors. FDCs from bone marrow reconstituted SCID mice were also found to be of donor phenotype, indicating bone marrow contained FDC precursors (Kapasi et al. 1994).

Following a SCID bone marrow reconstitution experiment similar to that described above, FDCs were found to express the SCID host phenotype suggesting they were not of a bone marrow origin (Imai et al. 1993). Ultrastructural studies highlighting the structural similarities between the FDC and fibroblasts outlined the structural characteristics of a population of cells morphologically similar to both fibroblasts and FDCs, known as Fibrohistiocytoid Cells (FH). Their studies indicated that FDCs might be derived from fibroblasts, while FH cells may be the intermediate between the two cell types (Heusermann et al. 1980; Imai et al. unpublished data cited in (Imai & Yamakawa 1996)). Although this matter remains an issue for contention, it is generally accepted that FDCs are not bone marrow derived.

The regulation of the humoral immune response depends directly on lymphocyte and accessory cell population interactions, during which FDCs play an important role. The primary function of FDCs within the lymphoid follicles is the trapping and retention of immune complexes via the C3b and Fc cell surface receptors. Complexes are retained at the cell surface without undergoing endocytosis (Heinen et al. 1985;

Radoux et al. 1985b; Tew et al. 1990), where they may remain from several months or even years (Tew et al. 1997). FDCs trap antigen via complement receptors only when it is complexed with an antibody and complement (Klaus & Humphrey 1977; Radoux et al. 1985a). Ferritin was not observed in conjunction with FDCs in mice that were not pre-immunised with this antigen, but, instead, was localised in large quantities in macrophages. In contrast, after a secondary immunisation with ferratin, sub-cellular analysis revealed accumulation of this antigen in the electron-dense material surrounding FDC dendritic processes (Radoux et al. 1985a). In addition, the ferritin antigen / antibody complex seemed to localise within the extracellular space between adjacent dendrites, resulting in an almost uniform spacing between dendrites. This arrangement could be due to the fixation of the antigen / antibody complex on adjacent dendrites, the complex thus acting as a bridge. Antigen / antibody complexes retained by the FDC may be involved in the periodic re-stimulation of B, and perhaps, T cells (Heinen et al. 1995). In studies with aged mice, it has been demonstrated that functional FDCs are required for the development of antibody-forming cells, and subsequent secondary response (Kosco et al. 1989). This study concluded that in young mice, FDCs readily attach antigen / antibody complex, and subsequently stimulate the proliferation of centrocytes into antibody-forming cells. However, in aged mice, it was observed that FDCs retained little antigen, and released no immune complex coated bodies; thus, few antibody-forming cells were formed. It was concluded that failure of old mice to respond to antigen was due to the lack of functional FDCs and resulted in the absence of germinal centres (Szakal et al. 1990). This was further shown in aged mice that were unable to induce a normal

secondary antibody response in the absence of released immune complex coated bodies, termed "ICCOSOMES" (Szakal et al. 1989; Burton et al. 1991).

It is possible that circulating B cells trap antigen, move towards the germinal centre where they present immune complex to FDCs (Heinen et al. 1986), however the involvement of B cells at this stage remains controversial. The alternative hypothesis now considered more likely, involves the binding of secreted low affinity antibodies at extrafollicular sites to the respective antigen, which complex and finally localise on the FDC in the primary follicle, although exactly how the complexes reach the FDC in the spleen remains unclear (Tew et al. 1997). The major accessory cell role of the FDC is in the stimulation of B cells. Antigen encountered within the primary follicle leads to the induction of the germinal centre, where B cells rapidly proliferate and divide. Immune complex-retaining FDCs can create a microenvironment for centrocytes within the light zone of the follicle. The FDC-expressed antigen is then believed to interact with specific immunoglobulin receptors on the centrocytes, thus inducing proliferation into antibody-producing or memory B cells (Petrasch et al. 1991). B cells which are not surrounded, or "emperipolesed" by the FDC, are considerably more likely to undergo apoptosis (Kosco & Gray 1992). The exact mechanism for the inhibition of apoptosis by FDC emperipolesis, and also by T cell stimulation was also investigated (Lindhout et al. 1995). The primary characteristic of apoptosis is the fragmentation of DNA by an endogenous endonuclease. Following FDC interaction, endonuclease activity within B cells of the germinal centre is irreversibly blocked. Both FDCs and T cells provide stimuli to B cells that prevent apoptosis, and promote differentiation into memory or plasma cells. In addition to Fc and complement receptors, many adhesion molecules are expressed on

germinal centre FDCs, and also on B cells. These receptor molecules have been shown to mediate cell to cell, or cell to the extracellular matrix binding and play an important role in the interactions between these two cell types (Koopman et al.1991; Bosseloir et al. 1995). Stimulation of B cell adhesion molecules, cross linking of immunoglobulin receptors by antigen associated with FDCs, and cross-linking of the T cell CD40 ligand with B cell CD40, have been shown to prevent apoptosis of B cells within the germinal centre (Koopman et al. 1997). It was later demonstrated that FDCs are responsible for both the maintenance of anamnestic responses as a result of antigen presentation, and, along with T cells (Kosco et al. 1992; Burton et al. 1995), for co-stimulatory signals to induce B cell proliferation. FDCs also play an important role in the induction of B cell response to chemotactic factors that induce migration.

FDC complex retention relies on activation of complement. If activation does not occur, complexes will not be retained on the FDC cell surface and ultimately, memory B cells and antigen specific antibody will not be produced (Imai & Yamakawa 1996). Complement receptors expressed by the FDC are necessary for binding immune complexes, and the presence of complement receptors such as CD21 are essential for the production of antibodies against both T cell dependent and independent antigen during the primary immune response. CD21 is also essential for the long-term retention of immune complex within the germinal centre.

The expression of adhesion molecules by FDCs also plays an important role in B cell binding to create the B cell / FDC network (Kosco et al. 1992; Ogata et al. 1996). In addition, cytoplasmic processes of the FDC have been demonstrated to bind to

extracellular fibres. This mechanism is thought to play an important role in the creation of a three dimensional framework within the follicle.

In 1948, Marshall et al. reported metallophillic cells in germinal centres which were later given the name "Dendritic reticular cells" due to their abundance of dendritic extensions (Maruyami et al. in (Heinen 1995)). The morphological features of these cells, later termed follicular dendritic cells, have been thoroughly described. FDCs frequently have a large, clear, bi- or multi-lobed nucleus, delineated peripherally with only a thin line of chromatin along the lamina densa. These features and the restricted distribution of the cell to one pole of the light zone of the follicle assist the morphological identification at the light microscopical level. Mature FDCs bear well-developed cytoplasmic dendritic profiles, which extend between many lymphocytes within the germinal centre of the follicle. Desmosomal junctions between dendrites serve to maintain the convoluted dendritic network. The cytoplasm is sparse and contains limited organelles. FDCs of the germinal centre were sub-divided into seven distinct morphological types (Rademakers 1992). These categories were distinguished on the basis of cell organelle content, cellular extension morphology, the presence of plasmalemmal-associated electron-dense deposit, and the occurrence of intermediate filaments. The distribution of FDC subtypes differs between the dark and light zone, with the more primitive types predominantly located in the dark zone, and more differentiated types appearing in the light zone.

1.3.3.4. Origin, function and morphology of TBMs

TBMs, so named due to their dark-staining, phagocytosed nuclear remnants in their cytoplasmic vesicles, are normal constituents of the germinal centres of secondary lymphoid tissues (Smith et al. 1998; Steiniger & Barth 2000). These cells are large with indented nuclei and well-developed Golgi complexes, while many other cellular organelles are present in small quantities. Many electron-dense granules, thought to be lysosome precursors are also present, while the cytoplasm of activated macrophages contains multiple developed lysosomes. This group of macrophages are a subset of the long-lived mononuclear phagocytic cells, which are derived from bone marrow, and after differentiation into blood monocytes, finally settle in a specific tissue, which, in the case of TBMs, is the germinal centre of the spleen. Macrophages may finally come to reside at many different locations. Their specific function is partly determined by the microenvironment in which they are located (Smith et al. 1998). Within the germinal centres of the follicles, B cells which fail to produce functional immunoglobulin receptors by affinity selection (see section 1.3 2. 2.) undergo apoptosis and are removed by TBMs. This occurs via a mechanism known as endocytosis, which can be divided into phagocytosis and pinocytosis, depending on the size of the endocytosed vesicles. Pinocytosis occurs in most cells and involves the ingestion of pieces of their plasma membrane in the form of small pinocytic vesicles. These vesicles are formed from specialised invaginated areas of the cell membrane, which are coated in proteins, predominantly clathrin. A dynamin ring forms around the neck of the invagination to cause 'budding' of the vesicle into the cell (Hill et al. 2001). As soon as the intracellular vesicle is formed, the clathrin

and associated proteins dissociate from the membrane, and return to the plasma membrane. The vesicle is then able to fuse with endosomes, where unless their contents are specifically retrieved, will finally be digested by hydrolytic enzymes within lysosomes. The movement of endosome contents from peripheral to perinuclear endosomes and subsequently lysosomes remains unclear (Brown et al. 1986).

Macrophages are capable of ingesting many apoptotic cells, up to twenty have been observed in a single macrophage (Ghadially 1982). Apoptotic B cells are engulfed by TBMs by the process of phagocytosis. The apoptotic cells first attach to the macrophage membrane; however, the receptors for this process are unknown. Pseudopodia are extended around the dying cell and phagosomes are formed, the diameter of which is determined by the size of the particle being ingested, and at this stage, some components of the phagocytosed cellular plasma membrane are recycled to the macrophage membrane, where they are presented in complexes with major histocompatibility complex glycoproteins. This presentation then serves to stimulate T helper cells to mount an immune response. However, TBM-enriched preparations were shown to be poor antigen presenters and therefore were determined not to be involved in the regulation of the germinal centre reaction (Smith et al. 1998). In addition to the cell-scavenging role of TBMs, it has been suggested that these cells are a major determinant of interleukin 2 suppression, thereby serving as regulatory cells by downregulating the germinal centre reaction (Smith et al. 1998). As in pinocytosis, endocytosed vesicles fuse with lysosomes, where the contents are digested. Indigestible materials remain within the lysosomes to form residual bodies,

while digested material is expelled into the cell cytosol where it is excreted or reutilised by the cell (Bainton 1981).

Although it has been suggested that TBMs are resident germinal centre macrophages (Kotani et al. 1982), it seems more likely, due to the transient nature of germinal centres that these macrophages migrate to the germinal centre as a result of immunological stimulation. Ultrastructural studies by Szakal et al. (unpublished data) suggest they migrate into the germinal centre from the sub-capsular sinus. This is supported by the findings of Smith et al. who failed to immunolabel macrophages within primary follicles (Smith et al. 1988).

The kinetics of the TBM response have also been investigated, and it was demonstrated that proliferation of B cells as a result of an immune reaction, directly correlated with an increase in TBM numbers, and the ratio of B cells to TBM remained relatively constant throughout germinal centre development (Smith et al. 1991).

1.4. Project background

Initial sub-cellular investigations of scrapie-infected tissues were undertaken in murine brain (Jeffrey et al. 1994a; Jeffrey et al. 1995; Jeffrey & Goodsir 1996; Liberski et al. 1996). These studies determined the sub-cellular localisation of PrP^{d} and its relationship to the pathological changes associated with disease in brain tissue.

More recent light microscopical studies have suggested follicular dendritic cells and / or B cells of the LRS play a vital role in the peripheral pathogenesis of scrapie (McBride et al.1992; Klein et al. 1997; Brown et al. 2000).

The investigations detailed in this thesis attempt to verify the hypotheses that PrP^d is located both intracellularly and extracellularly within the LRS, FDCs are intrinsically involved in the accumulation of PrP^d, and that sub-cellular pathology of the LRS occurs following TSE infection.

1.5. Project aims

Light microscopical immunohistochemical and morphological analysis of TSE infection within the LRS has been well documented during the past decade, however, ultrastructural analyses have, to date, been limited.

This thesis will investigate aspects of scrapie infection within the lymphoreticular system of mice and, to a lesser extent, sheep.

The principal aims of the study can be divided into technical, structural and pathogenesis.

Technical development

To determine methods for the fixation of lymphoid tissues and labelling of PrP^d. This should permit both high quality preservation of cellular structure, while retaining essential antigenic epitopes that will allow localisation of PrP^d in the electron microscope.

Ultrastructural morphology

To determine the structure of the secondary follicles of murine spleen and sheep lymph node in normal and scrapie-infected animals. Morphologic changes will be sought from early in the incubation period through to the development of clinical disease.

Pathogenesis

To determine the sub-cellular location of PrP^d accumulation, and to relate this to the pathogenesis of disease.

2. MATERIALS AND METHODS

2.1. Experimental animals

2.1.1. Murine – C57Bl mice: ME7 inoculation (intracerebral – i.c.).

All experimental mice were maintained under specific pathogen free conditions at the Institute of Animal Health (IAH) Neuropathogenesis Unit (NPU) in Edinburgh. The ME7 strain of scrapie was used in the majority of experiments, as it is one of the best-characterised strains. It has been established that i.c. ME7 scrapie inoculation causes peripheral infection, therefore, due to the short incubation period, this inoculation route was used for the initial experiments. As limited tissues were available, either i.c. or intra-peritoneal (i.p.) inoculations were used for each of the other experimental models. It was therefore impossible to directly compare experimental models, however, this was taken into consideration when results were analysed.

C57Bl mice, infected with the ME7 scrapie strain by i.c. injection of 20 µl of a 1% brain homogenate, were available for study. An average of 40 spleen tissue blocks were taken from each of two scrapie-infected mice at day 70, and an average of 33 spleen tissue blocks were taken from each of three scrapie-infected mice at terminal stages of the disease (mean incubation period approximately 170 days following i.c. injection). From two age-matched (70 dpi) normal brain (NB) inoculated control mice, 70 blocks of spleen tissue were available for examination, while 90 tissue blocks were available from the NB inoculated control group at 170 dpi. At least 5

tissue blocks were studied from each animal. An average of three white pulp areas were present within each of the blocks studied.

2.1.2. Murine - Sheep red blood cell inoculation (SRBC).

C57Bl mice were challenged by i.p. injection with a 10^{-2} dilution of ME7 scrapie brain or a homogenate consisting of normal mouse brain. I.p. ME7 inoculation gives a mean incubation period of 270 days.

One group of ME7 infected, and one group of NB mice were given one immunization of SRBC (1×10^7 SRBC in sterile saline in a total volume of 100µl) or saline, followed by a boost 21 days later (approximately 63 days post infection (dpi)). A duplicate set of mice were immunologically challenged with SRBC or saline at 240 dpi, followed by a boost 21 days later (approximately 261 dpi) (see table 2.1). These mice were allowed to become terminally diseased. From each experimental group, at least 5 tissue blocks containing white pulp areas were studied.

	Number of animals (average no. tissue blocks per animal)			
	42 dpi		240 dpi	
	SRBC	Saline	SRBC	Saline
ME7 scrapie inoculated	2 animals (30)	2 animals (30)	2 animals (38)	2 animals (30)
Normal brain inoculated	2 animals (30)	2 animals (30)	2 animals (25)	2 animals (25)

Table 2.1. Scrapie and SRBC innoculation. Table shows numbers of animals / tissue blocks (number within bracket) from each experimental group.

2.1.3. Murine – strain / agent studies. 139A, 79A, ME7, 87V. Scrapie inoculation

Phenotypic properties of different scrapie strains were analysed ultastructurally within the spleen. Initial PrP^d detection, incubation periods and cellular targeting differences between TSE strains were compared. All mice were challenged i.c. with a 10^{-2} dilution of the TSE agent.

Tissues from each of the inoculated groups were collected 5 weeks after scrapie infection, 10 weeks after scrapie infection and finally at terminal disease (see table 2.2). At lease 5 tissue blocks containing white pulp were identified from each group for study.

The ME7 scrapie strain was originally isolated from a Suffolk sheep with naturally acquired scrapie. Maintenance of the strain is achieved by serial passage in C57Bl mice.

The 79A scrapie strain was originally isolated from a goat which had been inoculated experimentally with the SSBP / 1 scrapie strain. Passage was undertaken in C57Bl mice.

139A scrapie was isolated form a murine source that originated from the same caprine source as 79A scrapie. The strain was maintained in C57Bl mice.

87V scrapie was originally isolated from a Cheviot / Border Leicester cross sheep which had natural scrapie. Passage was achieved in a VM strain of mice.

Scrapie strain (mouse strain)	Number of animals (average No. of tissue blocks)		
	5weeks	10 weeks	Terminal
ME7 (C57Bl)	2 (29)	2 (35)	2 (32)
79A (C57Bl)	2(31)	2 (35)	2 (30)
139A (C57Bl)	2 (30)	2 (28)	2 (34)
87V (VM)	2 (36)	2 (27)	4 (35)

Table 2.2. Number of animals / average number of tissue blocks per scrapie strain group at 3 different timepoints.

2.1.4. Murine – cytokine inoculation

Signalling between lymphocytes and FDCs by cytokines is essential in the formation of the germinal centre and maintenance of FDC networks (Matsumoto et al. 1997; Pasperakis et al. 1996). These studies investigate the effect of the inhibition of specific cytokine signals from B-lymphocytes on the sub-cellular localisation of PrP^d, and transmission of scrapie infectivity to the CNS.

2.1.4.1. Murine - Tumour Necrosis factor fusion protein inoculation

C57Bl mice (8 –12 weeks old) were treated i.p. with Human Tumour Necrosis Factor Receptor Fusion protein (huTNFR: Fc) or human Immunoglobulins (hu-Ig) at either 14 or 38 days after i.p. injection, with 20 µl of a 1% dilution of brain homogenate from a terminally affected scrapie mouse. Mice were sacrificed 7 days after huTNFR:Fc / hu-Ig treatment. The experimental animals are detailed in Table 2.3. Significant numbers of tissue blocks were processed and examined in each case. These were examined by toluidine blue, initially to determine the structure of the spleen, and in order to locate several secondary follicles in appropriate stages of development and orientation. At least 5 tissue blocks were studied from each animal, however, follicles were sparse in blocks from huTNFR:Fc treated animals. Subsequently, many more blocks were studied from these animals. The precise number of follicles detected varied from animal to animal and between experiment groups.

Number of animals (Average No. tissue blocks)		
Treatment day post scrapie infection	hu-Ig	huTNFR:Fc
14	2 (13)	2 (18)
38	2 (18)	2 (19)

Table 2.3. Number of animal / average number of tissue blocks (number within bracket) per treatment group.

2.1.4.2. Murine - Lymphotoxin β fusion protein inoculation

C57Bl mice were i.p treated with human Lymphotoxin β Receptor immunoglobulin Fusion protein (LTβR: Ig) or hu-Ig, at either 42 or 70 days after i.p. injection with ME7 scrapie (20 μl of a 1% dilution of brain homogenate from a terminally affected scrapie mouse). Mice were then sacrificed either 3 or 35 days after treatment. At least 5 tissue blocks were studied from each animal from each experimental group. Experimental details are summarised in Table 2.4.

Treatment day after ME7 scrapie infection (necropsy after ME7 infection)	Number of animals (Average No. tissue blocks per animal)	
	hu-Ig	LTβR-Ig
42 (45)	4 (27)	2 (23)
42 (77)	3 (23)	2 (20)
70 (73)	3 (19)	2 (21)
70 (105)	2 (18)	2 (19)

Table 2.4. Number of animal / average number of tissue blocks (number within bracket) per treatment group.

2.1.5. Ovine studies.

For all ovine studies, mesenteric lymph node (MLN) from clinically affected Suffolk sheep were used. Tissues were obtained from sheep of the most susceptible genotype: $PrP^{ARQ/ARQ}$. MLN was studied due to the consistency of infection and ease of access in scrapie-infected animals. Many tissue blocks were studied from at least 10 sheep.

2.2. Experimental techniques

2.2.1. Tissue fixation technique

2.2.1.1.Murine

Following a previously established animal perfusion technique protocol (see Appendix 6.1.a), mice were anaesthetised and perfused with one of two aldehyde-based fixatives (see Appendices 6.1.b and 6.1.c for fixative recipes). Spleen tissue was chosen due to both the vast abundance of literature available regarding splenic involvement in murine scrapie, and due to ease of tissue removal. Spleens were removed following perfusion and immediately immersed in corresponding fixative for 24 hours at 4°C.

Spleens were also immediately removed from mice following death by cervical dislocation. Within 5 minutes, these tissues were sectioned into 2-3 mm slices, and immersed in one of four fixatives for 24 hours at 4°C (see Table 2.5).

Fixation Procedure	Fixative
Perfusion	0.5% paraformaldehyde / 0.5% gluteraldehyde
Perfusion	4% paraformaldehyde / 0.1% gluteraldehyde
Immersion	4% paraformaldehyde / 0.5% gluteraldehyde
Immersion	4% paraformaldehyde / 1% gluteraldehyde
Immersion	0.5% paraformaldehyde / 0.5% gluteraldehyde

Table 2.5. Table showing details of initial tissue fixation study

Previous ultrastructural tissue processing carried out at VLA Lasswade, have produced a standard technique for the processing of brain tissue, using 4% paraformaldehyde / 0.1% gluteraldehyde as a perfusate. In order to identify whether this fixative was equally useful for splenic fixation, various other fixative mixtures were also compared. Phosphate buffer is relatively safe for handling, and exerts the appropriate osmolality when combined with aldehyde-based fixatives (Hayat 1989). Gluteraldehyde is the most commonly used fixative. It was demonstrated that gluteraldehyde is the most effective fixative for the preservation of fine structure. Using paraformaldehyde in conjunction with gluteraldehyde, has the added advantage of rapid penetration of the tissue (Sabatini & Bensch 1962; Sabatini & Bensch 1963).

Following standard techniques detailed in sections 2.2.2 - 2.2.4. and 2.2.6, these tissues were processed, embedded in resin, sectioned and counterstained in order to identify the optimal fixative and fixation procedure.

Multiple blocks from each fixation group were studied, and quality of fixation judged on the basis of overall tissue structure and the degree of organelle and membrane preservation.

Spleens obtained from animals perfused with either 0.5% paraformaldehyde / 0.5% gluteraldehyde, or 4% paraformaldehyde / 0.1% gluteraldehyde,
showed equally poor cell / cell apposition, mitochondrial turgidity and poor membrane integrity. As a result of this, various adjustments were made to the perfusion protocol (Appendix 6.1.a.). Chloral hydrate, which, in conjunction with intracardiac perfusion is an accepted rodent anaesthetic, was used routinely for murine perfusion. This is not barbiturate based and is unlikely to cause adverse affects on the spleen such as splenic congestion.

Cannulation pressure was also decreased to 110-120 mm Hg (Hayat 1989) to ensure no capillary damage of the highly vascularised tissue. However, tissue ultrastructure did not appear to be improved by these modifications.

All immersion fixed spleens showed considerably greater membrane definition and an improvement in tissue structure. Based on these findings, immersion fixation was chosen as the standard fixation technique for murine spleen tissue. As no discernable difference was apparent between different paraformaldehyde / gluteraldehyde concentrations, that with the lowest gluteraldehyde content was chosen, as this aldehyde is known to reduce the ability of antibody to recognise antigen (Totterdell et al. 1992). Both 4% and 0.5% paraformaldehyde gave equally good results, therefore the lower fixative content was chosen in order to reduce the possibility of the fixative interfering with antigen recognition due to protein cross linking.

2.2.1.2. Ovine

As with murine tissues, samples were immersed in various fixatives. 4% paraformaldehyde / 0.1% gulteraldehyde was found to be the optimal fixative for ovine lymphatic tissue. Paraformaldehyde is a slow penetrating fixative, while gluteraldehyde fixes tissues in a short space of time and provides excellent maintenance of tissue structure. However, gluteraldehyde is also known to impair antigen localisation by altering cellular components (Glauert & Lewis. 1998). It was therefore decided that the lowest possible concentration of gluteraldehyde should be used. Where no gluteraldehyde was used, tissue structure was noticeably impaired.

2.2.2. Tissue processing

Following fixation, spleens were trimmed into 1 mm^2 blocks and embedded in araldite resin according to the protocol detailed in Appendix 6.1.d. Blocks were cured at both 37°C and 60°C in order to determine whether curing temperature affected tissue structure. Subject to the tissue block size, embedding capsules with a conical or flat base were used. Following tissue sectioning and staining methods detailed in sections 2.2.3, 2.2.4 and 2.2.6, structure of ovine MLN was analysed and was found to be comparable to murine spleen in terms of tissue morphology and preservation. Based on these previous criteria (see section 2.2.2.1), araldite-embedded tissue cured at 60°C was used routinely for all ovine studies.

2.2.3. Tissue sectioning

Flat-based resin blocks were trimmed into a conical shape using a Leica EM trim. This method can be found in the instruction manual.

A Leica Ultracut E microtome was used to further remove excess resin from conical resin blocks. Using a freshly cut glass knife, remaining resin is cut to form a sloping rectangular shape, known as a mesa (see Figure 2.1). Mesa formation allows accurate orientation of tissue blocks for ultrastructural analysis (see section 2.2.6).

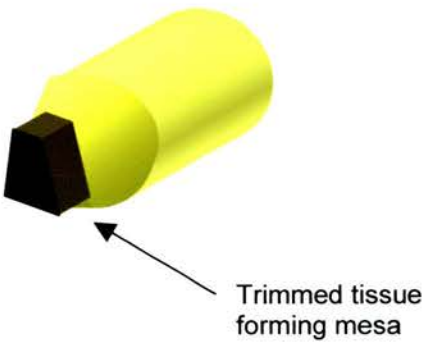

Figure 2.1. A trimmed resin embedded tissue block.

2.2.3.1. LM sectioning

Prior to sectioning, plastic troughs (TAAB Laboratories Equipment LTD, Berkshire, England; Agar Scientific LTD Essex, England) were attached to cut glass knives using molten wax. Dental wax (TAAB) heated on a wax hot plate (Multiplate LKB, Agar Scientific) was most commonly used. Freshly cut glass knives were used, and formed a sealed water bath with the trough onto which cut sections were floated.
1 μm sections were cut from tissue blocks and floated into the water bath. They were then stretched using a TAAB heat pen and removed using a fine hair. For immunolabelling, sections were placed onto a water drop on BDH charged glass slides, (VWR International Ltd., Leics) allowed to dry naturally then placed in a 60°C oven for 24 hours.
The protocol for staining 1μm sections is detailed in Appendix 6.1.e., and protocols for immunolabelling 1μm sections are detailed in Appendix 6.1.g.

2.2.3.2. EM sectioning

Excess tissue was trimmed from blocks containing areas of interest. Orientation of blocks was possible due to the formation of a mesa that could be directly correlated with the 1μm immunolabelled sections.
55 nm sections were cut from blocks chosen for ultrastructural analysis using a 2.4 mm Diatome ultra diamond knife. Sections were straightened in the water bath using the heat pen, and were lifted from the water bath by gold grids held by Dumont fine forceps (TAAB). Excess water was removed from grids by touching fine filter paper

to the periphery of the grid. Grids were allowed to air dry completely before being placed in a dial-a-grid box (TAAB, Agar Scientific).

2.2.3.2.i. Grid suitability for immunolabelling

Following initial investigations, standard nickel grids were found to be unsuitable for use with formic acid pre-treatment, as grids disintegrated due to the intensity of the acid reaction. Formic acid had a similar effect on copper and rhodium grids. The inert nature of gold resulted in these grids being stable when incubated with formic acid.

Due to the intense etching procedure required to expose ovine PrP, a smaller support mesh was also required. 400 mesh gold grids were therefore used routinely when immunolabelling murine tissue, while 600 mesh gold grids were used when immunolabelling ovine tissues.

As nickel grids are considerably less expensive that gold grids, and no formic acid treatment was required, sections were placed on 400 mesh nickel grids for all counterstaining.

2.2.4. Light microscopical staining method

1μm sections were stained using 1% Toluidine Blue dye. See Appendix 6.1. e.

2.2.5. Light microscopical immunolabelling methods

1 μm sections were immunolabelled using one of the following techniques. Selected blocks with appropriate immunolabelled areas were then taken for ultrastructural studies. Although PrP^c can be detected in cells of lightly fixed spleen by light microscopy (McBride et al. 1992), the combination of fixatives and pre-treatments employed destroys PrP^c immunoreativity and reveals only PrP^d accumulations. Whether these deposits are protease-resistant, or protease-sensitive, cannot be determined by the immunocytochemical methods described.

2.2.5.1. Peroxidase anti-peroxidase technique (PAP)

Initial murine studies were carried out using the peroxidase anti-peroxidase technique (Appendix 6.1.f)

The peroxidase anti-peroxidase method is an indirect method; that is the antibody is not directly labelled, but the secondary antibody binds to the primary antibody and it is this reagent that is bound to the label. As more than one secondary molecule can bind to the primary antibody, this step amplifies the reaction. A peroxidase anti-peroxidase pre-formed conjugate then binds to the secondary antibody. The peroxidase in this complex is involved in the visualisation reaction involving 3'3-Diamiobenzidine Tetra-hydrochloride (DAB) and hydrogen peroxide. During this reaction, peroxidase reacts initially with hydrogen peroxide, and then oxidises the chromagen (DAB) to give a coloured product. See Figure 2.2a.

2.2.5.2. Avidin Biotin amplification method (ABC)

This technique was used for all later immunolabelling of murine tissue, and all ovine work (see Appendix 6.1.g). ABC kits are obtained from Vector Laboratories Inc. Peterborough, UK. In both species, abundant FDC and intralysosomal TBM labelling was present.

This is also an indirect labelling method, however, due to the affinity of avidin for biotin the technique is considerably more sensitive. The avidin / biotin / HRP molecule is bound to a biotinylated secondary antibody, which is attached to the primary antibody. Again, peroxidase is the enzyme involved in the colour reaction. See Figure 2.2b.

2.2.5.3. Envision system

The Dako Envision system (Appendix 6.1.h.) (DakoCytomation, Cambridgeshire, UK), was used to immunolabel both murine and ovine tissue. Investigations showed this system to be slightly less sensitive than the ABC technique, thus its use was discontinued.

The technique is a direct method, whereby a polymer chain consisting of many secondary antibodies bound to the primary antibody can bind a large number of horseradish peroxidase molecules, which are then visualised using DAB as described above. See Figure 2.2c.

Figure 2.2.

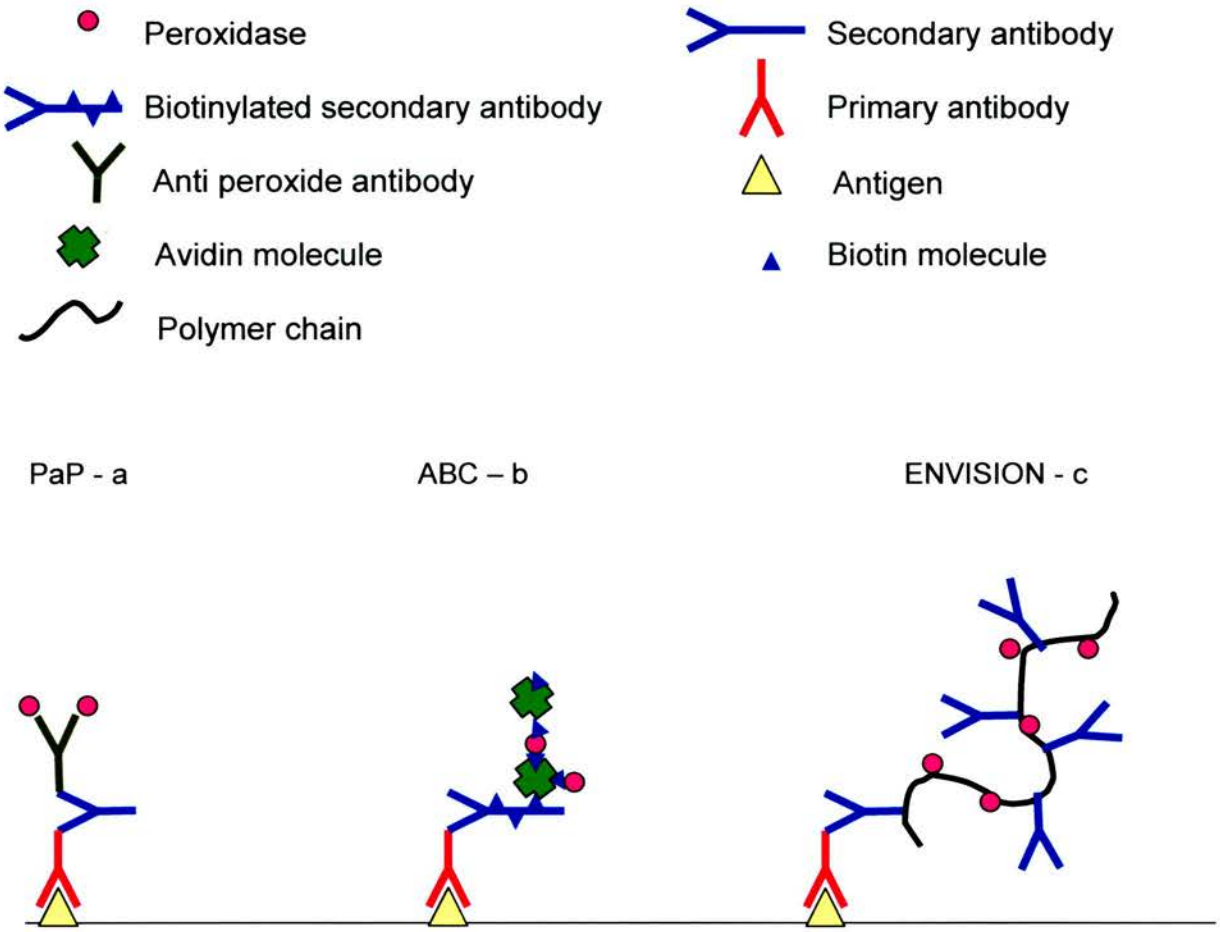

Figure 2.2. Diagrammatical representation of LM immunohistochemical techniques used.

Figure2.2a. Peroxidase anti-peroxidase labelling. A secondary antibody is attached directly to the specific primary antibody, followed by a peroxidase anti-peroxidase molecule.

Figure 2.2b. Avidin-biotin complex immunolabelling. A biotinylated secondary antibody is attached to the specific primary antibody. Avidin / biotin / HRP complexes are then attached, amplifying the signal.

Figure2.2c. Envision system amplification. A polymer chain consisting of many secondary antibodies bind to the specific primary antibody. This complex also binds to a large number of horseradish peroxidase molecules.

2.2.5.4 Antibodies – murine tissues

Polyclonal primary antibodies against PrP, previously shown to give excellent labelling in murine tissues, include 1A8 and 1B3 obtained from the IAH – NPU in Edinburgh (Farquhar et al. 1993). 1A8 was used routinely for all LM and ultrastructural murine studies.

2.2.6. Ultrastructural staining method

Tissue sections mostly contain molecules of a low atomic weight, thus, they are predominantly electron transparent (Hayat 1989). Ultrathin sections must therefore firstly be stained with heavy metals to improve contrast.

The simplest method for staining 55 nm sections for EM analysis employs the heavy metals lead citrate and uranyl acetate. The protocols for making these stains can be found in Appendices 6.1.i and 6.1.j. respectively.

These heavy metal stains are used in conjunction to label ultrathin sections (Appendix 6.1.k).

2.2.7. Ultrastructural immunolabelling method – murine

2.2.7.1. Use of Auroprobe 1nm Immunogold silver stain technique (IGSS) for murine studies - 1A8.

Ultrastructural immunological studies of murine splenic tissues were carried out using the Auroprobe 1 nm gold probe (Amersham Biosciences, NJ, USA) as

described in Appendix 6.1.l. See figure 3.5.7a. This probe consists of a gold molecule attached directly to a secondary antibody.

2.2.7.2. Use of Nanoprobe 1nm gold probe (Nanoprobes, NY, USA) with gold enhancement for murine studies – 1A8[2]

Nanoprobe 1 nm gold probe was substituted for Auroprobe 1 nm probe. Again, this probe is a gold molecule directly conjugated to a secondary antibody. Using Amersham silver enhancement, poor results were obtained on murine spleen tissue. Using Nanoprobe gold enhancement with Nanoprobe gold probe (Figure 2.3a), results were more positive, however, they were not comparable to those using Auroprobe 1nm with silver enhancement. Results from using Auroprobe 1 nm with gold enhancement were considerably better than those from the original IGSS technique (Figure 2.3b).

[2] Ovine

Details of all methods specific to the ultrastructural visualisation of PrP^d in ovine tissues are discussed in chapter 3.5.

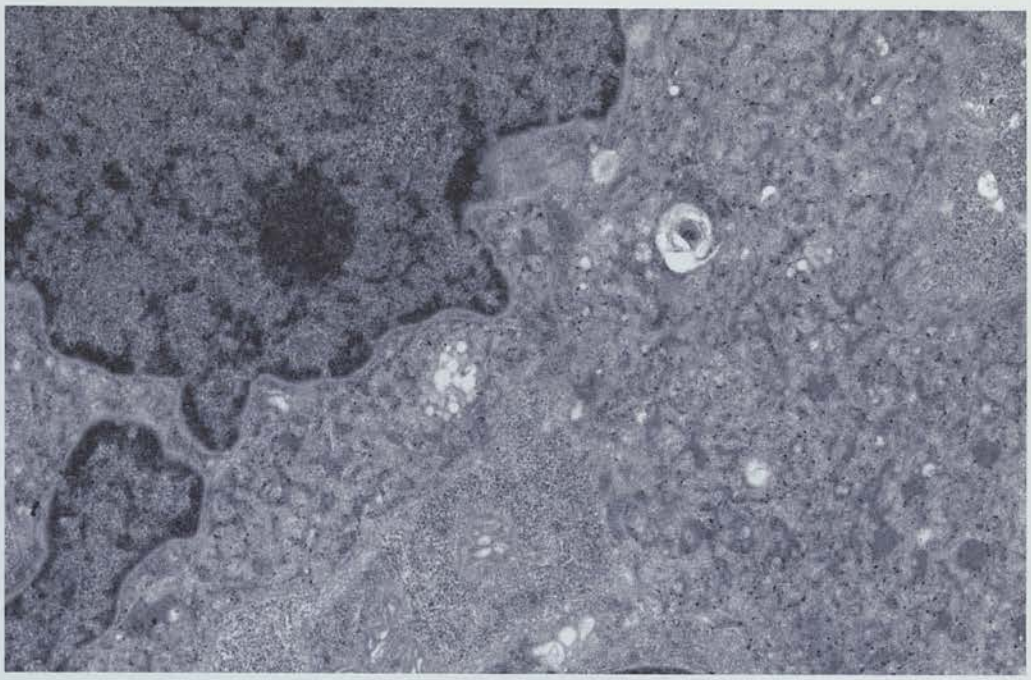

Figure 2.3a. x15K magnification. Terminally scrapie affected murine spleen. Limited Immunolabelling is observed following immunolabelling with 1A8 anti PrP serum, 1nm Nanoprobe immunogold and enhanced using Nanoprobe goldenhance technique.

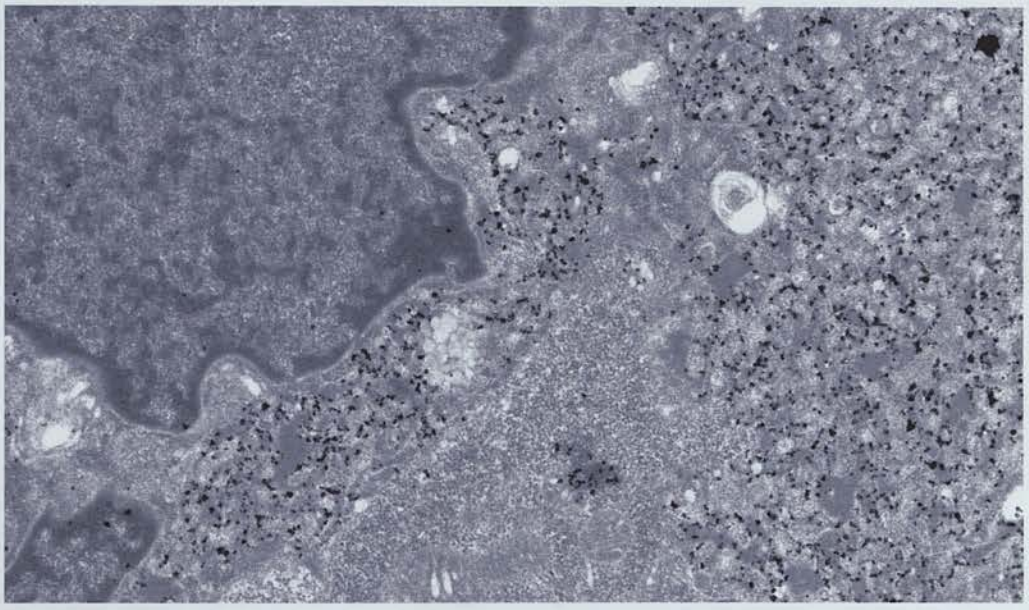

Figure 2.3b. x15K magnification. Terminally scrapie affected murine spleen. Immunolabelled with 1A8 anti PrP serum, 1nm Auroprobe immunogold and enhanced using Nanoprobe goldenhance technique. Considerably more immunolabelling is present than the serial section above.

3. RESULTS

3.1. Sub-cellular sites of prion protein accumulation in scrapie-infected mouse spleen

Introduction

In most experimental models, PrP^d is a reliable indicator of the presence of TSE infectivity (Diringer et al. 1983). Light microscopical studies have suggested that both PrP^c and PrP^d are associated with follicular dendritic cells (FDCs) (Kitamoto et al. 1991; McBride et al. 1992; Brown et al. 1999). Using immunogold electron microscopy, the aim of this project was to demonstrate sub-cellular accumulation of PrP^d in the spleens of C57Bl 70 days after i.c. infection with the ME7 strain of scrapie and at the terminal stage of disease (170 days). Following i.p inoculation, scrapie infectivity in the spleen is known to plateau at 70 dpi, however, no direct correlation can be made with the i.c. inoculated 70 day timepoint in this study. This timepoint was therefore extrapolated from i.p. inoculation data.

This study was undertaken to try and better understand the cellular origin and sub-cellular distribution of PrP^d in the spleen.

Light microscopical and Ultrastructural staining and immunolabelling procedures.

Mice were obtained from IAH – NPU in Edinburgh (see section 2.1.1). C57Bl mice were infected with an ME7 scrapie strain homogenate. An average of 40 spleen tissue blocks were taken from each of two scrapie-infected mice at day 70, and an average of 33 spleen tissue blocks were taken from each of three scrapie-infected mice at terminal stages of the disease (mean incubation period approximately 170 days following i.c. injection). From two age-matched (70 dpi) normal brain (NB) inoculated control mice, 70 blocks of spleen tissue were available for examination, while 90 tissue blocks were available from the NB inoculated control group at 170 dpi. At least 5 tissue blocks were studied from each animal. An average of three white pulp areas were present within each of the blocks studied.

Spleens were immersion fixed, processed and labelled as described in sections 2.2.1. – 2.2.7.

Light Microscopy

At terminal stages of disease, PrP^d was detected in the white pulp in of the majority of macrophage-like cells with open nuclei containing little nuclear chromatin (Figure 3.1.1), and showing multiple intense puncta of labelling adjacent to the nucleus. These cells were located throughout the white pulp and occasionally in red pulp immediately surrounding white pulp, in the mantle zones, and in both the dark and light zones of germinal centres. They were provisionally interpreted as TBMs. All germinal centres were affected.

Another cell type, also with marginated nuclear chromatin and presumptively identified as the FDC, showed a diffuse pattern of labelling adjacent to the nucleus, and in a pattern suggestive of cytoplasmic processes (Figure 3.1.1). These processes extended from the cell body.

Although more subtle, the patterns of PrP^d labelling at 70 dpi were essentially the same as terminally diseased spleens described above. No immunolabelling was seen in the red or white pulp of age-matched, normal brain inoculated controls.

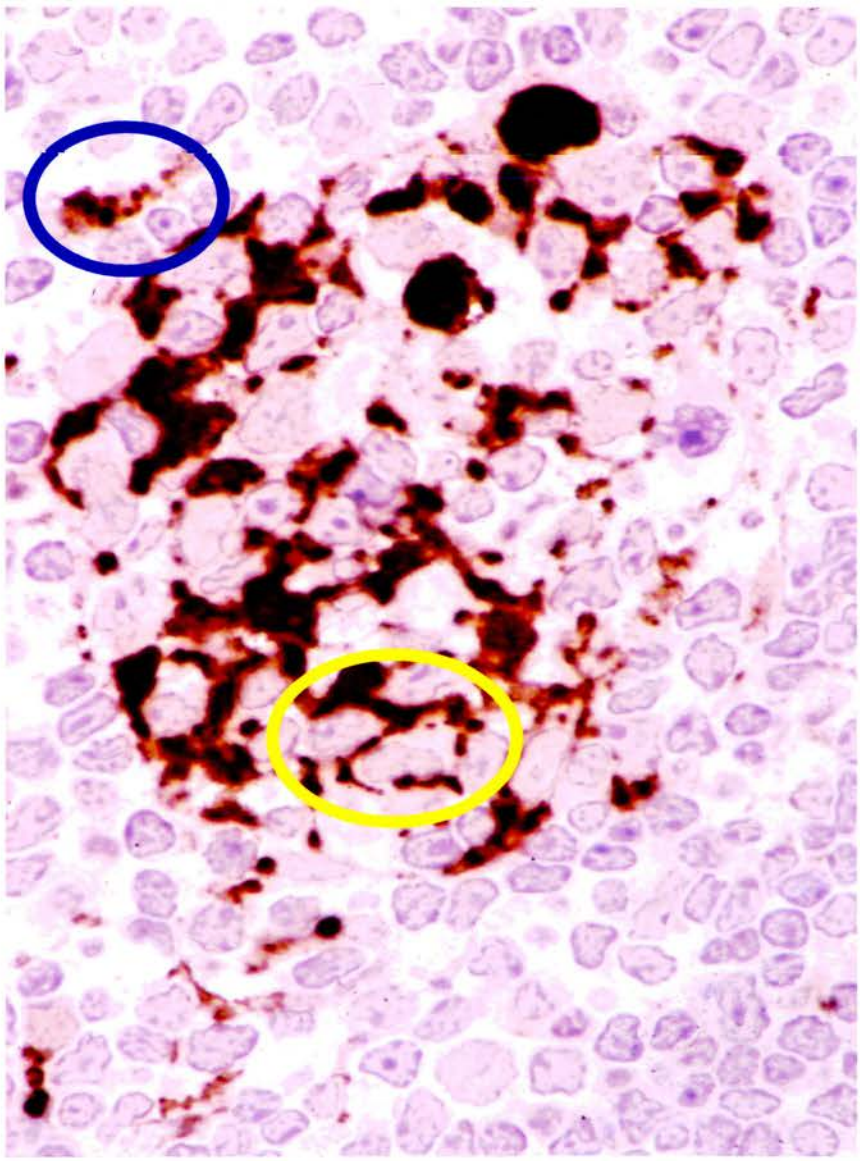

Figure 3.1.1. Resin embedded spleen (1 µm thick) from a terminally affected mouse. The germinal centre shows two types of PrP^d labelling. There is an interrupted linear pattern (yellow oval) and condensed granular pattern (blue oval).

Uninfected tissues: morphology and immunolabelling

Control tissues did not show any immunolabelling when examined by electron microscopy. In areas of white pulp directly adjacent to red pulp, small lymphocytes between which were small FDC filiform dendritic processes could be seen. At the centre of some areas of white pulp, secondary lymph follicles could be identified. These follicles contained FDCs that had highly irregular nuclei and were often bi-nucleate and occasionally multi-nucleate. The nuclei were clear with abundant euchromatin and a distinctive band of heterochromatin adjacent to the nuclear membrane. The perikaryonal cytoplasm was limited when compared with lymphocytes, and contained moderate amounts of cell organelles. Dendritic processes of mature FDC ran between germinal centre lymphoid cells. These processes were often extensive and sometimes formed small knots; occasionally, more complex arrangements of dendrites (labyrinthine glomerular complexes) were present. Where several processes ran between cells they were usually uncomplicated and ran in parallel straight or curved lines. No visible structural features were present between the plasmalemmae of adjacent dendrites. Only rare desmosomes were found joining two processes. In part of these follicles, lymphocytes were larger (the germinal centre light zone), and between them, arranged in small knots, were more complex branching processes (labyrinthine glomerular complexes) of FDCs (Figure 3.1.2). The processes were uncomplicated and associated with limited electron-dense deposits, held in a uniform curvi-linear manner between the plasmalemma of

adjacent dendrites. This electron-dense deposit formed an intermediate lamina between dendrites and was held at roughly 0.14 μm from each dendritic process.

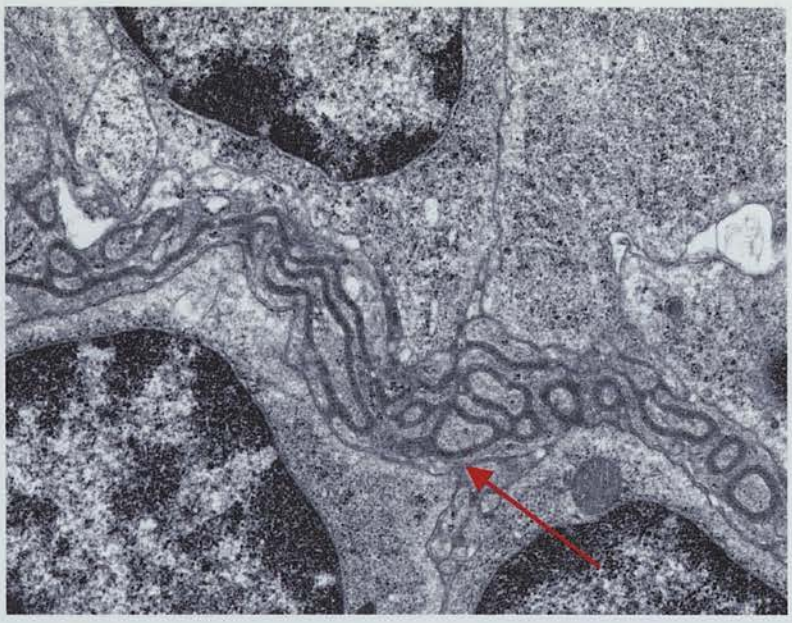

Figure 3.1.2. x17K magnification. FDC dendritic processes from an uninfected mouse spleen (arrow). Simple FDC processes run between lymphocytes. The associated electron-dense deposit is uniform and linear.

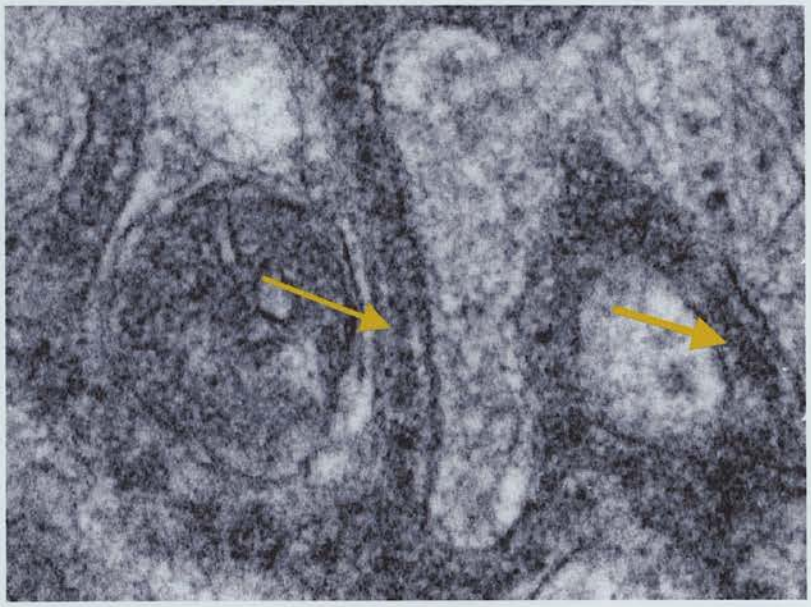

Figure 3.1.3. x50K magnification. Detail of labyrinthine glomerular complex from the spleen of an uninfected mouse. The extracellular space surrounding dendritic process plasmalemmae consists of an intermediate dense lamina (arrows), bound on either side by two less electron-dense zones. This assembly is of a consistent width.

The intermediate lamina itself was on average 0.18 μm in width. FDCs of a similar size and complexity were present in all control spleens (Figure 3.1.3).
TBMs, identifiable by their frequent lysosomes, abundant rough endoplasmic reticulum and open nuclei containing mainly euchromatin with a peripheral margin of heterochromatin, were identified in white pulp and less frequently in red pulp.

Scrapie-infected tissues: morphology and immunolabelling

In tissues obtained from ME7 infected mice at 70 dpi and at terminal disease, TBMs showed marked immunogold labelling for PrP^d within lysosomes (Figure 3.1.4). In some of these lysosomes, immunogold deposits were concentrated at one particular pole associated with a more electron-dense floccular material. Very occasionally, TBMs showed immunogold affinity for fibrillar structures within a lysosome. Only a proportion of TBMs were so labelled.

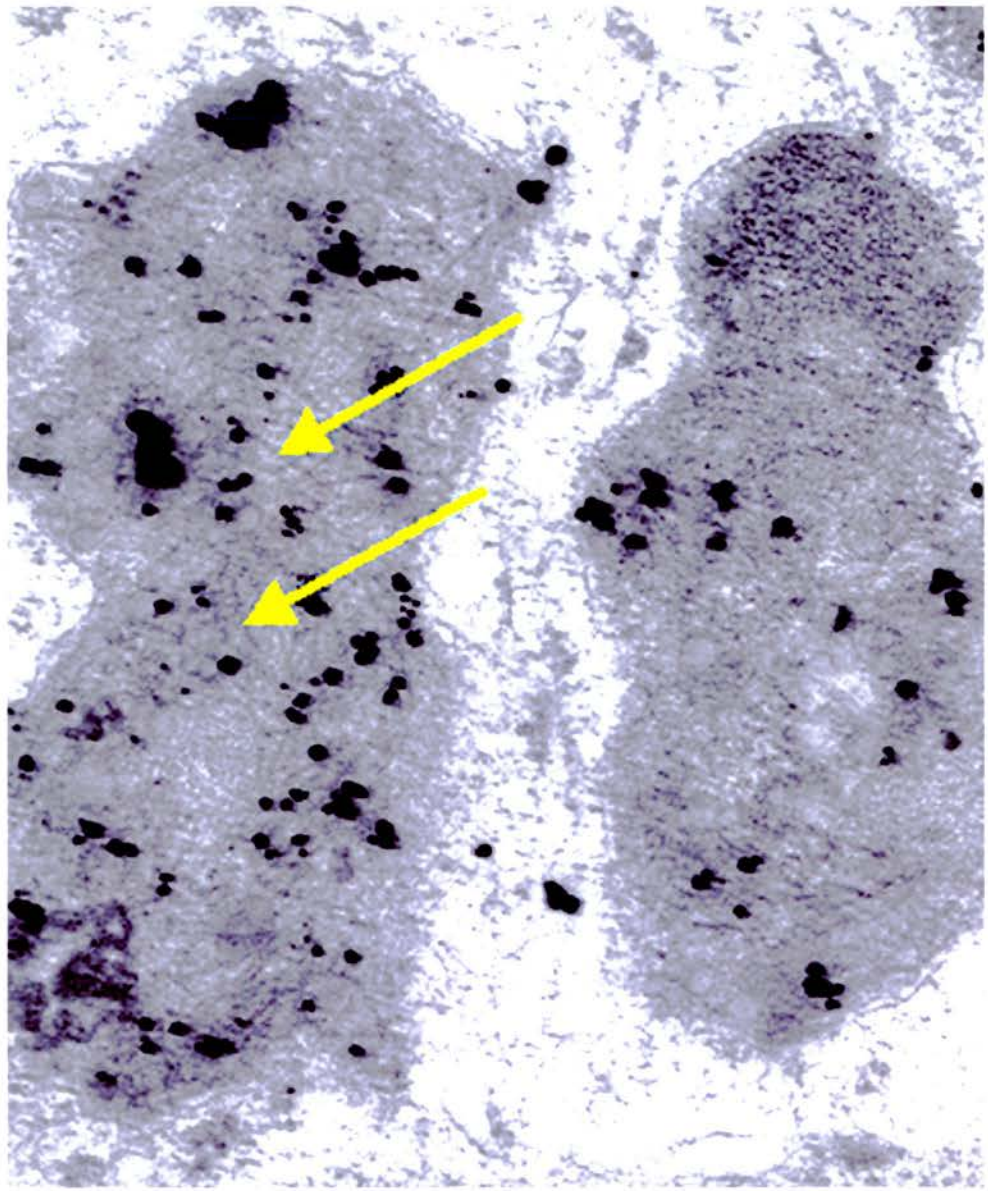

Figure 3.1.4. x54K magnification. Intralysosomal TBM immunolabelling within the spleen of a terminally diseased mouse. Short linear filamentous structures are present within one lysosome (arrows).

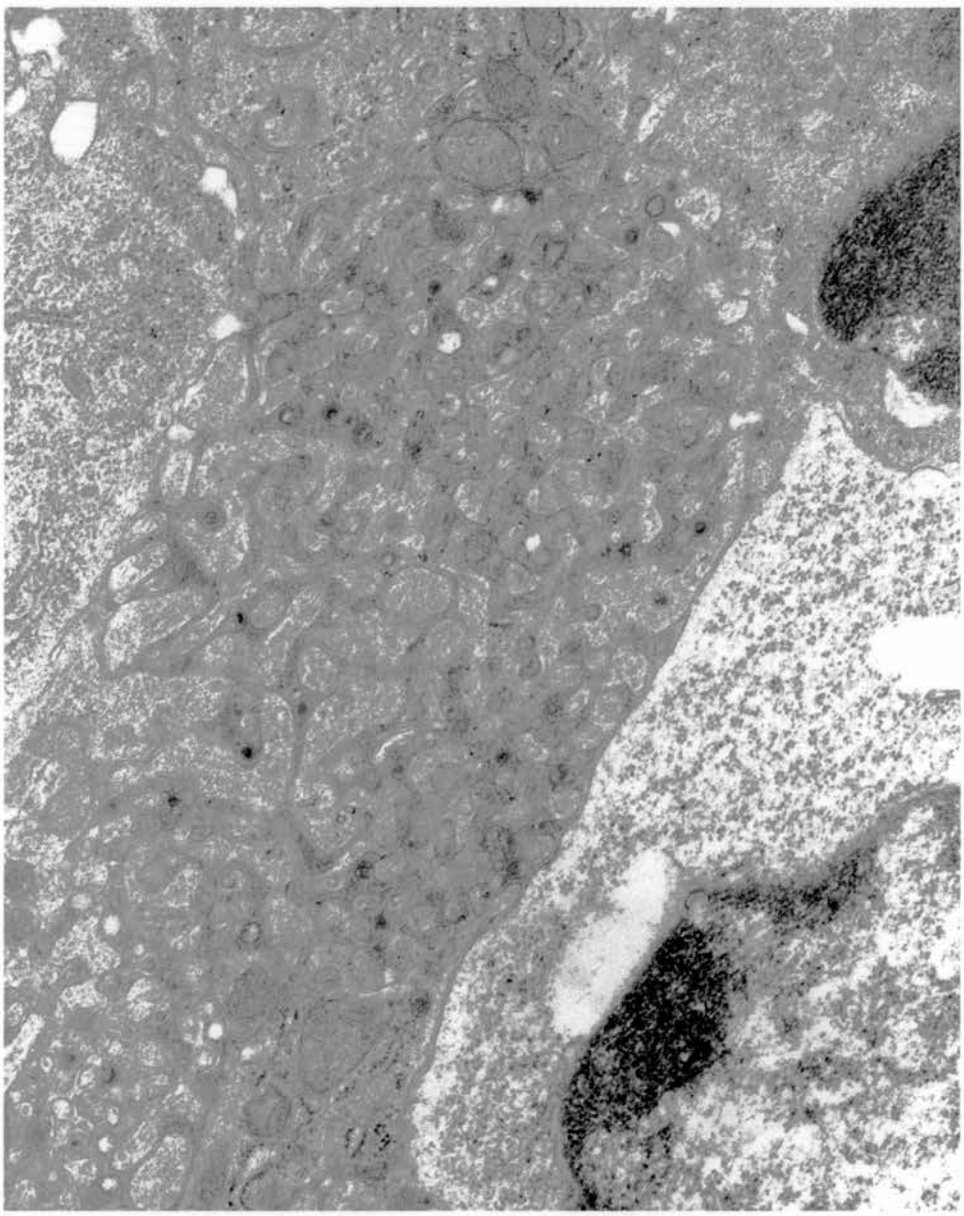

Figure 3.1.5. x28K magnification. Hypertrophic FDC labyrinthine complex from the spleen of a terminally diseased mouse. Dendrites are highly convoluted and abundant associated electron-dense deposit is present between dendritic profiles.

In addition to TBM labelling of secondary follicles containing mature FDCs, intralysosomal PrP^d labelling of macrophages was seen less consistently in the red pulp, mantle zone and PALS.

At both timepoints, immunogold / silver complex labelling was also associated with a second population of cells. These were characterised by a nucleus containing abundant euchromatin and marginal heterochromatin and complex hypertrophic branching processes (dendrites) which identified them as FDCs.

In the light zone of follicles obtained from spleens of clinically affected mice, the FDC dendrites invariably formed large and complex labyrinthine glomeruli, indicating a highly reactive response to stimulation. These were considerably larger, with more florid branching and interweaving of dendritic processes than in control tissues. Around each dendritic process, a significant margin of amorphous electron-dense material was present (Figure 3.1.5). This electron-dense deposit was abundant and irregular generally with the loss of the electron-dense lamina present in normal tissues.

At both the terminal stage of disease, and, to a lesser extent at 70 dpi, a proportion of immunogold labelling of both immature extended linear processes and mature labyrinthine glomerular complexes was not associated with areas where the amorphous electron-dense material situated between reactive FDC dendritic processes was abundant. At these points, PrP^d was seen to co-localise with the plasma membrane itself. Labelling intensity of dendritic plasmalemma and the complexity of branching of dendritic processes, increased in proportion to the amount of electron-dense material within the extracellular space (Figure 3.1.6a). This electron micrograph has been artificially coloured for ease of identification

(Figure 3.1.6b). These changes were more evident in terminally affected spleens when compared with the earlier stage of disease.

Immunolabelling of immature FDCs was rare in 70 day spleens and few mature hypertrophic FDCs expressing PrP accumulations were present at this timepoint. Most FDCs in the follicular light zones had relatively inconspicuous dendrites that formed small knots of labyrinthine complexes interspersed between lymphocytes, and, thus, were similar to controls. Any such processes had no obvious amorphous electron-dense deposit at the plasmalemma, although some electron-dense material was present around a minority of FDC dendrites.

Immunolabelling was generally weaker at the pre-clinical stage of disease, although PrP^d immunoreactive fibrils were located at both timepoints in the extracellular space around some large labyrinthine complexes (see figure 3.4.1.1). These fibrillar forms were seen within the extracellular space and generally involved the loss of the majority of membrane-associated electron-dense deposit. Fibrils were of approximately 20 nm diameter and from 40 to 300 nm long.

Coated pits were present at the surface of reactive FDC dendrites and adjacent lymphocytes (see Figure 3.2.7). They were observed in both control and scrapie-infected spleens, but numbers in scrapie-infected tissues were considered to be at least doubled. These pits did not co-localise with PrP^d accumulations.

Terminally differentiated plasmablasts with distended rough endoplasmic reticulum containing electron-dense material consistent with accumulation of globulins, were also present in the light zones of secondary follicles of all scrapie-infected tissues. These were often fully surrounded, or engulfed by PrP^d-expressing FDC dendrites.

This process will be referred to as "emperipolesis". At this terminal stage of differentiation, these cells are known as plasma cells (see Figure 3.2.8).

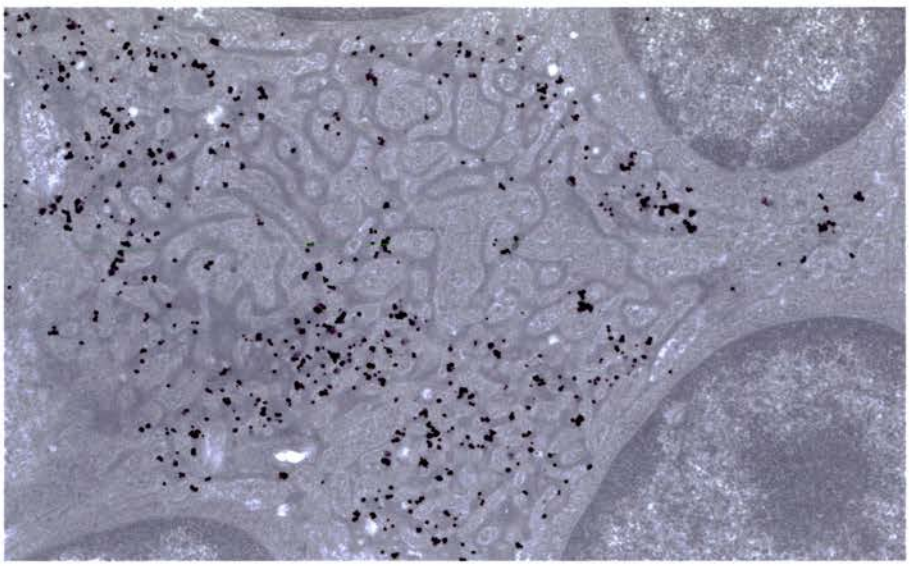

Figure 3.1.6a. x13K magnification. Hypertrophic FDC labyrinthine glomerular complex from the spleen of a terminally diseased mouse. PrP^d immunolabelling is clearly associated to a greater extent with the more convoluted dendritic extensions. Immunolabelling is sparse in areas where an intermediate dense lamina remains and excess electron-dense deposit has not accumulated.

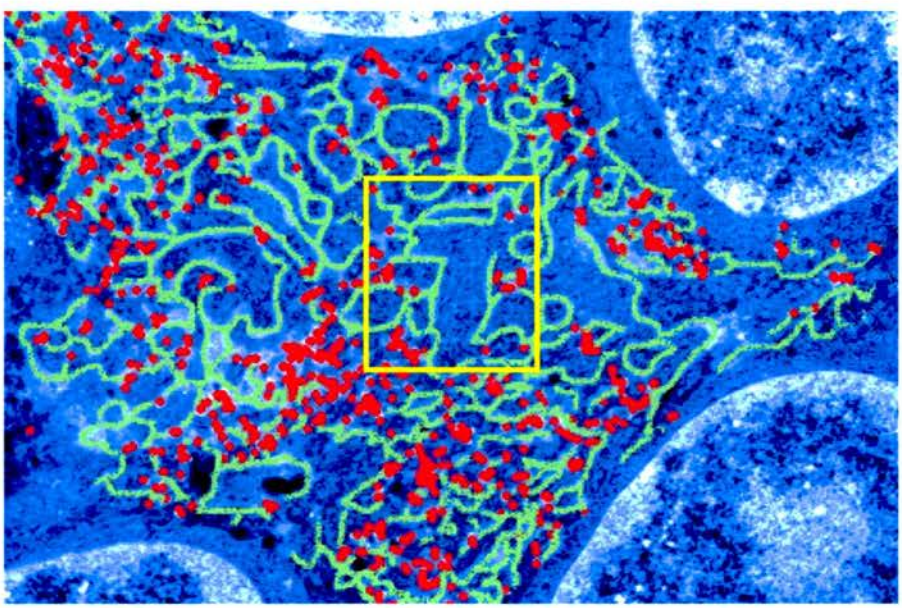

Figure 3.1.6b. Figure 6a has been digitally colourised to emphasise the lack of PrP^d immunolabelling (red), associated with the less convoluted dendritic profiles that lack electron-dense deposit accumulation (green). The area highlighted by the yellow rectangle shows limited dendritic complexity, which correlates with little PrP^d immunolabelling. The area immediately below this shows an abundance of PrP^d (red) immunolabelling and considerably more complex dendritic profiles

Discussion

These results confirm previous light microscopy studies showing that accumulations of PrP^d occur in the white pulp of spleen. Ultrastructural analysis revealed that PrP^d is associated with the plasmalemma of FDCs, and is localised intralysosomally within macrophages. FDCs in scrapie-infected tissues demonstrated an exaggerated or hypertrophic response to infection. Cell processes were elongated and considerably more complex, forming large glomerular structures within the secondary follicle, while electron-dense deposit previously presumptively identified as antigen / antibody complexes which associated with these processes, was more abundant in these tissues.

Although the antibody used does not distinguish between the protease-sensitive and protease-resistant isoforms of PrP, it may be anticipated that at least some of the PrP^d accumulations, particularly those in fibrillar forms, would be protease-resistant. In agreement with previous transmission and light microscopy studies (Brown et al. 1999), my observations do not suggest that PrP^d accumulation occurs within B-lymphocytes in ME7 scrapie-affected spleens (Klein et al. 1997).

During the development of germinal centres, FDC's lose the capacity to synthesise matrix elements, and begin to produce specific surface antigens. As increasing quantities of immune complexes are retained, imported by lymphoid cells or by other means, the surfaces of FDCs enlarge, form plicae, and dendrites develop. Immune complexes are bound to the cytoplasmic extensions (dendrites) of FDCs, where they may remain for weeks or months. The mechanism of antigen / antibody complex attachment was found to be the fixation of the antigen in the extracellular space to

adjacent FDC membranes via the complexed antibody attachment to FDC expressed C3b and Fc receptors (Bosseloir et al. 1995). These complexes are not endocytosed, but are held at the surface of the dendrite by receptors. Free antigens are not bound to the surface of FDCs. Antigen / antibody complexes serve to periodically re-stimulate B cells although many of the complexes are deep within the cytoplasmic invaginations of FDCs and not readily revealed to other cells.

In uninfected tissues, these antigen / antibody complexes form an ordered line or lamina equidistant from FDC dendritic process plasmalemma. The ordered binding of antibody / ferritin complex as an electron-dense line, within the dense material between adjacent FDC membranes has been previously described (Radoux et al. 1985a). This would suggest the lamina seen in the extracellular space surrounding normal uninfected FDC dendritic processes is a feature of the normal antigen / antibody complex binding mechanism. However, no normal lamina was associated with dendritic processes of FDCs in scrapie-infected tissues. Hypertrophic ME7-infected FDCs did not show the tri-laminar assembly indicative of normal antigen / antibody complex binding, but demonstrated an excess binding affinity for these complexes. These complexes are visualised in the form of dendrite-associated electron-dense deposit. Complex binding is greatly increased in these tissues suggesting that the normal immune complex trapping mechanism associated with normal FDC function has been disrupted in scrapie-infected animals, resulting in the loss of lamina and subsequent FDC hypertrophy. Thus, as previously described, the greater concentration of antigen / antibody complex in the extracellular space surrounding FDC dendrites and subsequent increased attachment of immune complexes to FDC plasmalemma, triggers FDC hypertrophy (Terashima et al. 1992;

Heinen et al. 1995a; Heinen et al. 1995b). Insofar as it is possible to determine the localisation of FDCs within the follicles of mice, immature FDCs similar in maturity to those found in the dark zone of the follicle of other species, were similar in controls and in infected mice. However, in presumed light zones all FDCs at terminal stages of disease and a proportion of FDCs at 70 dpi had large and highly complex labyrinthine glomeruli. This appears to represent an abnormal reactive or hypertrophic change of FDCs compared to controls.

Unlike the FDCs described by Rademakers et al. (1992) in which classification was based on both nuclear and dendrite morphology, unless otherwise specified, FDC in this thesis will be defined on dendritic appearance alone. FDCs will be deemed "mature" if inter-dendritic electron-dense deposits are observed, and dendritic profiles are considered to be extended. Immature FDCs have no accumulated electron-dense deposit and possess simple, unbranched dendritic profiles of limited length. Dendrites of mature FDCs extend for considerable distances from the cell body, interweaving between lymphocytes of the germinal centre. It is therefore often impossible to determine which dendrites extend from a specific cell body. For this reason, the above definitions will be used throughout this thesis. The term "immature" is used frequently to describe FDCs associated with some immunologically-altered models, for example SCID or TNF-null mice (Brown et al.1997; Mabbott et al.2002). These authors employ molecular tools for FDC classification, which do not directly correlate with those in this thesis.

Transmission studies using chimaeric mice in which some immune system cells carry the PrP gene and some do not, and light microscopy immunocytochemical studies of spleen and lymph nodes, suggest that mature FDCs accumulate PrP^{d}. Our sub-

cellular immunolabelling confirms that FDCs are associated with PrP^d accumulation. It could be observed that immunogold-labelled PrP^d is associated with the plasmalemma of dendritic processes and not electron-dense deposits which suggests that PrP^d remains membrane-bound and is not released into the extracellular space until stimulated to aggregate into a fibrillar form, as is also found in the brain (Jeffrey et al. 1994b). However, the mechanism for this change remains unclear. Where present, amyloid fibrils that are known to form from full-length PrP^d correlate with a marked reduction in excess antigen / antibody trapping. It is therefore possible that some PrP^d associated with the plasmalemma in scrapie-infected FDCs, is directly responsible for excess complex trapping.

The observations presented in this study indicate that there is an excess accumulation of electron-dense deposit at the FDC dendrite plasmalemma, increased complexity of FDC dendritic branching and accumulation of excess or abnormal PrP associated with scrapie infection. As attachment of immune complexes is the trigger for a marked increase in the complexity of dendritic processes, the pattern of dendritic branching and distribution of immunogold deposit in terminally diseased mice indicates that the FDCs were highly stimulated by either (or both) of the abundant or abnormal PrP, or by excess trapping of immune complexes. These findings suggest that PrP^d is involved in dendritic process elongation or in the process of trapping immune complexes.

In support of this hypothesis, accumulation of PrP^d associated with one cell type in scrapie-infected sheep lymph nodes and spleen, is co-localised with the cell surface marker CD 21 and is confined to the light zone of germinal centres (M. Jeffrey, personal observations). Only fully mature, process-bearing FDCs express CD21 in

the light zone. In the present study, at the terminal stage and to a lesser extent at 70 dpi, immunolabelling of FDCs with limited plasmalemma-associated electron-dense deposits suggest that early PrP^d accumulation may occur initially in the absence of antigen / antibody complex trapping. In the terminal stages of disease, more linear dendritic processes were associated with PrP^d, indicating infection of immature FDCs in the later stages of disease. This would suggest PrP^d accumulation precedes the follicular changes described.

TBMs ingest apoptotic cells, mostly B cells that are not selected to form clones of immunoglobulin-producing cells. However, they also scavenge the ends of FDC processes, and perhaps effete FDCs themselves (Smith et al. 1991). Intralysosomal PrP^d accumulation has also been seen within phagocytic cells of the CNS, including microglia, astroglia and Kolmer or epiplexus cells. TBMs may be ingesting excess or abnormal PrP. It is unclear whether this is the result of phagocytosis of entire degenerate FDCs or their processes or merely by scavenging the extracellular space. TBMs containing intralysosomal PrP^d were found adjacent to PrP^d accumulation associated with FDCs and as individual labelled cells distant from other foci of PrP^d immunoreactivity. In terminally diseased animals, the presence of intralysosomal PrP^d labelling of macrophages outwith the germinal centre suggest that these cells play an important role in the transportation of infectivity away from the secondary follicle.

All known amyloids are formed within the extracellular space from precursor proteins and therefore, as some macrophages possess intralysosomal filaments consistent with amyloid, these at least would presumably have been internalised to the macrophage from the extracellular space around FDCs.

In the present study it has also been observed that scrapie-infected FDCs are associated with the abnormal retention and maturation of B cells within the secondary follicle (refer to plasmablast discussion, results page 73). If scrapie infection of FDCs induces abnormal antigen / antibody trapping, the presentation of these immune complexes to B cells may also occur abnormally or in excess, thus inducing the prolonged retention of B cells within the secondary follicle. It is generally accepted that FDCs shed part of their cell membrane and associated immune complex (ICCOSOME), which then binds to B cell surface immunoglobulins before being internalised (Szakal et al. 1988). During this process, the FDC creates an enclosed environment that allows B cells to be selected based on the affinity of their receptors for the antigen retained by the FDC. Perhaps the release of immune complexes from the plasmalemma of FDCs exhibiting PrP^d accumulations is somehow impaired. Thus the emperipolesed B cell is not stimulated adequately, no immune complex is internalised, and the cell is unable to be released from the stimulating FDC. This might be due either to the alteration of the mechanical FDC binding to the B cell itself via the immune complex, or the lack of internal signal by the B cell to leave the secondary follicle. In support of this hypothesis, plasma cell PrP^d accumulation has not been observed.

At this stage, coated pit activity associated with FDC hypertrophy is also upregulated. The reason for this increased pit activity remains unclear, however, it can be hypothesised that although coated pits do not directly associate with the PrP^d, they may still relate indirectly to disease pathology. It has been noted that in purified preparations of coated pits from the brain, PrP^c co-localises with these structures (Harris 1999). In diseased animals, normal PrP might be upregulated resulting in

increased endocytic trafficking, however, this has to date, not been tested. Alternatively, coated pits might be attempting to remove abnormal PrP from the cell surface or plasmalemma. Abnormal increased frequency of coated pits also occurs in scrapie-infected brain tissue (Ersdal et al. 2003).

Disruption of the normal immune complex binding mechanism and cellular PrP^c-trafficking, increased plasma cell retention within the secondary follicle and infection of immature FDCs in the later stages of disease, all suggest a basic pathology and possibly an alteration to immune system output, occur within scrapie-infected tissues. It has previously been demonstrated that some scrapie infections upset the control of IgG production, as increased amounts of IgG have been detected in cerebrospinal fluid (CSF) of sheep, and serum of scrapie affected mice (Collis et al. 1979; Collis & Kimberlin 1983; Collis & Kimberlin 1989). However, what remains unclear is whether the pathological effects and possible alteration to normal immune function observed here are all scrapie-specific, or whether immune challenge from any antigen could cause these sub-cellular reactions. In order to test the hypothesis that scrapie alone causes these abnormal changes, normal mice must be antigenically challenged and the splenic ultrastructure analysed for the presence of morphologic and immunologic changes.

3.2. An ultrastructural study of the morphological changes associated with immune challenge in scrapie-infected mouse spleen.

Introduction

In the previous chapter, the experimental design rendered it impossible to determine whether pathological responses described were specific to scrapie infection, or were simply a part of the normal or exaggerated or otherwise altered immunological response to antigenic stimulation in a scrapie-affected mouse. To help discriminate between these possibilities, we immunologically stimulated scrapie-infected and scrapie-uninfected mice, and examined the tissue response. As before, immunogold labelling was used to determine the sub-cellular localisation of PrP^d in scrapie-infected and uninfected tissues, with and without immune stimulation.

Light microscopical and Ultrastructural staining and immunolabelling procedures.

Mice were obtained from IAH – NPU in Edinburgh (see section 2.1.2). ME7 scrapie was administered i.p, and is known to give a mean incubation period of 270 days. One group of ME7 infected, and one group of NB mice were given one immunization of SRBC or saline followed by a boost 21 days later (approximately 63 days post infection (dpi)). A duplicate set of mice were challenged with SRBC or saline at 240 dpi, and were given one immunization of SRBC or saline followed by a boost 21 days later (approximately 261 dpi) (see table 2.1). These mice were allowed to become terminally diseased. Spleens were immersion fixed, processed and labelled as described in sections 2.2.1. – 2.2.7. From each experimental group, at least 5 tissue blocks containing white pulp areas were studied.

Results

Light Microscopy

At both 70 dpi and terminal stages of disease, morphological examination indicated that reactive germinal centres were more abundant in scrapie and scrapie / sheep red blood cell (SRBC) challenged spleens than in the corresponding NB and NB / SRBC inoculated controls at these timepoints. The germinal centres from scrapie-infected tissues showed PrP^d labelling mainly within the secondary follicles, though some TBM labelling was seen at the periphery of follicles. The intensity of immunolabelling in the terminally diseased spleens was considerably greater than in the 70 dpi spleens, with most follicles showing extensive PrP^d accumulation of a magnitude similar to that seen in Figure 3.1.1. PrP^d immunolabelling provisionally identified as TBM labelling, was also detected in the red pulp, mantle zone and PALS of ME7 infected tissues. No immunolabelling was seen in spleens of age-matched normal brain inoculated control mice, with or without immune stimulation.

Electron Microscopy

Uninfected tissues: morphology and immunolabelling

Tissues from normal brain homogenate inoculated mice and normal brain homogenate inoculated mice treated with SRBC demonstrated very similar ultrastructural morphology. When examined by electron microscopy, follicles of

uninfected tissues contained FDCs at various stages of maturation. Mature FDCs were confined to the secondary follicle. The ultrastructural morphology of uninfected murine splenic tissue is described in detail in section 3.1. FDCs of a similar size and complexity were observed in all control and immune stimulated uninfected spleens. Within the secondary follicles, some FDCs appeared less mature as they had more rounded, mono-nuclei and poorly developed processes. In contrast to other species such as sheep and humans, lymphocytes within the germinal centre of rodents are only slightly larger and paler than those outwith this area. This effectively means that distinguishing between the light and dark zones in rodents is difficult using morphological parameters alone (Steiniger & Barth 2000). The location of the immature FDCs relative to the dark and light zones was therefore not determined. Numerous TBMs, with phagocytosed nuclear remnants in their cytoplasm and containing abundant lysosomes, were present within secondary follicles. Occasionally whole degenerate (presumed apoptotic lymphocytes) cells were found within the cytoplasm of these macrophages. Most lymphocytes showed little or no evidence of differentiation within the light zone of the secondary follicle. Only rarely did lymphocytes show signs of early B cell differentiation. These cells had distended, oval or rough endoplastic reticulum (RER) containing floccular material. In the mantle and PALS, occasional lymphocytes showed even more recognisable differentiation towards plasma cells. Such cells had numerous cisternae of widely distended RER containing an amorphous electron-dense material (presumed immunoglobulins). No PrP^d immunolabelling was detected in these tissues.

Infected tissues: morphology

In tissues obtained from all terminally affected ME7 groups, the majority of dendritic processes of FDCs within secondary follicles formed large labyrinthine glomerular structures. These were estimated to be in the order of 10 to 20 times larger in diameter than those of control tissues, with more florid branching and interweaving of dendritic processes. The space between dendrites was markedly increased, and contained an electron-dense material that apparently obliterated the intermediate electron-dense lamina described in normal tissues. In some parts of hypertrophic labyrinthine glomerular complexes the membrane associated electron-dense deposit was not abundant, or was absent. Where the electron-dense material was limited, the space between dendritic processes remained relatively constant. In these areas, the intermediate electron-dense line could clearly be seen (see Figure 3.1.3). In yet other FDC dendritic complexes, there was no abnormal electron-dense deposit and the size and frequency of branching of dendrites was similar to that of controls. This was more frequently the case in 70 dpi-infected mice that showed a similar yet more restricted FDC response. The complexity of branching of dendritic processes, and the abundance of extracellular electron-dense material were directly proportionate: less complex branching of dendrites correlated with less electron-dense material. In some of the highly hypertrophic labyrinthine glomerular complexes there was a reduction in electron density of the material in the extracellular space around the dendrites. Within these areas were short, usually single fibrillar structures though occasionally small groups of randomly oriented fibrils were also seen (Figure 3.2.1).

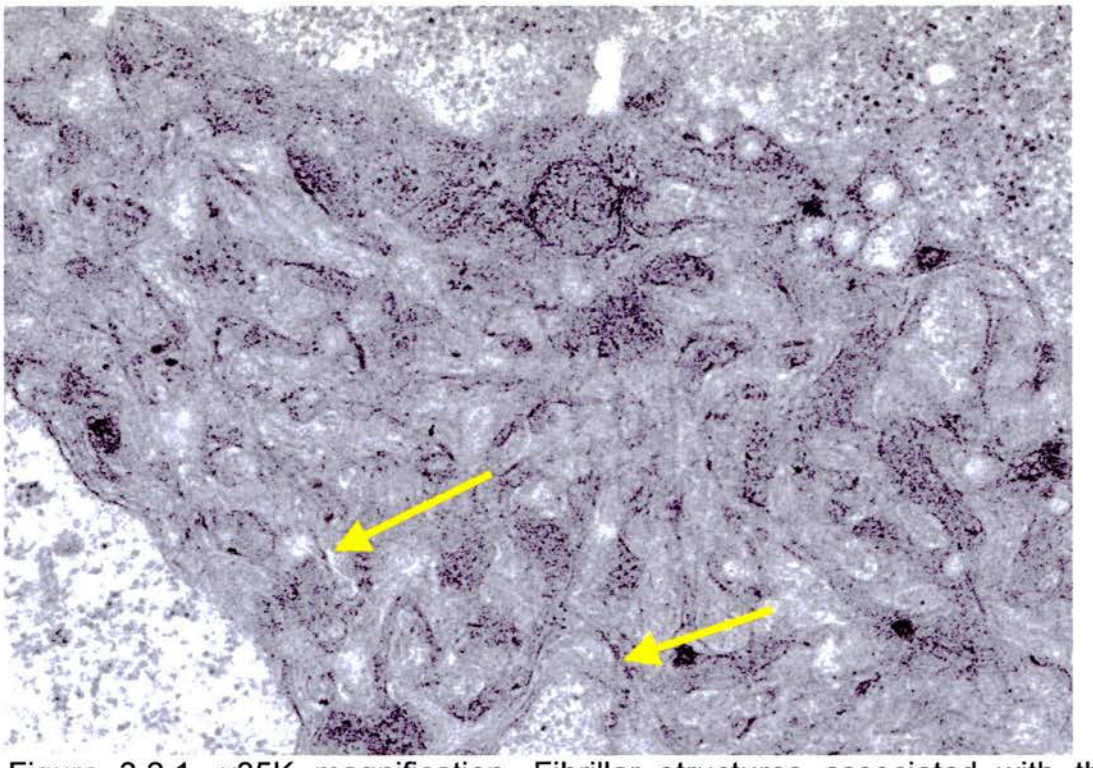

Figure 3.2.1. x35K magnification. Fibrillar structures associated with the spleen from a terminally affected mouse treated with SRBC. Fibrillar structures (arrows) are present in the expanded extracellular space surrounding mature FDC dendritic profiles.

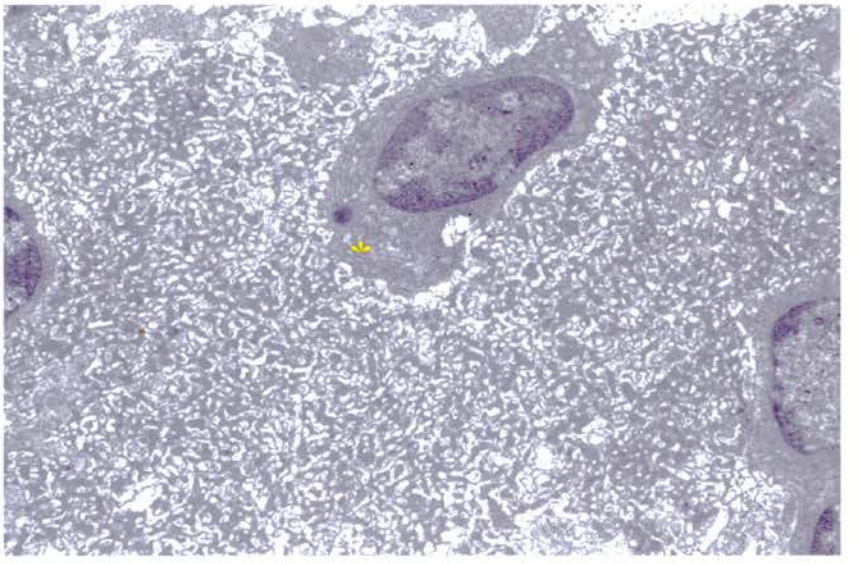

Figure 3.2.2. x8K magnification. Hypertrophic FDC complex from the spleen of a terminally affected mouse treated with SRBC. A markedly hypertrophic FDC labyrinthine complex with highly convoluted dendrites and abundant associated electron-dense deposit is shown. Embedded within the hypertrophic dendrites is a differentiating plasmablast (asterisk), which is dwarfed by the hypertrophic FDC complex.

When compared with terminally diseased ME7 infected tissues, both the overall size of the hypertrophic labyrinthine glomerular complexes, and the amount of extracellular material between labyrinthine glomerular complexes were increased in SRBC challenged ME7 infected mice (Figure 3.2.2).

In both terminally diseased and SRBC boosted terminally diseased tissues, TBMs of secondary follicles contained abundant lysosomal compartments. Apoptotic cells were occasionally seen within these compartments, including B-lymphocytes with distended RER. Similarly sized TBMs were observed in 70 dpi-infected spleens. Well-differentiated plasmablasts with distended RER containing moderate electron-dense material, presumed to be globulins, were present in the secondary follicles of both ME7 and ME7 SRBC boosted tissues. They were frequently surrounded or emperipolesed by FDC dendritic processes. Less mature B cells still with distended RER were found in the secondary follicles of scrapie-infected animals. The differentiated B cells were generally more abundant in all scrapie-infected tissues than in either of the control groups.

Coated pits and vesicles were observed in all experimental groups, but these structures were considerably more numerous in ME7 infected tissues. Up-regulation was primarily confined to the plasmalemma of reactive FDC dendrites, although pits were also observed less frequently at the cell surface of lymphocytes, adjacent to infected FDCs. Infected FDCs at 70 dpi showed similar coated pit up-regulation.

Infected tissues: immunogold labelling

Immunogold labelling of both immune stimulated and unstimulated ME7 mice was associated with FDC dendritic plasmalemma of both immature extended linear processes (Figure 3.2.3), and mature labyrinthine glomerular complexes. Where the immunogold / silver reaction product was of a sufficiently small dimension, labelling was generally associated with the plasma membrane itself. Only a minority of the reaction product was found within the electron-dense material of the extracellular space. This was conspicuous in the SRBC challenged animals where the extra-cellular electron-dense material was particularly abundant between separated adjacent FDC dendrites making the distinctions between plasmalemma-associated PrP^d and PrP^d accumulation in electron-dense material more readily apparent (Figure 3.2.4). Within the extracellular space surrounding some FDC labyrinthine glomerular complexes, immunolabelled short fibrillar forms were observed.

Although immunolabelling of hypertrophic labyrinthine glomerular complexes was identical in both 70 dpi and terminal spleens, subtle differences in the distribution of immunogold labelling occurred in respect of immature FDCs and smaller groups of dendrites. At 70 dpi, all PrP^d accumulations were restricted to mature hypertrophic FDC glomeruli, with no PrP^d accumulations associated with smaller dendritic knots.

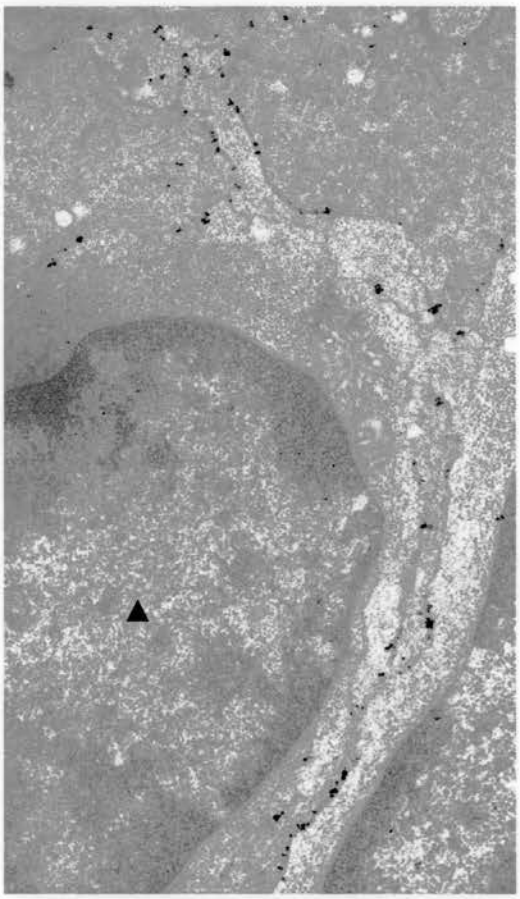

Figure 3.2.3. x16K magnification. Immunolabelled immature FDC profiles from the spleen from a terminally affected mouse treated with SRBC. A lymphocyte emperipolesed by FDC dendrites is shown at ▲. Immunolabelling is associated with the plasmalemma of dendritic processes. There is no electron-dense material surrounding simple FDC dendrites.

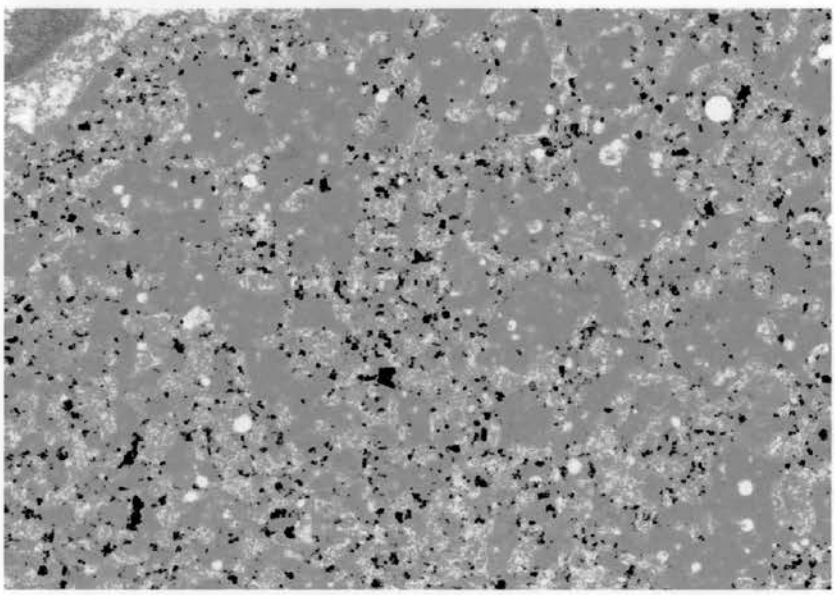

Figure 3.2.4. x17K magnification. Immunolabelled spleen from a terminally affected mouse treated with SRBC. Detail of a hypertrophic FDC complex. Immunogold PrP^d labelling is primarily associated with the plasmalemma of dendrites and not the adjacent electron-dense deposit. The abundant amorphous electron-dense material is unstructured and lacks an intermediate dense lamina.

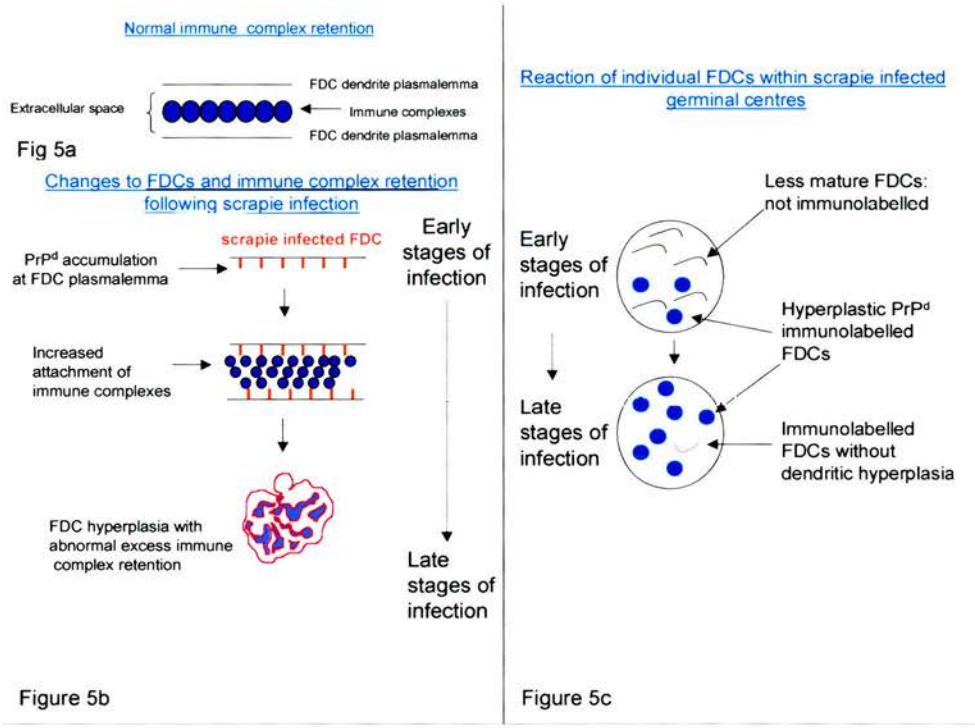

Figure 3.2.5. Schematic diagram showing relationship between immune complexes and FDC in normal and scrapie-infected mice.

Figure 3.2.5a. Antigen / antibody complexes (blue circles) are held in the extracellular space at a regular interval between FDC dendrites.

Figure 3.2.5b. Following scrapie infection, abnormal PrP (PrP^d) accumulates at the surface of FDC dendritic plasmalemma. This is associated with increased extracellular electron-dense material (presumptively immune complexes) and FDC hypertrophy.

Figure 3.2.5c. At early stages of infection, few FDCs within a germinal centre / secondary follicle show evidence of PrP^d accumulation. However, where PrP^d accumulation is found, evidence of hypertrophy is present. In contrast, at late stages of disease, almost all FDCs show PrP^d accumulation. Most of these are hypertrophic but occasionally PrP^d can be found at the plasmalemma of unreactive FDCs.

Where labelling occurred it was invariably associated with more abundant amounts of electron-dense material. At the terminal stage of disease, very few FDCs did not form hypertrophic complexes. However, immunolabelling was found at the plasmalemma of dendrites of rare immature FDC dendrites, where no intermediate lamina was present and no extracellular electron-dense material was formed. These observations suggest a progression of events illustrated schematically in Figure 3.2.5.

Large TBMs containing many apoptotic bodies within their lysosomes, were more frequently observed within the secondary follicle of scrapie-infected groups than in both the NB and NB / SRBC immunized control groups. In addition to TBM labelling of secondary follicles, intralysosomal PrP^d labelling of TBMs was seen in the red pulp, mantle zone and PALS of both immune-stimulated and unstimulated terminally infected ME7 mice (Figure 3.2.6). In some cases, PrP^d accumulations appeared to associate with dense floccular material within lysosomes.

Intralysosomal PrP^d labelling of TBMs was not seen outwith the secondary follicle in pre-terminal tissues.

As described above, coated vesicles and pits were more abundant in scrapie-infected tissue groups. However, immunolabelling did not associate with these structures (Figure 3.2.7).

Transformation of B lymphoblasts into plasmablasts and differentiated plasma cells was associated with immunolabelled emperipolesing PrP^d expressing FDC dendrites. An association between lymphocyte emperipolesis and PrP^d immunolabelling could also be seen within areas of the follicle where labyrinthine glomerular complexes were not observed. A full range of differentiating B cells could be visualised within the follicle of all scrapie-infected groups, from undifferentiated lymphocytes to fully

mature plasma cells (Figure 3.2.8). Less mature B cells, still with distended endoplasmic reticulum similar to the maturity seen at the bottom of figure 3.2.8, were found in the secondary follicles of both control and scrapie-infected animals; however, B cells were generally more prolific in scrapie-infected tissues.

	70dpi				Terminal			
	Norm	Norm SRBC	ME7	ME7 SRBC	Norm	Norm SRBC	ME7	ME7 SRBC
FDC hypertrophy	-	-	++	++	-	-	+++	++++
Increased electron-dense deposit accumulation	-	-	++	++	-	-	++	+++
PrP^d labelling of immature FDCs	-	-	-	-	-	-	+++	+++
Coated pit activity	+	+	++	++	+	++	+++	+++
Lysosomal TBM labelling	-	-	++	++	-	-	+++	+++
Increased follicular B cell maturity	-	-	++	++	-	-	+++	+++

Table 3.2.1. Nature and frequency of the morphological changes in each of the four groups.

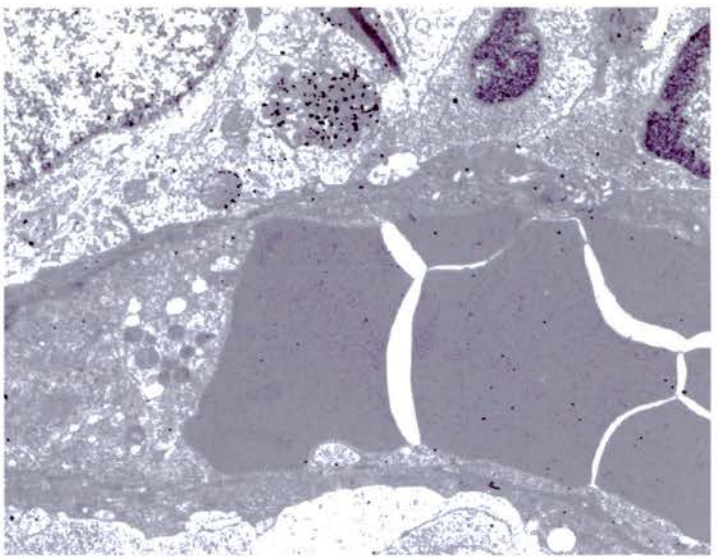

Figure 3.2.6. x8K magnification. Immunolabelled spleen from a terminally affected mouse treated with SRBC. Lysosomal TBM labelling is seen in the red pulp adjacent to a capillary containing erythrocytes.

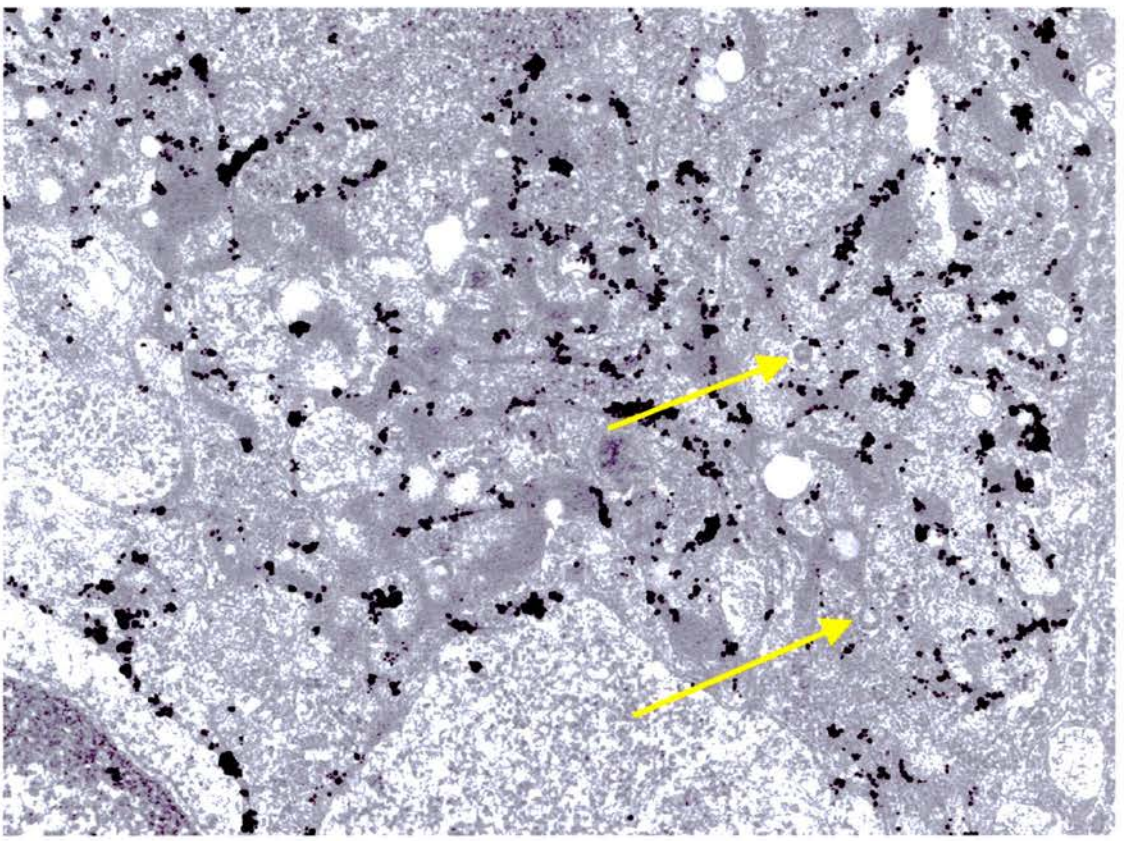

Figure 3.2.7. x22K magnification. Immunolabelled spleen from a terminally affected mouse treated with SRBC. Numerous coated pits are associated with FDC dendritic profiles (arrows), but are not associated with immunogold labelling. Immunogold plasmalemmal PrP^{d} labelling is present both in areas with and without excess electron-dense deposit.

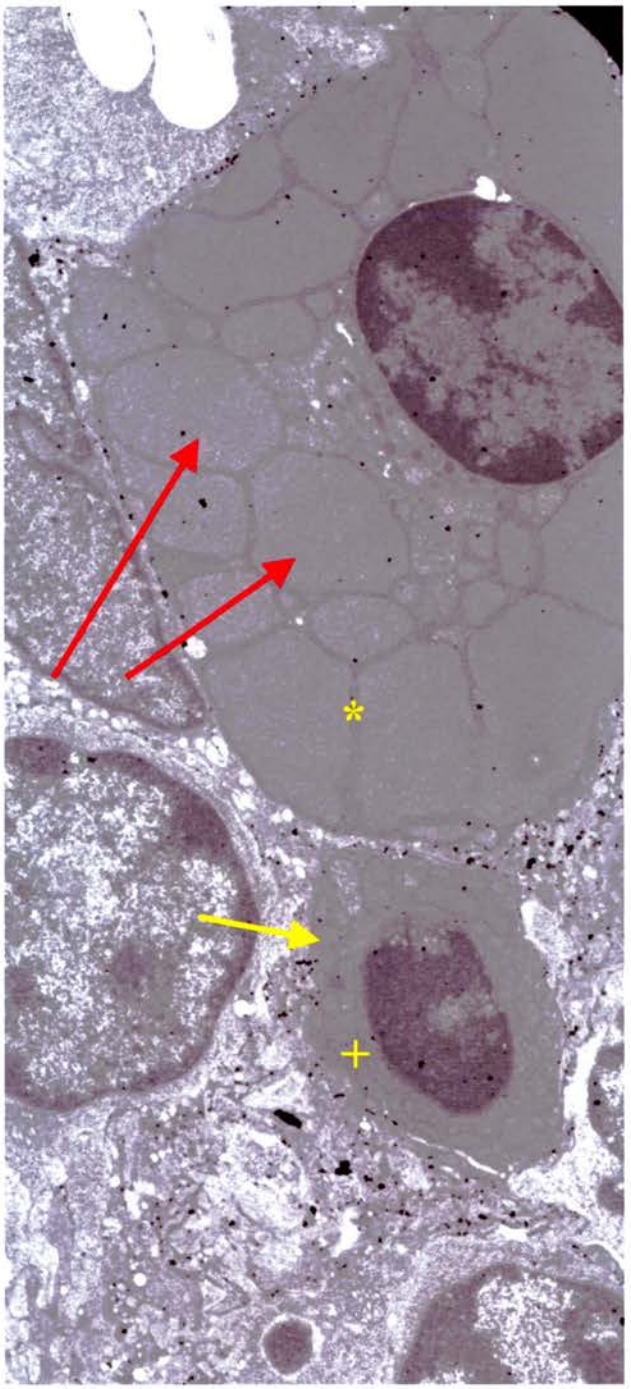

Figure 3.2.8. x9K magnification. Immunolabelled spleen from a terminally affected mouse treated with SRBC. Two differentiated B cells emperipolesed by PrP^d accumulating FDC dendrites are shown. The B cell indicated by an asterisk is terminally differentiated and shows endoplasmic reticulum organised into globulin-producing compartments (red arrow). The B cell indicated by a cross is less mature, with distended rough endoplasmic reticulum (yellow arrow).

Discussion

Following on from initial investigations described in section 3.1, this study confirms that the pathological changes observed within the spleen, previously hypothesised as a specific response to scrapie infection, are not present following SRBC antigenic challenge and are therefore likely to be scrapie-specific.

All scrapie-infected tissues studied, whether or not challenged with SRBCs, demonstrated an exaggerated or hypertrophic response of FDC dendrites within germinal centres. Cell processes were elongated and considerably more convoluted, forming large glomerular structures within the secondary follicle, while an electron-dense deposit accumulated around and between these processes. Both the accumulated electron-dense material and the hypertrophic FDC glomerular responses were more conspicuous in the scrapie / SRBC challenged animals than those infected with ME7 scrapie alone.

In uninfected tissues, an ordered electron-dense line or lamina, equidistant from FDC dendritic process plasmalemma, could be seen within extracellular electron-dense deposit. This line was visualised as a tri-laminar assembly in conjunction with two FDC plasmalemmal membranes. As discussed in the previous section, antibody / ferritin complex binds to adjacent FD plasmalemmae in the form of a line, equidistant between adjacent FDC membranes (Radoux et al. 1985a). The mechanism of antigen / antibody complex attachment was later shown to be the fixation of the antigen in the extracellular space to adjacent FDC membranes via the complexed antibody attachment to FDC receptor molecules C3b and Fc (Bosseloir et al. 1995). This would suggest the electron-dense lamina seen in detailed electron

micrographs of the extracellular space surrounding normal uninfected FDC dendritic processes is the site of normal antigen / antibody complex binding.

The extracellular space around hypertrophic ME7 infected FDCs did not show the tri-laminar assembly indicative of normal antigen / antibody complex binding, but demonstrated an abundant electron-dense material within the extracellular space. Because of its location and similarities in the electron density of the intermediate dense line, I suggest that this is representative of accumulated antigen / antibody complexes, although the exact nature of these complexes is yet to be determined. An abnormal or excessive antigen / antibody complex trapping by FDC dendrites with a subsequent breakdown of the normal binding and structural relationships between antigen-antibody complex receptors is therefore implied by the presence of abnormal amounts of this extracellular electron-dense material. The amount of FDC hypertrophy, and extracellular electron-dense material was greater in SRBC challenged ME7 infected animals when compared with mice infected with ME7 alone. It has previously been shown that the triggers for FDC process extension are an increased concentration of antigen / antibody complexes in the extracellular space surrounding FDC dendrites, and the subsequent attachment of these complexes to FDC plasmalemma (Terashima et al. 1992; Heinen et al. 1995). Thus, the increase in FDC hypertrophy and assumed immune complex attachment in SRBC boosted scrapie-infected tissues may simply be due to an increase in available antigens and complexes.

In the present study, I have noted changes that suggest scrapie infection perturbs the processes of B cell maturation and development. In the normal situation, antigen / antibody complexes retained at the surface of FDCs, and the presence of

$CD4^+$ T-lymphocytes are initial requirements for the formation of a germinal centre follicle. Where primed circulating B cells recognise their cognate antibody held at the surface of FDCs they cease their cycle of recirculation, proliferate and hypermutate. Many hypermutated B cells (centrocytes) are immediately destroyed by apoptosis, but B cells with improved antigen binding affinity of their surface immunoglobulins survive. Interaction with $CD4^+$ cells results in affinity maturation of the immunoglobulin produced by centrocytes. Some centrocytes become memory B cells; others join the pool or recirculating lymphocytes, while others migrate into body tissues where they further differentiate into long-lived antibody-secreting plasma cells.

Increased numbers of plasmablasts, and morphologically mature plasma cells were observed to be present within the germinal centre of scrapie-infected spleens when compared with controls. In addition there is an increase in the number of TBMs containing large amounts of apoptotic debris (presumed apoptotic B cells).

I therefore suggest that scrapie infection leads to an increase in the number of B cells that are selected for hypermutation. Although many of these will undergo apoptosis, many continue to survive and are retained beyond the normal states at which they would migrate from the germinal centre. If scrapie infection induces FDC hypertrophy and subsequent abnormal antigen / antibody trapping by facilitation of the C3b or Fc receptor binding or by impairing the release of transiently attached immune complexes, the presentation of these immune complexes to B cells may also occur abnormally or in excess, thus inducing the prolonged retention of B cells within the secondary follicle. During this process, the FDC creates an enclosed environment that allows B cells to be selected based on the affinity of their

immunoglobulins for the antigen retained by the FDC. It can be hypothesised that the release of immune complexes from the plasmalemma of FDCs from scrapie-infected spleens is somehow impaired. Thus the emperipolesed B cell is unable to be released from the stimulating FDC. Whether these morphologically mature B cells are in fact secreting antibody was not tested in the present study.

At all stages of ME7 infection in mice, with and without SRBC stimulation, increased numbers of coated pits and vesicles are found in association with FDC hypertrophy. The reason for this increased coated pit activity remains unclear, however, it can be hypothesised that although coated pits do not directly associate with the disease-specific form of PrP, they may still relate indirectly to disease pathology (Harris 1999). Immunogold labelling was found at the plasmalemma of FDC dendrites and in adjacent associated extracellular space, on extracellular fibrils and in lysosomes of TBMs. As in the previous study, the intensity of immunolabelling is increased in proportion to the tortuosity of process convolutions, complexity of branching of dendrites and the amount of extracellular electron-dense material. In the present study a smaller size of immunogold reaction product allows for the localisation of the majority of FDC associated PrP^d to the plasmalemma of dendrites within labyrinthine glomerular complexes. That most immunogold labelled PrP^d associates with the plasmalemma of dendritic processes and not electron-dense deposit suggests PrP^d remains membrane-bound and is not released into the extracellular space. A minority of extracellular PrP^d is located within the extracellular space around FDC dendrites, mostly visualised on fibrils. These FDCs are conspicuous not only by the increased amount of fibrils within the extracellular space, but also by the lack of membrane associated electron-dense deposit and highly

convoluted dendritic profiles. The mechanism or sequence of events leading to PrP^d aggregation, complex release and increase in dendrite complexity remains unclear. These findings suggest that PrP^d is initially attached to the FDC membrane until released or otherwise stimulated to aggregate and form fibrils.

The amounts of extracellular electron-dense material, dendritic hypertrophy and tortuosity and plasmalemmal PrP^d are directly proportional to each other. However, in terminally diseased mice, some immature FDCs that lack any intermediate dense lamina between FDC dendrites, or in some cases lack any extracellular electron-dense material, show PrP^d accumulation at the plasmalemma. The accumulation or presence of PrP^d at the plasma membrane would appear to precede pathological change. As both the accumulation of electron-dense material (presumed immune complexes) and hypertrophy of FDCs are considered to be the sequel to increased immune complex trapping, I suggest that excess PrP^d retained at the FDC dendritic plasmalemma may enhance capacity to trap complexes via C3b or Fc receptors. PrP^d accumulation at the plasmalemma of immature FDCs may be interpreted to suggest that PrP^d accumulation at the cell surface initiates this chain of events.

In this and previous studies of both sheep and mice infected with scrapie, I have found that all or virtually all follicles at the stage of terminal disease are scrapie-infected, as shown by the accumulation of PrP^d. This further suggests that follicles do not regress but are stimulated to continue to produce antibody. That excess numbers of mature plasma cells are present is also consistent with delayed or impeded B cell migration from the follicle. PrP^d immunolabelling was observed at the plasmalemma of all emperipolesing FDC dendritic profiles.

Again, within the spleens of terminally diseased animals, intralysosomal PrP^d labelling of macrophage was apparent outwith the germinal centre, suggesting these cells play an important role in the transportation of infectivity away from the secondary follicle.

In summary, several scrapie-specific changes have been identified in the spleens of scrapie-infected mice. Taken together, the loss of the membrane associated electron-dense lamina, FDC hypertrophy and increased plasma cell retention within the secondary follicle all suggest that germinal centre functionality is pathologically affected as a result of scrapie infection. The nature of these changes suggests that there is a change in immune complex binding mechanisms, normal plasma cell maturation and perhaps cellular PrP^c trafficking. I can speculate that these changes are due to the presence of abnormal PrP at the surface of FDCs and that this PrP^d retains a functional role in facilitation of immune complex trapping. In order to challenge disease at the cellular level, the sub-cellular progression of the disease must also be clearly understood; we have shown PrP^d accumulation precedes immunopathology while PrP^d may be transported from the germinal centre in macrophage lysosomal compartments. PrP^d accumulation associated with the plasmalemma of FDCs has a function: it is directly related to excess immune complex trapping which in turn induces FDC hypertrophy. While the exact mechanism for the delayed release of B cells from the secondary follicle and increase in coated pit expression are unknown, it is clear that scrapie infection induces these pathological effects. It can therefore be concluded that scrapie infection causes both morphological and functional pathology of the LRS, and seems to alter the way in which the host responds to immunological challenge.

3.3. Ultrastructural strain specific localisation of disease-specific PrP in murine spleen.

Introduction

The importance of FDCs in the neuroinvasion of the ME7 strain of scrapie has been extensively discussed in previous sections. However, the involvement of FDCs in disease progression has to date, only been tested in the ME7 scrapie strain and Rocky Mountain Laboratory (RML) isolate(Klein et al. 1998; Weissmann et al. 2001). Different murine scrapie strains have different incubation periods when inoculated by i.c., oral or peritoneal injections (Kimberlin & Walker 1979b). Neuroinvasion takes place at approximately 50% of the incubation period after i.p. challenge. This investigation aims to ascertain whether different TSE strains target different cell types in murine spleen. In the event that FDCs are invariably targeted by different scrapie strains, the structure of the secondary follicles will be studied to determine whether the nature and progression of morphological changes are the same in models with differing incubation periods.

Materials and methods

Mice were obtained from IAH – NPU in Edinburgh (see section 2.1.3). Scrapie-infected tissues taken are detailed in table 2.2. Spleens were immersion fixed, processed and labelled as described in sections 2.2.1. – 2.2.7. Phenotypic properties of different scrapie strains were analysed ultastructurally within the spleen. Initial PrP^d detection, incubation periods and cellular targeting differences between TSE strains were compared. All mice were challenged i.c. with the TSE agent. Tissues from each of the inoculated groups were collected 5 weeks after scrapie infection, 10 weeks after scrapie infection and finally at terminal disease (see table 2.2). At lease 5 tissue blocks containing white pulp were identified from each group for study.

Results

Light microscopy: morphology

5 weeks after scrapie infection: within the spleens of all scrapie-infected groups, white pulp areas were easily distinguished. These areas varied greatly in size, although no consistent pattern was seen when the different strains were compared. FDC like cells were identified within the white pulp areas of all scrapie strains studied, while cells presumptively identified as TBMs were present both within the follicle and adjacent sites.

10 weeks after scrapie infection: the morphology of the spleens of mice at the 10week after scrapie infection timepoint was not subjectively different from those at the 5 week timepoint. White pulp areas were easily identified, and contained both FDCs and TBM like cells.

Terminal stages of disease: again, distinct white pulp areas were identified within the spleens of all experimental groups.

Light microscopy: PrP^d immunolabelling

5 weeks after scrapie infection: PrP^d immunolabelling was observed only in the spleens of mice infected with the 139A strain of scrapie. This labelling present in very few follicles, and, where present was not abundant. It was consistent with an FDC-type pattern of labelling as described in the previous sections 3.1 and 3.2. No

immunolabelling was seen in any of the tissue blocks studied from the 87V, 79A or ME7 scrapie-infected groups at the 5 week timepoint.

10 weeks after scrapie infection: spleens from 79A, ME7 and 139A scrapie-infected groups showed PrP^d accumulation within the secondary follicles. Within the spleens of mice infected with the 87V strain of scrapie, no immunolabelling was observed. Within spleens from mice infected with the 139A, 79A and ME7 strains of scrapie, PrP^d immunolabelling was widespread, with the majority of follicles affected. Patterns of labelling within the follicles from these infected animals are consistent with both FDCs and TBMs. No labelling was observed outwith the follicle in any of these spleens.

Terminal stages of disease: within the white pulp of spleens from the 139A, 79A and ME7 scrapie-infected animals at the terminal stage of disease, extensive PrP^d immunolabelling was observed. Patterns of labelling indicate PrP^d is associated with both macrophage and FDC-like cells. Immunolabelling was present within the dark and light zones of most follicles in the spleens of mice infected with the 139A, 79A and ME7 strains of scrapie. Occasional intense puncta of immunolabelling were observed adjacent to red blood cells outwith the follicle, and in areas provisionally identified as the marginal zones. At the terminal stages of disease, immunolabelling of spleens infected with the 87V strain of scrapie was absent.

Ultrastructural morphology and immunolabelling.

Tissue blocks with previously identified white pulp areas were examined ultrastructurally. The morphology of the spleens of the i.c. inoculated 139A, 79A

and ME7 strains of scrapie correspond to the previously seen i.c. inoculated ME7 spleens, at both 10 weeks after inoculation and the terminal stage of infection (see section 3.1). FDCs at various stage of hypertrophy were observed at these timepoints, while TBMs with many intracytoplasmic lysosomal bodies were prolific. Other scrapie-specific pathological effects such as prolonged follicular B cell retention, were observed intermittently in all three scrapie strains studied, with increased frequency at the terminal stages of infection. These morphological observations are described in detail in sections 3.1 and 3.2. Spleens at the 5 week timepoint were not studied ultrastructurally. As no immunolabelling was observed in the 87V experimental group, these spleens were also not examined at the sub-cellular level. Patterns of immunolabelling in the 3 groups studied were similar to the results discussed in previous chapters. At the 10 week timepoint, a proportion of mature and rarely, immature FDCs accumulate PrP^d on the plasma membrane of dendrites, while labelling was also seen within TBM lysosomes. At the terminal stage of disease, FDCs that were not associated with PrP^d immunolabelling were not observed in any of the tissue blocks from the mice inoculated with 79A, 139A and ME7 strains of scrapie. Patterns of immunolabelling correspond to those described in sections 3.1.and 3.2. (and Figure 3.2.1).

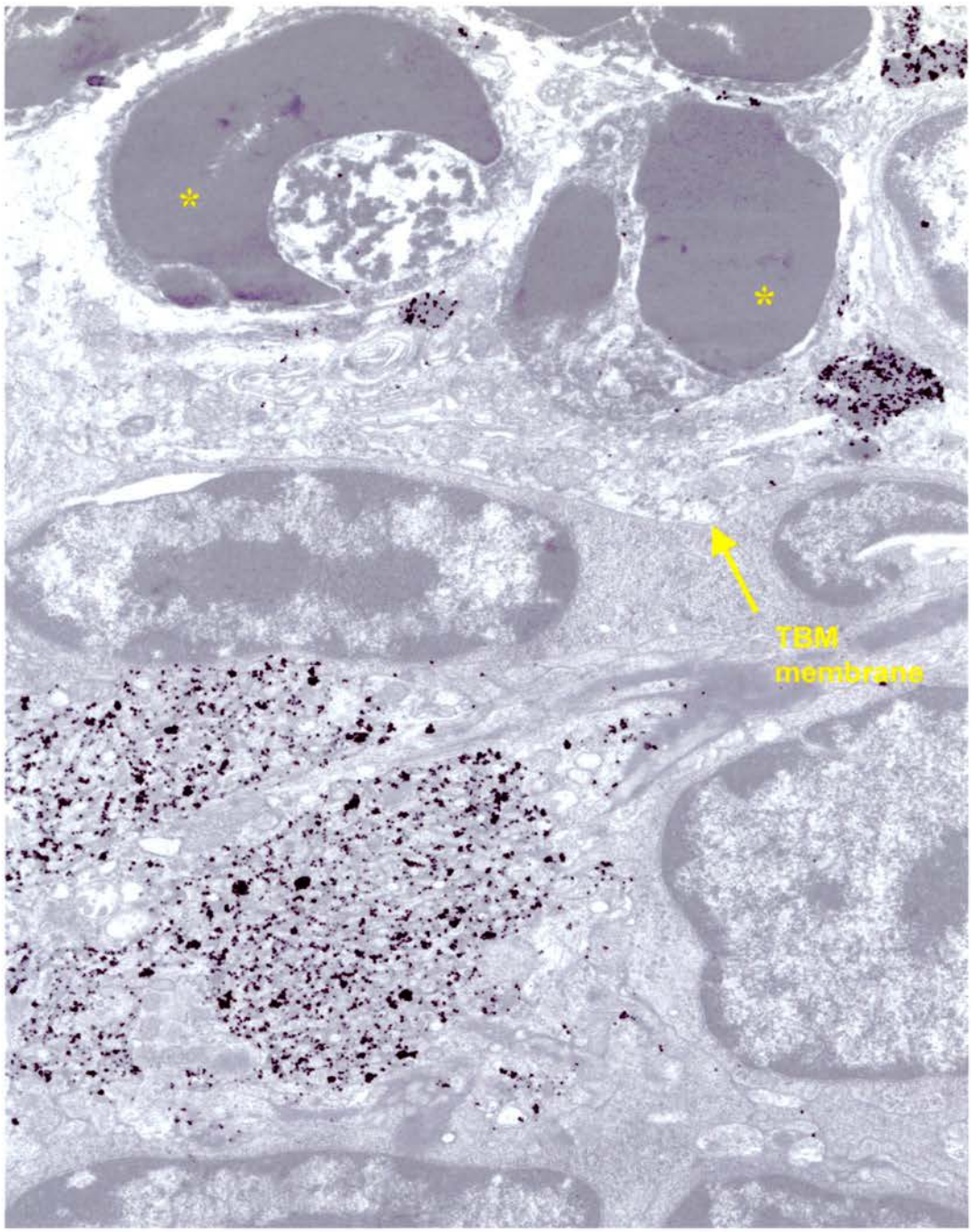

Figure 3.3.1. x13K magnification. Spleen from a terminally affected mouse infected with 139A scrapie. FDC and TBM immunolabelling patterns do not differ from those described in previous sections FDC labelling is associated with dendritic plasmalemmae, while TBM labelling is limited to lysosomal compartments. The TBM seen here contains many apoptotic cell remains (asterisks).

Discussion

Much discussion of murine scrapie strain variation has reflected upon the mechanisms of incubation period differences, and the severity and distribution of pathological changes seen in the brains of mice of defined genotypes. Based on these criteria, about 20 phenotypically distinct murine scrapie strains have been identified (Dickinson & Fraser 1977). This study demonstrates that pathological variation and disease-specific localisation of PrP within the spleen is not scrapie strain specific, at least for the ME7, 139A, and 79A scrapie strains.

Incubation period, i.e. the time between initial infection and clinical endpoint, is generally very similar where a single cloned scrapie strain is used to infect genetically uniform mice. Incubation periods with standard errors of <2% of the mean are measured following i.c. inoculation of mice with a high dose of a single scrapie strain (Bruce 1996). The host gene which influences incubation period and pathology is known as the *Sinc* or Scrapie incubation gene, and can exist in one of two forms: s7, indicative of a short incubation period with the ME7 strain of scrapie, and p7 which gives a more prolonged incubation period with this strain.

Of the four strains studied, only the 87V strain of scrapie was injected into a Sinc ^{p7} mouse strain (the VM mouse strain). I.c. inoculation was used in this experiment as a time limiting factor; peripheral routes of infection have considerably longer incubation periods. Incubation period following i.c. inoculation determined from this and previous studies, is in the order of 285 days, which is in stark contrast to the remaining strains which were injected into mice of the Sinc ^{s7} strain (the C57Bl strain). The incubation periods for the 139A, 79A and ME7 strains of scrapie are 170

days, 175 days and 185 days respectively (Bruce 1996). Initial PrP^d accumulations within the spleen correlate with previous studies of PrP^d accumulations in the brain in so far as the earliest disease-specific PrP accumulations are to be found in the spleens of mice infected with the 139A strain of scrapie. This could be anticipated due to the short incubation period of this strain in C57Bl mice. At the 10 week timepoint, all C57Bl mice strains demonstrate moderate PrP^d accumulations within secondary follicles, while PrP^d could not be located within germinal centres of VM mice inoculated with the 87V strain of scrapie.

The results of this study suggest that, unlike the brain, splenic PrP^d accumulations within the spleen are associated with the same cell types. Although there were differences in the onset of PrP^d detection in FDCs with different strains, no significant magnitude differences in PrP^d accumulation or pathology of FDCs were noted at terminal stages. Although this study examined only a few mice infected by i.c., rather than i.p. inoculation, the changes seen did not suggest variability of FDC susceptibility to infection, which could explain the limited variation in times of neuroinvasion for the three scrapie strains which show splenic PrP accumulation. However, the early detection of FDC-associated PrP^d in the 139A strain suggests that this strain may replicate faster that the other strains in FDCs. Faster replication of 139A in FDCs offers a potential explanation for the more rapid neuroinvasion in this strain by i.p. or oral inoculation, when compared with other strains. Such a suggestion would need to be further studied in oral or i.p. challenged mice.

The combination of murine strain or genotype, and scrapie strain may explain the absence of peripheral PrP^d immunolabelling in the VM mouse strain following 87V scrapie inoculation. For example, in sheep, peripheral PrP^d accumulation does not

occur in certain sheep genotypes following natural infection (Jeffrey et al. 2002), while in cattle, there is no peripheral involvement following natural BSE infection (Wells et al. 1996). Where i.c. scrapie inoculations of susceptible sheep genotypes are carried out, magnitude and frequency of peripheral involvement is dependent upon infective dose, i.e. low dose inoculation results in no peripheral accumulation (Martin et. al., submitted). It therefore seems likely that 87V scrapie does not have an effective LRS phase.

3.4. Inhibition of Follicular Dendritic Cell maturation and subsequent effect on scrapie pathogenesis.

The role of some lymphoreticular cell types in the peripheral pathogenesis of TSEs has been extensively studied using mouse models deficient in particular cell populations of the immune system, or in specific signalling molecules. The involvement of T cells, B cells and FDCs has been explored using mice lacking specific cellular components. Signalling between lymphocytes and FDCs by cytokines is essential in the formation of the germinal centre. Many studies have demonstrated the importance of LT and TNF in the formation of B cell follicles, FDC networks and germinal centres (Matsumoto et al. 1997; Pasperakis et al. 1996). The studies discussed in this section were carried out in collaboration with colleagues at the IAH -NPU in Edinburgh, and investigated FDC involvement in scrapie pathogenesis. Sections 3.4.1. and 3.4.2., investigate the effect of the inhibition of specific cytokine signals from B-lymphocytes on the sub-cellular localisation of PrP^{d}, and transmission of scrapie infectivity to the CNS.

3.4.1. Ultrastructural analysis of the effect of the blockade of the Tumour Necrosis Factor signalling pathway on scrapie neuroinvasion.

Introduction

Studies of immunodeficient mice infected with scrapie have shown that mature FDCs which express host derived PrP, are necessary for PrP^d accumulation in the lymphoid tissues. Immunodeficient mouse models have demonstrated that the absence of mature FDCs significantly impairs the spread of infection to the CNS (Brown et al. 1999).

It has been demonstrated that B-lymphocyte derived tumour necrosis factor (TNF-α) signalling is critical for FDC development as mice deficient in this cytokine lack mature FDCs in lymphoid tissues (Pasparakis et al. 1996). TNF-α influences FDC development via the cell surface receptor TNF receptor 1 (TNFR-1), expressed on FDCs and /or their precursors (Tkachuk et al. 1998). Lack of signal via this pathway leads to the temporary inactivation of FDCs, suggesting they require constant stimulation from TNF-α to maintain their differentiated state (Mackay & Browning 1998). Temporary blockade of this cell signalling pathway was achieved using a single i.p injection of human TNFR fusion protein (huTNFR:Fc), which binds TNF-α, thus inactivating the cell signalling process (Mohler et al. 1993).

This study was undertaken to investigate the effect of TNF-α signal blockade on the morphology of FDCs, and the sub-cellular localisation of PrP^d in scrapie-infected mice treated with TNF-α at early stages of infection.

Materials and Methods

Mice were obtained from IAH – NPU in Edinburgh (see section 2.1.4.1). Details of tissues from these experimental groups are shown in table 2.3. Animals were sacrificed 7 days after human immunoglobulin (hu-Ig) or huTNFR:Fc boost. Spleens were immersion fixed, processed and labelled as described in sections 2.2.1. – 2.2.7.

Results

Light microscopy

At 14 dpi, few spleen tissue blocks from each experimental group showed defined germinal centre development. Those tissue blocks in which a mature follicle could be identified, were immunolabelled using the technique described in section 2.2.5. No PrP^d immunolabelling was observed in tissue sections taken from animals in any of the experimental groups.

Mature secondary follicles were easily identified in mice treated with hu-Ig 38 days after scrapie infection and sacrificed at day 45. Follicles showed moderate PrP^d immunolabelling within germinal centres. Patterns of labelling were those associated with FDCs, and punctate intracytoplasmic labelling typical of intralysosomal TBM PrP^d deposits.

Although secondary follicles were again relatively abundant, mice treated with huTNFR:Fc showed less follicular PrP^d immunolabelling. Where present, immunolabelling was not of a typical linear FDC type pattern. TBMs contained many ingested apoptotic cells, although little immunolabelling.

Electron Microscopy

As observed at light microscopy, ultrastructural morphological analysis of spleens at 14 days after scrapie infection revealed few follicles in all experimental groups. FDCs were occasionally identified due to their large irregular nuclei containing a

peripheral margin of chromatin, but did not exhibit extended or hypertrophic dendritic profiles associated with scrapie infection. Of the limited morphologically identifiable FDCs present in huTNFR:Fc treated spleens, no FDC apoptosis was observed, however, a small number of ingested apoptotic B cells were seen within TBMs in these spleens. No morphological evidence of B cell apoptosis was observed in hu-Ig treated spleens.

At the later timepoint (38 days + 7), hu-Ig inoculated scrapie spleens showed some FDC hypertrophy, with extended dendritic profiles forming both large labyrinthine glomerular complexes and small knots of dendritic processes between lymphocytes of the secondary follicle. FDC glomeruli were occasionally observed to loose extracellular electron-dense deposit in favour of the formation of fibrillar structures (Figure 3.4.1.1) As discussed in previous chapters, there fibrillar structures were seen to co-localise with immunogold labelling. A proportion of FDCs identified by their typical nuclear morphology, were in an immature state with poorly developed dendritic profiles. TBMs, with phagocytosed nuclear remnants in their cytoplasm and containing abundant lysosomes, were also present within the secondary follicle. Occasionally, whole degenerate (presumed apoptotic lymphocytes) cells were found within the cytoplasm of these macrophages.

Mice treated with huTNFR:Fc 38 days after scrapie infection showed extensive cellular degeneration. Apoptotic lymphocytes with dark fragmented nuclei were present within the secondary follicle when mice were killed one week after the treatment (Figure 3.4.1.2). Many TBMs with abundant cytoplasm containing intralysosomally digested lymphocytes, and occasionally whole B cells, were also present.

Some limited FDC networks were observed, however, most dendritic processes were relatively uncomplicated when compared to hu-Ig treated control mice.

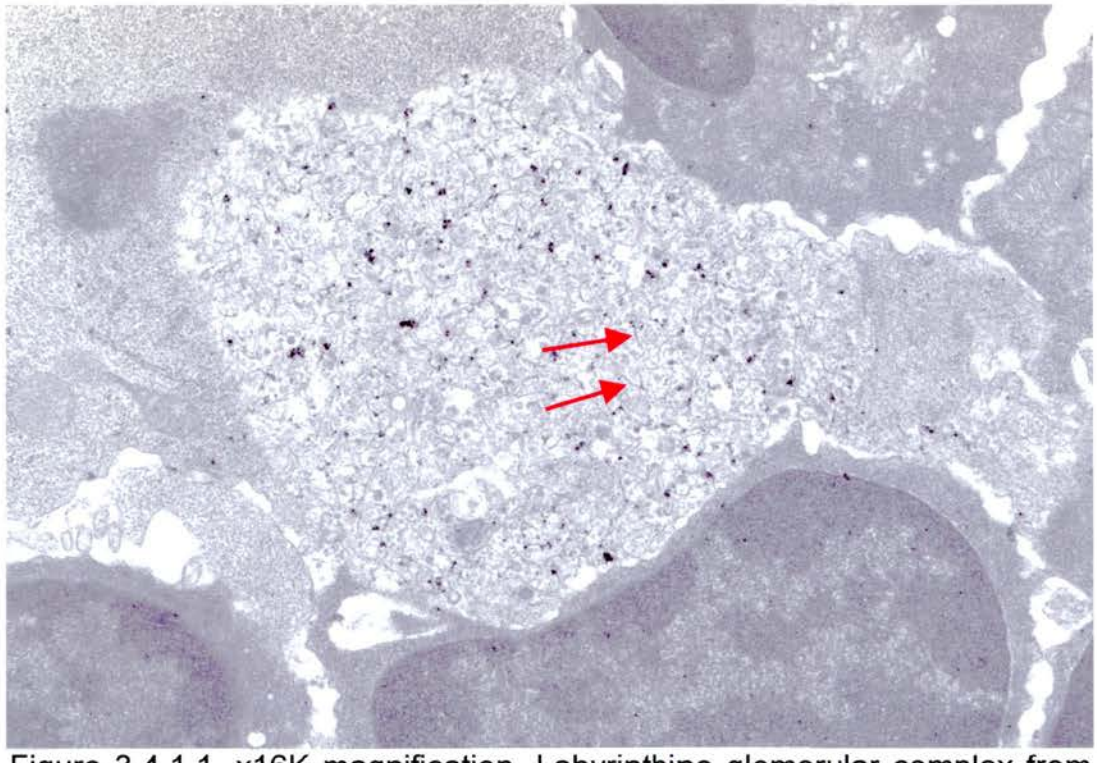

Figure 3.4.1.1. x16K magnification. Labyrinthine glomerular complex from a hu-Ig inoculated mouse spleen 42 days after scrapie infection. Many fibrillar structures are present within the extracellular space (arrows) and are associated with PrP^d immunolabelling.

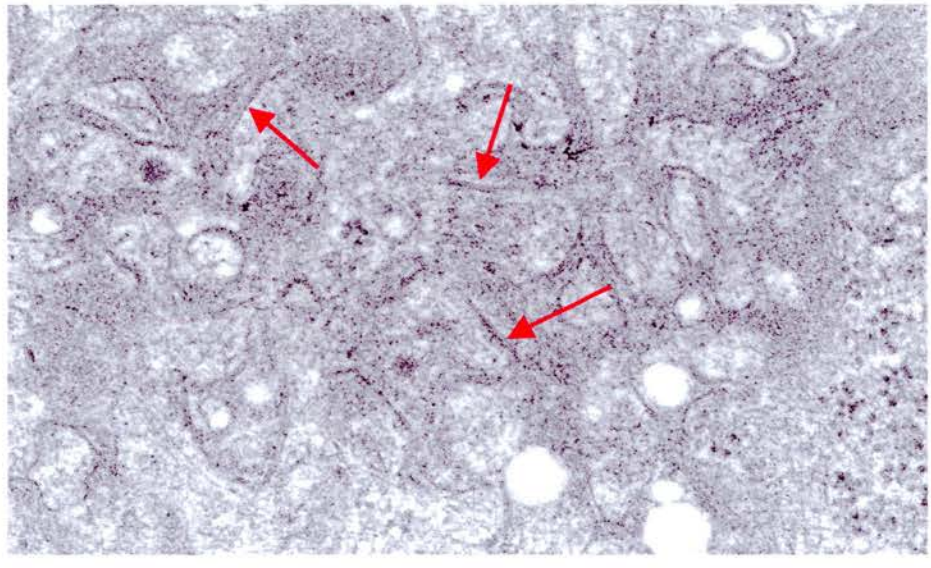

Figure 3.4.1.1a. x63K magnification. Detail of fibrillar structures (Arrows) within the extracellular space surrounding FDC dendrites.

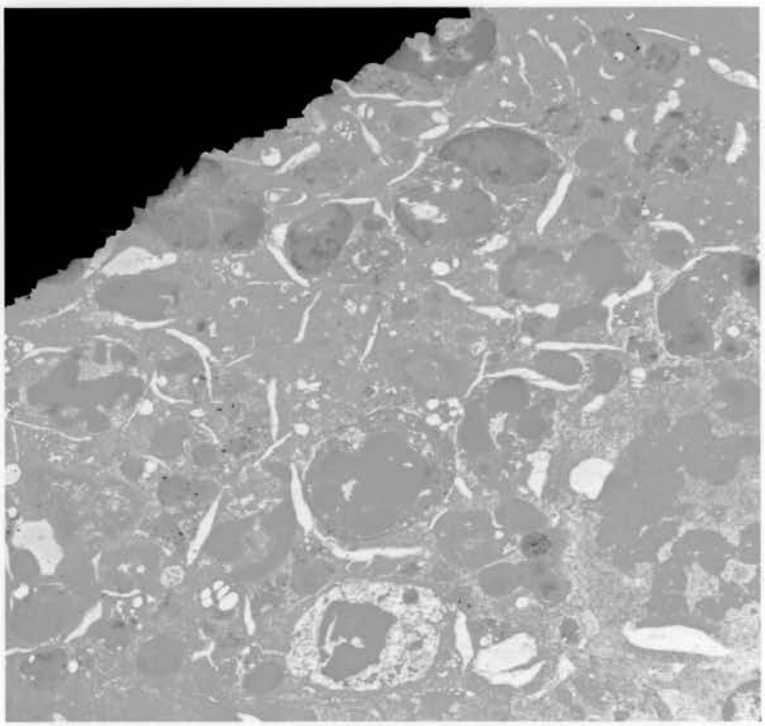

Figure 3.4.1.2. x5K magnification. Immunolabelled spleen from a scrapie-infected mouse inoculated with huTNFR:Fc 38 days after scrapie infection (killpoint = 45 days). Extensive cellular degeneration can be seen, in addition to many TBMs containing intralysosomal PrP^d.

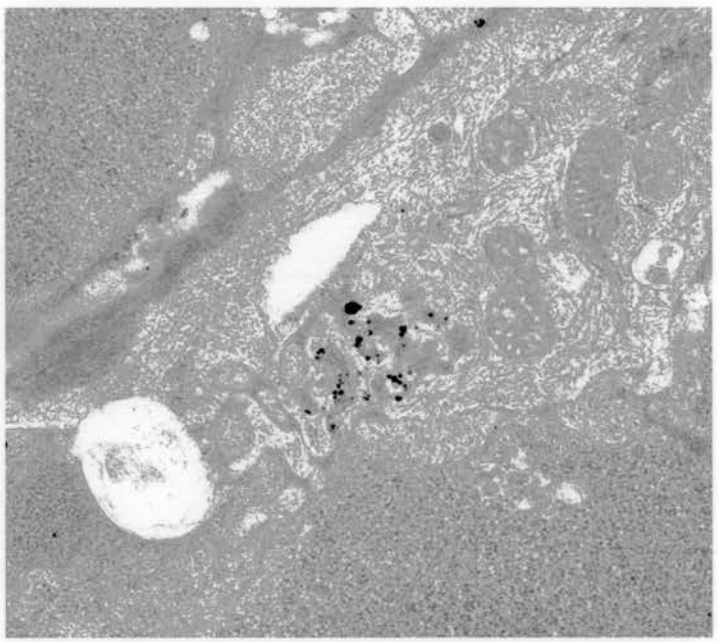

Figure 3.4.1.3. x23K magnification. Immunolabelled FDC complex from the spleen of a scrapie-infected mouse inoculated with huTNFR:Fc 38 days after scrapie infection (killpoint = 45 days). Limited dendritic profiles are sparsely labelled.

As no PrP^d was observed in any spleen blocks at the 14 day timepoint using light microscopical techniques, no ultrastructural immunolabelling was carried out on these tissues.

Immunoelectron microscopical analysis of hu-Ig treated spleens killed at the 45 day timepoint revealed as anticipated from earlier studies, that PrP^d accumulations were associated with mature FDCs. Labelling was observed primarily at the FDC plasmalemma of both convoluted labyrinthine complexes, and to a lesser extent more linear immature processes. In some follicles, occasional fibrillar structures could be seen within the extracellular space between FDC dendrites. Immunolabelling was associated with these structures. Intralysosomal TBM PrP^d labelling was also observed.

PrP^d immunolabelling of huTNFR:Fc treated mice, revealed light PrP^d labelling in association with only the more developed FDC dendritic profiles (Figure 3.4.1.3). Although TBMs were morphologically identified in the tissue sections more frequently than the h-Ig controls, immunolabelling was light and limited to a small portion of the lysosomes present.

Discussion

Work undertaken at the IAH - NPU by Neil Mabbott and his colleagues, demonstrated that a single treatment of mice with huTNFR:Fc before peripheral inoculation with the scrapie agent, significantly reduced PrP^d accumulation in the spleen, which, in turn, delayed the onset of CNS disease (Mabbott et al. 2002). It was further demonstrated that the mean incubation period of control mice inoculated with hu-Ig 14 days after i.p. scrapie infection was 262± 8 days (SE), while those mice treated with huTNFR:Fc at this timepoint developed disease at 281± 7 days. Inoculation with huTNFR:Fc at the later timepoint of 38 days after scrapie infection did not significantly alter incubation periods. Treatment with huTNFR:Fc before or after peripheral scrapie inoculation did not have an effect infectivity at 70dpi when compared to controls. These results are consistent with previous findings that suggest that the absence of mature FDCs in lymphoid tissues leads to impaired neuroinvasion following peripheral scrapie inoculation (Brown et al. 1999).

Ultrastructural analysis of the secondary follicles from mice treated at 14 days after scrapie infection revealed a TNF influence upon maintenance of B cell differentiation, although differences in FDC development between hu-TNFR:Fc and hu-Ig treated were insignificant, with no extended dendritic processes present in either experimental group. As FDCs are known to provide necessary co-stimulatory factors which prevent B cells from undergoing apoptosis (Tew et al. 1997), the detection of an increased level of B cell apoptosis in hu-TNFR:Fc treated spleens suggests a lack of antigen, co-stimulatory or cytokine signalling due to the loss of FDCs. It might be anticipated that developing immature FDCs may gradually express

more cell surface molecules. A parallel light microscopical study by Neil Mabbott at the IAH - NPU demonstrated that in mice treated with hu-TNFR:Fc or hu-Ig 14 days after scrapie infection and allowed to reach a terminal stage of disease, survival time of those animals inoculated with hu-TNFR:Fc was seen to increase. This suggests hu-TNFR:Fc inoculation in the early stages of infection causes a significant delay in neuroinvasion. This delay may be due to the absence of mature FDCs as a result of hu-TNFR:Fc inoculation, suggesting FDCs are not able to sustain or multiply infection until fully mature. Alternatively, de-differentiated FDCs may be partly susceptible to scrapie infection with low levels of inoculum able to infect FDCs followed by limited PrP^d amplification. The absence of morphologically identifiable mature FDCs and related ultrastructural PrP^d immunolabelling in both hu-Ig and hu-TNFR:Fc inoculated spleens at this stage would suggest a level of FDC associated PrP^d accumulation, which is not detectable using ultrastructural immunohistochemical methods.

An alternative hypothesis may be that the de-differentiated FDCs are as susceptible as mature FDCs to initial scrapie infection. However, the PrP^d is unable to amplify due perhaps to a physical or chemical alteration to the cell. Both of these last two hypotheses imply that following hu-TNFR:Fc exposure, the capacity of FDCs to produce a sufficient quantity of PrP^d to allow neuroinvasion is impaired.

At 38 days after scrapie infection, colleagues at NPU demonstrated that hu-TNFR:Fc inoculation did not significantly alter survival time when compared to that of hu-Ig inoculated controls. Temporary de-differentiation of FDCs as a result of hu-TNFR:Fc inoculation was demonstrated to last for between 7 and 14 days, while at 38 days after scrapie infection high levels of scrapie infectivity are present in the spleen. This

observation suggests that either infection of peripheral nerves has already occurred by this timepoint, or the period of FDC de-differentiation is inadequate to alter incubation periods significantly once infectivity is established. Again, at this later timepoint, extensive B-lymphocyte apoptosis suggests the loss of mature FDCs causes major degenerative changes in the follicle. When compared with hu-Ig treated murine spleens, hu-TNFR:Fc treatment results in extensive FDC de-differentiation and associated pathological effects, with many whole apoptotic B-lymphocytes phagocytosed by TBMs. FDC networks, where present were very limited in extent, and only occasionally formed small knots. Whether these processes were consistent with regenerating FDCs, or mature FDCs unaffected by the cell signalling blockade remains unclear. It has been suggested that FDCs participating in a strong antigenic response may be unaffected by treatments which inhibit the TNFR signalling pathway (Mackay & Browning 1998).

PrP^d immunolabelling within the spleen of hu-TNFR:Fc inoculated mice, was considerably more limited than the hu-Ig treated controls at the 38 day timepoint, with light FDC labelling and low PrP^d accumulation within TBM lysosomes. Following de-differentiation of FDCs, it might be expected that FDC-related PrP^d would be released into the extracellular space to be internalised by macrophage. As PrP^d levels within lysosomal compartments of TBMs were lower in hu-TNFR:Fc treated murine spleens, it may be hypothesised that the rate of lysosomal digestion of PrP^d is sufficient to allow the digestion of the majority of PrP^d prior to the regeneration, re-infection and subsequent disease amplification by FDCs, and re-internalisation of FDC related PrP^d by TBMs.

If cytokines are inhibited at an early timepoint of scrapie infection, subsequent FDC dedifferentiation causes an increased scrapie incubation period. However, the connection between this and neuroinvasion remains provocative. Although peripheral nerves have been detected in the light zone of sheep Peyer's patches (Heggebo et al. 2003), no peripheral nerves were seen in the secondary follicles of mice in the present studies. There is therefore no clear structural relationship between sub-cellular sites of PrP^d accumulation and peripheral nerves. The possibility that the infectious agent is delivered to the CNS via mechanisms independent of PrP^d accumulation of FDCs or any cell type, cannot be eliminated.

3.4.2. Ultrastructural analysis of the germinal centres of scrapie-infected murine spleen, following treatment with an inhibitor of the lymphotoxin pathway.

Generation and maintenance of FDCs within germinal centres is dependent on signals from cytokines, including lymphotoxins, members of the tumour necrosis factor family (De Togni et al. 1994). Lymphotoxin α and β (LTα and LTβ, respectively) are known to be produced by activated B cells, activated T cells and Natural Killer cells (Paul & Ruddle 1988; Ware et al. 1995), and their absence results in an almost complete loss of germinal centres and FDC networks (Koni et al. 1997). However, previous studies have shown that residual FDC-like cells are present within B cell follicles in spleens of LTβ and LTβ receptor (LTβR) deficient mice (Alimzhanov et al. 1997).

In normal mice, the LTα molecule lacks a transmembrane domain, and can only be retained on the cell surface in complex with LTβ, which is a transmembrane protein (Browning et al. 1993). This complex signals though the LTβR, expressed on stromal cells such as the FDC and / or its precursor. In mice born with the absence of either LTα / β or its corresponding receptor, no splenic B or T cell zones, or germinal centres are formed, and FDCs do not differentiate. Likewise, if a specific inhibitor blocks the LTβR signalling pathway, FDCs quickly de-differentiate (Mackay & Browning 1998).

Recent studies have shown that in the absence of FDCs caused by blockage of the LTβR pathway, early accumulation of PrP^d in the spleen is impaired and neuroinvasion is delayed (Mabbott et al. 2000b).

In order to further understand the effects of the blockade of the LTβR pathway on scrapie pathogenesis, we studied the spleens of scrapie-infected mice ultrastructurally, following treatment with both LTβR immunoglobulin fusion protein (LTβR:Ig) and human immunoglobulin IgG (hu-Ig) as a control.

Mice were obtained from IAH – NPU (see section 2.1.4.2.). Details of tissues from these experimental groups are shown in Table 2.4. ME7 scrapie was administered i.p, and animals were sacrificed 3 or 35 days after hu-Ig or LTβR:Ig treatment. Spleens were immersion fixed, processed and labelled as described in sections 2.2.1. – 2.2.7. Mice were then sacrificed at a later scrapie incubation period, again, either 3 or 35 days after LTβR:Ig or hu-Ig treatment.

Details of tissues from these experimental groups are shown in table 2.4.

Results

Light Microscopy

Control hu-Ig treated mice

Within the spleens of mice treated with hu-Ig 42 days after scrapie infection and harvested 3 days later, follicles were relatively abundant in all tissue sections studied. Slight PrP^d immunolabelling, with a linear pattern consistent with an FDC association, and a more punctuate, intracytoplasmic PrP^d labelling, were observed. Immunolabelling was extremely limited and was restricted to the more mature follicular germinal centres. Immunolabelling was not consistent in all mice studied, with 2 of the 4 mice studied showing no PrP^d accumulation within splenic tissue blocks studied.

In spleens of control mice treated at 42 days and killed at day 77, mature germinal centres were more abundant, with more florid FDC and TBM type immunolabelling. At the 73 and 105 day killpoints (see Table 3.4.2), germinal centres were more developed with well defined FDC and TBM labelling. At these timepoints, all mice studied showed PrP^d accumulation within the spleen.

At the 45 and 73 / 77 day kill points, the morphology and immunolabelling of hu-Ig treated ME7 infected mice within the spleen were similar to those of ME7 infected mice at 45 dpi (section 3.4.1), and 70 dpi described in section 3.2.

LTβR-Ig treated spleens

In tissues inoculated with LTβR-Ig at the 42 day timepoint and killed 3 days later, areas of white pulp appeared relatively abundant. Germinal centres however, were not readily apparent, and, subsequently, very little PrP^d immunolabelling was observed. Due to the sparseness of labelling, it was impossible to determine whether this immunolabelling was associated with cells of a FDC or TBM type morphology. In spleens from mice inoculated with LTβR-Ig at day 42 after scrapie infection, and killed at day 70, mature follicles were again present. Extensive PrP^d immunolabelling was observed within a portion of these follicles and was consistent with both an FDC and TBM type pattern.

Follicles from the spleens of mice inoculated with LTβR-Ig at day 70 after scrapie infection, and killed 3 days later were again present, however they generally appeared less organised than corresponding hu-Ig controls, with less well defined white pulp areas. Immunolabelling for PrP^d was profuse and was associated with FDC and TBM type cells. Within spleens of mice inoculated with LTβR-Ig at day 70 and killed 35 days later, again white pulp appeared generally disorganised, with few identifiable germinal centres. Within these white pulp areas, low - moderate levels of PrP^d immunolabelling was observed. It was not possible to determine the exact location of these labelling patterns, or indeed which cells they were associated with. Labelling patterns did not appear as intense as hu-Ig controls.

Electron microscopy

Controls hu-Ig inoculated tissues: morphology

Ultrastructural study of scrapie-infected spleens inoculated with hu-Ig, showed a marked increase in FDC hypertrophy as incubation period increased, as previously described in section 3.4.1. At all timepoints, FDCs with extended dendritic profiles forming small knots of dendritic processes between lymphocytes of the secondary follicle were observed; however, at the 70 day killpoint and beyond, an increasing proportion of FDCs also formed large extended labyrinthine glomerular complexes. At the 45 day killpoint, although smaller labyrinthine glomerular complexes were present, the majority of FDCs, with a typical nuclear morphology, were in an immature state with poorly developed dendritic profiles.

Within all hu-Ig inoculated experimental groups, TBMs, identified by their abundant lysosomes and cytoplasmic phagocytosed nuclear remnants, were present within the secondary follicle. Occasionally, whole degenerate (presumed apoptotic lymphocytes) cells were found within the cytoplasm of these macrophages. Within the PALS region of a spleen from a mouse inoculated with hu-Ig at the 70 day timepoint and killed 35 days later, a macrophage containing two B-lymphocytes at different stages of maturity was observed.

Control hu-Ig inoculated tissues: Immunolabelling

Ultrastructural immunolabelling of scrapie-infected spleens at the 45 day killpoint produced low levels of immunogold labelling in some tissue blocks from two of the four mice studied. There were no differences in patterns of immunolabelling of these control tissues at this stage of infection, when compared to those described in section 3.4.1. Other tissue blocks that showed a more restricted pattern of immunolabelling at the light microscopical level showed no specific labelling by electron microscopy. It therefore seems likely, that the lesser sensitivity of ultrastructural immunolabelling when compared with light microscopic methods of PrP^d detection, is responsible for this effect.

At both the 73 day (hu-Ig inoculation at day 70), the 75 day (hu-Ig inoculation at day 42) and the 105 day (hu-Ig inoculation at day 70) killpoints, PrP^d immunolabelling was associated with the plasmalemma of a proportion of FDCs which formed labyrinthine glomerular complexes, while other FDC dendritic profiles, which interweaved between lymphocytes, were only immunolabelled in a small proportion of tissues from the 105 day killpoint. TBMs, present in close association with FDCs, demonstrated low levels of PrP^d immunolabelling both at the periphery of lysosomes and in association with denser intralysosomal areas.

These latter observations are in line with those anticipated from the 70 and terminal disease labelling patterns described for ME7 scrapie described in section 3.2.

LTβR-Ig inoculated spleens: morphology

At all timepoints, FDCs identified by their large, irregular nucleus containing a peripheral margin of chromatin, were present within germinal centres

At the 45 day killpoint (3 days after lymphotoxin inoculation), no FDCs observed formed labyrinthine structures, although FDC nuclei and dendritic profiles were easily identified, the profiles running between lymphocytes forming small knots. This contrasts to the corresponding control tissues at this timepoint that did exhibit labyrinthine-like structures. However, limited conclusions may be drawn from this as the LTβR-Ig inoculated group consists of only two animals, while the four animals were studied in the control group. TBMs containing multiple lysosomes were also identified in areas adjacent to FDCs.

Within the spleens of mice inoculated with LTβR-Ig 42 days after scrapie infection, and killed 35 days later, a proportion of FDC dendrites present formed small to moderately sized glomerular complexes between lymphocytes within the germinal centre. Again, TBMs were easily identified in areas populated by FDCs, and these contained lysosomal compartments.

At the 73 day kill point (3 days after lymphotoxin inoculation), both FDC nuclei and dendritic networks were observed within germinal centres (Figure 3.4.2.1). Easily recognisable knots of FDC dendritic profiles were interspersed between germinal centre lymphocytes, as well as limited linear profiles. FDCs demonstrated characteristics previously seen in hu-Ig inoculated control tissues at this timepoint. TBMs containing many lysosomes were observed in close proximity to FDCs.

Similar morphological observations were made of spleens obtained from mice inoculated with LTβR-Ig 70 days after scrapie infection and killed 35 days later. Within tissue blocks studied at this timepoint, neither FDCs nor TBMs varied in size and complexity from those observed at the 73 day killpoint. Apoptotic cells, presumed to be B cells due to the dense concentric circles surrounding the nuclear remnants, were observed within the follicle.

LTβR-Ig inoculated spleens: immunolabelling

Ultrastructural immunoelectron analysis of spleens inoculated with LTβR-Ig following scrapie infection, revealed PrP^d immunolabelling associated with FDC dendritic processes in all experimental groups, with the exception of the earliest killpoint of 45 days. At this point, all FDC processes observed were limited in development, with no formation of labyrinthine complexes. The immature linear processes that run between lymphocytes of the germinal centre did not show any immunolabelling. As immature FDC processes do not accumulate PrP^d during the early stages of infection, this result could be expected. TBMs were also unlabelled at this timepoint.

Within spleens from mice inoculated both at 42 days and 70 days after scrapie infection and killed 35 and 3 days later respectively, immunolabelling of the plasmalemma of mature FDCs complexes could be seen within germinal centres. FDC were readily identified in both experimental groups with mature processes forming both small knots and, to a lesser extent labyrinthine glomeruli (Figure 3.4.2.2). PrP^d immunolabelling of these structures was similar in magnitude to

corresponding control tissue blocks. A proportion of lysosomes within TBMs adjacent to mature FDCs were also immunolabelled.

Spleens from mice inoculated with LTβR-Ig 70 days after inoculation and killed at day 105, showed similar patterns of immunolabelling to those discussed in the previous paragraph. These levels of immunolabelling were conspicuously lower than those observed in the corresponding control tissues at 105 days. Labelling of immature FDC dendrites, where present was extremely limited. FDC nuclei, surrounded by small knots of relatively uncomplicated dendritic profiles with electron-dense deposit held uniformly between adjacent dendrites, were occasionally seen at this timepoint. No PrP^d immunolabelling was associated with these cytoplasmic extensions. As discussed in Section 3.2, at 70 days after i.p. scrapie infection, all stimulated FDCs would be expected to show pathological effects of scrapie infection, with only immature dendritic profiles that have not accumulated any excess electron-dense deposit, remaining unaffected. At this timepoint FDC dendrites that accumulate any electron-dense deposit, no longer do so uniformly, while immunolabelling is associated with the plasmalemmae of all stimulated FDC dendrites. Spleens from mice inoculated with LTβR-Ig 70 days after inoculation and killed at day 105, did not show this magnitude of PrP^d immunolabelling. Immunolabelling of TBMs did not appear to vary from the matching controls. Conclusions that can be drawn from this result are again limited due to the small group size.

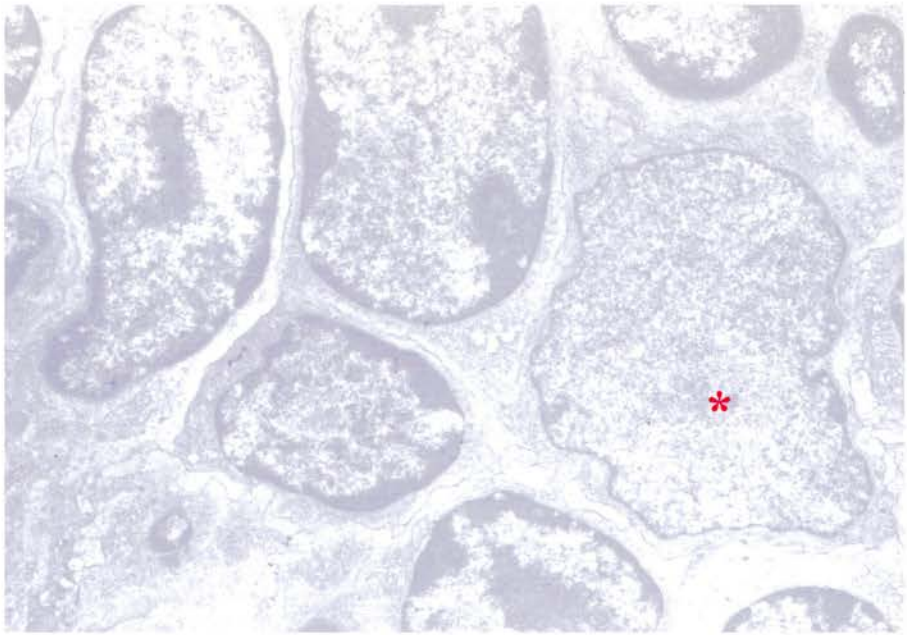

Figure 3.4.2.1. x6K magnification. Immunolabelled spleen from a scrapie-infected mouse inoculated with LTβR-Ig 70 days after scrapie infection (killpoint = 73 days). An FDC nuclei (asterisk) and limited dendritic profiles are present.

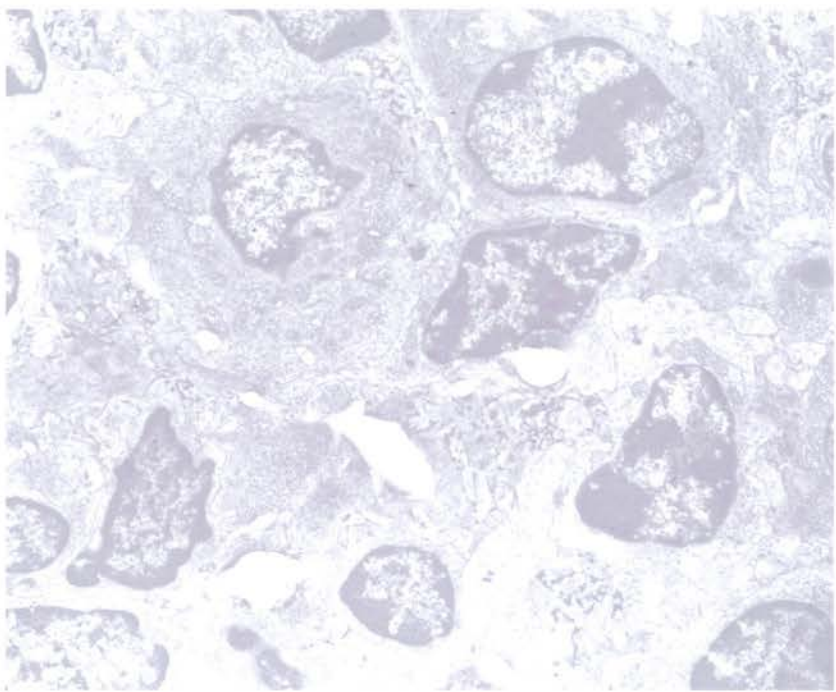

Figure 3.4.2.2. x4K magnification. Immunolabelled spleen from a scrapie-infected mouse inoculated with LTβR-Ig 70 days after scrapie infection (killpoint = 73 days). Interspersed between lymphocytes of the follicle FDC dendritic complexes can be seen. PrP^d immunolabelling is present in addition to excess accumulation of electron-dense deposit.

Discussion

Due to both the small experimental group size and investigated timepoints, it is difficult to draw many conclusions from this study. With hindsight, it may have been better to study the morphological effect and putative altered distribution of PrP^d at several time intervals after LTβR-Ig treatment in mice sacrificed at a single (e.g. 75 dpi) stage of scrapie infection. Nevertheless, it can be clearly seen that LTβR-Ig inoculation of scrapie-infected mice does not result in complete de-differentiation of FDCs, either 3 days or 35 days after LTβR-Ig inoculation. Whether complete de-differentiation of FDCs is achieved between these two points cannot be determined within this study.

In contrast to the present findings, previous studies have demonstrated that, after LTβR-Ig inoculation, FDC networks temporarily de-differentiate within 72 hours and return approximately 28 days later. FDC markers such as FDC-M1, FDC-M2 and CR1 disappear within 1 day (Mackay & Browning 1998; Mabbott et al. 2003). However, following the discovery that within spleens of mice already infected with scrapie, PrP^d immunolabelling remains apparent 72 hours after LTβR-Ig inoculation, it was suggested that this PrP^d immunolabelling may be associated with macrophages or unknown extracellular sites (Mabbott et al. 2000b). Our study indicates not only the presence of FDCs in 70 dpi scrapie-infected murine spleens 72 hours after LTβR-Ig inoculation, but that these FDCs have not lost their previous PrP^d accumulation, and exhibit other scrapie-specific pathological effects such as abnormal antigen / antibody complex retention and labyrinthine glomerular complex formation.

Although no mature FDCs were observed in 42 dpi scrapie inoculated spleens 3 days after LTβR-Ig inoculation, it is difficult to state conclusively the significance of this finding due to the small group size. The presence of mature FDCs 35 days after LTβR-Ig inoculation is perhaps expected, as previous evidence suggests that the period of de-differentiation following a single inoculation of LTβR-Ig is in the region of 4 weeks (Mabbott et al. 2003). There is some indication that the FDCs present at this timepoint are regenerating, with FDCs present that have a uniform electron-dense deposit held between dendrites. These mature FDCs, which do not exhibit scrapie-specific pathology or immunolabelling, are present in the follicles of spleens inoculated with LTβR-Ig 70 days after scrapie infection, then killed 35 days later. Following extensive ultrastructural studies of murine spleens 70 days after scrapie infection (see section 3.2), where all mature FDCs show evidence of scrapie-specific pathology, the presence of these apparently normal cells may indicate FDCs are regenerating, having lost scrapie infection. In addition, where PrP^d immunolabelling was present and associated with mature FDCs in these tissues, it appeared considerably less abundant than that of the corresponding hu-Ig controls. Again, this suggests that dendritic extensions have regressed due to LTβR-Ig inoculation, with PrP^d released in to the extracellular space or phagocytosed by adjacent macrophages.

The absence of FDC cell markers 72 hours after LTβR-Ig inoculation, may indicate an alteration in FDC cell marker expression as opposed to complete de-differentiation of these cells. This may explain the light microscopic pattern of FDC cell marker immunolabelling observed 72 hours after LTβR-Ig inoculation as described in earlier studies of these mice (Mabbott et al. 2003). Investigations

regarding the absence of cell markers following cytokine inoculation have, however, not been undertaken following scrapie infection. If scrapie infection was established within the spleen prior to cytokine inoculation, perhaps FDCs would be unable to de-differentiate to the same extent as uninfected cells, and persist in the spleen due to this abnormal scrapie-infected state, Alternatively, FDCs observed ultrastructurally may still be in the process of degenerating. Ultrastructural morphological observations do not allow quantification of FDCs or associated dendritic networks, therefore conclusions cannot be drawn concerning the possible degree of de-differentiation.

Light microscopical analysis of scrapie-infected mice, inoculated with LTβR-Ig prior to i.p. scrapie infection, revealed a significantly reduced susceptibility to scrapie infection, increased survival time (Mabbott et al. 2003), with scarcely detectable levels of infectivity in the spleen 70 days after scrapie challenge (Mabbott et al. 2000b). At this point, scrapie infection within the spleen should reach plateau levels (Farquhar et al. 1994; Brown et al. 1999). In comparison to this single dose treatment, consecutive prolonged treatments were given at 21 day intervals. Despite this extended cytokine inhibition, both survival time and susceptibility were similar to those of animals given only a single treatment. This suggests LTβR-Ig induces de-differentiation of FDCs that prevents initial uptake of scrapie infection, but has little or no effect on replication of the agent. In mice inoculated with LTβR-Ig 14 and 42 days after i.p. scrapie infection, levels of infectivity in the spleen at 70 days after scrapie infection were similar to those of controls even though incubation periods were extended. Following FDC de-differentiation the inhibitory effects of the LTβR-Ig would be absent allowing for further amplification of the scrapie agent.

Following oral scrapie infection, LTβR-Ig inoculation 14 days later does not increase survival time or affect disease susceptibility when compared to control mice. In contrast to this, inoculation with LTβR-Ig prior to infection remained asymptomatic of scrapie infection for at least 518 days, while post mortem findings suggested no scrapie-specific pathology or PrP^d accumulation (Mabbott et al. 2003). This would suggest LTβR-Ig blocked PrP^d accumulation in gut associated LRS and prevented CNS infection. Administration of LTβR-Ig after scrapie inoculation did not achieve this effect. These results suggest oral scrapie inoculation has a quicker or easier route to peripheral nerves than following i.p infection. This has recently been clarified: a close contact has been established between FDCs and TBMs of Peyer's patches with the peripheral nerves that innervate the gut (Heggebo et al. 2003).

The study detailed in this section suggests LTβR-Ig involvement in scrapie intervention is only possible before neuroinvasion occurs. In addition, levels of PrP^d accumulation within the spleen do not directly correlate with disease progression if LTβR-Ig inoculation occurs after scrapie infection.

Further study of the effects and subsequent possible intervention potential of LTβR-Ig must depend on confirmation of FDC de-differentiation. In addition, further study should be undertaken to investigate the fate of FDC-associated PrP^d following LTβR-Ig inoculation.

3.5. Visualisation of disease-specific PrP in the LRS of sheep.

Introduction

The sub-cellular pathology of scrapie-infected murine spleens has been characterised in detail in the previous sections. Much research has also been undertaken regarding gross and cellular pathology of scrapie infection in its natural host: the sheep. However, the sub-cellular localisation of PrP^d has not been studied in this species. In this section, I will discuss the development of ultrastructural immunocytochemical techniques for the visualisation of abnormal PrP in the MLN of clinical scrapie-affected sheep.

Materials

MLNs were obtained from clinically affected Suffolk sheep of the most susceptible genotype: $PrP^{ARQ/ARQ}$, as described in section 2.1.5. This tissue was chosen for all ovine studies as, with the exception of the spleen, it is the largest lymph node in the sheep, and therefore available in abundance for this and related studies. Infection of follicular areas is also consistent in this tissue (M. Jeffrey, personal observation). Spleen was not chosen for study, as the method of anaesthesia used was barbiturate based, and is known to cause splenic distension. Immersion fixation would not allow for adequate removal of all red blood cells from the tissue, which would prove detrimental to immunolabelling and morphological study of the tissue.

Many tissue blocks were studied from at least 10 sheep.

Methods and Results

Studies of ovine tissue were carried out using a variety of PrP specific antibodies. PrP antibodies, initially found to give good immunolabelling in paraffin embedded ovine tissues (Jeffrey et al. 2001a), were tested on resin embedded tissues. At the light microscopical level, the rabbit polyclonal antibody R486 was found to give excellent results, and was therefore used routinely for all light microscopic work on ovine tissues.

As a result of difficulties arising from ultrastructural immunolabelling studies (see below), a wide variety of PrP antibodies were used to label PrP^d-positive ovine tissues using the standard ABC technique.

The PrP antibodies tested and their specific amino acid target sites are detailed in Figure 3.5.1. Those highlighted in red gave specific PrP^d labelling of both FDCs and macrophages, while those in blue gave no labelling. Antibody sources are listed in table 3.5.1.

Antibody	Source
1A8	IAH, NPU, Edinburgh, UK
6H4	Prionics, Schlieren, Switzerland
BG4	IAH, Compton, UK
F89	K O'Rourke, Washington State University, Washington, USA
L42	M Groschup, Insel Riems, Germany
R145	R Jackman, CVL, Weybridge, UK
8G8	CEA, Gif sur Yvette cedex, France
P4	R–Biopharm, Darmstadt, Germany
R505.5	J Langeveld, ID –Lelystad The Netherlands
R521.7	J Langeveld, ID –Lelystad The Netherlands
R523.7	J Langeveld, ID –Lelystad The Netherlands
SAF 32	CEA, Gif sur Yvette cedex, France
R486	R Jackman, CVL, Weybridge, UK

Table 3.5.1. Table identifying the source of all antibodies tested. Those in blue are not available commercially

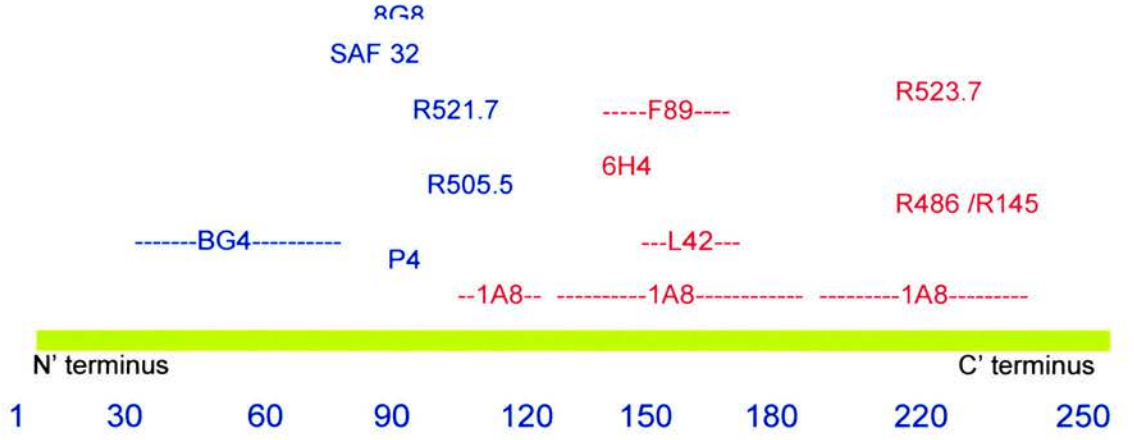

Figure 3.5.1. PrP antibody epitopes. Antibodies in red immunolabel ovine PrP^d to varying extents, those in blue do not. The amino acid sequence recognised by antibody is indicated on the bottom axis.

Light microscopical staining method (see section 2.2.4 and Appendix 6.1.e)

Using this technique, MLN tissue blocks containing developed germinal centres were identified. No discernable difference in the amount of secondary follicles present in the uninfected and scrapie-infected animals was observed in tissue blocks studied.

Light microscopical immunolabelling: Avidin Biotin amplification method (see section 2.2.5.2 and Appendix 6.1.g)

This method was used routinely for all light microscopical immunolabelling. PrP antibody R486 was found to give the most intense labelling patterns, although as can be seen from Figure 3.5.1, R145, L42, 523.7, 6H4, F89 and 1A8 all immunolabel both FDCs and TBMs to some degree. The intensity and relative abundance of immunolabelling was deemed to be greater following immunolabelling using R486 antibody. Patterns of PrP^d immunolabelling of samples of scrapie-infected MLN impregnated with resin were consistent with those from previous studies of paraffin wax embedded tissues (Van Keulen et al. 1996; Jeffrey et al. 2001b; Heggebo et al. 2002). Uninfected ovine MLNs were also immunolabelled using this technique; no PrP^d immunolabelling was observed. Within the MLN of a clinically affected scrapie-infected sheep, PrP^d was associated with cells of the light zone of the secondary follicle that resembled FDCs. Another pattern of labelling consistent with TBMs was observed within the light zone, dark zone and mantle zone of the follicle (Figure 3.5.2).

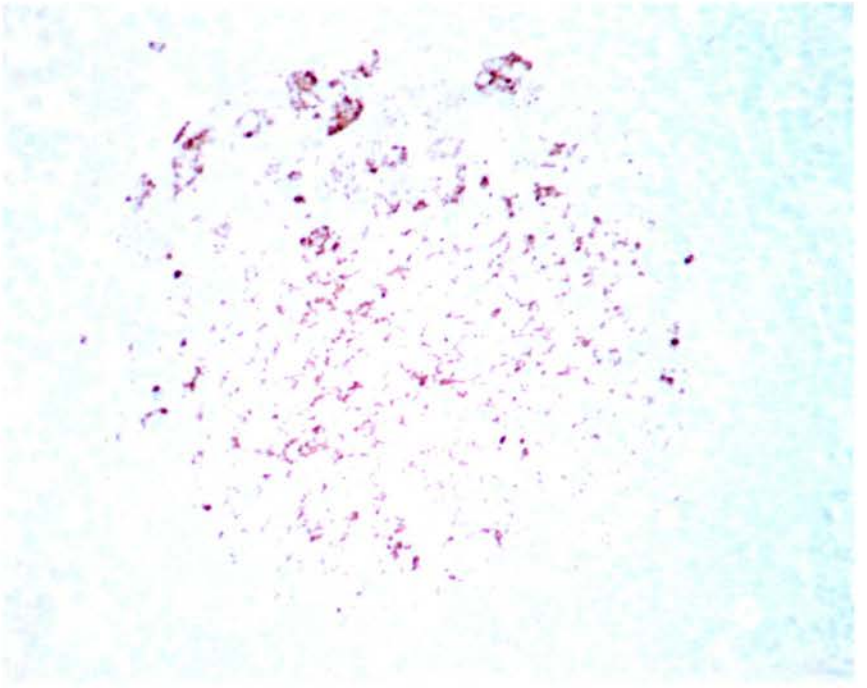

Figure 3.5.2. Light microscopically immunolabelled follicle from a scrapie-infected ovine MLN. Two distinct patterns of immunolabelling are present. A linear pattern, consistent with FDC labelling predominates the lower part of the follicle, while more intense foci of granular immunolabelling is present in the upper part of the follicle. This pattern of labelling is consistent with TBM labelling.

Light microscopical immunolabelling: Envision system (see section 2.2.5.3. and Appendix 6.1.p)

Although this method gave good immunolabelling, when serial sections were labelled by different techniques, results were inferior to those of tissues labelled with the ABC method.

Ultrastructural staining method (see section 2.2.6, and Appendices 6.1.i, 6.1.j, 6.1.k)

55 nm thick sections from tissue blocks previously shown to contain secondary follicles, were stained using the method described.

FDCs within the light zone of the secondary follicles of normal uninfected ovine MLNs had greater numbers and more complexly folded dendrites than those of normal FDCs within murine spleens. Processes formed small knots between lymphocytes, and although electron-dense deposit was uniform between adjacent processes, many spherical profiles were observed within this space (Figure 3.5.3). These were similar in both size and frequency to those previously described (Landsverk 1987; Landsverk et al. 1990). The MLN often has more numerous and larger secondary follicles than other lymph nodes of the sheep. This finding has been noticed for several species and it has been suggested that this is because of the constant exposure of the MLN to dietary associated antigens (M. Jeffrey, personal communication). It is possible that the increased complexity of sheep MLN FDC profiles relative to those found in the white pulp of murine spleens (Figure 3.1.2) may be because of diet-related antigenic challenge.

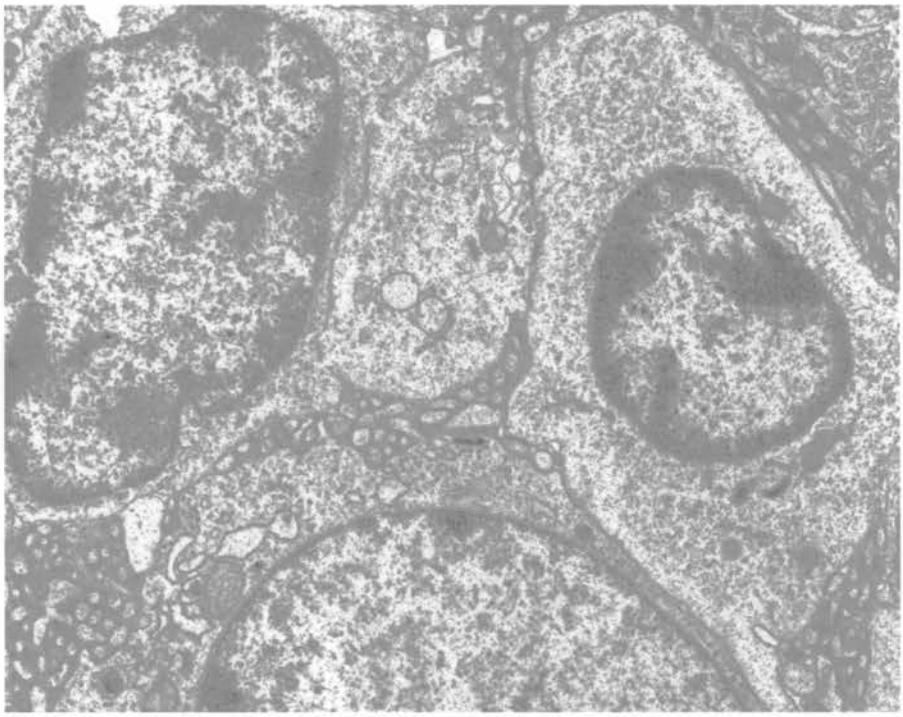

Figure 3.5.3. x10K magnification. Detail from a secondary follicle of a normal uninfected ovine MLN. FDC processes form small knots between lymphocytes, while electron-dense deposit is held uniformly between adjacent processes.

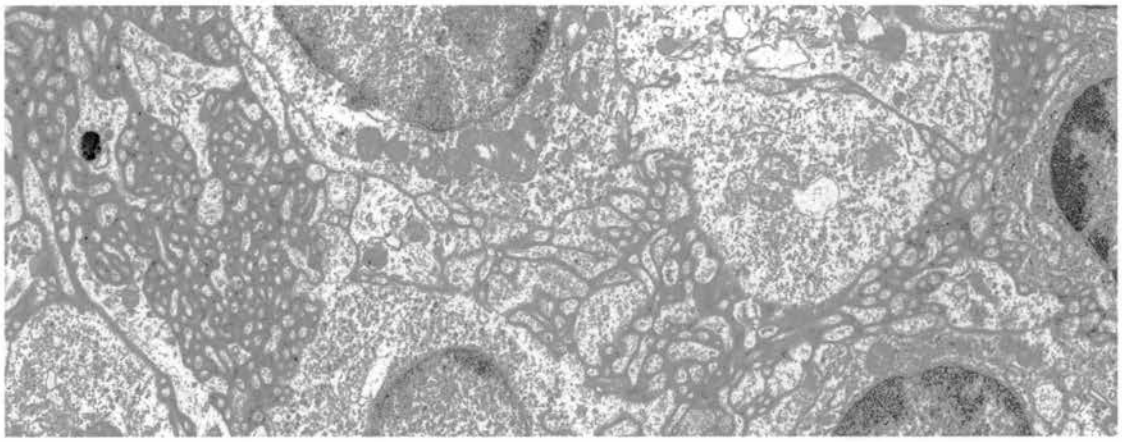

Figure 3.5.4. x8K magnification. Detail from a secondary follicle from a scrapie-infected ovine MLN. FDC profiles form hypertrophic labyrinthine glomerular complexes interspersed between lymphocytes. Abundant electron-dense deposit is held between adjacent dendrites.

To further explore this possibility, sub-mandibular lymph nodes were studied. Similar profiles were observed in comparable quantities.

TBMs containing lysosomes were also present in the light zone and dark zone of the follicle. Occasionally, TBMs contained whole apoptotic lymphocytes.

Ultrastructural analysis of MLN from a clinically scrapie-infected sheep revealed extensive FDC networks within easily definable germinal centres. In comparison to FDC networks from scrapie-infected murine spleens, dendritic profiles were more widespread and stretched to sites distant from the FDC nucleus. Hypertrophic FDC networks were more abundant, although they rarely formed labyrinthine complexes of a similar magnitude to those observed in murine spleen. Instead, FDCs formed smaller yet more numerous glomerular complexes that were interspersed between many light zone lymphocytes (Figure 3.5.4). At some points, FDC dendrites were not associated with an excess electron-dense deposit. Rather, simple, yet extended linear profiles stretched between cells to form small knots again, joined by other more linear processes.

Extracellular electron-dense deposit was associated with all mature FDC dendritic profiles and was highly irregular. Within the extracellular space, many small spherical bodies could be seen (Figure 3.5.5). Mature B-lymphocytes were present within the light zone of the follicle, surrounded by extended FDC dendritic profiles (Figure 3.5.6). FDC processes which formed labyrinthine complexes were seen adjacent to blood vessels. TBMs were again numerous and were present in both the light and dark zones of the secondary follicle, and at sites distant from the germinal centre. These TBMs contained abundant lysosomes and remnants of apoptotic cells.

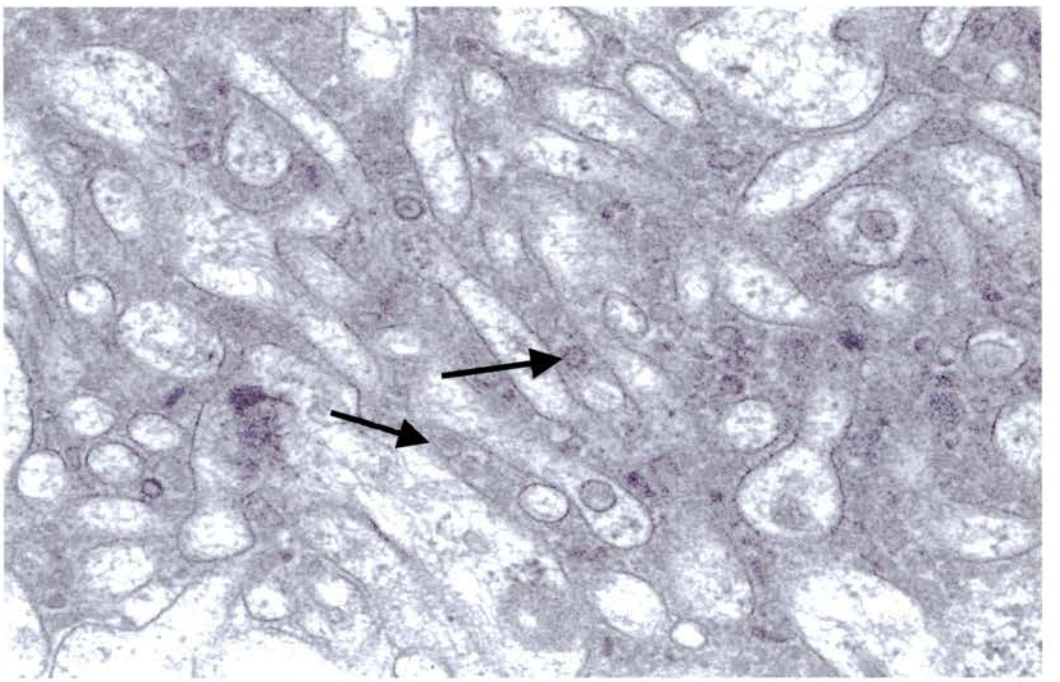

Figure 3.5.5. x45K magnification. Detail from a hypertrophic labyrinthine glomerular complex from a scrapie-infected ovine MLN. Many small spherical bodies are present within the extracellular electron-dense deposit.

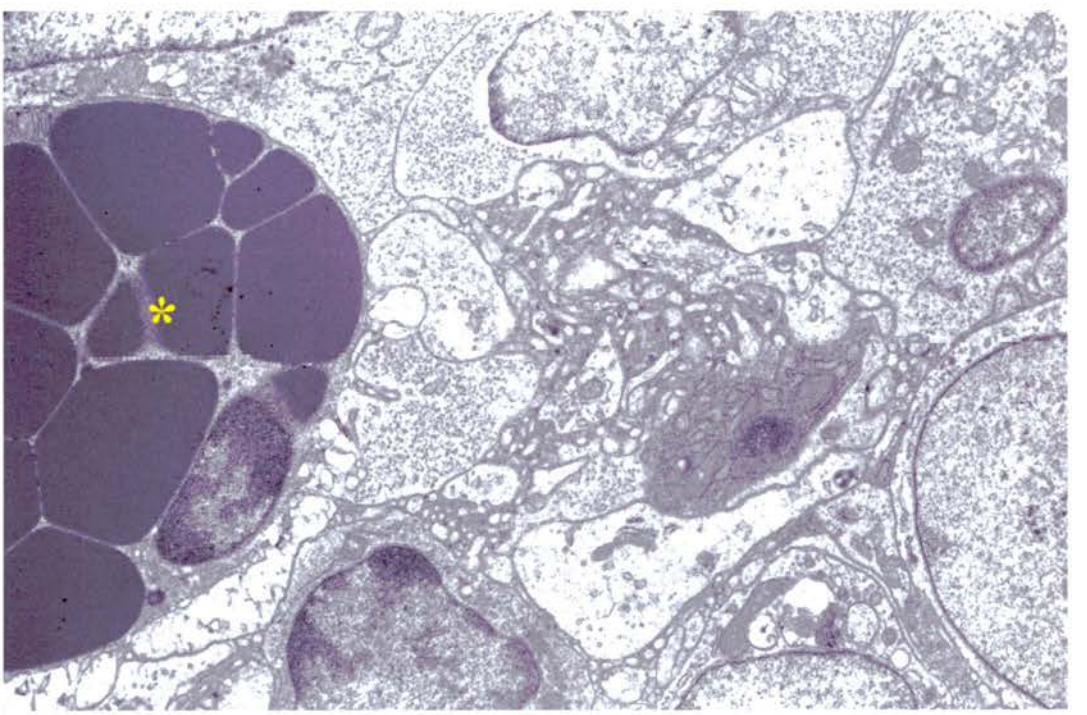

Figure 3.5.6. x8K magnification. Scrapie-infected ovine MLN. FDC dendritic profiles surround a mature B-lymphocyte (asterisk).

Ultrastructural immunolabelling method: use of Auroprobe 1 nm or Nanoprobe 1 nm Immunogold probe, and either silver stain or gold enhancement (See Appendix 6.1.l. and Figure 3.5.7a).

The standard technique used in all ultrastructural immunolabelling of murine tissue was applied to ovine MLN i.e. the Auroprobe 1 nm gold probe as described in section 2.2.7. This technique was also adapted for the use of 1 nm Nanoprobe gold probe. All primary anti-PrP antisera, found to give immunolabelling using the ABC method at the light microscopical level, yielded poor results using this technique. Following a series of titrations of the primary and gold conjugated antibodies, 1A8 and R486 antibodies were not found to immunolabel known positive ovine tissue adequately using the Auroprobe or Nanoprobe 1 nm immunogold techniques with either silver stain or gold enhanced methods. PrP^d labelling, where present, was very light and confined to TBM lysosomes, and, occasionally, small areas of larger FDC labyrinthine glomerular complexes.

Ultrastructural immunolabelling: tyramide amplification with anti-biotin gold (See Appendix 6.1.n. and Figure 3.5.7b).

The Dako Catalysed signal amplification technique was adapted for use at the ultrastructural level. This technique is a recently devised amplification system used to enhance light microscopical immunohistochemical techniques, where antigen is present in small quantities, or where primary antibody has a low affinity for the studied antigen. This technique is based on the principle that peroxidase already

present in the form of attached immune complex can catalyse the deposition of biotinylated tyramide molecules at the antigen / antibody complex site (Mayer & Bendayan 2001). Neither a 1 nm nor 5 nm anti-biotin gold probe (British Biocell International, Cardiff, UK) enhanced with silver (Amersham Plc, Buckinghamshire, UK) improved PrP^d immunolabelling in ovine tissues when compared to the Auroprobe and Nanoprobe methods detailed above.

Ultrastructural immunolabelling: NEN tyramide amplification with anti-biotin gold

The working principles of the NEN tyramide amplification system are similar to those of the Dako system detailed above, however, the NEN system has previously been used in conjunction with gold probes to visualise ultrastructural antigens (NEN life sciences, Boston, USA). Again, silver-enhanced 1 and 5 nm anti biotin gold probes were used. This technique did not improve the 1 nm Nanoprobe technique.

Ultrastructural immunolabelling: ABC with anti biotin gold probe (see Appendix 6.1.o. and Figure 3.5.7c)

The ABC technique described in section 2.2.5.2. was adapted for use at the ultrastructural level using both anti-biotin gold probes described above. This method resulted in no PrP^d immunolabelling of ovine tissue.

Ultrastructural immunolabelling: Envision with anti HRP gold probe (see Appendix 6.1.p. and Figure 3.5.7d)

The Envision system described in section 2.2.5.3. was adapted and applied to ovine and murine control tissue. A silver enhanced 1 or 5 nm anti HRP conjugated gold probe was used as a visualisation product. No immunolabelling was seen in ovine or murine tissue.

As none of the amplification systems tested enhanced immunolabelling, this would suggest the antigen itself or the attached primary antibody are unavailable for further amplification steps.

Figure 3.5.7. Ultrastructural immunolabelling

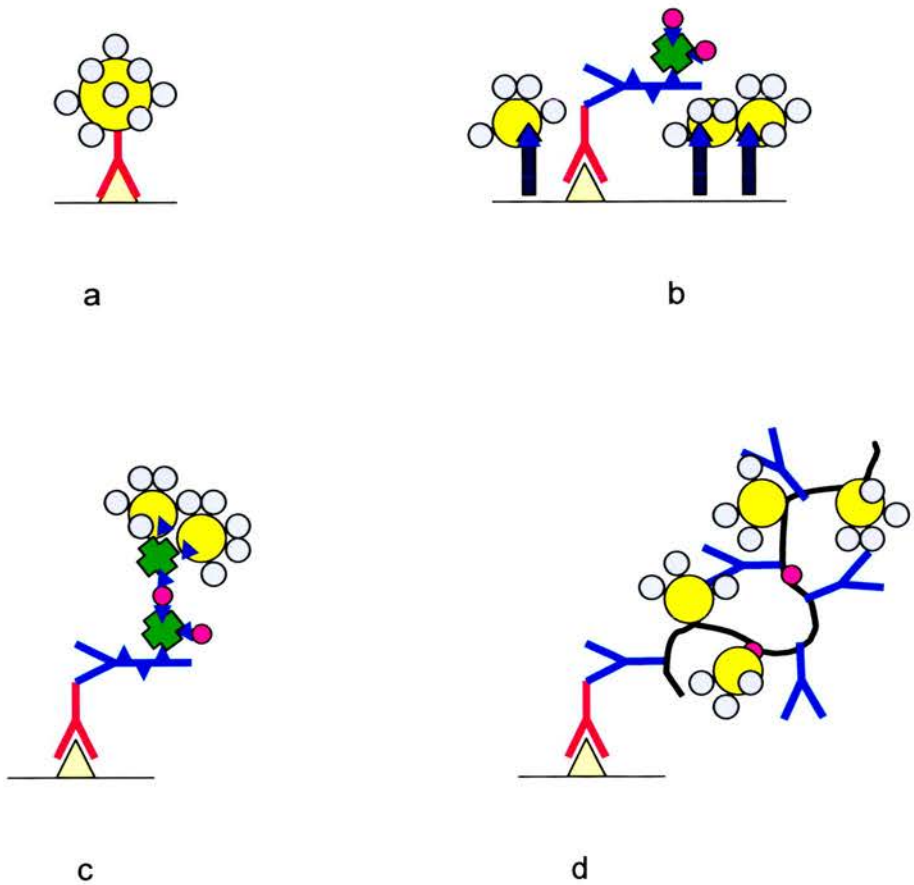

Figure 3.5.7a. Direct immunogold labelling. A gold probe is attached directly to the specific primary antibody and is enhanced using a silver or gold enhancement technique.

Figure 3.5.7b. Tyramide amplification. Peroxidase immune complex catalyses biotinylated tyramide deposition of gold molecules at the antigen / antibody complex site. Gold is enhanced using silver or gold enhancement.

Figure 3.5.7c. Avidin / biotin amplification. This is an indirect labelling method. An avidin / biotin complex is attached to the biotinylated secondary antibody. A gold probe is attached to the complex that is then enhanced.

Figure 3.5.7d. Envision system amplification. This is a direct method whereby a polymer chain consisting of many secondary antibodies bound to the primary antibody can bind a large number of horseradish peroxidase molecules. A gold probe is attached to the HRP molecules followed by enhancement.

Light microscopical immunolabelling: application of ultrastructural Immunogold silver stain (IGSS) technique

In order to ascertain whether immunogold labelling of ovine MLN was possible, i.e. if the gold probes couple with primary antibodies, the Nanoprobe gold probe technique was adapted for use at the light microscopical level. Using the etch and pre-treatments applied to 1μm sections using the ABC technique, followed by application of R486 PrP anitsera, Nanoprobe 1 nm and finally Nanoprobe LM silver enhancement, good follicular PrP^d immunolabelling was obtained. Using sodium meta-periodate etch technique, no immunolabelling was obtained.

Fixative / embedding medium comparison

As described above, poor immunolabelling of ovine tissue at the ultrastructural level following application of immunohistochemical methods was observed. To ensure antigenicity was not compromised as a result of fixation or processing, formalin-fixed lymph node was processed into resin, and paraformaldehyde-fixed lymph node was embedded in paraffin wax. Levels of immunolabelling in paraformaldehyde fixed tissue were found to be similar to that of formalin-fixed paraffin-embedded tissue. Formalin-fixed resin-embedded tissue also gave poor immunolabelling at the ultrastructural level.

Effect of section thickness at LM

The effect of section thickness on antigenicity was tested in order to identify whether the lack of immunolabelling at the ultrastructural level was as a result of the reduction in section thickness and subsequent decrease of detectable antigen. 100 nm, 250 nm, 400 nm, 600 nm and 1 μm sections were immunolabelled using the avidin biotin technique and R486 PrP antisera. At all antibody concentrations, all tested sections showed immunolabelling, however, decreased section thickness resulted in very pale DAB reaction product. Retention of counterstain also became increasingly poor as section thickness decreased, suggesting visualisation of a labelled molecule or molecules is dependent on molecular density.

Section thickness study at EM

Ovine lymph nodes were sectioned at various thicknesses ranging from 55 nm to 1 μm. These grids were then counterstained (see Appendix 6.1.k). At thicknesses greater than 100 nm, it became impossible to determine tissue ultrastructure due to the decreasing penetration of electrons through the tissue. Thick sections were therefore not immunolabelled for ultrastructural study.

Etching techniques for ultrastructural study

Araldite is an epoxide resin that is tightly bonded allowing very little penetration of aqueous reagents and antibodies into the hydrophobic matrix. Permeation of this

plastic matrix is only possible if a surface gel layer is created which can be swollen with water and subsequently allows reagents and antibodies to reach the tissue.

A gel layer may be created in 2 ways:

1. Treatment with an oxidising agent e.g. hydrogen peroxide, sodium meta-periodate. Hydrophobic alkane side chains are oxidised, which increases the hydrophillicity of the resin.
2. Treatment with an alkoxide, e.g. sodium ethoxide. The curing system for epoxy resin involves ester cross-linking. The addition of sodium ethoxide causes the ester cross links to be broken, resulting in a net increase in hydrophilic groups (Causton 1984).

In order to investigate which "etching" techniques would be suitable for ovine ultrastructural PrP^d immunolabelling, 1μm sections on glass slides were studied. Light microscopical resin labelling is a considerably easier technique, therefore a more appropriate initial method for this study.

- Sodium meta-periodate

The immunogold technique previously identified for use with murine tissues (see section 2.2.7. and Appendix 6.1.l) involves the application of saturated sodium meta-periodate to tissue sections as an oxidising reagent, allowing penetration of reagents into the resin matrix. Although murine tissues could be etched appropriately to reveal immunolabelling, when this reagent was applied as an etching technique to ovine tissues for ultrastructural study, no PrP^d immunolabelling was observed. This was confirmed at the light microscopical level, where no immunolabelling was observed using a sodium meta-periodate etch and the standard ABC technique.

It was therefore considered possible that the sodium meta-periodate etching technique resulted in the loss of antibody (R486) epitopes. Therefore, a wide cross section of PrP^d antibodies, each targeting different amino acid sequences within the PrP molecule were used to immunolabel PrP^d at the light level using the ABC technique. Neither R145, 1A8, 505.5 nor 521.7, immunolabelled PrP^d positive ovine MLN at the ultrastructural level, using the Auroprobe technique with a sodium-meta periodate etch. Murine brain and spleen were also treated with a sodium-meta periodate etch. Moderate immunolabelling was observed in all murine tissues studied.

- Hydrogen peroxide.

10% hydrogen peroxide is commonly used to oxidise the resin matrix (Newman & Jasani 1984). Chemically, this has a similar effect to sodium meta-periodate. When hydrogen peroxide was applied to 1 μm murine tissues, PrP^d immunolabelling was observed. However, PrP^d was not immunolabelled in 1 μm ovine tissues when similarly treated. Therefore no ultrastructural studies were undertaken utilising this etching technique.

- Periodic acid

10% aqueous periodic acid was used in conjunction with sodium meta-periodate to etch 1 μm sections; however, again, no immunolabelling was observed at light microscopy in ovine tissues using this technique.

- Iodine solution (acetone)

Iodine in absolute acetone is known to soften epoxy resin, and can be employed in conjunction with absolute acetone washes to remove resin prior to immunolabelling. Slides were placed in a 10% iodine solution in acetone for 16 hours, followed by consecutive washes in 100% acetone for between 4 and 24 hours. Limited immunolabelling was observed in all murine tissues, regardless of the length of acetone wash. No immunolabelling was seen in any ovine tissue sections.

- Sodium ethoxide

Unlike the previous etching techniques, this technique involves the breaking of ester cross links within the resin matrix. It is routinely used for light level resin immunohistochemistry, and is therefore known to remove resin sufficiently from tissue sections to allow immunolabelling.

In order to ascertain an appropriate etching time for 55 nm sections for ultrastructural study, sections on grids were etched at various dilutions of neat sodium ethoxide in ethanol for various times (see Table 3.5.2). Sections were counterstained and analysed ultrastructurally. Good tissue integrity and reasonably good structure were obtained using 1:4 dilution of sodium ethoxide for 10 seconds, followed by graded alcohol / water washes. Shorter times, or more dilute etching solution, maintained good structure while longer etching times or more concentrated etching solution, resulted in loss of tissue.

Etch Time	Etch Conc.	Tissue structure / integrity	Immunolabelling
3 sec	1:1	Damaged	N/A
3 sec	1:2	Damaged	N/A
3 sec	1:4	Damaged	N/A
3 sec	1:10	Damaged	N/A
10 sec	1:1	Damaged	N/A
10 sec	1:2	Damaged	N/A
10 sec	1:4	Good	Moderate
10 sec	1:10	Very good	None
30 sec	1:1	Damaged	N/A
30 sec	1:2	Damaged	N/A
30 sec	1:4	Damaged	N/A
30 sec	1:10	Good	Light

Table 3.5.2. Table showing sodium ethoxide concentrations and times, and results obtained.

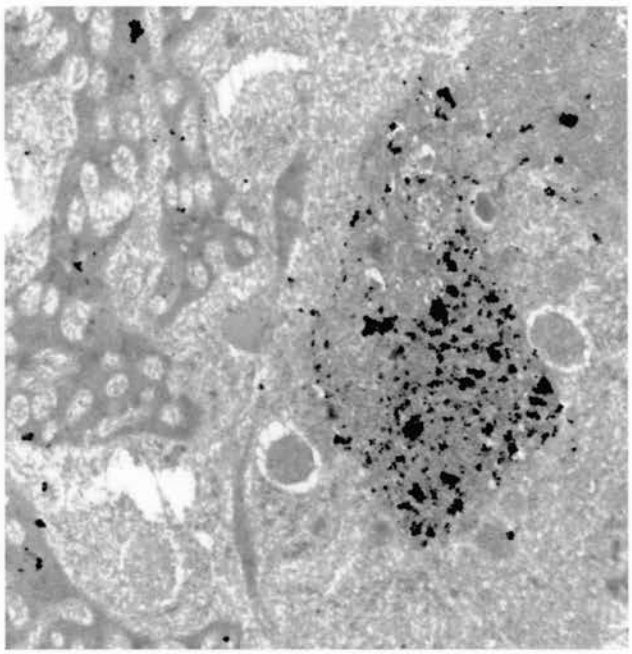

Figure 3.5.8. x16K magnification. Immunolabelled secondary follicle from the MLN of a scrapie-infected sheep. FDC dendritic profiles are sparsely labelled, while PrP^d immunolabelling is abundant within an adjacent TBM lysosome.

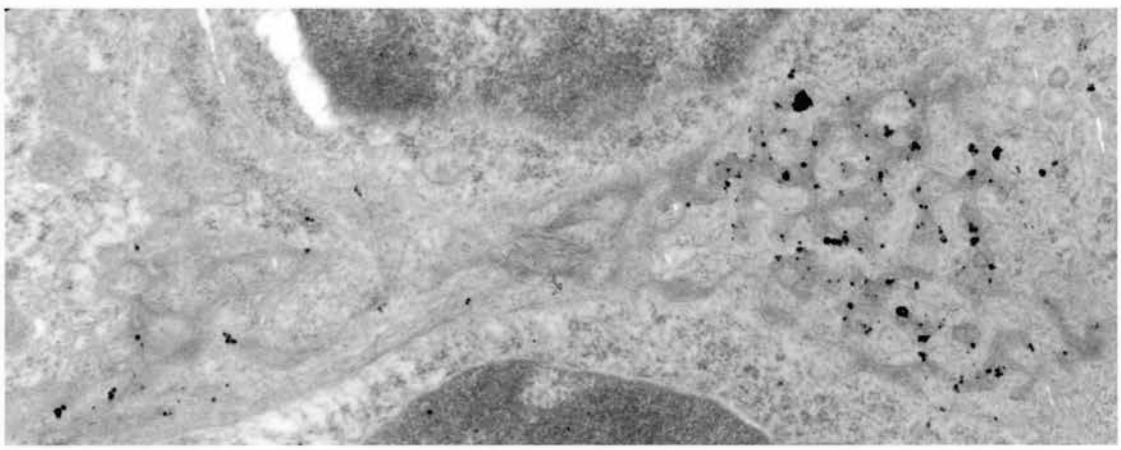

Figure 3.5.9. x20K magnification. Immunolabelled secondary follicle from the MLN of a scrapie-infected sheep. Moderate PrP^d immunolabelling is associated with the plasmalemma of FDC dendritic profiles.

When this etching solution was applied to 55 nm sections of ovine MLN, followed by the standard Nanoprobe / gold enhance immunogold technique, light to significant immunolabelling was observed within TBM lysosomal compartments (Figure 3.5.8), and in association with FDC labyrinthine complexes (Figure 3.5.9). Replication of this technique was extremely difficult to achieve on consecutive tissue sections. Where tissue was retained following the immunolabelling procedure, only very slight labelling was observed, a large portion of sections treated demonstrated no immunolabelling. Although etching times and concentrations were considered to be very accurate, some tissue sections were lost during immunolabelling, presumably due to over-etching of the tissue. This was considered the likely explanation, as some tissues, although present, were virtually destroyed, membranes were unrecognisable, while intracellular organelles were absent or appeared distorted. As the chemical process involved in alkoxide etching is considerably more aggressive than the oxidation reaction, it appears tissue destruction is more likely using this technique. Even tissues that were briefly etched appeared more damaged than those that were etched using an oxidation reaction. Although four different antibodies were applied using this technique, the TBM and FDC labelling described was only seen using R486 antibody.

Routinely, ultrastructural studies involved immunolabelling sections from ovine brain in conjunction with the MLN tissues. Surprisingly, where tissue sections were not over-etched, some immunolabelling was consistently seen. In scrapie-infected brain tissue sampled at the dorsal motor nucleus of the vagal nerve both intracellular and extracellular labelling patterns were detected. Intracellular labelling consisted of intralysosomal labelling in neurons and astrocytes. Additionally, labelling was found

within the extracellular space, where it was occasionally seen in association with short rods or amyloid-like filaments. It was also detected in association with abnormal coated pits. As mentioned previously, tissues did appear less well-preserved than following oxidation etching. Light and electron microscopical immunolabelling techniques applied are summarised in Table 3.5.3.

Etch technique	Immunolabelling technique							
	Direct immunogold		Tyramide amplification		ABC amplification		Envision Amplification	
	LM	EM	LM	EM	LM	EM	LM	EM
Sodium m-periodate	-	+	n/t	-	-	-	n/t	-
Hydrogen peroxide	n/t	n/t	n/t	n/t	-	n/t	n/t	n/t
Periodic acid	n/t	n/t	n/t	n/t	-	n/t	n/t	n/t
Iodine	n/t	n/t	n/t	n/t	-	n/t	n/t	n/t
Sodium ethoxide	++	++	n/t	n/t	+++	-	++	-

n/t: not tested
- : negative
+ : light immunolabelling
++: Moderate immunolabelling
+++: good immunolabelling

Table 3.5.3. Table showing the degree of positive immunolabelling of ovine MLN using a variety of etching and immunolabelling techniques.

Discussion

Despite the satisfactory immunolabelling of scrapie-infected murine spleen, it has proved extremely problematic to achieve adequate sub-cellular visualisation of PrP^d within the LRS of sheep. Immunolabelling of resin-embedded, scrapie-infected ovine MLNs at the light microscopical level demonstrated abundant labelling of comparable magnitude to that of routine paraffin wax light microscopy. However, when the technique is adapted for use at the sub-cellular level, limited immunolabelling of the LRS, and to a lesser extent the CNS, is achieved. Sub-cellular murine PrP^d is easily obtained using this method.

The results discussed in this chapter suggest perhaps that inter-species and inter-tissue conformational differences of the PrP^d molecule may be paramount in understanding differences in immunolabelling between both ovine and murine tissues, and CNS and LRS tissues of sheep.

Using antibodies specific to ovine PrP in conjunction with the technique developed for light microscopical immunolabelling of murine splenic tissue, two distinct patterns of immunolabelling were observed within easily defined secondary follicles of the MLN from scrapie-infected sheep. Unlike murine spleen, these follicles were clearly outlined by a distinct margin of cells known as the mantle zone, while PrP^d within germinal centres of scrapie-infected sheep was considerably more easily defined and abundant using immunolabelling techniques. These results correlate with previous light microscopical studies of paraffin embedded ovine lymph nodes obtained from clinically sick sheep (Van Keulen et al. 1996; Schreuder et al.1998; Jeffrey et al. 2001b).

Ultrastructural study of scrapie-infected MLNs, revealed a much more widespread network of hypertrophic FDCs within the light zone of the germinal centre, than was previously observed within scrapie-infected murine spleen. Again, this correlates with light microscopical findings insofar as FDC networks have been observed to occupy most of the space between lymphocytes of the light zone of the follicle. This may simply be due to the inherent size difference between murine and ovine lymph nodes, but what is clear is that the abnormal FDC hypertrophy, and subsequent increase in electron-dense deposit as a result of scrapie infection, is not restricted to murine spleen. Small vesicular bodies observed within the extracellular space surrounding FDC cytoplasmic extensions from ovine MLN, were not present within the spleens of mice. Spherical bodies of unknown cause and function within the ileal Peyer's patches similar to the particles seen in this study, have been previously described. These authors suggest that the particles may initially be membrane-bound to the follicle associated epithelium then shed into the intercellular space. Later, these particles are found within the follicles of the Peyer's patches in association with both FDCs and lymphocytes (Landsverk 1987; Landsverk et al. 1990; Landsverk et al. 1991).

All murine immunolabelling is undertaken using the 1A8 PrP antisera. This antibody recognises epitopes of the PrP molecule at 3 different amino acid sequences from the N' terminus, through the globular domain to the C' terminus (Farquhar et al. 1993) (see also Figure 3.5.1 in this chapter). 1A8 gives excellent immunolabelling of all murine tissues tested, both at the light and ultrastructural levels. Using the same light microscopical and ultrastructural immunolabelling techniques, ovine CNS and LRS tissues immunolabelled poorly at the LM level, and not at all the sub-cellular level

using 1A8 antisera. This suggests the configuration of the PrP^d molecule differs between species, and that the antigenic sites, recognised by the 1A8 antisera, remain hidden in ovine tissues. Not only do interspecies differences in the protein conformation of PrP lead to antibody specificity differences, but inter-tissue conformation changes probably also occur. The conversion of the normal PrP molecule to that of the disease-specific form has been well documented (Caughey et al. 1991; Pan et al. 1993). This conversion results in structural change, and the PrP^d may be present in many truncated and non-truncated forms (Hope et al. 1986; Jeffrey et al. 2001a). It may therefore be possible that PrP^d can be released or accumulated in many different conformational forms, depending on cell type or location, for example, an N' terminally truncated form is known to be present within macrophages (Jeffrey et al. 2001a).

Resin removal techniques, such as oxidation and transesterification, also influence levels of immunolabelling. Resin removal at the light microscopical level is sufficient to allow good immunolabelling of ovine tissues, however, using many different ultrastructural etching techniques, immunolabelling is inconsistent and at a considerably lower level than murine labelling patterns. PrP^d immunolabelling can be achieved at the light microscopical level using transesterification etch, and ultrastructural level following both oxidation and transesterification in murine brain (Jeffrey & Goodsir 1996) and spleen (chapter 3.1 and 3.2). Although light microscopical labelling can be obtained in sheep tissue using the same etch techniques as defined for murine tissue, none of the ultrastructural etching techniques employed allow for comparable levels of labelling as seen in murine tissue. This would infer that the nature of the chemical etch is important for antigen exposure. In

ovine tissue, resin removal may be inadequate to expose the specific antigenic site, or alternatively, the site may be damaged by the etching techniques. As PrP immunolabelling was easier to obtain in the CNS of sheep, it may be more resilient within the CNS than the LRS. This may suggest the specific PrP epitope recognised by the antibody has been damaged in the LRS. However, PrP within the CNS may also be more abundant, suggesting the lack of LRS immunolabelling may relate to sensitivity of the immunolabelling technique. To further address the problem of sensitivity, more must be understood regarding cross linkage and bonding between tissue molecules and the resin matrix. This may in turn result in more study of the nature of the PrP protein itself.

Although formalin fixed, resin embedded tissue did not yield an increase in immunolabelling over gluteraldehyde-fixed resin-embedded tissues, the fixative may nevertheless have some influence upon antigenicity. The detrimental effects of fixation have been well documented (Sabatini & Bensch 1963; Hayat 1989), and the cumulative negative effect of fixation and resin embedding may be significant. In this case, pre-embedding techniques may need to be deployed in order to achieve any significant immunolabelling of ovine lymphoreticular tissues.

Future study must involve experimentation with different forms of embedding; for example, water-based resins require no etching, although fine structure is compromised. At the very least, this would allow further analysis of the conformation of the PrP protein and its interactions with fixatives and resin polymers. If, as seems likely, chemical etching is the key to PrP^d exposure, further investigation of post-embedding immunohistochemistry of ovine tissue should be

based on this premise. Trans-esterification etching techniques must be modified to allow better tissue preservation while exposing the PrP^d molecule more thoroughly.

4. SUMMARY

In these studies I have determined methods for the ultrastructural detection of abnormal disease-associated PrP (PrP^d), characterised previously unreported sub-cellular scrapie-associated lesions and determined the sub-cellular localisation of PrP^d in the spleen of mice, and, to a lesser extent, the lymphoreticular system of sheep.

Ultrastructural immunohistochemistry is a technically demanding procedure. In order to determine methods of fixation which retain good ultrastructural morphology but allow the de-plasticization of tissues without loss of relevant antigenic epitopes, meticulous and carefully performed chequer-board investigations were needed to compare the effect of many different parameters. My studies of murine spleens have shown that satisfactory tissue morphology, combined with a significant level of antigenic recovery, may be obtained using a 0.5 % paraformaldehyde / 0.5% gluteraldehyde fixation procedure, followed by oxidative de-plasticization and an indirect immunogold visualisation method. Nevertheless, when all the different forms of PrP^d labelling seen at the light microscopical level are taken into account, the optimal ultrastructural immunogold technique developed still appears to have a reduced level of sensitivity, when compared to light level immunohistochemistry. It is not clear what parameters affect these differences in labelling sensitivity. It is possible that only the more robust and more highly aggregated forms of PrP^d are labelled by immunogold, with some accumulations of PrP^d observed by LM apparently remaining undetected at the sub-cellular level. Harsh fixation and processing techniques required for the ultrastructural analysis of tissues may degrade

or mask some forms of the PrP^d protein, and impair the ability of PrP antibodies to recognise the relevant epitopes present. Whether these epitopes have been irreversibly damaged, or whether they remain masked by resin polymer remains to be determined. This, coupled with the lack of signal amplification using the relatively basic indirect immunogold technique, may explain the probable lowered sensitivity of sub-cellular immunohistochemistry, when compared with light microscopical immunohistochemistry.

Loss of sensitivity was more conspicuous following immunolabelling of ovine lymphoid tissues, where only weak labelling was observed with different immunogold techniques, fixation and unmasking procedures. In addition to this, ovine sub-cellular studies have been restricted by the apparent difficulty of adequate resin removal. In conjunction with the indirect immunolabelling method used for murine ultrastructural studies, limited sub-cellular immunolabelling was achieved using a trans-esterification de-plasticization technique, normally reserved for light microscopical immunohistochemical techniques. With tissue de-plasticization proving to be a vital constituent of the immunolabelling procedure, both at the light and ultrastructural levels, the resin / tissue interaction that renders ovine lymphoid tissue completely impregnable to oxidative etching techniques, must be further examined.

Observations of the sub-cellular localisation of PrP^d in murine spleen tissue correlate with light microscopical immunohistochemistry studies (McBride et al. 1992, Brown et al. 1999). Patterns of immunolabelling observed at the light microscopical level, tentatively described as both follicular dendritic cell (FDC)-associated and tingible body macrophage (TBM) labelling patterns, were confirmed using the ultrastructural

immunocytochemical techniques described above. PrP^d immunolabelling was associated with the plasmalemma of both mature, and to a lesser extent, immature FDC dendritic profiles. Lysosomal TBM labelling is a feature common to all scrapie-infected spleens studied, but perhaps the most striking ultrastructural immunolabelling is related to convoluted FDC dendrites, which form labyrinthine glomerular complexes, a feature specific to all strains of scrapie which exhibit a peripheral accumulation phase, and in some cases occurring as early as 6 weeks post infection (at 15 % of the incubation period following i.p. inoculation). FDCs have been reported to be involved in various disorders affecting lymphoid tissues and in inflammation, and may be the target cell type following some viral infections. FDC proliferation is observed in several types of non-Hodgkin's lymphoma, for example follicle centre lymphoma and T cell lymphoma (Petrasch et al. 1992; Suchi et al.1987) . Lymphoid tissues also demonstrate an inflammatory reaction by becoming enlarged, and can exhibit hyperplasia. Viral particles have been observed in association with FDCs, and viral replication has been demonstrated in lymphoid follicles. This suggests that the immune complex trapping mechanism of FDCs may play an important role in the pathogenesis of such diseases (Armstrong & Horne 1984; Smith et al. 2001). FDCs are considered to play a vital role in HIV infection of germinal centres by infecting $CD4^+$ T cells. They are thought to process the virus as antigen, whereby infecting $CD4^+$ T cells as they pass through the germinal centre (Tenner-Racz et al. 1988). Ultrastructural analysis has revealed that the viral particles are located within the extracellular electron-dense deposit between adjacent dendritic profiles (Racz &.Tenner-Racz 1995). In patients with persistent generalised lymphadenopathy, FDCs reveal an increased number of organelles, and can become

hypertrophic forming small labyrinthine glomerular complexes (Armstrong & Horne 1984). These complexes appear smaller than those observed following scrapie infection, and have less abnormal accumulation of electron-dense deposit. As the HIV disease progresses and the follicle becomes increasingly distorted, in areas with abundant viral particles FDC networks degenerate and in the later stages of disease are completely lost (Tenner-Racz et al. 1985; Armstrong 1991).

The strain inoculation involving the Sinc ^{p7} mouse strain did not result in peripheral accumulation, and only minor variations of the immunolabelling patterns were observed when different strains of murine scrapie were examined in Sinc ^{s7} mouse strains. Variability was confined to differences in the temporal progression of changes, albeit these changes were consistent with the clinical disease onset and incubation times specific to the different scrapie strains examined (Bruce et al. 1994; Bruce 2003). Sub-cellular pathology of disease is indistinguishable in these strains. Excess extracellular electron-dense deposits accumulate, and occasional fibrils were found between individual FDC dendritic processes. This results in the loss of the normal tri-laminar arrangement consisting of a central electron-dense line corresponding to the site of accumulation of antigen / antibody complexes (Radoux et al. 1985) between the plasmalemmae of two adjacent FDC dendrites. Coated pits are upregulated within the follicles of scrapie-infected murine spleens, while B-lymphocytes mature to become plasmablasts within the follicle, probably due to an abnormal prolonged retention of clonally selected B cells by PrP^{d} expressing FDC dendrites. Contrary to previous dogma, these results provide morphological evidence to suggest that immune surveillance mechanisms are altered in scrapie.

Studies of scrapie - infected murine spleens following inhibition of cytokine signalling and subsequent FDC development have provided little conclusive data. Although light microscopical results suggest FDCs play a role in neuroinvasion during the early stages of scrapie infection (Mabbott et al. 2000b), the studies undertaken in section 3.4. do not conclusively reveal the relationship between these manipulated murine models and neuroinvasion. Larger experimental groups with both longer scrapie incubation periods and varying time intervals between cytokine inhibition and tissue collection may enable more definitive conclusions to be drawn. I have also confirmed that scrapie infection of sheep causes similar disease-specific pathological effects within the lymphoreticular system to those identified in the spleen of mice. As previously seen in murine spleens, FDCs within the follicle of mesenteric lymph nodes of sheep form highly convoluted dendritic complexes with excess associated electron-dense deposit and the loss of intermediate dense line. Unlike that seen within murine spleens, this electron-dense deposit contains many as yet unidentified spherical structures. Other pathological changes associated with scrapie infection, such as up-regulation of clathrin-coated pits, fibril formation and abnormal retention of B-lymphocytes are also present within ovine lymph nodes. Although sensitive methods of immunolabelling of ovine MLN remain to be developed, it may be hypothesised from the limited results obtained that PrP^d within ovine MLN has a similar pattern of expression to that previously recognized within murine spleen. In order to confirm these preliminary observations, further investigation of the nature of resin / tissue interaction with antigen recovery must be obtained.

A more complete understanding of the pathological features of scrapie infection already discussed within this thesis must also be acquired. The exact nature of the disease-specific excess extracellular electron-dense deposit surrounding FDC plasmalemmae, and the cause and mechanisms of coated pit upregulation must be further investigated.

In conclusion, the work undertaken in this thesis has both advanced the understanding of immunohistochemical techniques for the sub-cellular study of scrapie infection in the lymphoreticular system of mice and sheep and distinguished abnormal sub-cellular features associated with scrapie infection. I have also analysed the importance of FDCs in the pathogenesis of the disease. Collectively, these results have increased our knowledge of the pathogenesis of scrapie infection in the lymphoreticular system.

5. REFERENCE LIST

Aguzzi, A. & Weissman, C.1997. Prion Research: The Next Frontiers. *Nature* 389: 795 - 798.

Alimzhanov, M. B., Kuprash, D. V., Kosco-Vilbois, M. H., Luz, A., Turetskaya, R. L., Tarakhovsky, A., Rajewsky, K., Nedospasov, S. A. & Pfeffer, K. 1997. Abnormal development of secondary lymphoid tissues in lymphotoxin beta-deficient mice. *Proc Nat Acad Sci* 94: 9302 - 9307.

Alper, T., Cramp, W. A., Haig, D. A. & Clarke, M. C. 1967. Does the agent of scrapie replicate without nucleic acid? *Nature* 214: 764 - 766.

Armstrong, J. A. & Horne, R. 1984. Follicular dendritic cells and virus-like particles in AIDS-related lymphadenopathy. *Lancet* ii: 370-2.

Armstrong, J. A. 1991. Ultrastructure and significance of the lymphoid tissue lesions in HIV infection. In Racz, P., Dijkstra, C. D. & Gluckman J.C. (Eds). Accessory cells in HIV and other retroviral infections (pp. 69 - 82). Basel: Karger.

Bainton, D. F. 1981. The discovery of lysosomes. *J Cell Biol* 91: 66s - 76s.

Beekes, M., Baldauf, E., Cassens, S., Diringer, H., Keyes, P., Scott, A. C., Wells, G. A. H., Brown, P., Gibbs, C. J., Jr. & Gajdusek, D. C. 1995. Western blot mapping of disease-specific amyloid in various animal species and humans with transmissible spongiform encephalopathies using a high-yield purification method. *J Gen Virol* 76: 2567 - 2576.

Begara-McGorum, I., Gonzalez, L., Simmons, M., Hunter, N., Houston, F. & Jeffrey, M. 2002. Vacuolar lesion profile in sheep scrapie: Factors influencing its variation and relationship to disease-specific PrP accumulation. *J Comp Path* 127[1]: 59 - 68.

Belt, P. B. G. M., Muileman, I. H., Schreuder, B. E. C., Bosderuijter, J., Gielkens, A. L. J. & Smits, M. A. 1995. Identification of 5 allelic variants of the sheep PrP gene and their association with natural scrapie. *J Gen Virol* 76: 509 - 517.

Bencsik, A., Lezmi, S. & Baron, T. 2001. Autonomous nervous system innervation of lymphoid territories in spleen: A possible involvement of noradrenergic neurons for prion neuroinvasion in natural scrapie. *J Neurovirol* 7: 447 - 453.

Beringue, V., Demoy, M., Lasmézas, C. I., Gouritin, B., Weingarten, C., Deslys, J. P., Andreux, J. P., Couvreur, P. & Dormont, D. 2000. Role of spleen macrophages in the clearance of scrapie agent early in pathogenesis. *J Pathol* 190: 495 - 502.

Blattler, T., Brandner, S., Raeber, A. J., Klein, M. A., Voigtlander, T., Weissmann, C. & Aguzzi, A. 1997. PrP-expressing tissue is required for transfer of scrapie infectivity from spleen to brain. *Nature* 389: 69 - 73.

Blattler, T. 2002. Implications of prion diseases for neurosurgery. *Neurosurg Rev* 25: 195 - 203.

Bolam, J. P. 1992. Preparation of central nervous system tissue for light and electron microscopy. In: Bolam, J. P. (Ed). Experimental Neuroanatomy; A practical approach (pp. 1 - 29). Oxford University Press.

Bosseloir, A., Bouzahzah, F., Simar, L. & Heinen, E. 1995. B cells in contact with FDC. In: Heinen, E. (Ed). Follicular dendritic cells in normal and pathological conditions (pp. 53 - 78). Springer, Heidelberg, Germany.

Bossers, A., Schreuder, B. E. C., Muileman, I. H., Belt, P. B. G. M. & Smits, M. A. 1996. PrP genotype contributes to determining survival times of sheep with natural scrapie. *J Gen Virol* 77: 2669 - 2673.

Bostock, C. J. 2000. The nature of TSEs. *Microbiol Today* 27: 164-166.

Brandner, S., Isenmann, S., Raeber, A., Fischer, M., Sailer, A., Kobayashi, Y., Marino, S., Weissmann, C. & Aguzzi, A. 1996. Normal host prion protein is necessary for scrapie-induced neurotoxicity. *Nature* 379: 339 - 343.

Brown, K. L., Stewart, K., Bruce, M. E. & Fraser, H. 1997. Severely combined immunodeficient (SCID) mice resist infection with bovine spongiform encephalopathy. *J Gen Virol* 78: 2707-2710.

Brown, K. L., Stewart, K., Ritchie, D. L., Mabbott, N. A., Williams, A., Fraser, H., Morrison, W. I. & Bruce, M. E. 1999. Scrapie replication in lymphoid tissues depends on prion protein-expressing follicular dendritic cells. *Nat Med* 5: 1308 -1312.

Brown, P. 1998. Transmission of spongiform encephalopathy through biological products. *Dev Biol Stand* 93: 73 - 78.

Brown, W. J., Goodhouse, J. & Farquhar, M. G. 1986. Mannose-6-phosphate receptors for lysosomal enzymes cycle between the Golgi complex and endosomes. *J Cell Biol* 103: 1235 - 1247.

Browning, J. L., Ngam-ek, A., Lawton, P., DeMarinis, J., Tizard, R., Chow, E. P., Hession, C., O'Brine-Greco, B., Foley, S. F. & Ware, C. F. 1993. Lymphotoxin beta, a novel member of the TNF family that forms a heteromeric complex with lymphotoxin on the cell surface. *Cell* 72: 847 - 856.

Bruce, M. E. & Fraser, H. 1981. Effect of route of infection on the frequency and distribution of cerebral amyloid plaques in scrapie mice. *Neuropathol and Appl Neurobiol* 7: 289 - 298.

Bruce, M., Chree, A., McConnell, I., Foster, J., Pearson, G. & Fraser, H. 1994. Transmission of bovine spongiform encephalopathy and scrapie to mice: strain variation and the species barrier. *Philosophical Transactions - Royal Society of London.Series B* 343: 405 - 411.

Bruce, M. E. 1996. Strain typing studies of scrapie and BSE. In: Baker, H. F. & Ridley, R. M. (Eds) Prion Diseases (pp. 223 - 236). Humana Press Inc.

Bruce, M. E., Will, R. G., Ironside, J. W., McConnell, I., Drummond, D., Suttie, A., McCardle, L., Chree, A., Hope, J., Birkett, C., Cousens, S., Fraser, H. & Bostock, C.

J. 1997. Transmissions to mice indicate that 'new variant' CJD is caused by the BSE agent. *Nature* 389: 498 - 501.

Bruce, M. E. 2003. TSE strain variation. *Brit Med Bull* 66: 99 - 108.

Bueler, H., Fischer, M., Lang, Y., Bluethmann, H., Lipp, H-P., DeArmond, S. J., Prusiner, S. B., Aguet, M. & Weissmann, C. 1992. Normal development and behaviour of mice lacking the neuronal cell-surface PrP protein. *Nature* 356: 577 - 582.

Bueler, H., Aguzzi, A., Sailer, A., Greiner, R. A., Autenried, P., Aguet, M. & Weissmann, C. 1993. Mice devoid of PrP are resistant to scrapie. *Cell* 73: 1339 - 1347.

Burton, G. F., Kosco, M. H., Szakal, A. K. & Tew, J. G. 1991. ICCOSOMES and the secondary antibody response. *Immunology* 73: 271 - 276.

Burton, G. F., Kupp, L. I., McNalley, E. C. & Tew, J. G. 1995. Follicular dendritic cells and B cell chemotaxis. *Eur J Immunol* 25: 1105 - 1108.

Carp, R. I. & Callahan, S. M. 1982. Effect of mouse peritoneal macrophages on scrapie infectivity during extended in vitro incubation. *Intervirol* 17: 201 - 207.

Carp, R. I., Callahan, S. M., Patrick, B. A. & Mehta, P. D. 1994. Interaction of scrapie agent and cells of the lymphoreticular system. *Arch Virol* 136: 255 - 268.

Caughey, B. W., Dong, A., Bhat, K. S., Ernst, D., Hayes, S. F. & Caughey, W. S. 1991. Secondary structure analysis of the scrapie-associated protein PrP 27-30 in water by infrared spectroscopy. *Biochem (Washington)* 30: 7672 - 7680.

Causton, B. E. 1984. The choice of resins for electron immunocytochemistry. In: Polak, J. M. & Varndell, I. M. (Eds). Immunolabelling for electron microscopy (pp. 29 - 36). Elsevier science.

Chandler, R. L. 1961. Encephalopathy in mice produced by inoculation with scrapie brain material. *Lancet* i: 1378 - 1379.

Chaplin, D. D. & Fu, Y. 1998. Cytokine regulation of secondary lymphoid organ development. *Curr Opin Immunol* 10: 289 - 297.

Clarke, M. C. & Kimberlin, R. H. 1984. Pathogenesis of mouse scrapie: distribution of agent in the pulp and stroma of infected spleens. *Vet Microbiol* 9: 215 - 225.

Collinge, J., Whittington, M. A., Sidle, K. C. L., Smith, C. J., Palmer, M. S., Clarke, A. R. & Jefferys, J. G. R. 1994. Prion protein is necessary for normal synaptic function. *Nature* 370: 295 - 297.

Collinge, J., Palmer, M. S., Sidle, K. C., Gowland, I., Medori, R., Ironside, J. & Lantos, P. 1995. Transmission of fatal familial insomnia to laboratory animals. *Lancet* 346: 569 - 570.

Collis, S. C. & Kimberlin, R. H. 1989. Polyclonal increase in certain IgG subclasses in mice persistently infected with the 87V strain of scrapie. *J Comp Path* 101: 131-141.

Collis, S. C., Kimberlin, R. H. & Millson, G. C. 1979. Immunoglobulin G concentrations in the sera of Herdwick Sheep with natural scrapie. *J Comp Path* 89: 389-396.

Collis, S. C. & Kimberlin, R. H. 1983. Further studies on changes in immunoglobulin G in the sera and CSF of Herdwick sheep with natural and experimental scrapie. *J Comp Path* 93: 331-338.

Cuille, J. & Chelle, P. L. 1936. La maladie dite tremblante du mouton - est elle inoculable? *Compte Rendu de L'Academie des Sciences, Paris* 203: 1552 - 1554.

De Togni, P., Goellner, J., Ruddle, N. H., Streeter, P. R., Fick, A., Mariathasan, S., Smith, S. C., Carlson, R., Shornick, L. P. & Strauss-Schoenberger, J. 1994. Abnormal development of peripheral lymphoid organs in mice deficient in lymphotoxin. *Science* 264: 703 - 707.

Dickinson, A. G., Meikle, V. M. & Fraser, H. 1968. Identification of a gene which controls the incubation period of some strains of scrapie agent in mice. *J Comp Path* 78: 293 - 299.

Dickinson, A. G. 1976. Scrapie in sheep and goats. In: Kimberlin, R. H. (Ed). Slow virus diseases of animals and man (pp. 209 - 241). Amsterdam: North Holland.

Dickinson, A. G. & Fraser, H. 1977. Scrapie pathogenesis in inbred mice: an assessment of host control and response involving many strains of agents. In: ter Meulen, V. & Katz, M. (Eds). Slow virus infections of the central nervous system (pp. 3 - 14). Springer-Verlag, New York.

Diringer, H., Gelderblom, H., Hilmert, H., Ozel, M. & Edelbluth, C. 1983. Scrapie infectivity, fibrils and low molecular weight protein. *Nature* 306: 476 - 478.

Elsen, J. M., Khang, T. V. T. & Clouscard, C. 1996. Genetic susceptibility to subacute transmissible spongiform encephalopathies. *Point Veterinaire* 28: 27 - 32.

Ersdal, C., Simmons, M. M., Goodsir, C., Martin, S. & Jeffrey, M. 2003. Sub-cellular pathology of scrapie: coated pits are increased in PrP codon 136 alanine homozygous scrapie-affected sheep. *Acta Neuropathol (Berl)* 106: 17 - 28.

van Ewijk, W., Rozing, J., Brons, N. H. C. & Klepper, D. 1977. CellulareEvents during the primary immune response in the spleen. *Cell Tissue Res* 183: 471 - 489.

Farquhar, C. F., Somerville, R. A., Dornan, J., Armstrong, D., Birkett, C. & Hope, J. 1993. A review of the detection of PrP^{sc}. In Bradley, R. and Marchant, B. (Eds) Transmissible Spongiform Encephalopathies. 301 - 313. Brussels.

Farquhar, C. F., Dornan ,J., Somerville, R. A., Tunstal, A. M. & Hope, J. 1994. Effect of *Sinc* genotype, agent isolate and route of infection on the accumulation of protease-resistant PrP in non-central nervous system tissues during the development of murine scrapie. *J Gen Virol* 75: 495 - 504.

Ford, M. J., Burton, L. J., Morris, R. J. & Hall, S. M. 2002. Selective expression of prion protein in peripheral tissues of the adult mouse. *Neuroscience* 113: 177 - 192.

Ford, W. L. 1975. Lymphocyte migration and immune responses. *Prog Allergy* 19: 1 - 59.

Fraser, H. & Dickinson, A. G. 1970. Pathogenesis of scrapie in the mouse: the role of the spleen. *Nature* 226: 462 - 463.

Fraser, H. & Dickinson, A. G. 1973. Scrapie in mice: Agent strain differences in the distribution and intensity of grey matter vacuolation. J *Comp Path* 83: 29 - 40.

Fraser, H. 1976. The pathology of natural and experimental scrapie. In: Kimberlin, R. H. (Ed). Slow virus diseases of animals and man (pp. 267 - 305). Amsterdam: North-Holland Publishing Company. Fraser, H. & Dickinson, A. G. 1978. Studies of lymphoreticular system in the pathogenesis of scrapie. The role of spleen and thymus. *J Comp Path* 88: 563 - 573.

Fraser, H. & Farquhar, C. 1987. Ionising radiation has no influence on scrapie incubation period in mice. *Vet Microbiol* 13: 211 - 223.

Fraser, H. 1993. Diversity in the neuropathology of scrapie-like diseases in animals. *Brit Med Bull* 49: 792 - 809.

Fraser, H., Brown, K. L., Stewart, K., McConnell, I., McBride, P. & Williams, A. 1996. Replication of scrapie in spleens of SCID mice follows reconstitution with wild-type mouse bone marrow. *J Gen Virol* 77: 1935 - 1940.

Fu, Y.-X. & Chaplin, D. D. 1999. Development and maturation of secondary lymphoid tissues. *Annu Rev Immunol* 17: 399 - 433.

Gajdusek, D. C. 1977. Unconventional viruses and the origin and disappearance of kuru. *Science* 197: 943 - 960.

Ghadially, F. N. 1982. Ultrastructural pathology of the cell matrix. Butterworths.

Glauert, A. M. & Lewis, P. R. 1998. Biological specimen preparation for transmission electron microscopy. London: Portland press.

Gonzalez, L., Martin, S., Begara-McGorum, I., Hunter, N., Houston, F., Simmons, M. & Jeffrey, M. 2002. Effects of agent strain and host genotype on PrP accumulation in the brain of sheep naturally and experimentally affected with scrapie. *J Comp Path* 126: 17 - 29.

Gonzalez, L., Martin, S. & Jeffrey, M. 2003. Distinct profiles of PrP^{d} immunoreactivity in the brain of scrapie and BSE-infected sheep: implications for differential cell targeting and PrP processing. *J Gen Virol* 84: 1339 - 1350.

Gordon, W. S. 1946. Advances in veterinary research - louping ill, tick-borne fever and scrapie. *Vet Rec* 58: 516 - 520.

Griffith, J. S. 1967. Self-replication and scrapie. *Nature* 215: 1043 - 1044.

Groschup, M. H., Kuczius, T., Junghans, F., Sweeney, T., Bodemer, W. & Buschmann, A. 2000. Characterization of BSE and scrapie strains / isolates. *Arch Virol* 217 - 226.

Hadlow, W. J., Kennedy, R. C. & Race, R. E. 1982. Natural infection of Suffolk sheep with scrapie virus. *J Infect Dis* 146: 657 - 664.

Harris, D. A. 1999. Cell biological studies of the prion protein. In: Harris, D. A (Ed). Prions – molecular and cellular biology (pp. 53 - 66). Norfolk: Horizon scientific press.

Hayat, M. A. 1989. Electron microscopy biological applications principles and techniques. Hampshire: Macmillan press Ltd.

Heggebo, R., Press, C. M., Gunnes, G., Gonzalez, L. & Jeffrey, M. 2002. Distribution and accumulation of PrP in gut-associated and peripheral lymphoid tissue of scrapie-affected Suffolk sheep. *J Gen Virol* 83: 479 - 489.

Heggebo, R., Gonzalez, L., Press, C. M., Gunnes, G., Espenes, A. & Jeffrey, M. 2003. Disease-associated PrP in the enteric nervous system of scrapie-affected Suffolk sheep. *J Gen Virol* 84: 1327 - 1338.

Heinen, E., Radoux, D., Kinet-Denoel, C., Moeremans, M., de Mey, J. & Simar, L. J. 1985. Isolation of follicular dendritic cells from human tonsils and adenoids III. Analysis of their Fc receptors. *Immunology* 54: 777 - 784.

Heinen, E., Braun, M., Coulie, P. G., Van Snick, J., Moeremans, M., Cormann, N., Kinet-Denoel, C., Simar, L. J et al. 1986. Transfer of immune complexes from lymphocytes to follicular dendritic cells. *Eur J Immunol* 16: 167 - 172.

Heinen, E. 1995. History of FDCs. In: Heinen, E. (Ed) Follicular dendritic cells in normal and pathological conditions (pp. 5 - 22). Heidelberg: Springer-Verlag.

Heinen, E., Bosseloir, A. & Bouzahzah, F. 1995. Follicular Dendritic cells: origin and function. *Curr top Microbiol Immunol* 201: 15 - 47.

Heusermann, U., Zurborn, K. H., Schroeder, L. & Stutte, H. J. 1980. The origin of the dendritic reticulum cell. *Cell Tissue Res* 209: 279 - 294.

Hill, E., van Der, K. J., Downes, C. P. & Smythe, E. 2001. The role of dynamin and its binding partners in coated pit invagination and scission. *J Cell Biol* 152: 309 - 323.

Hope, J., Morton, L. J. D., Farquhar, C. F., Multhaup, G., Beyreuther, K. & Kimberlin, R. H. 1986. The major protein of scrapie-associated fibrils (SAF) has the same size, charge distribution and N-terminal protein sequence as predicted for the normal brain protein (PrP). *EMBO J* 5: 2591 – 2597.

Horiuchi, M. & Caughey, B. 1999. Specific binding of normal prion protein to the scrapie form via a localized domain initiates its conversion to the protease-resistant state. *EMBO J* 18: 3193 - 3203.

Humphrey, J. H. 1981. Tolerogenic or immunogenic activity of hapten-conjugated polysaccharides correlated with cellular localization. *Eur J Immunol* 11: 212 – 220.

Humphrey, J. H. 1985. Splenic macrophages: antigen presenting cells for T1-2 antigens. *Immunol lett* 11: 149 - 152.

Hunter, N., Dann, J. C., Bennett, A. D., Somerville, R. A., McConnell, I. & Hope, J. 1992. Are *Sinc* and the PrP Gene Congruent? Evidence from PrP Gene Analysis in Sinc Congenic Mice. *J Gen Virol* 73: 2751 - 2755.

Hunter, N. 1996a. Genotyping and susceptibility of sheep to scrapie. In: Baker, H. F. & Ridley, R. M. (Eds) Prion Diseases (pp. 211 - 221). Humana Press Inc.

Hunter, N. 1996b. Prion protein (Prnp) genotypes and natural scrapie in closed flocks of Cheviot and Suffolk sheep in Britain. In: Court, L. & Dodet, B. (Eds) Transmissible subacute spongiform encephalopathies: Prion Diseases (pp. 47 - 50). Elsevier Editions Scientifiques.

Hunter, N., Goldmann, W., Foster, J. D., Cairns, D. & Smith, G. 1997. Natural scrapie and PrP genotype: case-control studies in British sheep. *Vet Rec.* 141: 137 - 140.

Imai, Y., Maeda, K., Yamakawa, M., Karube, Y., Matsuda, M., Dobashi, M., Sato, H. & Terashima, K. 1993. Heterogeneity and cellular origin of follicular dendritic cells. *Adv Exp Med Biol* 329: 339 - 344.

Imai, Y. & Yamakawa, M. 1996. Morphology, function and pathology of follicular dendritic cells. *Pathol Int* 46: 807 - 833.

Ironside, J. W. 1996. Human prion diseases. *J Neural Transm Suppl* 231 - 246.

Jeffrey, M. & Wells, G. A. 1988. Spongiform encephalopathy in a nyala (Tragelaphus angasi). *Vet Pathol* 25: 398 - 399.

Jeffrey, M., Goodsir, C. M., Bruce, M., McBride, P. A., Scott, J. R. & Halliday, W. G. 1994a. Correlative light and electron microscopy studies of PrP localisation in 87V scrapie. *Brain Res* 656: 329 - 343

Jeffrey, M., Goodsir, C. M., Bruce, M. E., McBride, P. A. & Farquhar, C. 1994b. Morphogenesis of Amyloid Plaques in 87V Murine Scrapie. *Neuropathol Appl Neurobiol* 20: 535 - 542.

Jeffrey, M., Goodbrand, I. A. & Goodsir, C. M. 1995. Pathology of the transmissible spongiform encephalopathies with special emphasis on ultrastructures. *Micron* 26: 277 - 298.

Jeffrey, M. & Goodsir, C. M. 1996. Immunohistochemistry of resinated tissues for light and electron microscopy. In Baker, H. F. & Ridley, R. M. (Eds) Prion diseases (pp. 301 - 312). Humana Press.

Jeffrey, M., Martin, S., Gonzalez, L., Ryder, S. J., Bellworthy, S. J. & Jackman, R. 2001a. Differential diagnosis of infections with the bovine spongiform encephalopathy (BSE) and scrapie agents in sheep. *J Comp Path* 125: 271 - 284.

Jeffrey, M., Martin, S., Thomson, J. R., Dingwall, W. S., Begara-McGorum, I. & Gonzalez, L. 2001b. Onset and distribution of tissue PrP accumulation in scrapie-affected Suffolk sheep as demonstrated by sequential necropsies and tonsillar biopsies. *J Comp Path* 125: 48 - 57.

Jeffrey, M., Ryder, S., Martin, S., Hawkins, S. A. C., Terry, L., Berthelin Baker, C. & Bellworthy, S. J. 2001c. Oral inoculation of sheep with the agent of bovine spongiform encephalopathy (BSE). 1. Onset and distribution of disease-specific PrP accumulation in brain and viscera. *J Comp Path* 124: 280 - 289.

Jeffrey, M., Begara-McGorum, I., Clark, S., Martin, S., Clark, J., Chaplin, M. & Gonzalez, L. 2002. Occurrence and distribution of infection-specific PrP in tissues of clinical scrapie cases and cull sheep from scrapie-affected farms in Shetland. *J Comp Path* 127: 264 - 273.

Jeffrey, M., Martin, S. & Gonzalez, L. 2003. Cell-associated variants of disease-specific prion protein immunolabelling are found in different sources of sheep transmissible spongiform encephalopathy. *J Gen Virol* 84: 1033 - 1046.

Kapasi, Z. F., Burton, G. F., Shultz, L. D., Tew, J. G. & Szakal, A. K. 1993. Induction of functional follicular dendritic cell development in severe combined immunodeficiency mice. Influence of B and T cells. *J Immunol* 150: 2648 - 2658.

Kapasi, Z. F., Kosco-Vilbois, M. H., Shultz, L. D., Tew, J. G. & Szakal, A. K. 1994. Cellular origin of follicular dendritic cells. *Adv Exp Med Biol.* 355: 231 - 235.

Kapasi, Z. F., Haley, S. T., Tew, J. G. & Szalak, A. K. 1995. Origin of the follicular dendritic cell. In: Heinen, E. (Ed) Follicular dendritic cells in normal and pathological conditions (pp. 23 - 34). Springer-Verlag, Heidelberg:Germany.

Katz, J. B., Pedersen, J. C., Jenny, A. L. & Taylor, W. D. 1992. Assessment of western immunoblotting for the confirmatory diagnosis of ovine scrapie and bovine spongiform encephalopathy (BSE). *J Vet Diag Invest* 4: 447 - 449.

Kimberlin, R. F. & Walker, C. A. 1979a. Pathogenesis of mouse scrapie:effect of route of inoculation on infectivity titres and dose response curves. *J Comp Path* 89: 39 - 47.

Kimberlin, R. H. & Walker, C. A. 1979b. Pathogenesis of mouse scrapie: dynamics of agent replication in spleen, spinal cord and brain after infection by different routes. *J Comp Path* 89: 551 - 562.

Kimberlin, R. H. & Walker, C. A. 1986. Pathogenesis of scrapie (strain 263K) in hamsters infected intracerebrally, intraperitoneally or intraocularly. *J Gen Virol* 67 (Pt 2): 255 - 263.

Kimberlin, R. F. & Walker, C. A. 1988a. Pathogenesis of experimental scrapie. In: Bock, G. & Marsh, J. (Eds). Novel infectious agents and the central nervous system (pp. 37 - 54). Chichester, New York: John Wiley and Sons.

Kimberlin, R. H. & Walker, C. A. 1988b. Incubation periods in six models of intraperitoneally injected scrapie depend mainly on the dynamics of agent replication

within the nervous system and not the lymphoreticular system. *J Gen Virol* 69: 2953 - 2960.

Kimberlin, R. H. & Walker CA. 1988c. Pathogenesis of scrapie in mice after intragastric infection. *Virus res.* 12: –213 - 220.

Kitamoto, T., Muramoto T., Mohri S, Doh-Ura, K. & Tateishi, J. 1991. Abnormal isoform of prion protein accumulates in follicular dendritic cells in mice with Creutzfeldt-Jakob disease. *J Virol* 65: 6292 - 6295.

Klaus, G. G. & Humphrey, J. H. 1977. The generation of memory cells. I. The role of C3 in the generation of B memory cells. *Immunology* 33: 31 - 40.

Klein, M. A., Frigg, R., Flechsig, E., Raeber, A. J., Kalinke, U., Bluethmann, H., Bootz, F., Suter, M., Zinkernagel, R. M. & Aguzzi, A. 1997. A crucial role for B cells in neuroinvasive scrapie. *Nature* 390: 687 - 690.

Klein, M. A., Frigg, R., Raeber, A. J., Flechsig, E., Hegyi, I., Zinkernagel, R. M., Weissmann, C. & Aguzzi, A. 1998. PrP expression in B-lymphocytes is not required for prion neuroinvasion. *Nat Med* 4: 1429 - 1433.

Knight, R. & Collins, S. 2001. Human prion diseases: cause, clinical and diagnostic aspects. In: Rabenau, H. F., Cinatl, J. & Doerr, H. W. (Eds). Prions. A challenge for science, medicine and public health system (pp. 68-92). Karger.

Koni, P. A., Sacca, R., Lawton, P., Browning, J. L., Ruddle, N. H. & Flavell, R. A. 1997. Distinct roles in lymphoid organogenesis for lymphotoxins alpha and beta revealed in lymphotoxin beta-deficient mice. *Immunity* 6: 491 - 500.

Koopman, G., Parmentier, H. K., Schuurman, H. J., Newman, W., Meijer, C. J. & Pals, S. T. 1991. Adhesion of human B cells to follicular dendritic cells involves both the lymphocyte function-associated antigen 1/intercellular adhesion molecule 1 and very late antigen 4/vascular cell adhesion molecule 1 pathways. *J Exp Med* 173: 1297 – 1304.

Koopman, G., Keehnen, R. M., Lindhout, E., Zhou, D. F., de Groot, C. & Pals, S. T. 1997. Germinal center B cells rescued from apoptosis by CD40 ligation or attachment to follicular dendritic cells, but not by engagement of surface immunoglobulin or adhesion receptors, become resistant to CD95-induced apoptosis. *Eur J Immunol* 27: 1 - 7.

Kosco, M. H., Burton, G. F., Kapasi, Z. F., Szakal, A. K. & Tew, J. G. 1989. Antibody-forming cell induction during an early phase of germinal centre development and its delay with ageing. *Immunology* 68: 312 - 318.

Kosco, M. H. & Gray, D. 1992. Signals involved in germinal center reactions. *Immunol Rev* 126: 63 - 76.

Kosco, M. H., Pflugfelder, E. & Gray, D. 1992. Follicular dendritic cell-dependent adhesion and proliferation of B cells in vitro. *J Immunol* 148: 2331 - 2339.

Kotani, M., Ezaki, T., Ekino, S., Matsuno, K., Fujii, H. & Nawa, Y. 1982. Lymph macrophages enter the germinal center of regional lymph nodes. *Adv Exp Med Biol* 149: 837 - 841.

Krasemann, S., Groschup, M. H., Harmeyer, S., Hunsmann, G. & Bodemer, W. 1996. Generation of monoclonal antibodies against human prion proteins in $PrP^{0/0}$ mice. *Mol Med* 2: 725 - 734.

Krasemann, S., Jurgens, T. & Bodemer, W. 1999. Generation of monoclonal antibodies against prion proteins with an unconventional nucleic acid-based immunization strategy. *J Biotechnol* 73: 119 - 129.

Landsverk, T. 1987. The follicle-associated epithelium of the ileal Peyer's patch in ruminants is distinguished by its shedding of 50 nm particles. *Immunol Cell Biol* 65: 251 - 261.

Landsverk, T., Trevella, W. & Nicander, L. 1990. Transfer of carbonic anhydrase-positive particles from the follicle-associated epithelium to lymphocytes of Peyer's patches in foetal sheep and lambs. *Cell Tissue Res.* 261: 239 - 247.

Landsverk, T., Halleraker, M., Aleksandersen, M., McClure, S., Hein, W. & Nicander, L. 1991. The intestinal habitat for organized lymphoid tissues in ruminants; comparative aspects of structure, function and development. *Vet Immunol Immunopathol* 28: 1 - 16.

Le Hir, M., Bluethmann, H., Kosco-Vilbois, M. H., Muller, M., di Padova, F., Moore, M., Ryffel, B. & Eugster, H. P. 1996. Differentiation of follicular dendritic cells and full antibody responses require tumor necrosis factor receptor-1 signaling. - *J Exp Med* 183: 2367-72.

Liberski, P. P., Jeffrey, M. & Goodsir, C. 1996. Immunogold electron microscopy studies of tubulovesicular structures: they are not composed of prion protein (PrP). In: Court, L. & Dodet, B. (Eds) Transmissible subacute spongiform encephalopathies: prion diseases (pp. 137 - 142). Elsevier Editions Scientifiques.

Ligios, C., Jeffrey, M., Ryder, S., Bellworthy, S. & Simmons, M. 2002. Distinction of scrapie phenotypes in sheep by lesion profiling. *J Comp Path* 127: 45 - 57.

Lindhout, E., Lakeman, A. & De Groot, C. 1995. Follicular dendritic cells inhibit apoptosis in human B-lymphocytes by a rapid and irreversible blockade of preexisting endonuclease. *J Exp Med* 181: 1985 - 1995.

Liu, Y. J., Oldfield, S. & MacLennan, I. C. 1988. Memory B cells in T cell-dependent antibody responses colonize the splenic marginal zones. *Eur J Immunol* 18: 355 - 362.

Liu, Y. J. & Banchereau, J. 1996. Mutant mice without B-lymphocyte follicles. *J Exp Med* 184:1207 – 1211.

Liu, Y. J. & Banchereau, J. 1997. Regulation of B cell commitment to plasma cells or to memory B cells. *Semin Immunol* 9: 235 - 240.

Mabbott, N. A., Williams, A., Farquhar, C. F., Pasparakis, M., Kollias, G. & Bruce, M. E. 2000a. Tumor necrosis factor alpha-deficient, but not interleukin-6- deficient, mice resist peripheral infection with scrapie. *J Virol* 74[7]: 3338-3344.

Mabbott, N. A., Mackay, F., Minns, F. & Bruce, M. E. 2000b. Temporary inactivation of follicular dendritic cells delays neuroinvasion of scrapie. *Nat Med* 6: 719 - 720.

Mabbott, N. A., Bruce, M. E., Botto, M., Walport, M. J. & Pepys, M. B. 2001. Temporary depletion of complement component C3 or genetic deficiency of C1q significantly delays onset of scrapie. *Nature Med* 7: 485 - 487.

Mabbott, N. A., McGovern, G., Jeffrey, M. & Bruce, M. E. 2002. Temporary blockade of the tumor necrosis factor receptor signaling pathway impedes the spread of scrapie to the brain. *J Virol* 76: 5131 - 5139.

Mabbott, N. A., Young, J., McConnell, I. & Bruce, M. E. 2003. Follicular dendritic cell dedifferentiation by treatment with an inhibitor of the lymphotoxin pathway dramatically reduces scrapie susceptibility. *J Virol* 77: 6845 - 6854.

Mackay, F. & Browning, J. L. 1998. Turning off follicular dendritic cells. *Nature* 395: 26 - 27.

MacLennan, I. C., Gulbranson-Judge, A., Toellner, K. M., Casamayor-Palleja, M., Chan, E., Sze, D. M., Luther, S. A. & Orbea, H. A. 1997. The changing preference of T and B cells for partners as T-dependent antibody responses develop. *Immunol Rev* 156: 53 - 66.

Manson, J., McBride, P. & Hope, J. 1992. Expression of the PrP gene in the brain of *sinc* congenic mice and its relationship to the development of scrapie. *Neurodegen* 1: 45 - 52.

Manson, J. C., Clarke, A. R., Hooper, M. L., Aitchison, L., McConnell, I. & Hope, J. 1994. 129/Ola mice carrying a null mutation in PrP that abolishes mRNA production are developmentally normal. *Mol Neurobiol* 8: 121 - 127.

Manson, J. 1996. Prnp gene dosage, allelic specificity and gene regulation in the transmissible spongiform encephalopathies. In: Court, L. & Dodet, B. (Eds).Transmissible subacute spongiform encephalopathies: prion diseases (pp. 239 - 245). Elsevier Editions Scientifiques.

Matsumoto, M., Fu, Y. X., Molina, H. & Chaplin, D. D. 1997. Lymphotoxin-alpha-deficient and TNF receptor-I-deficient mice define developmental and functional characteristics of germinal centers. *Immunol Rev* 156: 137-44.

Mayer, G. & Bendayan, M. 2001. Amplification methods for the immunolocalization of rare molecules in cells and tissues. *Prog Histochem Cytochem* 36: 3 - 85.

McBride, P. A., Eikelenboom, P., Kraal, G., Fraser, H. & Bruce, M. E. 1992. PrP protein is associated with follicular dendritic cells of spleens and lymph nodes in uninfected and scrapie-infected mice. *Pathology* 168: 413 - 418.

McBride, P. A., Schulz-Schaeffer, W. J., Donaldson, M., Bruce, M., Diringer, H., Kretzschmar, H. A. & Beekes, M. 2001. Early spread of scrapie from the

gastrointestinal tract to the central nervous system involves autonomic fibers of the splanchnic and vagus nerves. *J Virol* 75: 9320 - 9327.

Mohler, K. M., Torrance, D. S., Smith, C. A., Goodwin, R. G., Stremler, K. E., Fung, V. P., Madani, H. & Widmer, M. B. 1993. Soluble tumor necrosis factor (TNF) receptors are effective therapeutic agents in lethal endotoxemia and function simultaneously as both TNF carriers and TNF antagonists. *J Immunol* 151: 1548 - 1561.

Mond, J. J., Lees, A. & Snapper, C. M. 1995. T cell-independent antigens type 2. *Annu Rev Immunol* 13: 655 - 692.

Montrasio, F., Frigg, R., Glatzel, M., Klein, M. A., Mackay, F., Aguzzi, A. & Weissmann, C. 2000. Impaired prion replication in spleens of mice lacking functional follicular dendritic cells. *Science* 288: 1257 - 1259.

Newman, G. R. & Jasani, B. 1984. Post embedding immunoenzyme techniques. In: Polak, J. M. & Varndell, I. M. (Eds) Immunolabeling for electron microscopy (pp. 53 - 70). Elsevier.

Nielsen, C. H., Fischer, E. M. & Leslie, R. G. 2000. The role of complement in the acquired immune response. *Immunology* 100: 4 - 12.

Oesch, B., Westaway, D., Walchi, M., McKinley, M. P., Kent, S. B. H., Aebersold, R., Barry, R. A., Teplow, D. B., Tempst, D. B., Hood, L. E., Prusiner, S. B. & Weissmann, C. 1985. A cellular gene encodes scrapie PrP 27-30 protein. *Cell* 40: 735 - 746.

Ogata, T., Yamakawa, M., Imai, Y. & Takahashi, T. 1996. Follicular dendritic cells adhere to fibronectin and laminin fibers via their respective receptors. *Blood* 88: 2995 - 3003.

Pan, K. M., Baldwin, M., Nguyen, J., Gasset, M., Serban, A., Groth, D., MEhlhorn, I., Huang, Z., Fletterick, R. J., Cohen, F. E. et al. 1993. Conversion of alpha-helices into beta-sheets features in the formation of the scrapie prion proteins. *Proc Nat Acad Sci USA* 90: 10962 - 10966.

Pasparakis, M., Alexopoulou, L., Episkopou, V. & Kollias, G. 1996. Immune and inflammatory responses in TNF alpha-deficient mice: a critical requirement for TNF alpha in the formation of primary B cell follicles, follicular dendritic cell networks and germinal centers, and in the maturation of the humoral immune response. *J Exp Med* 184: 1397 - 1411.

Paul, N. L. & Ruddle, N. H. 1988. Lymphotoxin. *Annu Rev Immunol* 6: 407 - 438.

Petrasch, S. G., Kosco, M. H., Perez-Alvarez, C. J., Schmitz, J. & Brittinger, G. 1991. Proliferation of germinal center B-lymphocytes in vitro by direct membrane contact with follicular dendritic cells. *Immunobiology* 183: 451 - 462.

Petrasch, S. G., Kosco, M. H., Schmitz, J., Wacker, H. H., Brittinger, G. 1992. Follicular dendritic cells in non-Hodgkin-lymphoma express adhesion molecules complementary to ligands on neoplastic B-cells. *Br J Haematol* 82:695-700.

Porter, D. D., Porter, H. G. & Cox, N. A. 1973. Failure to demonstrate a humoral immune response to scrapie infection in mice. *J Immunol* 111: 1407 - 1410.

Prinz, M., Montrasio, F., Klein, M. A., Schwarz, P., Priller, J., Odermatt, B., Pfeffer, K. & Aguzzi, A. 2002. Lymph nodal prion replication and neuroinvasion in mice devoid of follicular dendritic cells. *Proc Nat Acad Sci* USA 99: 919 - 924.

Prusiner, S. B. 1989. Scrapie prions. *Annu Rev Microbiol* 43: 345 - 374.

Prusiner, S. B., Scott, M., Foster, D., Pan, K.-M., Groth, D., Mirenda, C., Torchia, M., Yang, S.-L., Serban, D., Carlson, G. A., Hoppe, P. C., Westaway, D. & DeArmond, S. J. 1990. Transgenetic studies implicate interactions between homologous PrP isoforms in scrapie prion replication. *Cell* 63: 673 - 686.

Prusiner, S. B., Groth, D., Serban, A., Koehler, R., Foster, D., Torchia, M., Burton, D., Yang, S.-L. & DeArmond, S. J. 1993. Ablation of the prion protein (PrP) gene in mice prevents scrapie and facilitates production of anti-PrP antibodies. *Proc Nat Acad Sci USA* 90: 10608 - 10612.

Racz, P. & Tenner-Racz, K. 1995. Germinal center tropism of HIV-1 and other retroviruses. In: Heinen, E. (Ed.) Follicular dendritic cells in normal and pathological conditions (pp. 159-181). Springer, Heidelberg, Germany.

Rademakers, L. H. P. M. 1992. Dark and light zones of germinal centres of the human tonsil: an ultrastructural study with emphasis on heterogeneity of follicular dendritic cells. *Cell Tissue Res* 269: 359 - 368.

Radoux, D., Heinen, E., Kinet-Denoel, C. & Simar, L. J. 1985a. Antigen/antibody retention by follicular dendritic cells (FDC). *Adv.Exp Med Biol* 186: 185 - 191.

Radoux, D., Kinet-Denoel, C., Heinen, E., Moeremans, M., de Mey, J. & Simar, L. J. 1985b. Retention of immune complexes by Fc receptors on mouse follicular dendritic cells. *Scand J Immunol* 21: 345-353.

Rennert, P. D., Browning, J. L. & Hochman, P. S. 1997. Selective disruption of lymphotoxin ligands reveals a novel set of mucosal lymph nodes and unique effects on lymph node cellular organization. *Int Immunol* 9: 1627-39.

Rieger, R., Edenhofer, F., Lasmézas, C. I. & Weiss, S. 1997. The human 37-kDa laminin receptor precursor interacts with the prion protein in eukaryotic cells. *Nat Med* 3: 1383 - 1388.

Riesner, D., Kellings, K., Post, K., Wille, H., Serban, H., Groth, D., Baldwin, M. A. & Prusiner, S. B. 1996. Disruption of prion rods generates 10 nm spherical particles having high alpha-helical content and lacking scrapie infectivity. *J Virol* 70: 1714 - 1722.

Rohwer, R. G. 1991. The scrapie agent: "A virus by any other name". In: Chesebro, B.W. (Ed). Current topics in microbiology and immunology: Transmissible spongiform encephalopathies (pp. 195 - 232). Springer Verlag, Berlin.

Sabatini, D. D. & Bensch, K. B. R. J. 1962. New means of fixation for electron microscopy and histochemistry. *Anat Rec* 142: 274.

Sabatini, D. D. & Bensch, K. B. R. J. 1963. Cytochemistry and electron microscopy. The preservation of cellular structure and enzymatic activity by aldehyde fixation. *J Cell Biol* 17: 19.

Sakaguchi, S., Katamine, S., Nishida, N., Moriuchi, R., Shigematsu, K., Sugimoto, T., Nakatani, A., Kataoka, Y., Houtani, T., Shirabe, S., Okada, H., Hasegawa, S., Miyamoto, T. & Noda, T. 1996. Loss of cerebellar Purkinje cells in aged mice homozygous for a disrupted PrP gene. *Nature* 380: 528 - 530.

Schaller, O., Fatzer, R., Stack, M., Clark, J., Cooley, W., Biffiger, K., Egli, S., Doherr, M., Vandevelde, M., Heim, D., Oesch, B. & Moser, M. 1999. Validation of a western immunoblotting procedure for bovine PrP^{sc} detection and its use as a rapid surveillance method for the diagnosis of bovine spongiform encephalopathy (BSE). *Acta Neuropathol* 98: 437 - 443.

Schreuder, B. E. C., Van Keulen, L. J. M., Vromans, M. E. W., Langeveld, J. P. M. & Smits, M. 1998. Tonsillar biopsy and PrP^{sc} detection in the preclinical diagnosis of scrapie. *Vet Rec* 142: 564 - 568.

Scott, M. R., Supattapone, S., Nguyen, H. O. B., DeArmond, S. J. & Prusiner, S. B. 2000. Transgenic models of prion disease. *Arch Virol* 113 - 124.

Smith, J. P., Kosco, M. H., Tew, J. G. & Szakal, A. K. 1988. Thy-1 positive tingible body macrophages (TBM) in mouse lymph nodes. *Anat Rec* 222: 380 - 390.

Smith, J. P., Lister, A. M., Tew, J. G. & Szakal, A. K. 1991. Kinetics of the tingible body macrophage response in mouse germinal center development and its depression with age. *Anat Rec* 229: 511 - 520.

Smith, J. P., Burton, G. F., Tew, J. G. & Szakal, A. K. 1998. Tingible body macrophages in regulation of germinal center reactions. *Dev Immunol* 6: 285 - 294.

Smith, B. A., Gartner, S., Liu, Y., Perelson, A. S., Stilianakis, N. I., Keele, B. F., Kerkering, T. M., Ferreira-Gonzalez, A., Szakal, A. K., Tew, J. G. & Burton, G. F. 2001. Persistence of infectious HIV on follicular dendritic cells. *J Immunol* 166: 690-696.

Somerville, R. A. 2002. TSE agent strains and PrP: reconciling structure and function. *Trends Biochem Sci* 27: 606 - 612.

Stack, M. J., Keyes, P. & Scott, A. C. 1996. The diagnosis of bovine spongiform encephalopathy and scrapie by the detection of fibrils and the abnormal protein isoform. In: Baker, H. & Ridley, R. (Eds). Prion diseases (pp. 85-104). Humana.

Steiniger, B. & Barth, P. 2000. Microanatomy and function of the spleen. Beck, F., Brown, D., Christ, B., Kriz, W., Marani, E., Putz, R., Sano, Y., Schiebler, T.H. & Zilles, K. (Eds). *EMBO* 151. Springer-Verlag, Berlin.

Suchi, T., Lennert, K., Tu, L. Y., Kikuchi, M., Sato, E., Stansfeld, A. G , Feller, A.C. 1987. Histopathology and immunohistochemistry of peripheral T cell lymphomas: a

proposal for their classification. *J Clin Pathol* 40: 995-1015.

Szakal, A. K., Kosco, M. H. & Tew, J. G. 1988. A novel in vivo follicular dendritic cell-dependent iccosome-mediated mechanism for delivery of antigen to antigen-processing cells. *J Immunol* 140: 341 - 353.

Szakal, A. K., Kosco, M. H. & Tew, J. G. 1989. Microanatomy of lymphoid tissue during humoral immune responses: structure function relationships. *Annu Rev Immunol* 7: 91 - 109.

Szakal, A. K., Taylor, J. K., Smith, J. P., Kosco, M. H., Burton, G. F. & Tew, J. J. 1990. Kinetics of germinal center development in lymph nodes of young and aging immune mice. *Anat Rec* 227: 475 - 485.

Tenner-Racz, K., Racz, P., Dietrich, M. & Kern, P. 1985. Altered follicular dendritic cells and virus-like particles in AIDS and AIDS-related lymphadenopathy. *Lancet* i:105-106.

Tenner-Racz, K., Racz, P., Schmidt, H., Dietrich, M., Kern, P., Louie, A., Gartner, S. & Popovic, M. 1988. Immunohistochemical, electron microscopic and in situ hybridization evidence for the involvement of lymphatics in the spread of HIV-1. *AIDS* 199-309.

Terashima, K., Dobashi, M., Maeda, K. & Imai, Y. 1992. Follicular dendritic cell and ICCOSOMES in germinal center reactions. *Semin Immunol* 4: 267 - 274.

Tew, J. G., Kosco, M. H., Burton, G. F. & Szakal, A. K. 1990. Follicular Dendritic Cells as Accessory Cells. *Immunol Rev* 117: 185 - 211.

Tew, J. G., Wu, J., Qin, D., Helm, S., Burton, G. F. & Szakal, A. K. 1997. Follicular dendritic cells and presentation of antigen and costimulatory signals to B cells. *Immunol Rev* 156: 39 - 52.

Thorbecke, G. J., Amin, A. R. & Tsiagbe, V. K. 1994. Biology of germinal centers in lymphoid tissue. *FASEB J* 8: 832 - 840.

Tkachuk, M., Bolliger, S., Ryffel, B., Pluschke, G., Banks, T. A., Herren, S., Gisler, R. H. & Kosco-Vilbois, M. H. 1998. Crucial role of tumor necrosis factor receptor 1 expression on nonhematopoietic cells for B cell localization within the splenic white pulp. *J Exp Med* 187: 469 - 477.

Tobler, I., Gaus, S. E., Deboer, T., Achermann, P., Fischer, M., Rulicke, T., Moser, M., Oesch, B., McBride, P. A. & Manson, J. C. 1996 Altered circadian activity rhythms and sleep in mice devoid of prion protein. *Nature* 380: 639-42.

Totterdell, S., Ingham, C. A. & Bolam, J. P. 1992. Immunocytochemistry 1: pre-embedding staining. In: J.P. Bolam (Ed). Experimental neuroanatomy: a practical approach (pp. 1 - 29). Oxford University Press.

van den Eertwegh, A. J., Laman, J. D., Schellekens, M. M., Boersma, W. J. & Claassen, E. 1992. Complement-mediated follicular localization of T-independent type-2 antigens: the role of marginal zone macrophages revisited. *Eur J Immunol* 22:719 – 726.

van Ewijk, W. & Nieuwenhuis, P. 1985. Compartments, domains and migration pathways of lymphoid cells in the splenic pulp. *Experientia* 41: 199 - 208.

Van Keulen, L. J. M., Schreuder, B. E. C., Meloen, R. H., Poelen-van den Berg, M., Mooijharkes, G., Vromans, M. E. W. & Langeveld, J. P. M. 1995. Immunohistochemical detection and localization of prion protein in brain tissue of sheep with natural scrapie. *Vet Pathol* 32: 299 - 308.

Van Keulen, L. J. M., Schreuder, B. E. C., Meloen, R. H., Mooij-Harkes, G., Vromans, M. E. W. & Langeveld, J. P. M. 1996. Immunohistochemical detection of prion protein in lymphoid tissues of sheep with natural scrapie. *J Clin Microbiol* 34: 1228 - 1231.

Van Keulen, L. J. M., Schreuder, B. E. C., Vromans, M. E. W., Langeveld, J. P. M. & Smits, M. A. 2000. Pathogenesis of natural scrapie in sheep. *Arch Virol* 57 - 71.

Ware, C. F., Van Arsdale, T. L., Crowe, P. D. & Browning, J. L. 1995. The ligands and receptors of the lymphotoxin system. *Curr Top Microbiol Immunol* 198: 175 - 218.

Weiss, L. 1983. The Spleen. In: Weiss, L. (Ed). Cell and tissue biology: a textbook of histology. (pp. 517 - 538). 5th edition, Urban & Schwarzenberg, Baltimore.

Weissmann, C., Raeber, A. J., Montrasio, F., Hegyi, I., Frigg, R., Klein, M. A. & Aguzzi, A. 2001. Prions and the lymphoreticular system. *Philosophical transcations-Royal society of London* 356:177 – 84.

Wells, G. A. H., Scott, A. C., Johnson, C. T., Gunning, R. F., Hancock, R. D., Jeffrey, M., Dawson, M. & Bradley, M. 1987. A novel progressive spongiform encephalopathy in cattle. *Vet Rec* 121: 419 – 420.

Wells, G. A. H., Dawson, M., Hawkins, S. A. C., Austin, A. R., Green, R. B., Dexter, I., Horigan, M. W. & Simmons, M. M. 1996. Preliminary observations on the pathogenesis of experimental bovine spongiform encephalopathy. In: Gibbs, C. J., Jr. (Ed). Bovine spongiform encephalopathy - The BSE Dilemma (pp. 28 - 44). Springer-Verlag, New York, Inc.

Westaway, D., Goodman, P. A., Mirenda, C. A., McKinley, M. P., Carlson, G. A. & Prusiner, S. B. 1987. Distinct prion proteins in short and long scrapie incubation period mice. *Cell* 51: 651 - 662.

Wilesmith, J. W., Wells, G. A. H., Cranwell, M. P. & Ryan, J. B. N. 1988. BSE: epidemiological studies. *Vet Rec* 638 - 644.

Wilesmith, J. W., Ryan, J. B. M. & Atkinson, M. J. 1991. Bovine spongiform encephalopathy: Epidemiological studies on the origin. *Vet Rec* 199 - 203.

Wilkins, B. S. 1997. Simplifying the spleen: a new look at splenic pathology. In: Kirkham, N., Lemoine, N. R. (Eds). *Progress in Pathology* Vol 3 (pp. 211 - 231). Churchill & Livingstone, Edinburgh.

Will, R. G., Ironside, J. W., Zeidler, M., Cousens, S. N., Estibeiro, K., Alperovitch, A., Poser, S., Pocchiari, M., Hofman, A. & Smith, P. G. 1996. A new variant of Creutzfeldt-Jakob disease in the UK. *Lancet* 347: 921 - 925.

Williams, E. S., Miller, M. W., Kreeger, T. J., Kahn, R. H. & Thorne, E. T. 2002. Chronic wasting disease of deer and elk: A review with recommendations for management. *J Wildl Manage* 66: 551 - 563.

Yoshida, K., van den Berg, T. K. & Dijkstra, C. D. 1994. The functional state of follicular dendritic cells in severe combined immunodeficient (SCID) mice: role of the lymphocytes. *Eur J Immunol* 24: 464 – 468.

Zabel, M. D. & Weis, J. H. 2001. Cell-specific regulation of the CD21 gene. *Int Immunopharmacol* 1: 483 - 493.

6. APPENDICES

6.1. Technical protocols

6.1.a. Murine perfusion protocol.

Under deep anaesthesia with 0.3 ml of chloral hydrate (320-350 mg/kg i.p) animals are first injected with 1ml heparin (1000 units /ml buffer), slowly administered. Animals are perfused at a rate of 5 ml / min with 100 ml of fixative over a period of 20 min at room temperature via a cannula inserted through the left ventricle into the base of the aorta. Recommended perfusion pressure for murine brain is 150mmHg. Tissues are removed and allowed to fix for 24 hours in a fresh solution of the perfusate at 4°C.

6.1.b. Preparation of Phosphate buffer (PB) stock solution.

Reagents and equipment required:

1l flask

Magnetic stirrer and magnet

pH meter

Balance

Distilled water

di-sodium hydrogen orthophosphate ($Na_2HPO_4.2H_2O$)

Sodium di-hydrogen orthophosphate ($NaH_2PO_4.\ 2H_2O$)

Storage bottles

Method:

Prepare the following stock solutions in distilled water:

A: 0.2M $Na_2HPO_4.2H_2O$ = 35.6g/l

B: 0.2M $NaH_2PO_4.\ 2H_2O$ = 31.2g/l

- For stock solution 0.2 M phosphate buffer at pH 7.4, mix solutions A and B in a ratio of 4:1 and pH as necessary.
- To prepare a 0.1 M phosphate buffer solution, mix equal volumes of 0.2 M Phosphate buffer and distilled water.

Note: Stock solutions A and B may be stored for long periods at 4°C but should be warmed prior to use and stirred to dissolve crystals.

0.2 M PB can be stored for up to 1 week at 4°C.

Different pH values can be gained or adjusted by adding either solution A to increase the pH or solution B to decrease the pH.

6.1.c. Paraformaldehyde / Gluteraldehyde fixative protocol.

Reagents and equipment required:

Paraformaldehyde

Gluteraldehyde (supplied as 25% aqueous solution from all EM suppliers, stored at 4°C)

0.5 M NaOH

0.2 M phosphate buffer

Bunsen burner

Tripod and gauze

10" filter paper

Filter funnel

Parafilm

Method:

- Weigh out required volume of paraformaldehyde. Paraformaldehyde is a know respiratory allergen:all procedures must be carried out according to Health and Safety regulations – a particle facemask must be worn for this step.
- Using a Bunsen burner, heat distilled water (just under half the final required volume of fixative) to 70°C. Paraformaldehyde should be added while distilled water is between 65 and 70°C. Stir continuously with a magnetic stirrer in a fume hood.
- Allow paraformaldehyde solution to stir for 10 min.

- Slowly add 0.5 M NaOH drop wise until solution clears.
- Paraformaldehyde solution should be covered and allowed to cool.
- Filter paraformaldehyde solution.
- Add half the final volume of 0.2 M phosphate buffer (see appendix 6.1.b).
- Add the appropriate volume of 25% gluteraldehyde solution to give the desired final concentration. See Table 6.1.c.i. If this is less than the final required volume, add appropriate volume of distilled water.

Conc. Gluteraldehyde required	Volume of fixative (ml) required						
	100	200	300	400	500	750	1000
0.01%	0.04	0.08	0.12	0.16	0.2	0.3	0.4
0.05%	0.2	0.4	0.6	0.8	1.0	1.5	2.0
0.1%	0.4	0.8	1.2	1.6	2.0	3.0	4.0
0.2%	0.8	1.6	2.4	3.2	4.0	6.0	8.0
0.5%	2.0	4.0	6.0	8.0	10.0	15.0	20.0
1.0%	4.0	8.0	12.0	16.0	20.0	30.0	40.0
2.0%	8.0	16.0	24.0	32.0	40.0	60.0	80.0
2.5%	10.0	20.0	30.0	40.0	50.0	75.0	100.
5.0%	20.0	40.0	60.0	80.0	100.0	150.0	200.

Table 6.1.c.i. Volume of 25% gluteraldehyde solution required for the preparation of fixatives.Protocol and Table adapted from: Experimental Neuroanatomy – (Ed. J.P.Bolam) (Bolam 1992)

6.1.d. Araldite processing

Three days should be allowed for this process.

- Cut tissue into 1 mm blocks and place in vial containing 0.1 M PB. This is placed on shaker - 15 min.
- Replace PB with 2% Osmium tetroxide (4% stock diluted in 0.1 M PB) - 2 hours (Osmium concentrate protocol: 6.1.d.i.). This step must be carried out in a fume hood.
- Wash in 0.1 M PB - 2 x 5 min.
- Wash in dist. water - 2 x 5 min.
- Replace water with 40% acetone - 15 min.

  60% acetone - 15 min.

  80% acetone - 15 min.

  100% acetone - 15 min. x 2
- Replace acetone with 50 / 50 dilution of acetone/ araldite - overnight.
- Replace with 25 / 75 dilution of acetone/ araldite – daytime.
- Change to 100% araldite – overnight.
- Replace with fresh araldite - 2 hours fresh.
- Embed.
- Polymerize at 37°C or 60°C - 48 hours.

Stages 1 - 9 should be carried out on a shaker or mixer.

During this procedure temperature must remain relatively constant.

Reagent	Quantity required		
CY212	49g	24.5g	12.25g
DDSA	49g	24.5g	12.25g
Dib. Phthalate	0.75g	0.37g	0.185g
BDMA	1.5g	0.75g	0.37g

Table 6.1.d.i – Quantities of chemicals required for araldite production.

CY212, DDSA (Dodecenyl Succinic Anhydride) and Dibutyl Phthalate should be mixed thoroughly prior to the addition of BDMA (Benzyldimethylamine). This should take approximately 45 min.

After the addition of BDMA the araldite should be mixed for a further 30 min.

6.1.d.i. Stock osmium tetroxide preparation (4%).

Reagents / equipment required:

1 g ampule of solid osmium tetroxide (TAAB)

25 ml distilled H_2O

Dark glass bottle

parafilm

- The ampule of osmium tetroxide is opened by conventional glass scoring methods or using an ampule breaker.

- The contents of the ampule and 25 ml distilled water are placed into the glass bottle, a stirrer added and the lid tightly fixed.
- This should be stirred inside the fume hood until the crystals are seen to dissolve, i.e. for 2 - 3 hours.
- The lid is then covered in parafilm and the bottle placed in a sealed container.

This may be stored at 4°C for several months.

6.1.e. Staining 1μm sections with Toluidine blue dye.

Toluidine Blue dye:

1 g Toluidine blue

1 g Borax

100 ml distilled H_2O

Ingredients should be mixed on a magnetic stirrer until fully dissolved and solution filtered.

Equipment required:

Toluidine Blue dye

Hotplate

Hair stick

Beaker with distilled water

Method:

- Place a large droplet of toluidine blue dye onto a clean glass slide.
- Lift one stretched 1 μm section out of the water bath using hair stick and float onto the dye.
- Place the slide onto the hotplate (50°C) for 15 sec. or until the edges of the dye begin to evaporate.
- Remove slide and lift section from the dye into the water filled beaker. Water should be moved until excess dye is rinsed away.
- Place a drop of distilled water on a clean glass slide.
- Transfer section from the beaker to the water drop.
- Allow section to dry naturally.

Sections should not be coverslipped to allow for ease of mesa orientation.

6.1.f. Peroxidase anti-Peroxidase technique (PAP).

1 μm araldite embedded sections of tissue on glass slides. Dry sections in oven at 60°C overnight before immunolabelling.

Never allow sections to dry throughout the entire staining procedure.

Pre treatment:

- Plastic removal: Sections placed in a solution of saturated sodium ethoxide (See appendix 6.1.f.i.). A slide should be studied under the microscope at regular intervals to determine the degree of etching. As soon as visible resin is seen to begin disintegrating, the sodium ethoxide should be removed.

- Slides transferred to four consecutive washes in absolute ethanol (slides totally submerged) 4 x 5 min each.
- Inhibit endogenous peroxidase by treating with freshly prepared 6% hydrogen peroxide (H_2O_2) in methanol 10 min.
- Rinse in running water for 10 min.
- Enhance antigenicity with neat (98%) Formic Acid for 5 min.
- Rinse in running water for 10 min.
- Rinse sections in wash buffer (Appendix 6.1.f.ii.) before immunolabelling.

Peroxidase anti-peroxidase labelling method.

- Block non-specific binding: Incubate sections with normal swine serum diluted 1:10 in incubation buffer (Appendix 6.1.f.iv.) for 1 hour.
- Primary antibody incubation: Incubate sections with a 1:2000 dilution of 1A8 anti PrP serum. Antibody is diluted in incubation buffer. This should be carried out overnight at 4°C.
- Rinse the slides in washing buffer for 2 hours with regular buffer changes.
- Apply second layer antibody swine anti rabbit IgG at a 1:40 dilution in incubation buffer for 1 hour at room temperature.
- Rinse the slides in washing buffer for 4 x 10 min.
- Apply rabbit peroxidase anti-peroxidase complex at a 1:100 dilution in incubation buffer for 30 min at room temperature.
- Rinse the slides in washing buffer for 3 x 10 min.

- Reaction product is developed by the application of 3-3' Diaminobenzidine (DAB) (Appendix 6.1.f.v.) substrate for 10 min. This is diluted to a 1:100 with wash buffer. 50 µl H_2O_2 is added.
- Wash slides in running tap water for 5 min.
- Enhance DAB with copper sulphate (4g Cu SO_4 and 7.2g NaCl in 1 litre distilled water) solution for 10 min.
- Wash in water.
- Counterstain with Harris' haematoxylin for 30 min - check staining under a microscope.
- Blue the sections using Lithium Carbonate (0.5g $CLiCO_3$ in 1 litre distilled water). The term "Blue" refers to washing slides in a solution of pH>5.0. In most cases ordinary tap water will suffice, but may take a few minutes. Virtually instantaneous conversion can be obtained with a dilute solution of lithium carbonate.
- Dehydrate, clear and mount.

6.1.f.i. Saturated Sodium Ethoxide.

- 15 g NaOH pellets are added to 100ml absolute ethanol in a 250 ml flask, covered with parafilm and placed on a magnetic stirrer for 1 hour.
- The solution is left for 5 days at room temperature.
- The resultant transparent supernatant is decanted into a plastic 100 ml bottle, labelled and placed in a sealed container. Sodium ethoxide is ready for use.
- Sodium ethoxide should be freshly made on a weekly basis.

6.1.f.ii. Wash buffer.

Wash buffer consists of 10% Phosphate Buffer Saline concentrate in distilled water with 0.2% Tween 20 added.

6.f.iii. Phosphate buffer saline (PBS) protocol - concentrate.

Reagents required:

Sodium Chloride 80 g (mw 58.44)

Potassium Chloride 2 g (mw 74.55)

Di-Sodium Hydrogen Orthophosphate 11.5 g (mw 141.96)

Potassium Di-Hydrogen Orthophosphate 2 g (mw 136.09)

1l distilled H_2O

Ingredients should be mixed thoroughly on a magnetic stirrer and stored at room temperature.

6.1.f.iv. Incubation buffer.

Wash buffer as detailed above with the addition of 20% normal serum (this is dependent on the tracer system used) e.g. PAP technique will use normal swine serum.

6.1.f.v. Diaminobenzidine (DAB) protocol.

DAB concentrate

Reagents required: 3-3 Diaminobenzidine – 1 g

40 ml Distilled H_2O

- Mix ingredients thoroughly on a magnetic stirrer.
- Filter.
- Aliquot 0.5 ml into vials.
- Freeze at –20°C.

Working strength protocol:

- Defrost a vial of DAB concentrate.
- Dilute immediately in 50 ml wash buffer (see Appendix 6.1.f.ii.).
- Add 50 µl neat Hydrogen peroxide.

6.1.g. Avidin Biotin technique.

1μm araldite embedded sections of tissue are placed on charged glass slides (BDH,VWR International Ltd., Leics). Sections are dried in oven at 60°C for 48 hours before immunolabelling.

Never allow sections to dry throughout the entire staining procedure.

Pre-treatment:

- Plastic removal: A solution of saturated sodium ethoxide is placed on sections. (See Appendix 6.1.f.i) A slide should be studied under the microscope at regular intervals to determine the degree of etching. As soon as visible resin is seen to begin disintegrating, the sodium ethoxide should be removed.
- Slides transferred to consecutive washes in absolute ethanol (slides totally submerged). Agitate slides gently in the ethanol and repeat process until no more ethoxide can be removed from slides (approx. 4 times).
- Inhibit endogenous peroxidase by treating with freshly prepared 6% hydrogen peroxide (H_2O_2) in distilled water for 10 min. Rinse in running water for 10 min.
- Enhance antigenicity with Formic Acid for 5 min. Rinse in running water for 10 min.
- Remove slides individually from water and place onto plastic coverslip ensuring there is a layer of water trapped between the slide and coverslip and there are no air bubbles present. Do this by adding a few droplets of water to

the coverslip and slowly pressing the slide tissue side down towards the coverslip.

- Place slide and coverslip on the Sequenza rack and add 100 µl of PBST to prevent tissue from drying out. Allow sections to sit in PBST for 20 min before adding normal serum. Change PBST two times during this time.

ABC immunolabelling procedure:

- Block non-specific binding: - Incubate sections with normal serum diluted 1:10 in PBST (blocking buffer) for 60 min. Note the normal serum used depends on the ABC kit selected. Current EM R&D spec. is:- murine tissue with Rabbit Kit and normal goat serum, ovine tissue with Universal Kit and normal horse serum.
- Primary antibody incubation: - Incubate sections with appropriate dilution of specific primary antiserum in blocking buffer overnight at 27°C in Sequenza rack.
- Wash slides in two changes of PBST for 10 min each.
- Apply biotinylated second layer antibody IgG from the kit diluted in blocking buffer for 1 hour at room temperature.
- Make appropriate dilution of avidin biotin complex in PBST. This must be made at least 30 min. before use.
- Wash slides in two changes of PBST for 10 min. each.
- Apply avidin biotin complex for 30 min. at room temperature.
- Wash slides in two changes of PBST for 10 min. each.

- Prepare DAB in black plastic troughs by adding 2 x 1ml DAB to 200 ml PBST and 200 µl Hydrogen Peroxide. Slides placed in DAB for 10 min.
- Rinse slides in four quick changes of PBST.
- Immerse in 0.5% aqueous copper sulphate for 10min to enhance DAB reaction.
- Rinse in tap water.

Counterstain by hand as follows: -

- Mayer's Haematoxylin at 37°C for 30 min (use Haematoxylin preheated to 37°C).
- Rinse in tap water until it runs clear.
- Differentiate in 1% acid alcohol (1% HCl in ethanol) 2-3 sec.
- Rinse in tap water.
- Blue in 0.05% lithium carbonate.
- Rinse in tap water.
- Dehydrate in two changes of absolute ethanol, clear in xylene and mount in DPX.

6.1.h. Envision technique.

1µm araldite embedded sections of tissue on glass slides. Dry sections in oven at 60°C overnight before immunolabelling.

Never allow sections to dry throughout the entire staining procedure.

Pre treatment:

- Plastic removal: Sections placed in a solution of saturated sodium ethoxide. (See Appendix 6.1.f.i.) A slide should be studied under the microscope at regular intervals to determine the degree of etching. As soon as visible resin is seen to begin disintegrating, the sodium ethoxide should be removed.
- Slides transferred to four consecutive washes in absolute ethanol (slides totally submerged) 4 x 5 min each.
- Inhibit endogenous peroxidase by treating with freshly prepared 6% hydrogen peroxide (H_2O_2) in methanol 10 min.
- Rinse in running water for 10 min.
- Enhance antigenicity with Formic Acid for 5 min.
- Rinse in running water for 10 min.
- Remove slides individually from water and place onto plastic coverslip ensuring there is a layer of water trapped between the slide and coverslip and there are no air bubbles present. Do this by adding a few droplets of water to the coverslip and slowly pressing the slide tissue side down towards the coverslip.
- Place slide and coverslip on the Sequenza rack and add 100 µl of PBST to prevent tissue from drying out. Allow sections to sit in PBST for 20 min before adding normal serum. Change PBST two times during this time.

Note: no blocking serum is required as the envision kit is a polymer raised against a primary antibody. Therefore there will be no non-specific globulin binding.

- Primary antibody incubation: - Incubate sections with appropriate dilution of specific primary antiserum in incubation buffer overnight at 37°C in humidity chamber.
- Carefully drain slides onto absorbent paper and return to holder. Rinse in wash buffer with regular changes for 90 min.
- Apply labelled envision polymer diluted in wash buffer for 30 min. at room temperature.
- Carefully drain slides onto absorbent paper and return to holder. Rinse in wash buffer with regular changes for 30 min.
- Apply DAB (50 ml PBST + 500 µl DAB + 50 µl hydrogen peroxide) substrate for 10 min.
- Rinse slides in four quick changes of wash buffer.
- Immerse in 0.5% aqueous copper sulphate for 10min. to enhance DAB reaction.
- Rinse in tap water.

Counterstain by hand as follows: -

- Mayer's Haematoxylin at 37°C for 30 min (use haematoxylin preheated to 37°C).
- Rinse in tap water until it runs clear.
- Differentiate in 1% acid alcohol (1% HCl in ethanol) 2-3 sec.
- Rinse in tap water.
- Blue in 0.05% lithium carbonate.
- Rinse in tap water.

6.1.i. Reynolds Lead citrate.

Lead nitrate $Pb(NO_3)_2$	1.33 g
Tri Sodium Citrate $Na_3(C_6H_5O_7)2H_2O$	1.76 g
Boiled autoclaved Distilled H_2O	30 ml
NaOH	6 ml

- Lead nitrate, sodium citrate and H_2O are shaken vigorously for 1min.
- The resultant suspension is allowed to stand with intermittent shaking in order to ensure the complete conversion of lead nitrate to lead citrate.
- After 30 min, 6 ml NaOH is added and the suspension is diluted to 50 ml with Boiled autoclaved distilled water and mixed by inversion.
- Lead citrate should dissolve and the solution will be ready for use.
- pH the solution – if the pH is below pH 11.9 or above pH 12.1, discard.

Store in a labelled plastic bottle at 4°C.

The solution can be stored for up to 3 months although this depends on use, as the solution is unstable when exposed to air.

6.1.j. Uranyl acetate.

- Make 100 ml of 50% Ethanol.
- Filter 50 ml neat ethanol and add 50 ml Boiled Autoclaved Distilled water
- Add to brown glass bottle.
- To this add 2 g uranyl acetate.
- Stir for at least 1 hour.

pH the solution – if the solution is below pH 3.7 or above pH 4.5, discard.

Label and place in fridge.

This stain should be stored for a maximum of 3 weeks.

6.1.k. Lead citrate / uranyl acetate EM Counterstain.

Lead stains provide a general increase in contrast. Lead is a cumulative poison and all necessary precautions should be taken when handling.

Uranyl stains also increase contrast, but may also be used as semi specific stains for DNA containing structures. Membranous organelles are not stained well.

Safety

Gloves should be worn at all times when handling Uranyl acetate and Lead citrate.

All reagents should be disposed of in the sink with excess running water.

Materials

Chemicals:

5% hydrogen peroxide in boiled and filtered distilled water

2% uranyl acetate in ethanol

Reynolds lead citrate

50% ethanol (nylon membrane filtered)

Sodium hydroxide pellets

Distilled water

Fresh 0.02 M NaOH

Equipment:

3 staining dishes

2 disposable beakers

3 dental wax sheets

Disposable pipettes

Square filter paper

2 disposable 1ml syringe

0.2 μm nylon membrane filters

2 Eppendorf vials

Procedure

- Fill a beaker with 50% nylon filtered ethanol; fill the other with boiled autolcaved distilled water. This should be covered at all times.
- Place filter paper into the labelled staining dishes.

- For uranyl acetate, soak filter paper in 50% ethanol.
- For lead citrate, place pellets in dish
- For hydrogen peroxide soak in with boiled autolcaved distilled water
- Cover filter paper with dental wax and replace the lid on the dishes.
- Using a 1 ml disposable syringe, withdraw required amount of uranyl acetate from the bottle and filter using the 0.2 μm nylon filter into an Eppendorf vial. Clear filer by removing plunger to push air through.
- Repeat for Lead citrate.
- Place balanced eppendorf vials in the microcentrifuge at 13000 rpm for 5 min.
- Place Hydrogen peroxide on the wax (1 drop per grid).
- Float grid tissue side down on the drop for 5 min.
- Meanwhile, place appropriate amount of drops of uranyl acetate into the staining dish.
- After removing the grids from hydrogen peroxide, rinse in with boiled autolcaved distilled water for 15 sec.
- Float grids tissue side down on the drops of Uranyl acetate for the appropriate length of time.
- 5 min prior to completion of this step, place drops of lead citrate into staining dish.
- Remove grid and rinse in 50% ethanol for 15 sec followed by 15 sec in with boiled autolcaved distilled water.
- Place tissue side down onto the drops of lead citrate. Care should be taken keep the lid on this staining dish whenever possible.

- Leave for the appropriate length of time.
- Rinse grids in 0.02 M NaOH followed by with boiled autolcaved distilled water.
- Touch dry on filter paper and hold in forceps until visibly dry.
- Place the stained grid tissue side up onto a grid plate in a Petri dish.

6.1.l. Immunogold technique

AUROPROBE ONE (1nm gold probe) and INTENSE M (silver enhancement) and NANOPROBE (1nm gold probe) and NANOPROBE GOLDENHANCE (gold enhancement): staining on ultrathin araldite sections.

On grid staining.

All steps are performed at room temperature on reagent droplets on a sheet of dental wax. Never allow grids to dry throughout the procedure.

Pre-treatment:

- Etching step. Float grids section side down on a droplet of saturated filtered Sodium meta-periodate for 60 min.
- Rinse grids in boiled and filtered, distilled water for 3 x 5 min.
- Block endogenous peroxidase and de-osmicate with filtered (use nylon filter) 3% hydrogen peroxide in boiled filtered distilled water for 10 min.
- Rinse grids in boiled, filtered distilled water for 3 x 5 min.
- Enhance antigenicity with filtered Formic acid for 10 min.

- Rinse grids in boiled, filtered distilled water for 3 x 5 min.
- Rinse grids in filtered wash buffer (British Biocell Protocol – Appendix 6.1.l.i.), before immunolabelling for 2 x 10 min.

Immunogold staining procedure:

- Quench residual aldehyde groups with filtered 0.2 M glycine (Appendix 6.1.l.ii.) in PBS buffer pH 7.4 for 3 min.
- Rinse the grids on filtered washing buffer for 5 min.
- Blocking step. Incubate the grids on filtered washing buffer for 1 hour.
- Primary antibody incubation: Incubate grids with appropriate dilution of specific primary antiserum in filtered washing buffer overnight at 27°C.
- Rinse grids on filtered washing buffer for 6 x 10 min.
- Immunogold incubation. Incubate with Auroprobe One diluted 1:50 in filtered washing buffer for 2 hours, or Nanoprobe 1 nm gold probe diluted 1:50 in washing buffer for 2 hours.
- Rinse grids in washing buffer for 3 x 30 min and in PBS (see Appendix 6.1.f.iii.) for 3 x 5 min.
- Post fixation step. Post-fix the grids with filtered 2.5 % gluteraldehyde in PBS for 10 min.
- Rinse in excess boiled and filtered distilled water for 2 x 5 min.

Silver/gold amplification step:

- Prepare the silver solution by mixing equal parts of Enhancer and Initiator of the Intense M kit just before use. This should be removed from the fridge at least 1 hour prior to use. Perform silver amplification for 4 min.
- Prepare the goldenhance solution by mixing equal parts of component A and B. This should be allowed to develop for a minimum of 10 min. Equal parts of components C and D are added and the goldenhance solution as applied to grids for 10 min.
- Rinse grids in excess boiled and filtered distilled water for 3 x 10 min.
- Counterstain with uranyl acetate and lead citrate. See Appendix 6.1.k.

6.1.l.i. British Biocell buffer protocol.

- Make up fresh PBS (pH 7.6). Use boiled polished reverse osmosis pre-treated water.
- Add 2% Normal serum (depending on the 2° antibody host animal e.g. Goat anti Rabbit would be normal goat).
- Add 0.1% Tween 20.
- Add 1% BSA.
- Add 0.1% Sodium azide.
- Mix thoroughly.
- pH to 8.2 using 1 M NaOH.
- Pass buffer through a nylon filter and dispense into glass vials, label and freeze.

6.1.l.ii. Glycine – 0.2 M in PBS.

- Make up fresh PBS (pH 7.6). Use boiled polished reverse osmosis pre-treated water.
- Add 1.5 g glycine to 100 ml PBS.
- Filter into 1 ml vials, label and freeze.

6.1.l.iii. Gluteraldehyde - 2.5% in PBS.

- Make up fresh PBS (pH 7.6). Use boiled polished reverse osmosis pre-treated water.
- Add 10 ml neat EM grade gluteraldehyde (25%) to 90 ml PBS.
- Filter into 1 ml vials, label and freeze.

6.1.m. Immunogold for light microscopical analysis.

1 μm araldite embedded sections of tissue are placed on charged glass slides.

Sections are dried in oven at 60°C for 48 hours before immunolabelling.

Never allow sections to dry throughout the entire staining procedure.

Pre-treatment:

- Plastic removal: A solution of saturated sodium ethoxide is placed on sections. (See Appendix 6.1.f.i.) This procedure is carried out on a metal slide tray. A slide should be studied under the microscope at regular intervals

to determine the degree of etching. As soon as visible resin is seen to begin disintegrating, the sodium ethoxide should be removed. For 5 day old ethoxide this should be around 25-30 min.

- Slides transferred to consecutive washes in absolute ethanol (slides totally submerged). Agitate slides gently in the ethanol and repeat process until no more ethoxide comes off slides (approx. 4 times).
- Inhibit endogenous peroxidase by treating with freshly prepared 6.0% hydrogen peroxide in distilled water for 10 min. Rinse in running water for 10 min.
- Remove slides individually from water and place onto plastic coverslip ensuring there is a layer of water trapped between the slide and coverslip and there are no air bubbles present. Do this by adding a few droplets of water to the coverslip and slowly pressing the slide tissue side down towards the coverslip.
- Place slide and coverslip on the Sequenza rack and add 100 µl of PBST to prevent tissue from drying out. Allow sections to sit in PBST for 20 min before adding normal serum. Change PBST two times during this time.

ABC immunolabelling procedure:

- Block non-specific binding: - Incubate sections with normal serum diluted 1:10 in PBST (blocking buffer) for 60 min. Note the normal serum used depends on the ABC kit selected. Current EM R&D spec. is: - murine tissue with Rabbit Kit and normal goat serum, ovine tissue with Universal Kit and normal horse serum.

- Primary antibody incubation: - Incubate sections with appropriate dilution of specific primary antiserum (e.g. R486 is applied at a 1:1500 dilution) in blocking buffer overnight at 27°C in Sequenza rack.
- Wash slides in two changes of PBST for 10 min each.
- Apply Auroprobe 1nm or Nanoprobe 1nm gold probe at a dilution of 1:50 in PBST for 2 hours at room temperature.
- Wash slides in four changes of PBST for 10 min each.
- Remove slides from Sequenza rack and place in metal slide tray. Working strength silver stain (Intense M, Amersham, or LI silver enhance, Nanoprobes) is applied for 20 min.
- Wash slides in running tap water for 10 min.

Counterstain by hand as follows: -

- Mayer's Haematoxylin at 37°C for 30 min (use haematoxylin preheated to 37°C).
- Rinse in tap water until it runs clear.
- Rinse in tap water.
- Blue in 0.05% lithium carbonate.
- Rinse in tap water.
- Dehydrate in two changes of absolute ethanol, clear in xylene and mount in DPX.

6.1.n. Tyramide amplification for Ultrastructural analysis.

Carry out pre-treatments as detailed in Appendix 6.1.l.

Immunolabelling and tyramide amplification procedure:

- Quench residual aldehyde groups with filtered 0.2 M glycine (Appendix 6.1.l.ii) in PBS buffer pH 7.4 for 3 min.
- Rinse the grids on filtered washing buffer for 5 min.
- Blocking step. Incubate the grids on filtered washing buffer for 1 hour.
- Primary antibody incubation: Incubate grids with appropriate dilution of specific primary antiserum (R486 at 1:250) in filtered washing buffer overnight at 27°C.
- Rinse grids on filtered washing buffer for 6 x 10 min.
- Apply pre-prepared biotinylated secondary antibody for 15 min.
- Apply streptavidin-biotin complex for 15 min. This should be prepared at least 30 min prior to use.
- Apply biotinylated tyramide for 15 min according to manufacturers instructions.
- Incubate grids in 5nm goat anti biotin gold probe diluted to 1:50 in washing buffer for 2 hours.
- Rinse grids in filtered washing buffer for 6 x 10 min.
- Apply Nanoprobe goldenhance for 10 min (see Appendix 6.1.l. for details).
- Rinse in excess boiled and filtered distilled water for 2 x 5 min.
- Counterstain – see Appendix 6.1.k.

6.1.O. Avidin Biotin amplification for ultrastructural analysis.

Carry out pre-treatments as detailed in Appendix 6.1.l.

Immunolabelling and ABC amplification method:

- Quench residual aldehyde groups with filtered 0.2 M glycine (Appendix 6.1.l.ii.) in PBS buffer pH 7.4 for 3 min.
- Rinse the grids on filtered washing buffer for 5 min.
- Blocking step. Incubate the grids on filtered washing buffer for 1 hour.
- Primary antibody incubation: Incubate grids with appropriate dilution of specific primary antiserum (R486 at 1:250) in filtered washing buffer overnight at 27°C.
- Rinse grids in filtered washing buffer for 6 x 10 min.
- Apply biotinylated secondary antibody, diluted to 1:50 in washing buffer for 1hour. Rinse grids in filtered washing buffer for 3 x 10 min.
- Apply avidin biotin complex, diluted to 1:50 in filtered PBST for 30 min.
- Rinse grids in filtered washing buffer for 3 x 10 min.
- Incubate grids in 5 nm goat anti Biotin gold probe diluted to 1:50 in washing buffer for 2 hours.
- Rinse grids in filtered washing buffer for 6 x 10 min.
- Apply Nanoprobe goldenhance for 10 min (see Appendix 6.1.l. for details).
- Rinse in excess boiled and filtered distilled water for 2 x 5 min.
- Counterstain – see Appendix 6.1.k.

6.1.p. Envision system for ultrastructural analysis.

Carry out pre-treatments as detailed in Appendix 6.1.l.

Immunolabelling and Envision method:

- Quench residual aldehyde groups with filtered 0.2 M glycine (Appendix 6.1.l.ii.) in PBS buffer pH 7.4 for 3 min.
- Rinse the grids on filtered washing buffer for 5 min.
- Blocking step. Incubate the grids on filtered washing buffer for 1 hour.
- Primary antibody incubation: Incubate grids with appropriate dilution of specific primary antiserum (R486 at 1:250) in filtered washing buffer overnight at 27°C.
- Rinse grids in filtered washing buffer for 6 x 10 min.
- Dilute Envision reagent 1:1 in filtered PBST. Apply for 30 min.
- Rinse grids in filtered washing buffer for 3 x 10 min.
- Incubate grids in 5 nm goat anti-Horseradish peroxidase gold probe diluted to 1:50 in washing buffer for 2 hours.
- Rinse grids in filtered washing buffer for 6 x 10 min.
- Apply Nanoprobe goldenhance for 10 min (see Appendix 6.1.l for details).
- Rinse in excess boiled and filtered distilled water for 2 x 5 min.

Counterstain – see Appendix 6.1.k.

Journal of Pathology
J Pathol 2000; **191**: 323–332.

Original Paper

Sites of prion protein accumulation in scrapie-infected mouse spleen revealed by immuno-electron microscopy

Martin Jeffrey[1]*, Gillian McGovern[1], Caroline M. Goodsir[1], Karen L. Brown[2] and Moira E. Bruce[2]
[1] *VLA Lasswade, Pentlands Science Park, Bush Loan, Penicuik, Midlothian, Scotland, EH26 0PZ, UK*
[2] *Institute for Animal Health, Neuropathogenesis Unit, Ogston Building, West Mains Road, Edinburgh, Scotland, EH9 3JF, UK*

*Correspondence to:
M. Jeffrey, VLA Lasswade Laboratory, Pentlands Science Park, Bush Loan, Penicuik Midlothian, EH26 0PZ, UK.

Abstract

Prion protein (PrP) from the brains of animals with transmissible spongiform encephalopathies is partially protease resistant (PrP^{res}) compared with fully sensitive PrP (PrP^{sen}) from uninfected brains. In most experimental models, PrP^{res} is a reliable indicator of infectivity. Light microscopic studies have suggested that both PrP^{sen} and disease-specific accumulations of PrP are associated with follicular dendritic cells (FDCs). Using immunogold electron microscopy, this study has demonstrated disease-specific accumulation of PrP in the spleens of C57 BL mice, 70 days after intracerebral infection with the ME7 strain of scrapie and at the terminal stage of disease at 170 days. At both stages, tingible body macrophages contained PrP within lysosomes and PrP was also detected at the plasmalemma of FDCs. In the light zone of follicles of terminally diseased mice, all FDC dendrites were arranged in the form of highly reactive or hyperplastic labyrinthine glomerular complexes, within which PrP was consistently seen between FDC processes in association with abundant electron dense material, interpreted as antigen–antibody complexes. Within some glomeruli, fibrillar forms of PrP consistent with amyloid were seen. At 70 days after challenge, large or hyperplastic labyrinthine complexes were rare and invariably labelled for PrP. However, sparse PrP labelling was also seen on simple FDC processes at this stage. The ubiquitous accumulation of extracellular PrP in complex glomerular dendrites of FDCs in spleens from terminally affected mice, contrasted with simple FDC profiles, sparse PrP and limited electron dense deposits in all but a few FDCs of 70-day post-infected mice. This suggests that FDCs continually release PrP from the cell surface, where it is associated with trapped antigen–antibody complexes and dendritic extension. It is likely that tingible body macrophages acquire PrP following phagocytosis of PrP within iccosomes or from the extracellular space around FDC dendrites. These studies would not support an intracellular phase of PrP accumulation in FDCs but show that PrP is produced in excess by scrapie-infected cells from where it is released into the extracellular space. We suggest that PrP^{sen} is involved in dendritic extension or in the process of antibody–antigen trapping, perhaps as part of the binding mechanism for antigen–antibody complexes. © **Crown copyright 2000. Reproduced with the permission of Her Majesty's Stationery Office. Published by John Wiley & Sons, Ltd.**

Keywords: prion protein; scrapie; spongiform encephalopathies; immunogold; amyloid; spleen; follicular dendritic cells

Introduction

The transmissible spongiform encephalopathies (TSEs), or prion diseases, are a group of slowly progressive neurological disorders characterized by the accumulation of an abnormal post-translationally modified form of a host-encoded cell surface glycoprotein called prion protein (PrP). The abnormal form of the protein is partially protease resistant (PrP^{res}) and accumulates in brain and also in lymphoreticular tissues and peripheral nervous system in most experimental models and some natural disease. This abnormal isoform of PrP copurifies with infectivity [1]. The normal form of the prion protein (PrP^{sen}) is expressed abundantly in the CNS and at a lower level in many visceral tissues [2].

Many studies indicate that the lymphoreticular system is important for scrapie pathogenesis [3]. Within a few weeks of scrapie infection, agent replication can be detected in a variety of lymphoid tissues [4], and, at least in murine scrapie models, initial neuroinvasion is thought to occur following retrograde transportation of infectivity to the spinal cord via splanchnic nerves which innervate the spleen [5].

Studies employing a variety of experimental approaches, including the use of cell fractionation techniques, severe combined immunodeficient (SCID) mice and whole body gamma irradiation, suggest that the follicular dendritic cell (FDC) is important for scrapie pathogenesis [6–11]. Procedures which deplete mitotic cells, such as gamma irradiation, as well as genetic athymia or surgical thymectomy, do not significantly alter incubation periods [7,8], suggesting that scrapie replication does not depend upon B or T cells but requires radioresistant mitotically inactive

cells. Disease specific accumulations of PrP are also seen in association with FDCs of TSE infected mice, sheep and human beings [12–15]. PrP^{sen} can be detected in association with FDCs of the murine spleen [12].

SCID mice lack B and T cells and FDCs fail to mature [16]. They are relatively resistant to scrapie challenge by peripheral routes and fail to replicate infectivity in their spleens [9,17]. Following reconstitution by bone marrow grafting, these mice become fully susceptible to peripheral challenge and capable of supporting replication in their spleens. In further studies, chimeric mice have been produced by bone marrow grafting either SCID or gamma-irradiated mice which express PrP in FDCs but not lymphocytes, and vice versa. This has been possible because, in adult mice, FDCs probably derive from a stromal cell within the lymphoreticular system and are not replaced significantly from the bone marrow. Following ME7 scrapie infection, replication has been shown in the spleens of mice with a functional PrP gene ($PrP^{+/+}$) reconstituted with $PrP^{+/+}$ or PrP null ($PrP^{-/-}$) bone marrow, but not in the spleens of $PrP^{-/-}$ mice reconstituted with either $PrP^{+/+}$ or $PrP^{-/-}$ bone marrow [9,18]. These observations indicate that mature PrP-expressing FDCs are necessary for scrapie replication. However, other studies using a different murine scrapie strain have suggested that B cells may be involved, although this now appears to be in some doubt [20]. Nevertheless, it has been clearly shown that some lymphocytes express PrP^{sen} on their cell surface [21,22].

This study was undertaken to try to understand better the role of the spleen in the peripheral pathogenesis of scrapie. We have used immunogold electron microscopy to locate PrP at subcellular levels of ME7 infected spleen.

Materials and methods

C57 BL mice infected with the ME7 scrapie strain by intracerebral injection of 20 µl of a 1 per cent brain homogenate were available for study. 47 spleen tissue blocks were taken from 2 scrapie infected mice at 70 days after infection and 33 spleen tissue blocks were taken from 3 mice at terminal stages of the disease (mean incubation period approximately 170 days.) From 5 age-matched normal brain inoculated control mice, 70 blocks of spleen tissue were available for examination.

Light microscopical immunohistochemical staining procedure

Spleens were immersion fixed in 2 per cent PLP, 0.5 per cent paraformaldehyde/0.5 per cent glutaraldehyde or in a variety of concentrations of paraformaldehyde/glutaraldehyde for 24 hours at 4°C. One millimetre cubes of spleen were post fixed in osmium tetroxide, dehydrated and embedded in araldite. Thick sections were stained by toluidine blue or were etched (deplasticized) with saturated sodium ethoxide diluted 1 : 1 in absolute ethanol for up to 60 minutes. Endogenous peroxidase was blocked and sections de-osmicated with 6 per cent hydrogen peroxide in methanol for 10 minutes, followed by pre-treatment with formic acid for 30 minutes [23]. Normal serum was then applied for 1 hour to block non-specific staining. The peroxidase anti-peroxidase immunohistochemical staining method using 1A8 anti PrP serum [24] at a dilution of 1 : 2000, or pre-immune serum, was applied to the etched and pre-treated sections. Reaction product was developed using 3-3′ diaminobenzidine. Selected blocks with appropriate immunostained areas were then taken for ultrastructural studies.

Ultrastructural immunohistochemical methods

Serial 65 nm sections were taken from blocks previously identified as containing immunostained cells in white pulp. These sections were placed on 300 mesh nickel grids and etched in sodium periodate for 60 minutes. Endogenous peroxidase was blocked and sections de-osmicated with 3 per cent hydrogen peroxide in methanol for 10 minutes followed by enhancement of antigen expression with formic acid for 10 minutes. Residual aldehyde groups were quenched with 0.2 M glycine in PBS, pH 7.4 for 3 minutes. Primary antibody (1A8) at a 1 : 500 dilution in incubation buffer or pre-immune serum were then applied for 15 hours. After rinsing extensively, sections were incubated with Auroprobe 1 nm colloidal gold diluted 1 : 50 in incubation buffer for 2 hours. Sections were then post fixed with 2.5 per cent gluteraldehyde in PBS and staining was enhanced with IGSS for 4 minutes. Grids were counterstained with uranyl acetate and lead citrate. Tissues fixed in PLP fixative generally had better preservation of immunoreactivity but tissue fixed in mixtures of glutaraldehyde/paraformaldehyde had better tissue structure. In each case, observations were made on tissues fixed by PLP and by mixed aldehydes.

Although PrP^{sen} can be detected in cells of lightly fixed spleen by light microscopy [12], the combination of fixatives and pre-treatments described above destroys PrP^{sen} immunoreativity and reveals only disease-specific PrP accumulations. Whether these deposits are protease resistant or protease sensitive cannot be determined by the immunocytochemical methods described.

Results

Light microscopy

At terminal stages of disease, PrP was detected in the white pulp in a proportion of macrophage-like cells with open nuclei containing little nuclear chromatin, and these had multiple intense puncta of staining adjacent to the nucleus (Figure 1(a)). These cells were located throughout the white pulp and occasionally in

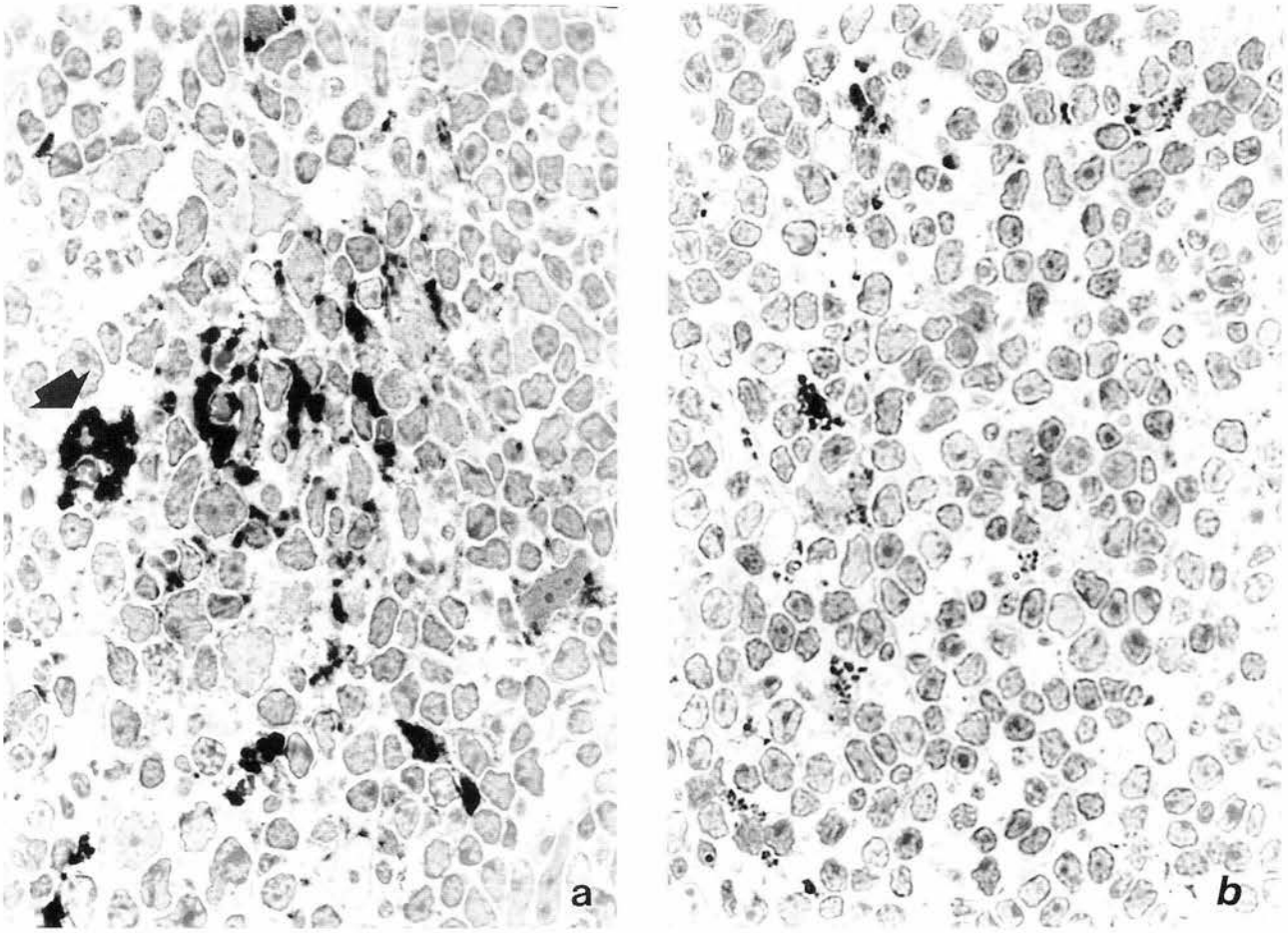

Figure 1. (a) One micrometre thick plastic embedded spleen from a terminally ill mouse showing immunostaining for PrP. Macrophage-like cells with punctate perinuclear immunoreactivity (arrow) are present. Other attenuated cell processes and larger areas of immunoreactivity are also immunostained. Peroxidase–anti-peroxidase (PAP) staining for PrP. (b) One micrometre thick plastic embedded spleen from a 70 dpi mouse immunostaining for PrP in a similar but less intense pattern than in terminally diseased mice. PAP staining for PrP

red pulp immediately surrounding white pulp, in the mantle zones, and in both the dark and light zones of germinal centres. They were provisionally interpreted as tingible body macrophages [25]. All germinal centres were affected.

A further cell type, also with marginated nuclear chromatin and presumptively identified as the FDC [26], showed a diffuse pattern of staining throughout the perikaryonal cytoplasm and in association with cytoplasmic processes which extended for considerable distances from the cell body (Figure 1(a)).

At 70 days post inoculation (dpi) the amount of immunostaining was considerably lower and not all follicles showed evidence of PrP accumulation. Although more subtle in amount, the patterns of staining at 70 dpi was essentially the same as that described above (Figure 1(b)).

No immunostaining was seen in the red or white pulp of age matched normal brain inoculated controls.

Electron microscopy

Control tissues did not show any immunostaining when examined by electron microscopy. The white pulp adjacent to red pulp contained small lymphocytes, between which were small filiform dendritic processes of FDCs. At the centre of some foci of white pulp, secondary lymph follicles could be identified. In part of these follicles lymphocytes were large (the germinal centre light zone) and between them, arranged in small knots, were more complex branching processes (labyrinthine glomerular complexes) of FDCs. At the plasmalemma of these dendrites was electron-dense material. Tingible body macrophages were identified in white pulp and less frequently in red pulp.

In tissues obtained from ME7 infected mice at 70 dpi and at terminal disease, a proportion of tingible body macrophages, identified by their frequent lysosomes, abundant rough endoplasmic reticulum and open nuclei containing mainly euchromatin with a peripheral margin of heterochromatin, showed marked immunogold affinity for PrP within lysosome-like structures (Figures 3, 4 and 9). In some of these lysosomes, immunogold deposits were concentrated at one particular pole, associated with a more electron-dense floccular material. A minority of tingible body macrophages showed immunogold affinity for fibrillar

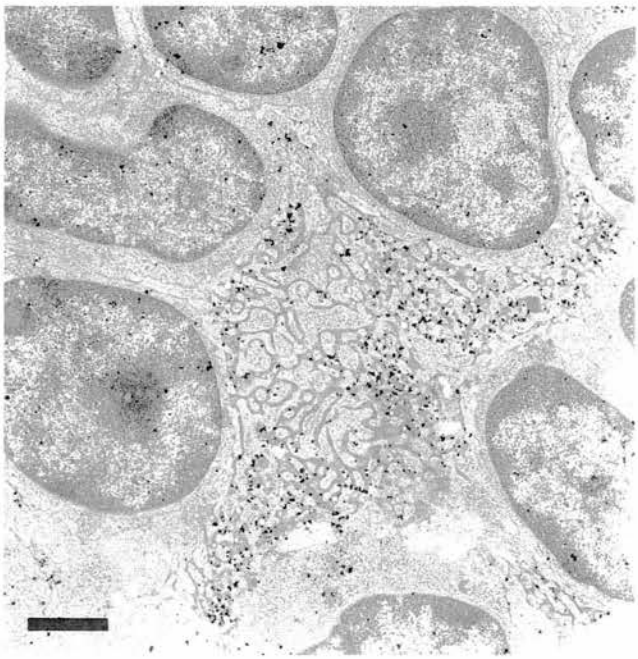

Figure 2. Terminal disease. Foci of immunoreactivity are present between lymphocyte cell nuclei in association with an FDC labyrinthine glomerular complex containing highly convoluted dendrites. Bar = 1.63 μm

structures within a lysosome (Figure 4). Only a proportion of tingible body macrophages was so stained. Some macrophages were found at sites

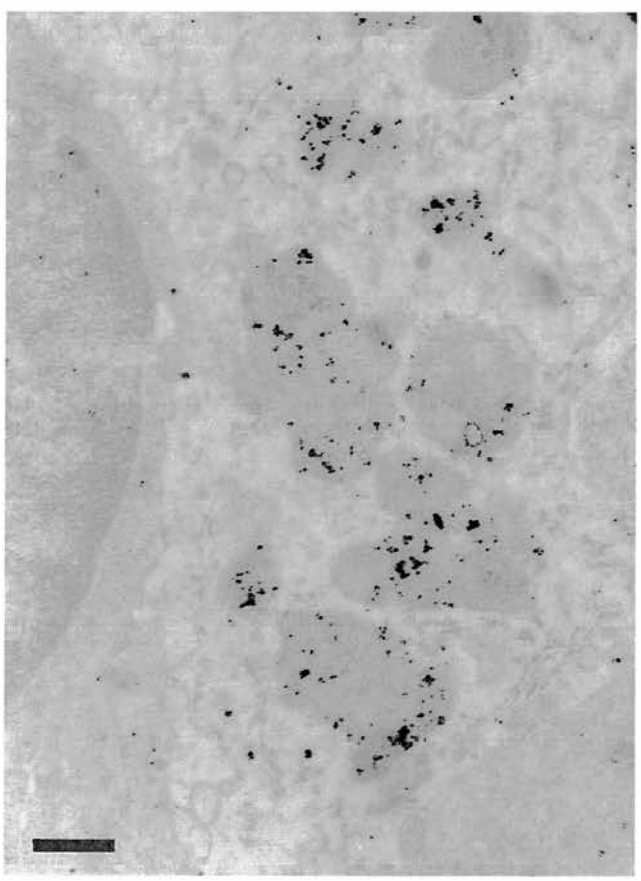

Figure 3. Terminal disease. Tingible body macrophage showing intra-lysosomal PrP accumulation. Bar = 0.45 μm

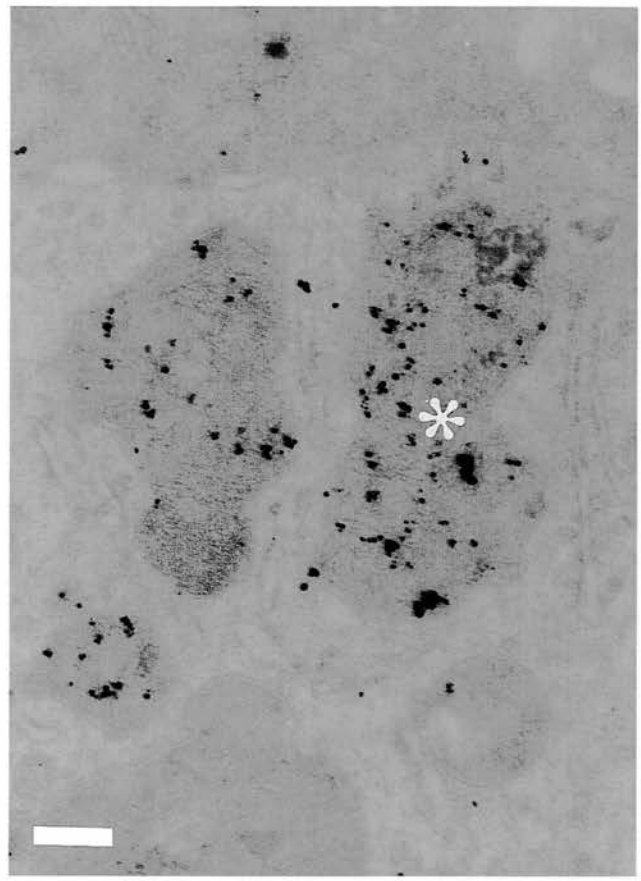

Figure 4. Terminal disease. Tingible body macrophage showing intra-lysosomal immunostaining. There are short linear filamentous structures within one lysosome (asterisk) which are closely associated with the reaction product. Bar = 0.34 μm

apparently distant from FDCs, whilst others were in close proximity to FDC-associated immunogold staining.

Immunogold/silver complex labelling was also associated with a second population of cells, characterized by a nucleus containing abundant euchromatin and marginal heterochromatin and complex branching processes (dendrites) which identified them as follicular dendritic cells (FDCs) (Figures 2 and 5). In the light zone of follicles obtained from spleens of clinically affected mice, the FDC dendrites invariably formed large and complex labyrinthine glomeruli (Figures 5 and 6) [27], indicating a highly reactive response to stimulation. Around each dendrite, a significant margin of amorphous electron-dense material was present (Figures 5 and 6). Immunogold staining was seen in the extracellular space surrounding the dendritic processes of FDCs and was associated with the electron-dense deposit. The immunogold staining intensity and the complexity of branching of dendritic processes within the glomeruli increased in proportion to the amount of electron-dense material within the extracellular space (Figures 5 and 6). In some areas, abundant short fibrillar forms were present within the extracellular space and were associated with the electron-dense deposit (Figure 6). Fibrils were of

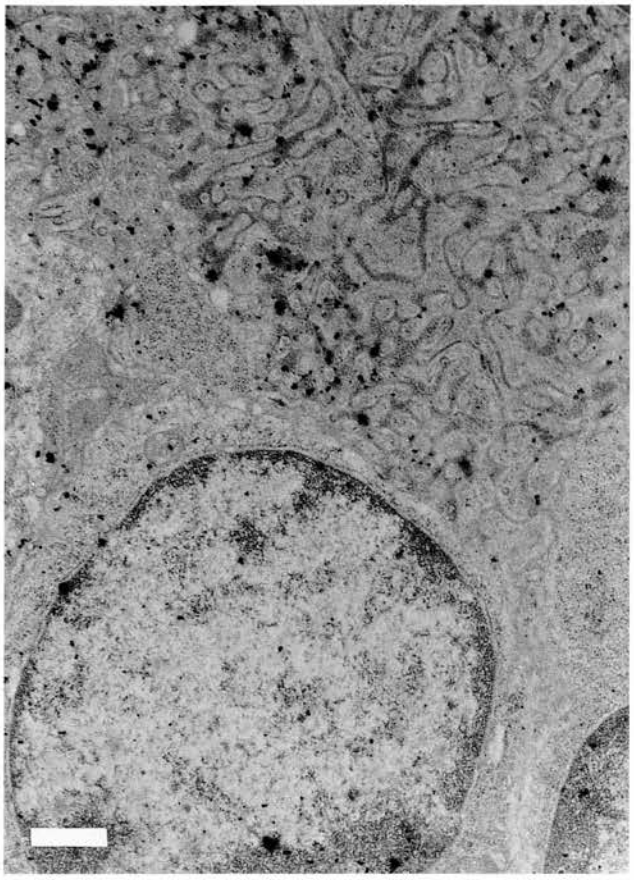

Figure 5. Terminal disease. Labyrinthine glomerulus with reactive FDC dendritic processes is present. The immunogold/silver reaction is associated with an electron-dense deposit at the plasmalemma of these dendrites. Bar = 0.8 μm

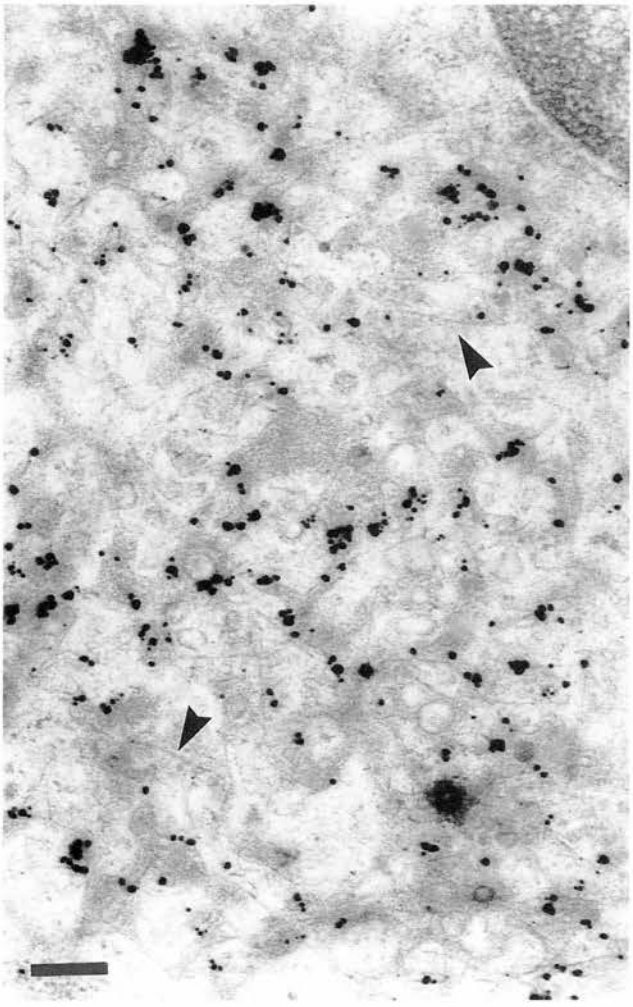

Figure 6. Terminal disease. FDC processes associated with intense immunogold reaction. There are frequent short filaments (arrowheads) present within the extracellular space. Bar = 0.28 μm

approximately 20 nm diameter and from 40 to 300 nm long. Immunogold localization was seen in coated pits at the surface of FDC dendrites. Rarely, coated pits at the surface of lymphocytes adjacent to labyrinthine complexes also contained immunoreactive products (Figure 7). Immunogold reaction was present in electron-dense material associated with FDC dendrites surrounding (emperipolesing) plasmablasts with dilated endoplasmic reticulum containing globulins (Figure 8).

In terminally affected mice, FDCs were recognized by electron microscopy in areas lacking PrP immunostaining at light microscopy (the dark zone and periarteriolar sheath). FDCs in this region had few filiform dendrites and did not show immunogold staining.

At 70 dpi most FDCs in the follicular light zones had relatively inconspicuous dendrites which formed small knots of labyrinthine complexes interspersed between lymphocytes and thus were similar to controls. Any such processes had no obvious amorphous electron-dense deposit at the plasmalemma although some electron dense material was present around the FDC dendrites of a minority of cells (Figure 9). Although the immunostaining was weaker than at terminal disease, nevertheless PrP accumulation was present at the plasmalemma of these FDC dendrites. FDCs with large labyrinthine glomerular complexes similar to those found in terminally affected mice were occasionally detected and invariably associated with intense immunogold staining. PrP immunoreactive fibrils were sometimes found in the extracellular space around these large labyrinthine complexes.

Discussion

These results confirm previous light microscopy studies showing that disease specific accumulations of PrP occur in white pulp of spleen. Although the antibody used does not distinguish between the protease sensitive and protease resistant isoforms of PrP, we would anticipate that at least some of the excess PrP accumulations, particularly those in fibrillar forms, would be protease resistant. In agreement with transmission and light microscopy studies of Brown *et al.* [18] our observations do not suggest that PrP accumulation occurs within B-lymphocytes in ME7 scrapie affected spleens.

Secondary follicles have at least three major morphological subdivisions. A peripheral circumferential

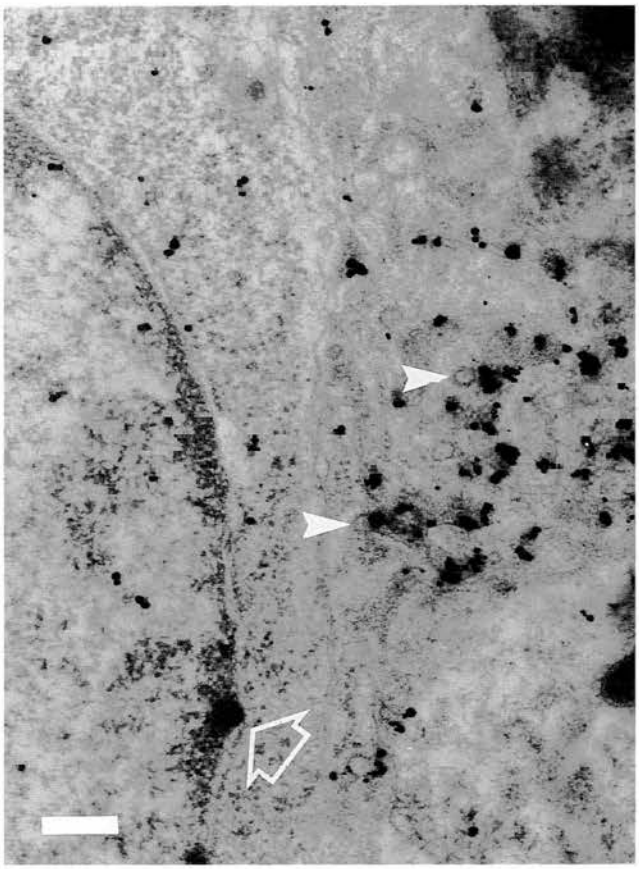

Figure 7. Terminal disease. Detail of convoluted dendrites of an FDC in association with frequent coated pits (arrowheads). A lymphocyte adjacent to the immunogold reaction shows PrP within a coated pit near the cell surface (arrow). Bar = 0.36 μm

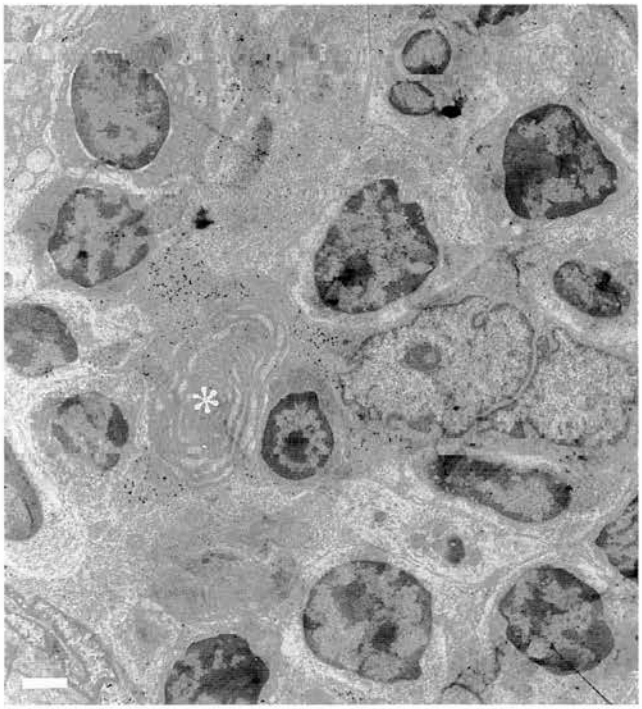

Figure 8. Terminal disease. Plasmablast (asterisk) with dilated (globulin containing) endoplasmic reticulum surrounded by immunoreactive dendrites of an FDC. Bar – 1.7 μm

arrangement of small recirculating lymphocytes forms the mantle zone around the dark and light zones of germinal centres [28]. The dark zone contains larger and more closely packed lymphocytes (centroblasts) and FDCs with poorly developed cytoplasmic extensions. In the light zone there are yet larger lymphoid cells (centrocytes) and FDCs with extensive cytoplasmic extensions. During the development of germinal centres, FDCs lose the capacity to synthesize matrix elements and begin to produce specific surface antigens. As increasing quantities of immune complexes are retained, imported by lymphoid cells or by other means, the surfaces of FDCs enlarge, form plicae and dendrites develop [24]. Immune complexes are bound to the cytoplasmic extensions (dendrites) of FDCs, where they may remain for weeks or months. These complexes are not endocytosed but are held at the surface of the dendrite by C3b or Fc receptors [27,29]. Free antigens are not bound to the surface of FDCs. Antigen–antibody complexes serve periodically to restimulate B and perhaps T cells, although many of the complexes are deep within the cytoplasmic invaginations of FDCs and not readily revealed to other cells.

In so far as we are able to determine the localization of FDCs within follicles, immature FDCs corresponding to those found in the dark zone were similar in controls and in infected mice. However, in presumed light zones, all FDCs at terminal stages of disease and a proportion of FDCs at 70 dpi had large and highly complex labyrinthine glomeruli. This appears to represent an abnormal reactive or hyperplastic change of FDCs compared with controls.

Transmission studies using chimeric mice [18] in which some immune system cells carry the PrP gene and some do not, and light microscopy immunocytochemical studies of spleen and lymph nodes, suggest that mature FDCs accumulate PrP [12,13,18]. The subcellular localization of PrP described above confirms that FDCs are associated with PrP accumulation. However, the PrP accumulation appears to be found at the cell surface of FDCs and not within the cytoplasm. This is similar to the extracellular localization of PrP around neurons in

Figure 9. (a) 70 dpi. An area of intense PrP labelling is present which extends over much of the upper portion of the field. Two FDC nuclei, one with only light staining (asterisk) of the adjacent parenchyma and one where the adjacent parenchyma is unstained (arrow), are also in the field. Arrowhead indicates a PrP containing tingible body macrophage. Bar = 4.5 μm. (b) Detail near tingible body macrophage at arrowhead in (a). An intense immunogold reaction is associated with the electron-dense deposit overlying complex labyrinthine convolutions of FDCs similar to those seen in terminal mice. Bar = 0.53 μm. (c) Detail near FDC at asterisk in (a). FDC processes extending between lymphocytes are simple and do not have conspicuous electron-dense deposits at the plasmalemma. Bar = 0.39 μm

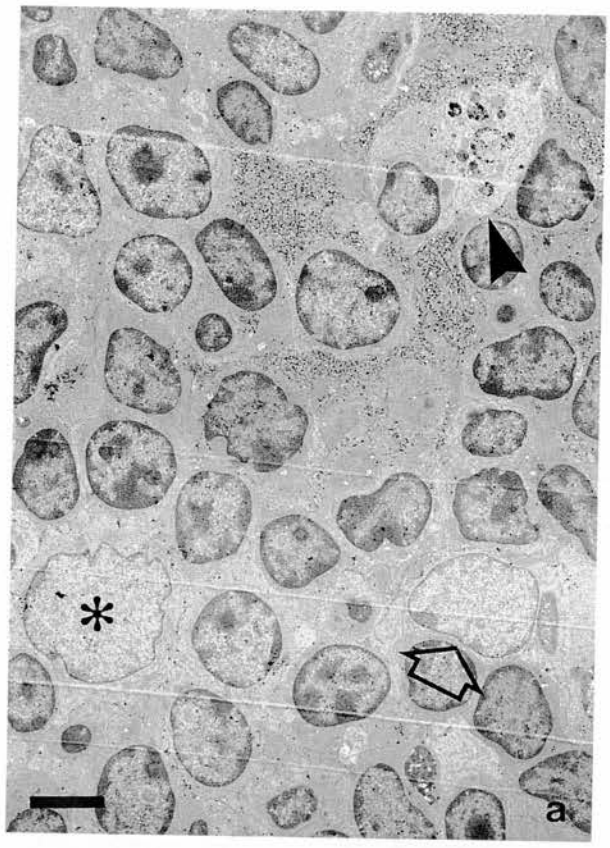
a

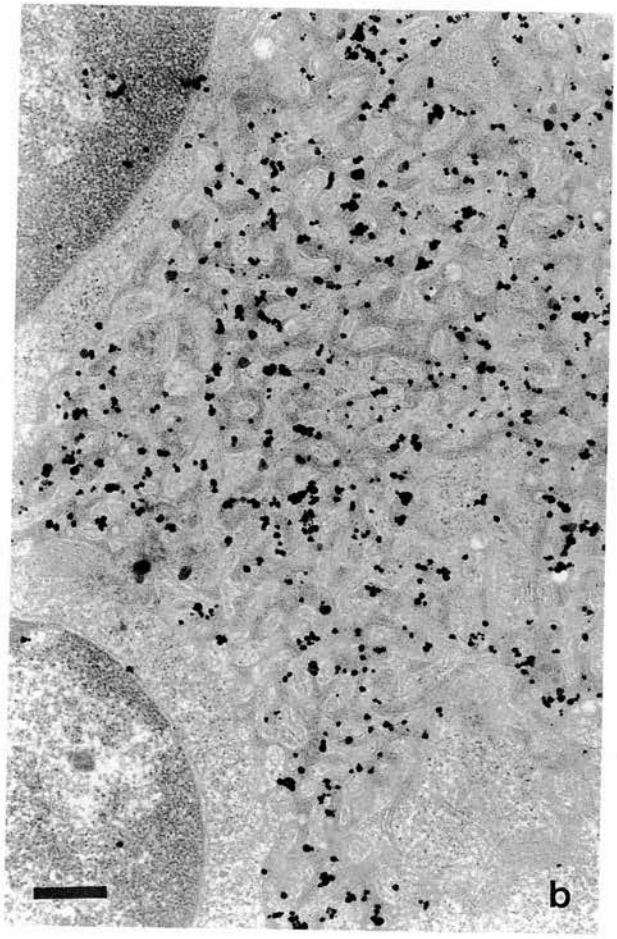
b

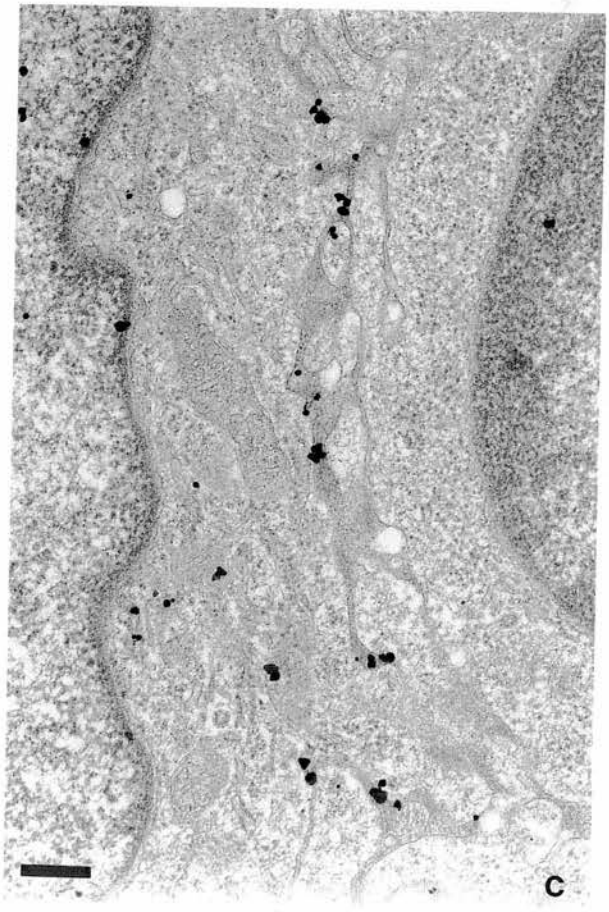
c

the brains of scrapie infected mice [30,31]. As is also found in brain, continued accumulation of PrP appears to lead to the formation of amyloid fibrils within the extracellular space [30,31]. Immature FDCs with poorly developed processes do not contain immunoreactive PrP in association with dendrites.

The observations presented in this study indicate that there is a proportionality of electron-dense deposits at the FDC dendrite plasmalemma, complexity of FDC dendritic branching and accumulation of excess or abnormal PrP. As attachment of immune complexes is the trigger for a marked increase in the complexity of dendritic processes [27,28], the pattern of dendritic branching and distribution of immunogold deposit in terminally diseased mice indicates that the FDCs were highly stimulated by either (or both) of the abundant or abnormal PrP, or by excess trapping of immune complexes. These findings suggest that PrP is involved in dendritic process elongation or in the process of trapping immune complexes. We suggest that this may reflect the normal function of PrP^{sen}. In support of this hypothesis we have also observed that disease specific accumulations of PrP in scrapie infected sheep lymph nodes and spleen are co-localized with the cell surface marker CD 21 and are confined to the light zone of germinal centres (M. Jeffrey, S. Martin, personal observations). Only fully mature process bearing FDCs posses CD21 in the light zone. In the present study, the uncomplicated nature of most FDC dendrites at 70 dpi and the paucity of plasmalemma associated electron-dense deposits suggest that early disease-specific PrP accumulation may occur initially in the absence of antigen–antibody complex trapping.

PrP immunostaining in FDC plasmalemma associated electron-dense material could also be interpreted as possible trapped antibody–PrP complexes. However, antibodies to PrP^{sen} would not be anticipated. Antibodies to PrP are not detected in TSE infected hosts, although infection does cause an immunological response in PrP null mice. PrP–antibody complexes would not therefore be expected at 70 dpi, but it is possible that low levels of antibodies may be formed to abnormal PrP^{res} as a result of structural changes, aggregation and fibrillization. Recent evidence using chimeric SCID-PrP null mice, irradiated and then reconstituted with either PrP null or $PrP^{+/+}$ bone marrow, indicate that scrapie replication and accumulation of PrP on FDCs [18] depends on PrP^{sen} expressing FDCs. These findings would suggest that most of the PrP detected at the cell surface of FDCs and within electron-dense material at the cell surface was initially expressed at the FDC surface and then released into the extracellular space.

If increased cell surface expression of PrP was involved in increased ability to scavenge non-specific antigen–antibody complex, then a breakdown in antibody homeostasis and a heightened non-specific polyclonal antibody response might be anticipated. Alterations in immunoglobulin levels have indeed been described in some scrapie–host model systems [11,32,33], including natural scrapie of sheep [33], but they are clearly not an essential aspect of disease, as most models do not exhibit changes in immunoglobulin levels. In some models, immunoglobulin levels may be altered at early stages of infection. The hyperplastic form of FDCs, evidence of emperipolesis associated plasmablast transformation, and marked increase in PrP associated antigen–antibody complexes suggests that scrapie infection may induce an enhanced presentation of immune complexes to B-lymphocytes. If, as suggested above, PrP is involved in non-specific binding of antigen–antibody complexes, then increased trapping of complexes may elicit alterations in homeostasis of antibody responses and an increased host polyclonal antibody response. These observations might suggest that the immunological response in scrapie is more complex than previously supposed. Further investigation of the immune system interactions with PrP may be of interest, not least as a potential for disease intervention strategies and diagnosis.

Tingible body macrophages ingest apoptotic cells, mostly B cells that are not selected to form clones of globulin producing cells. However, they also scavenge the ends of FDC processes and perhaps effete FDCs themselves [34,35]. Tingible body macrophages containing intra-lysosomal PrP were found adjacent to PrP accumulation associated with FDCs and as individual stained cells distant from other foci of immunostaining.

Intra-lysosomal PrP accumulation has also been seen within phagocytic cells of the CNS, including microglia, astroglia [30] and Kohler cells. We suggest that tingible body macrophages are ingesting excess or abnormal PrP. It is unclear whether this occurs as a result of phagocytosis of entire degenerate FDCs, or their processes, or merely by scavenging the extracellular space. All known amyloids are formed within the extracellular space from precursor proteins and therefore, as some macrophages possess intra-lysosomal filaments consistent with amyloid, these at least would presumably have been internalized to the macrophage from the extracellular space.

Scrapie associated fibrils are abnormal filamentous structures, which can be seen by negative stain electron microscopy following detergent extraction of brain [36] and spleen [4]. They are composed of PrP [37] and are observed only in the TSEs. Morphologically similar amyloid fibrils containing full length PrP are found *in vivo* in the brains of scrapie infected animals [31,38]. Although scrapie associated fibrils can be demonstrated in many of the TSEs, amyloid fibrils are not always seen in the brains of scrapie-infected animals and are in fact rare in scrapie of sheep and in BSE (M. Jeffrey, personal observations). In spleen, previous studies have shown that scrapie-associated fibrils may be found at early stages of disease and their numbers increase in correlation with infectious titre [4]. Although the inconsistent occurrence of PrP positive amyloid fibrils in the CNS suggests that the scrapie

associated fibrils seen by negative stain electron microscopy are an artefact of the tissue preparation process, nevertheless the similarity between scrapie associated fibrils and amyloid fibrils suggests that full length excess PrP has a propensity to form fibrils both *in vivo* and *in vitro*. It is possible that this propensity to aggregate carries with it the likelihood to acquire protease resistance, as with other amyloid proteins. Western blot analyses have demonstrated that PrP^{res} may be detected in ME7 infected spleens at very early stages of infection [24]. Our ultrastructural studies show that fibrillar forms of PrP may be detected deep in the folds of FDC dendrites even at early (70 dpi) stages of infection. We suggest therefore that western blots demonstrating PrP^{res} may be detecting these extracellular, fibrillar PrP aggregates and not necessarily the earlier, non-fibrillar disease specific accumulations of PrP.

In the light of recent reports indicating that PrP accumulates within the tonsil of clinical [15] and the appendix of preclinical vCJD patients [39], the importance of understanding the role of the lymphoreticular system in TSE pathogenesis has greatly increased. The present study provides an insight into the cellular and subcellular involvement of FDCs in the peripheral pathogenesis of scrapie and also suggests possible functions of PrP^{sen}

References

1. Diringer H, Gelderblom H, Hilmert H, Ozel M, Edelbluth C. Scrapie infectivity, fibrils and low molecular weight protein. *Nature* 1983; **306**: 476–478.
2. Oesch B, Westaway D, Walchi M, *et al.* Cellular gene encodes scrapie PrP 27–30 protein. *Cell* 1985; **40**: 735–746.
3. Fraser H, Dickinson AG. Pathogenesis of scrapie in the mouse. The role of the spleen. *Nature* 1970; **226**: 462–463.
4. Rubenstein R, Merz PA, Kascsak RJ. Scrapie-infected spleens: analysis of infectivity, scrapie associated fibrils, and protease-resistant proteins. *J Infect Dis* 1991; **164**: 29–35.
5. Kimberlin RH, Walker CA. Incubation periods in six models of intraperitoneally injected scrapie depend mainly on the dynamics of agent replication within the nervous system and not the lymphoreticular system. *Gen Virol* 1988; **69**: 2953–2960.
6. Ritchie DL, Brown KL, Bruce ME. Visualisation of PrP protein and follicular dendritic cells in uninfected and scrapie infected spleen. *J Cell Pathol* 1999; **1**: 3–10.
7. Fraser H, Dickinson AG. Studies of lymphoreticular system in the pathogenesis of scrapie. The role of spleen and thymus. *J Comp Pathol* 1978; **88**: 563–573.
8. Fraser H, Farquhar C. Ionising radiation has no influence on scrapie incubation period in mice. *Vet Micro* 1987; **13**: 211–223.
9. Brown KL, Stewart K, Bruce ME, Fraser H. Scrapie in immunodeficient mice. In *Transmissible Subacute Spongiform Encephalopathies*, Court L, Dodet B (eds). Elsevier: Paris, 1996; 159–166.
10. Laszemas CI, Cesbron J-Y, Deslys J-P, *et al.* Immune system-dependent and independent replication of the scrapie agent. *J Virol* 1996; **70**: 1292–1295.
11. Carp RI, Callaghan SM, Patrick BA, Mehta PD. Interaction of scrapie agent and cells of the lymphoreticular system. *Arch Virol* 1994; **136**: 255–268.
12. McBride PA, Eikelenboom P, Kraal G, Fraser H, Bruce ME. PrP protein is associated with follicular dendritic cells of spleens and lymph nodes in uninfected and scrapie-infected mice. *J Pathol* 1992; **168**: 413–418.
13. Kitamoto T, Muramoto T, Mohri S, Doh-ura K, Tatieishi J. Abnormal isoform of prion protein accumulates in follicular dendritic cells in mice with Creutzfeldt–Jakob disease. *J Virol* 1991; **65**: 6292–6295.
14. vanKeulen LJM, Schreuder BEC, Meloen RH, MooijHarkes G, Vromans MEW, Langeveld JPM. Immunohistochemical detection of prion protein in lymphoid tissues of sheep with natural scrapie. *J Clin Micro* 1996; **34**: 1228–1231.
15. Hill AF, Zeidler M, Ironside J, Collinge J. Diagnosis of new variant Creutzfeldt–Jakob disease by tonsil biopsy. *Lancet* 1997; **349**: 99–100.
16. Bosma GC, Fried M, Custer RP, Carroll A, Gibson DM, Bosma MJ. A severe combined immunodeficiency mutation in the mouse. *Nature* 1983; **301**: 527–530.
17. Brown KL, Stewart K, Bruce ME, Fraser H. Severely combined immunodeficient (SCID) mice resist infection with bovine spongiform encephalopathy. *J Gen Virol* 1997; **78**: 2707–2710.
18. Brown KL, Stewart K, Ritchie D, *et al.* TSE replication in lymphoid tissues depends on PrP-expressing follicular dendritic cells. *Nat Med* 1999; **5**: 1308–1312.
19. Blattler T, Brandner S, Raeber AJ, *et al.* PrP-expressing tissue required for transfer of scrapie infectivity from spleen to brain. *Nature* 1997; **389**: 69–73.
20. Klein MA, Frigg R, Raeber AJ, *et al.* PrP expresssion in B-lymphocytes is not required for prion invasion. *Nat Med* 1998; **4**: 1429–1433.
21. Cashman NR, Loertscher R, Nalbantoglu J. Cellular isoform of the scrapie agent protein participates in lymphocyte activation. *Cell* 1990; **61**: 185–189.
22. Mabbott NA, Brown KL, Manson J, Bruce ME. T lymphocyte activation and the cellular form of the prion protein. *Immunology* 1997; **92**: 161–165.
23. Jeffrey M, Goodsir CM. Immunohistochemistry of resinated tissues for light and electron microscopy. In *Methods in Molecular Medicine, Prion Diseases*, Baker HF, Ridley RM (eds). Humana Press: Totowa, New Jersey, 1996; 301–313.
24. Farquhar CF, Somerville RA, Dornan J, Armstrong D, Birkett C, Hope J. A review of the detection of PrPsc. Proceedings of a consultation on BSE with the ScientificVeterinary Committee of the CEC, 1993; 301–313.
25. Veerman AJO, van Ewijk W. White pulp in the spleen of mice and rats. A light and electron microscopy study of lymphoid and non lymphoid cells in T and B areas. *Cell Tissue Res* 1975; **156**: 417–423.
26. Heinen E. History of FDC. In *Follicullar Dendritic Cells in Normal and Pathological Conditions*, Heinen E (ed). Springer: Heidelberg, Germany, 1995; 5–17.
27. Terashima K, Dobashi M, Maeda K, Imai Y. Follicular dendritic cell and iccosomes in germinal centre reactions. *Sem Immunol* 1992; **4**: 267–274.
28. Heinen E, Bosseloir A, Bouzahzah F. Follicular dendritic cells: origin and function. *Curr Topics Microbiol Immunol* 1995; **201**: 15–47.
29. Bosseloir A, Bouzahzah F, Simar L, Heinen E. B cells in contact with FDC. In *Follicular Dendritic Cells in Normal and Pathological Conditions*, Heinen E (ed). Springer: Heidelberg, Germany, 1995; 53–78.
30. Jeffrey M, Goodsir CM, Bruce ME, McBride PA, Scott JR, Halliday WG. Correlative light and electron microscopy studies of PrP localization in 87 V scrapie. *Brain Res* 1994; **656**: 329–343.
31. Jeffrey M, Goodsir CM, Bruce ME, McBride PA, Fowler N, Scott JR. Murine scrapie-infected neurons *in vivo* release excess PrP into the extracellular space. *Neurosci Lett* 1994; **174**: 39–42.
32. Collis CS, Kimberlin RH. Long term persistence of scrapie infection in mouse spleens in the absence of clinical disease. *FEMS Microbiol Lett* 1985; **29**: 111–114.
33. Collis CS, Kimberlin RH. Further studies on changes in immunoglobulin G in the sera and CSF of Herdwick sheep

with natural and experimental scrapie. *J Comp Pathol* 1983; **93**: 331–338.
34. Tew JG, Kosco MH, Szakal AK. The alternative antigen pathway. *Immunol Today* 1989; **10**: 229–231.
35. Szakal AK, Kosco MH, Tew JG. A novel *in vivo* follicular dendritic cell-dependent iccosome-mediated mechanism for delivery of antigen to antigen-processing cells. *J Immunol* 1988; **140**: 342–353.
36. Merz PA, Somerville RA, Wisniewski HM, Iqbal K. Abnormal fibrils from scrapie-infected brain. *Acta Neuropathol* 1981; **54**: 63–74.
37. Merz PA, Kascsak RJ, Rubenstein R, Carp RI, Wisniewski HM. Antisera to scrapie-associated fibril protein and prion protein decorate scrapie-associated fibrils. *J Virol* 1987; **61**: 42–49.
38. Jeffrey M, Goodsir CM, Fowler N, Hope J, Bruce ME, McBride PA. Ultrastructural immunolocalization of synthetic prion protein peptide antibodies in 87 V murine scrapie. *Neurodegeneration* 1996; **5**: 101–109.
39. Hilton DA, Fathers E, Edwards P, Ironside JW, Zajicek J. Prion immunoreactivity in appendix before clinical onset of variant Creutzfeldt–Jacob disease. *Lancet* 1998; **352**: 703–704.

Arch Virol (2000) [Suppl] 16: 23–38

Archives of Virology

Cellular and sub-cellular localisation of PrP in the lymphoreticular system of mice and sheep

M. Jeffrey, G. McGovern, S. Martin, C. M. Goodsir, and K. L. Brown

Lasswade Veterinary Laboratory, Penicuik, Scotland, U.K.

Summary. Using immunocytochemistry or immunogold electron microscopy, abnormal PrP accumulation was found in lymphoreticular tissues of Suffolk sheep naturally exposed to scrapie and in the spleens of ME7 infected C57 BL mice at 70 days after infection and at the terminal stage of disease at 170 days. Clinically diseased scrapie affected sheep show widespread PrP accumulation within tingible body macrophages (TBMs) and follicular dendritic cells (FDCs) of secondary lymphoid follicles. Serial tonsillar biopsies taken from 171ARQ/ARQ sheep at 4 months of age did not contain abnormal PrP accumulations but 80% of biopsies were positive by 14 months. In contrast, whole body necropsies of sheep not previously biopsied failed to detect PrP in the tonsil of sheep at 4, 8, 12 or 16 months of age. These findings suggest that the biopsy procedure of susceptible sheep but not resistant sheep may induce tonsillar infection. In spleen of mice both at 70 and 170 dpi, accumulations of PrP were found within lysosomes of TBMs and also at the plasma-lemma of FDCs. In the light zone of follicles of terminally diseased mice, all FDC dendrites were arranged in the form of highly reactive or hyperplastic labrynthine glomerular complexes. PrP was consistently seen between FDC dendrites in association with abundant electron dense antigen-antibody complexes. At 70 days after challenge, labrynthine complexes were rare and invariably labelled for PrP. However, sparse PrP labelling was also seen on simple FDC dendrites at this stage. These observations suggests that scrapie infected FDCs continually release PrP from the cell surface where it accumulates in excess in association with trapped immune complexes and dendritic extension. It is likely that TBMs acquire lysosomal PrP following phagocytosis of effete FDC processes or from the extracellular space. We suggest that the normal function of PrP may involve cell process extension or immune complex trapping.

Introduction

Many studies indicate that the lymphoreticular system is important for scrapie pathogenesis. Within a few weeks of scrapie infection, agent

replication can be detected in a variety of lymphoid tissues [27] and, initial neuroinvasion is thought to occur following retrograde transportation of infectivity to the spinal cord via splanchnic nerves which innervate the spleen [20].

Studies employing a variety of experimental approaches, including the use of cell fractionation techniques, severe combined immunodeficient (SCID) mice and whole body γ irradiation, suggest that the follicular dendritic cell (FDC) is important for scrapie pathogenesis [6, 7, 12, 13, 24]. Procedures which deplete mitotic cells, such as γ irradiation as well as genetic athymia or surgical thymectomy do not significantly alter incubation periods [12, 13] suggesting that scrapie replication does not depend upon T cells but requires radioresistant mitotically inactive cells. Disease specific accumulations of PrP are also seen in association with FDCs of TSE infected mice, sheep and human beings [16, 22, 27, 33]. PrP^{sen} can be detected in association with FDCs of the murine spleen [27].

SCID mice lack B and T cells and FDCs fail to mature [2]. They are relatively resistant to scrapie challenge by peripheral routes and fail to replicate infectivity in their spleens [4, 6]. Following reconstitution by bone marrow grafting these mice become fully susceptible to peripheral challenge and capable of supporting replication in their spleens. In further studies, chimaeric mice have been produced by bone marrow grafting either SCID or γ-irradiated mice, which express PrP in FDCs but not lymphocytes, and vice versa. This has been possible because, in adult mice, FDCs probably derive from a stromal cell within the lymphoreticular system and are not replaced significantly from the bone marrow. Following ME7 scrapie infection, replication has been shown in the spleens of mice with a functional PrP gene ($PrP^{+/+}$) reconstituted with $PrP^{+/+}$ or PrP null ($PrP^{-/-}$) bone marrow but not in the spleens of $PrP^{-/-}$ mice reconstituted with either $PrP^{+/+}$ or $PrP^{-/-}$ bone marrow [4, 5]. These observations indicate that mature PrP expressing FDCs are necessary for scrapie replication. However, other studies using a different murine scrapie strain have suggested that B cells may be involved [1] although this now appears to be in some doubt [23]. Nevertheless, it has been clearlyd shown that some lymphocytes express PrP^{sen} on their cell surface [8, 25].

These studies were undertaken to try and better understand the role of the LRS in the peripheral pathogenesis of scrapie.

Materials and methods

Animals

Sequential tonsillar biopsies or necropsies were performed on lambs taken from a flock of Suffolk sheep which had experienced frequent cases of scrapie over a period of several years. All but 2 of 106 scrapie cases examined between 1990 and 1996 in this flock were homozygous for glutamine at codon 171 of the PrP gene with a mean age to clinical disease of 30 months. Clinically affected sheep had widespread PrP

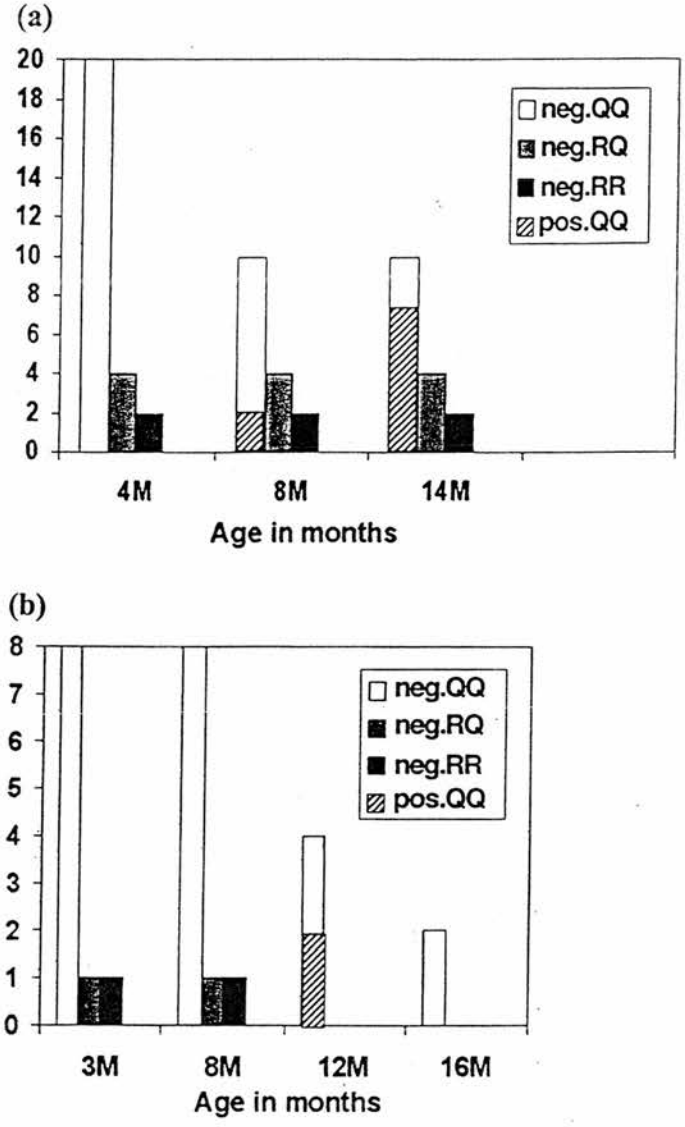

Fig. 1. a Numbers of positive and negative tonsillar biopsies by age and genotype; **b** numbers of positive necropsies with positive or negative immunostaining in viscera by genotype and age of sheep

accumulation in the lymphoreticular system and peripheral ganglia. Lambs born in Spring of 1998 were serially biopsied from tonsils or were subjected to whole body necropsy at selected time intervals (Fig. 1).

C57 BL mice infected with the ME7 scrapie strain by intracerebral injection of 20 µl of a 1% brain homogenate were available for electron microscopy studies. Forty-seven spleen tissue blocks were taken from two scrapie infected mice at 70 days after infection and 33 spleen tissue blocks were taken from three mice at terminal stages of the disease (mean incubation period approximately 170 days). From five age matched normal brain inoculated control mice, 70 blocks of spleen tissue were available for examination.

Light and electron microscopical immunohistochemical staining procedure

Details of light and electron microscopical techniques for immunostaining are as previously described [20]. Spleens were immersion fixed in 2% PLP, 0.5% paraformaldehyde/0.5% gluteraldehyde or in a variety of concentrations of paraformaldehyde/glutaraldehyde for 24 h at 4 °C. Primary antibody (1A8) at a 1:500 dilution in incubation buffer or pre-immune serum were then applied for 15 h. After rinsing extensively, sections were incubated with Auroprobe 1 nm colloidal gold diluted 1:50 in incubation buffer for 2 hours.

Tonsillar biopsies were prepared as described by van Keulen et al. [33] and stained using both the 521.2 antibody (kindly supplied by Dr. van Keulen) and a polyclonal rabbit anti-sheep PrP peptide antibody R482. None of the above antibodies can distinguish between PrP^{sen} and PrP^{res}. However, under the conditions of fixation and embedding employed in this study no staining was seen in control tissues. Immunocytochemically detected PrP therefore represents accumulation of abnormal amounts of PrP of unknown protease sensitivity.

Results

Natural sheep scrapie

Clinically affected sheep showed PrP accumulation in virtually all follicles of all lymph nodes. The numbers of secondary lymphoid follicles appeared to be more frequent than in controls and often penetrated into the medulla of the node. PrP was found in cells of the light zone which resembled mature FDCs and in serial sections co-localised with CD21 staining. Other cells which resembled TBMs were also immunostained and were found in light zone, dark zone, mantle zone and, in smaller numbers in the paracortex.

Serial tonsillar biopsies taken from lambs at 4, 8 and 14 months of age did not show any PrP accumulation in germinal centres of two ARR/ARR or four ARQ/ARR sheep. In serial biopsies from ARQ/ARQ lambs disease specific PrP accumulation was not seen in 20 lambs at 4 months of age, but was found in 2 of 10 lambs at 8 months and in 7 of 10 lambs at 14 months (Figs. 1 and 2). Initially, the earliest disease specific PrP accumulation seen was in TBMs within germinal centres and only later was it detected in a reticular pattern in the light zone of germinal centres. As in clinically diseased sheep, the latter staining was found to co-localise with CD21 suggesting that PrP was present in FDCs. At 12 months some immunostained TBMs were found in paracortical areas.

Eight ARQ/ARQ lambs necropsied at 3 or 8 months of age had no visceral PrP accumulations but at 12 months of age two of four ARQ/ARQ lambs had PrP accumulation in mesenteric lymph nodes alone. Other lymphoreticular tissues including tonsil were not affected. The remaining two 12-month-old ARQ/ARQ and two ARQ/ARQ sheep at 16 months had no CNS or visceral PrP (Fig. 1).

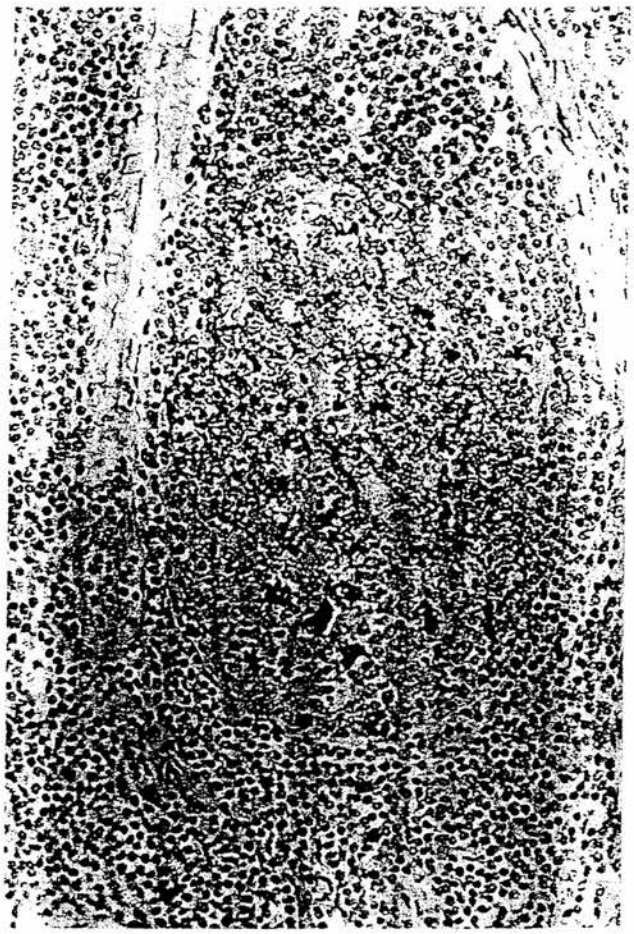

Fig. 2. Tonsillar biopsy of a 14-month-old sheep. The follicle shows marked immunostaining of cells with intense granular intracytoplasmic staining (Tingible body macrophages) throughout all regions of the follicle and diffuse punctate staining within the light zone (presumed FDCs). ABC staining for PrP

Murine scrapie infected spleen: light microscopy

In 1 μm thick sections of the spleens of mice at terminal stages of disease, PrP was detected in the white pulp in a proportion of macrophage like cells as multiple intense puncta of intracytoplasmic staining as described in sheep. These cells were located throughout the white pulp and occasionally in red pulp in the mantle zones and in both the dark and light zones of secondary lymphoid follicles and were provisionally interpreted as TBMs. All germinal centres were affected. A further cell type presumptively identified as the FDC, showed a diffuse pattern of staining in association with cytoplasmic processes which extended for considerable distances from the cell body.

At 70 days post inoculation (dpi) the overall amount of immunostaining was considerably lower and not all follicles showed evidence of PrP

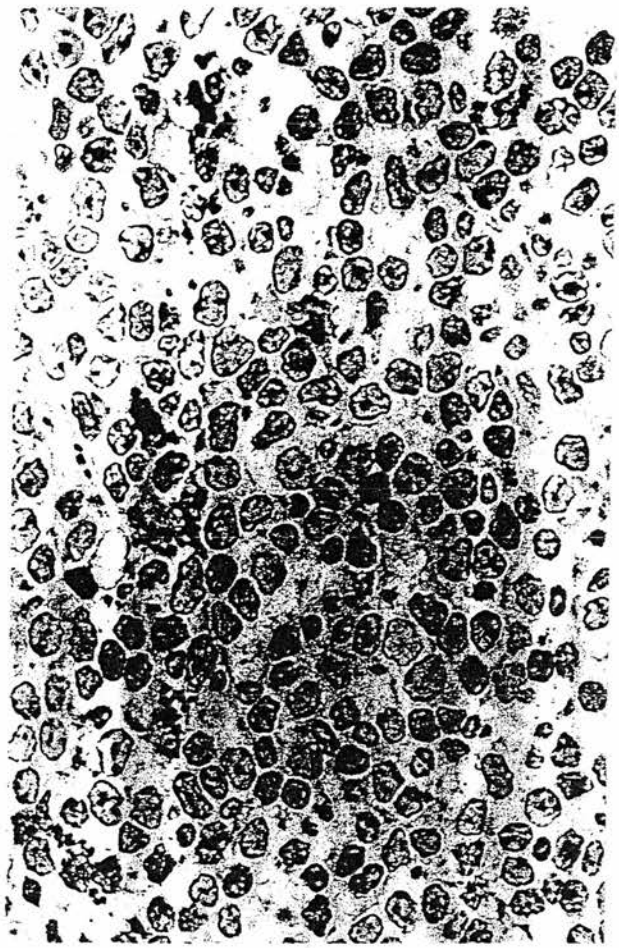

Fig. 3. Murine spleen. 70 days postinoculation showing staining of cells and processes. 1 μm thick section PAP for PrP

accumulation. Although more subtle in amount, the patterns of staining at 70 days post inoculation was essentially the same as in terminal diseased mice (Fig. 3). No immunostaining was seen in the red or white pulp of age matched normal brain inoculated controls.

Electron microscopy

Control tissues did not show any immunostaining when examined by electron microscopy. The dark zones of germinal centres contained lymphocytes between which were small filiform dendritic processes of FDCs. At the centre of some foci of white pulp, secondary lymph follicles could be identified. In part of these follicles lymphocytes were large often with indented nuclei, (the germinal centre light zone) and between them, arranged in small knots were more complex branching processes (labyrinthine glomerular complexes) of FDCs. At the plasmalemma of these dendrites

was electron dense material. TBMs were identified in white pulp and less frequently in red pulp.

In tissues obtained from ME7 infected mice at 70 dpi and at terminal disease, a proportion of TBMs showed marked immunogold affinity for PrP within membrane bound electron dense structures resembling lysosomes (Fig. 4). Only a proportion of TBMs showed immunogold staining.

Immunogold labelling was also associated with a second population of cells found only in the light zone and characterised by complex branching processes (dendrites), sometimes containing desmosome-like membrane specialisations, which identified them as FDCs (Fig. 5). In the light zone of follicles examined from the spleens of 170 dpi mice, the FDC dendrites invariably formed large and complex labyrinthine glomeruli (Figs. 5 and 6) [31] indicating a highly reactive response to stimulation. At the plasmalemma of dendrites there was an amorphous electron dense material (Figs. 5 and 6). Immunogold staining was seen in the extracellular space surrounding the dendritic processes of FDCs and was associated with the electron dense deposit. The immunogold staining intensity and the complexity of branching of dendritic processes within the glomeruli increased in

Fig. 4. Murine spleen. 70 days postinoculation. Tingible body macrophage showing intra-lysosomal PrP accumulation. Bar: 0.75 μm

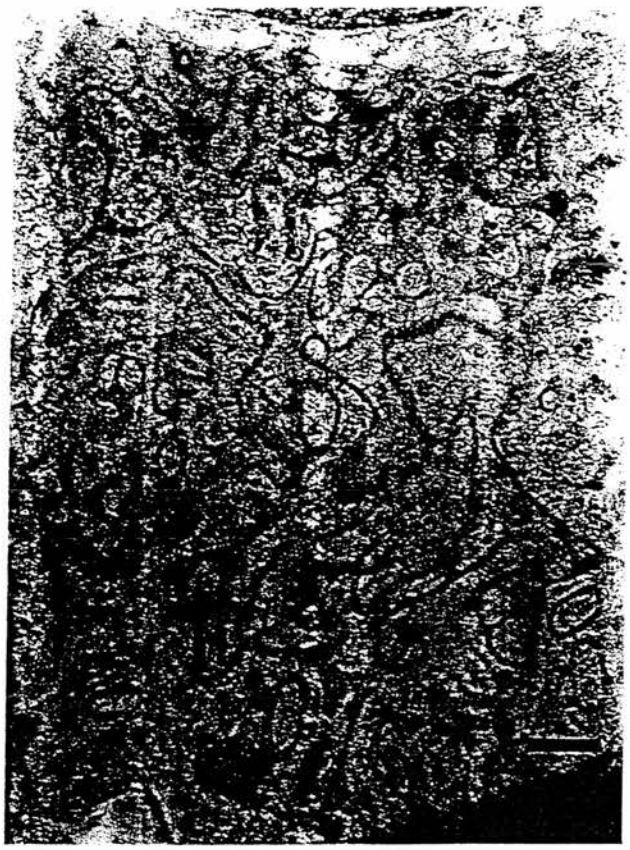

Fig. 5. Murine spleen. Terminal disease. Foci of immunoreactivity are present between lymphocyte cell nuclei in association with a FDC labyrinthine glomerular complex containing highly convoluted dendrites. Bar: 0.45 μm

proportion to the amount of electron dense material within the extracellular space (Figs. 5 and 6). In some areas amyloid fibrils were present within the extracellular space and were associated with the electron dense deposit (Fig. 6). Immunogold reaction was present in electron dense material associated with FDC dendrites surrounding (emperipolesis) plasmablasts with dilated endoplasmic reticulum. When compared with control material the frequency of plasmablast transformation within germinal centres was increased. Degenerate FDCs with condensation and fragmentation of nuclear chromatin and cytoplasmic vacuolation were also found in germinal centres of scrapie infected tissues but not in controls.

In terminal disease affected mice, most or all germinal centres in light zones were characterised by frequent reactive FDCs with highly complex labyrinthine glomeruli. FDCs were recognised by electron microscopy in areas lacking PrP immunostaining at light microscopy (the dark zone and periarteriolar sheath). FDCs in this region had a primitive morphology with few filiform dendrites and did not show immunogold staining.

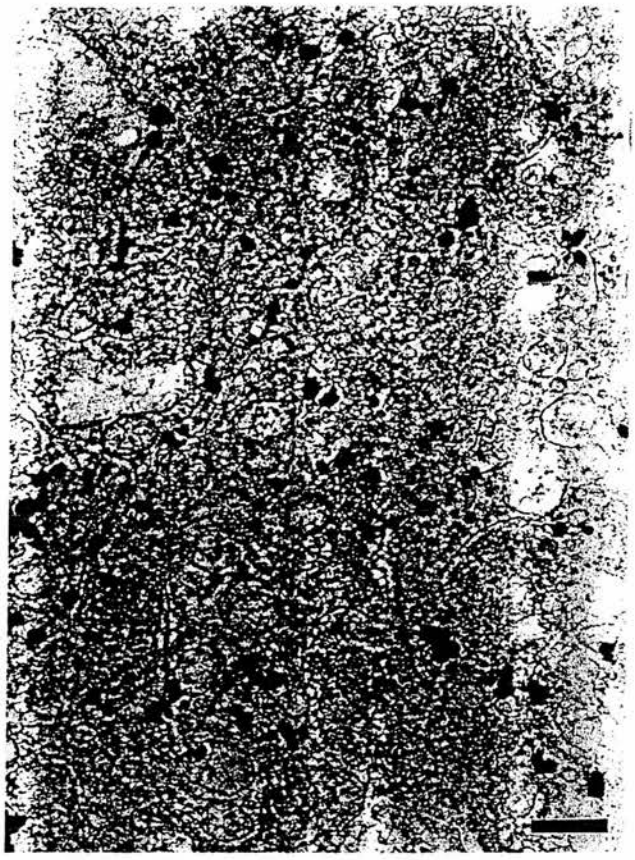

Fig. 6. Murine spleen. Terminal disease. FDC processes associated with intense immunogold reaction. There are frequent short filaments present within the extracellular space. Bar: 0.28 μm

At 70 days post inoculation most FDCs in the follicular light zones had relatively inconspicuous dendrites that formed small knots of labyrinthine complexes interspersed between lymphocytes and thus were similar to controls. Relatively smaller amounts of amorphous electron dense deposit were present at the plasmalemma. Weak immunostaining was seen within electron dense material around some mildly reactive FDC dendrites of a minority of cells (Fig. 7). FDCs with large labyrinthine glomerular complexes similar to those found in terminal diseased mice were occasionally detected and invariably associated with intense immunogold staining (Fig. 8). Some such areas showed amyloid fibril formation with increased numbers of coated pits.

Discussion

Although the study of sequential tonsillar biopsies and necropsies within our Suffolk flock are still incomplete, abnormal PrP accumulation has not been detected in tissues of sheep with ARR/ARR or ARQ/ARR

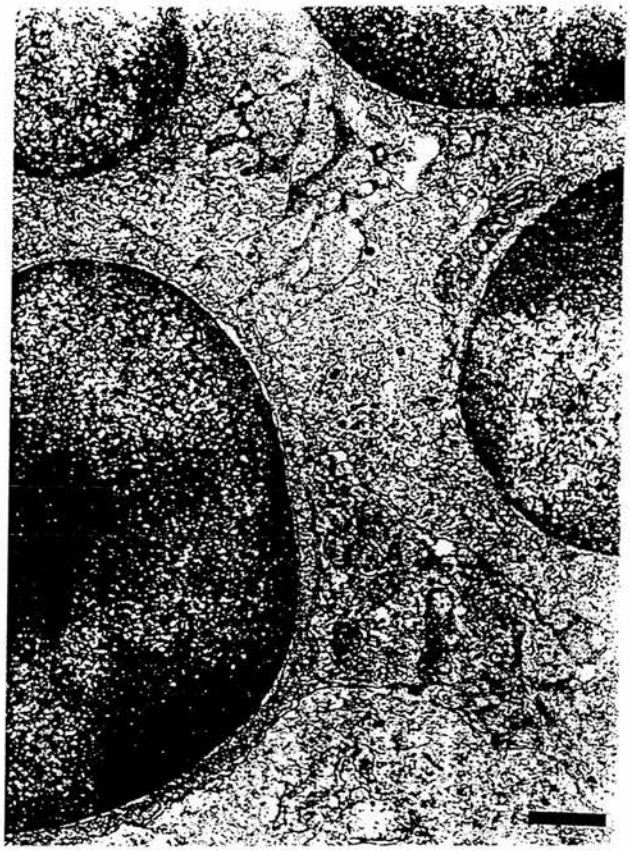

Fig. 7. Murine spleen. 70 days postinoculation. Small areas of immunogold reaction are present. These are located at the surface of FDC processes extending between lymphocytes. The dendrites are simple and do not have conspicuous electron dense deposits at the plasmalemma. Bar: 0.63 μm

genotypes. In contrast to the results of Dutch Texel and Swifter sheep reported by Schreuder and others [34], susceptible sheep upto 16 months of age have only low levels of immunohistochemically detectable PrP. This may reflect lower levels of susceptibility in Suffolk sheep generally when compared with Texel and Swifter sheep, or lower levels of infection within this flock compared to those studied by van Keulen et al. [33]. The disparity between abnormal PrP detection in tonsils at necropsy and following multiple tonsil biopsy is interesting. The results suggest that the biopsy procedure of susceptible sheep but not resistant sheep may increase susceptibility of FDCs within the remainder of the tonsil to infection.

The studies of murine spleen confirms previous light microscopy studies showing that disease specific accumulations of PrP occur in secondary follicles of spleen . Although the antibodies used do not distinguish between the protease sensitive and protease resistant isoforms of PrP, we would anticipate that at least some of the excess PrP accumulations, particularly

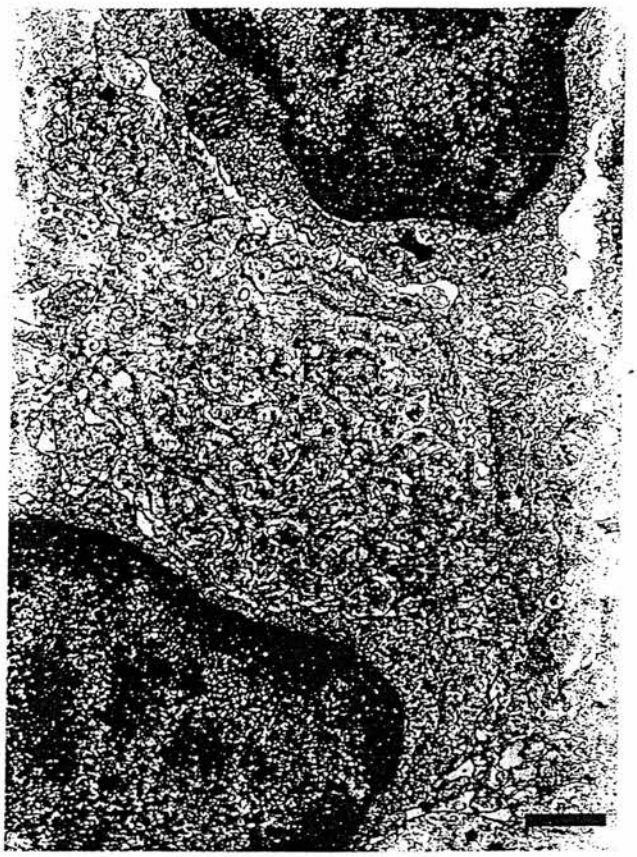

Fig. 8. Murine spleen. 70 days postinoculation. An intense immunogold reaction associated with the electron dense deposit overlying complex labrynthine convolutions of FDCs similar to those seen in terminal mice. Frequent fibrils are present in the extracellular space. Frequent coated pits are also present in association with these fibrils. Bar: 0.53 μm

those in fibrillar forms, would be protease resistant. In agreement with transmission and light microscopy studies of Brown et al. [5], our observations do not suggest that PrP accumulation occurs within B lymphocytes in ME7 scrapie affected spleens. Rather, the presence of PrP within TBMs in the paracortical zone or peri-follicular areas in spleen suggests that these cells or dendritic cells rather than plasma cells may possibly be responsible for transporting infection throughout the LRS.

Secondary follicles are divided into a mantle zone of small re-circulating lymphocytes surrounding the dark and light zones of germinal centres [15]. In the light zone there are large lymphoid cells (centrocytes) and FDCs with extensive cytoplasmic extensions. FDCs in the dark zone have immature processes. During the development of germinal centres, FDCs produce specific surface antigens. As increasing quantities of immune complexes are retained, the surfaces of FDCs enlarge, form plicae and dendrites develop [15]. Immune complexes are bound to the cytoplasmic extensions

(dendrites) of FDCs where they may remain for weeks or months. These complexes are not endocytosed but are held at the surface of the dendrite by C3b or Fc receptors [3, 31]. Free antigens are not bound to the surface of FDCs. Antigen-antibody complexes serve to periodically restimulate B and perhaps T cells.

Immature FDCs corresponding to those found in the dark zone were morphologically similar in controls and in infected mice. However, in light zones, all FDCs at terminal stages of disease and a proportion of FDCs at 70 dpi had large and highly complex labyrinthine glomeruli. This appears to represent an abnormal reactive or hyperplastic change of FDCs compared to controls. In addition, excess plasmablast differentiation and FDC degeneration were abnormal. These features show that pathological responses to scrapie infection are not confined to the CNS.

Transmission studies using chimaeric mice [5] in which some immune system cells carry the PrP gene and some do not, and light microscopy immunocytochemical studies of spleen and lymph nodes, suggest that mature FDCs accumulate PrP [5, 22, 27]. The sub-cellular localisation of disease specific PrP accumulations described above confirms that mature FDCs are associated with this accumulation. Outwith the light zone of the follicle, immature FDCs with poorly developed processes do not contain immunoreactive PrP. The disease specific PrP accumulation is not intracytoplasmic but is found at the cell surface of FDCs. This is similar to the plasmalemmal and extracellular localisation of PrP around neurons in the brains of scrapie infected mice [17, 18]. The continued accumulation of PrP both in brain and in spleen appears to lead to the formation of amyloid fibrils within the extracellular space [17–19], a feature consistent with other conventional amyloid diseases.

In this study, an increase in the complexity of FDC dendritic branching was associated with both an increase in the amount of electrondense deposit at the FDC dendrite plasmalemma and the intensity of immunostaining for PrP. As attachment of immune complexes are the trigger for a marked increase in the complexity of dendritic processes [14, 31], the pattern of dendritic branching and distribution of immunogold deposit in terminally diseased mice indicates that the FDCs were highly stimulated by abundant or abnormal PrP, or by excess trapping of immune complexes. In scrapie infected sheep tonsil and lymph nodes, PrP co-localised with CD 21, a marker confined to fully mature FDCs with well developed processes. The sites of accumulation of excess disease specific PrP and the morphological responses of the FDCs may reflect the normal function of PrP^{sen} . We suggest that PrP^{sen} is involved in dendritic process elongation or assisting in the adhesion of immune complexes to the cell surface. In the present study, the uncomplicated nature of most FDC dendrites at 70 dpi and the paucity of plasmalemma associated electron dense deposits suggest that early disease specific PrP accumulation may occur initially in the absence of antigen-antibody complex trapping.

PrP immunostaining in FDC plasmalemma associated electrondense material could also be interpreted as possible trapped antibody-PrP complexes. However, host antibodies to PrP^{sen} would not be anticipated. Antibodies to PrP are not detected in TSE infected animals although parenteral injection does cause an immunological response in PrP null mice. It is therefore possible that low levels of antibodies may be formed to abnormal PrP^{res} as a result of structural changes, aggregation and fibrillisation. Recent evidence using chimaeric SCID-PrP null mice irradiated and then re-constituted with either PrP null or $PrP^{+/+}$ bone marrow, indicate that scrapie replication and accumulation of PrP on FDCs [5] depends on PrP^{sen} expressing FDCs. These findings would suggest that most of the PrP detected at the cell surface of FDCs and within electron dense material at the cell surface, was initially expressed at the surface of FDCs and then released into the extracellular space to aggregate and form fibrils.

If increased surface expression of PrP increases the ability of FDCs to scavenge circulating immune complexes, then a breakdown in antibody homeostasis and a heightened non-specific polyclonal antibody response might be anticipated. The large number of lymphoid follicles with some penetrating into the medullary zones of lymph nodes in clinically diseased sheep [1] suggests an abnormal response of lymph nodes to scrapie infection. Sub-cellular pathology [2] including FDC degeneration, plasmablast differentiation, magnitude and ubiquity of labyrinthine glomerular complexes of FDCs in light zones of terminally diseased ME7 infected mice [3] further indicate an altered immunological response. Alterations in immunoglobulin levels have been described in some scrapie-host model systems [7, 9, 10] including natural scrapie of sheep [10] but they are clearly not an essential aspect of disease as most models do not exhibit changes in immunoglobulin levels. In some models immunoglobulin levels may be altered at early stages of infection. The widespread distribution of the hyperplastic form of FDCs with emperipolesis, and the marked increase in amounts of immunecomplexes suggests that scrapie infection may induce an enhanced trapping capacity of immunecomplexes. PrP may therefore be involved in non-specific binding of antigen-antibody complexes. Increased trapping of immune complexes caused by excess PrP at the FDC dendritic plasmalemma may elicit alterations in homeostasis of antibody responses and an increased host polyclonal antibody response. These observations suggest that the immunological response in scrapie is more complex than previously supposed and further investigation of the immune system interactions with PrP may be of interest, not least as a potential for disease intervention strategies and diagnosis.

TBMs ingest apoptotic cells, mostly B cells which are not selected to form clones of globulin producing cells. However, they also scavenge the ends of FDC processes and perhaps effete FDCs themselves [28, 30]. TBMs containing intra-lysosomal PrP were found adjacent to PrP accumulation associated with FDCs and as individual stained cells distant from other foci

of immunostaining. Intra-lysosomal PrP accumulation has also been seen within phagocytic cells of the CNS, including microglia [16], astroglia [16] and Kohler cells (unpubl. obs.). We suggest that TBMs ingest excess or abnormal PrP following phagocytosis of entire degenerate FDCs or their processes or by scavenging the extracellular space.

In the light of recent reports indicating that PrP accumulates within the tonsil of clinical [16] and pre-clinical CJD patients, the importance in understanding the role of the lymphoreticular system in TSE pathogenesis has been greatly increased. The present study indicates that natural and experimental scrapie induced pathological changes are not confined to the CNS. It also provides an insight into the cellular and sub-cellular involvement of FDCs in the peripheral pathogenesis of scrapie and also suggests possible functions of PrP^{sen}.

Acknowledgements

We gratefully acknowledge the assistance of Drs. J.R. Thomson and I. Begara-McGorum for tonsillar biopsies. The EU commission provided part funding of this work under grant 97/6013; UK MAFF provided part funding under SE1928.

References

1. Blattler T, Brandner S, Raeber AJ, Klein MA, Voigtlander T, Weissmann C, Aguzzi A (1997) PrP-expressing tissue required for transfer of scrapie infectivity from spleen to brain. Nature 389: 69–73
2. Bosma GC, Fried M, Custer RP, Carroll A, Gibson DM, Bosma MJ (1983) A severe combined immunodeficiency mutation in the mouse. Nature 301: 527–530
3. Bosseloir A, Bouzahzah F, Simar L, Heinen E (1995) B cells in contact with FDC. In: Heinen E (ed) Follicular dendritic cells in normal and pathological conditions. Springer, Berlin Heidelberg New York Tokyo, pp 53–78
4. Brown KL, Stewart K, Bruce ME, Fraser H (1997) Severely combined immunodeficient (SCID) mice resist infection with bovine spongiform encephalopathy. J Gen Virol 78: 2707–2710
5. Brown KL, Stewart K, Ritchie D, Mabbott NA, Williams A, Fraser H, Morrison WI, Bruce ME (2000) Scrapie replication in lymphoid tissues depends on prion PrP-expressing follicular dendritic cells. Nature Med 11: 1308–1311
6. Brown KL, Stewart K, Bruce ME, Fraser H (1996) Scrapie in immunodeficient mice. In: Court L, Dodet B (eds) Transmissible subacute spongiform encephalopathies. Elsevier, Paris, pp 159–166
7. Carp RI, Callaghan SM, Patrick BA, Mehta PD (1994) Interaction of scrapie agent and cells of the lymphoreticular system. Arch Virol 136: 255–268
8. Cashman NR, Loertscher R, Nalbantoglu J (1990) Cellular isoform of the scrapie agent protein participates in lymphocyte activation. Cell 61: 185
9. Collis CS, Kimberlin RH (1985) Long term persistence of scrapie infection in mouse spleens in the absence of clinical disease. FEMS Microbiol Lett 29: 111–114
10. Collis SC, Kimberlin RF (1983) Further studies on changes in immunoglobulin G in the sera and CSF of Herdwick sheep with natural and experimental scrapie. J Comp Pathol 93: 331–338

11. Diringer H, Gelderblom H, Hilmert H, Ozel M, Edelbluth C (1983) Scrapie infectivity, fibrils and low molecular weight protein. Nature 306: 476–478
12. Fraser H, Dickinson AG (1978) Studies of lymphoreticular system in the pathogenesis of scrapie. The role of spleen and thymus. J Comp Pathol 88: 563–573
13. Fraser H, Farquhar C (1987) Ionising radiation has no influence on scrapie incubation period in mice. Vet Microbiol 13: 211–223
14. Harris DA (1999) Cell biological studies of the prion protein. In: Harris DA (ed) Prions: molecular and cellular biology. Horizon Scientific Press, Norfolk, pp 53–66
15. Heinen E, Bosseloir A, Bouzahzah F (1995) Follicular dendritic cells: origin and function. Curr Top Microbiol Immunol 201: 15–47
16. Hill AF, Zeidler M, Ironside J, Collinge J (1997) Diagnosis of new variant Creutzfeldt–Jakob disease by tonsil biopsy. Lancet 349: 99–100
17. Jeffrey M, Goodsir CM, Bruce ME, McBride PA, Scott JR, Halliday WG (1994) Correlative light and electron microscopy studies of PrP localisation in 87V scrapie. Brain Res 656: 329–343
18. Jeffrey M, Goodsir CM, Bruce ME, McBride PA, Fowler N, Scott JR (1994) Murine scrapie-infected neurons in vivo release excess PrP into the extracellular space. Neurosci Lett 174: 39–42
19. Jeffrey M, Goodsir CM, Fowler N, Hope J, Bruce ME, McBride PA (1996) Ultrastructural immunolocalisation of synthetic prion protein peptide antibodies in 87V murine scrapie. Neurodegeneration 5: 101–109
20. Jeffrey M, McGovern G, Goodsir CM, Brown KL, Bruce ME (2000) Sites of prion protein accumulation in scrapie-infectd mouse spleen revealed by immuno-electron microscopy. J Pathol (in press)
21. Kimberlin RH, Walker CA (1988) Incubation periods in six models of intraperitoneally injected scrapie depend mainly on the dynamics of agent replication within the nervous system and not the lymphoreticular system. J Gen Virol 69: 2953–2960
22. Kitamoto T, Muramoto T, Mohri S, Doh-ura K, Tatieishi J (1991) Abnormal isoform of prion protein accumulates in follicular dendritic cells in mice with Creutzfeldt-Jakob Disease. J Virol 65: 6292–6295
23. Klein MA, Frigg R, Raeber AJ, Flechsig E, Hegyi I, Zinkernagel RM, Weissmann C, Aguzzi A (1998) PrP expresssion in B lymphocytes is not required for prion invasion. Nature Med 4: 1429–1433
24. Laszemas CI, Cesbron J-Y, Deslys J-P, Demaimay R, Adjou KT, Rioux R, Lemaire C, Locht C, Dormont D (1996) Immune system-dependent and independent replication of the scrapie agent. J Virol 70: 1292–1295
25. Mabbott NA, Brown KL, Manson J, Bruce ME (1997) T lymphocyte activation and the cellular form of the prion protein. Immunology 92: 161–165
26. Manson J, McBride P, Hope J (1992) Expression of the PrP gene in the brain of sinc congenic mice and its relationship to the development of scrapie. Neuro-degeneration 1: 45–52
27. McBride PA, Eikelenboom P, Kraal G. Fraser H, Bruce ME (1992) PrP protein is associated with follicular dendritic cells of spleens and lymph nodes in uninfected and scrapie-infected mice. Pathol 168: 413–418
28. Ritchie DL, Brown K[illegible], Bruce ME (2000) Visualisation of PrP protein and follicular dendritic cells in uninfected and scrapie infected spleen. J Cell Pathol 1: 3–[illegible]

29. Shyng S-L, Heuser JE, Harris DA (1994) A glycolipid-anchored prion protein is endocytosed via clathrin coate pits. J Cell Biol 124: 1239–1250
30. Szakal AK, Kosco MH, Tew JG (1988) A novel in vivo follicular dendritic cell-dependent iccosome-mediated mechanism for delivery of antigen to antigen-processing cells. J Immunol 140: 342–353
31. Terashima K, Dobashi M, Maeda K, Imai Y (1992). Follicular dendritic cell and iccosomes in germinal centre reactions. Semin Immunol 4: 267–274
32. Tew JG, Kosco MH, Szakal AK (1989) The alternative antigen pathway. Immunol Today 10: 229–231
33. van Keulen LJM, Schreuder BEC, Meloen RH, MooijHarkes G, Vromans MEW, Langeveld JPM (1996) Immunohistochemical detection of prion protein in lymphoid tissues of sheep with natural scrapie. J Clin Microbiol 34: 1228–1231
34. Schreuder BEC, van Keulen LJM, Vromans MEW, Langeveld JPM, Smits M (1998) Tonsillar biopsy and PrP^{Sc} detection in the preclinical diagnosis of scrapie. Vet Rec 142: 564–568

Authors' address: Dr. M. Jeffrey, Lasswade Veterinary Laboratory, Pentlands Science Park, Bush Loan, Penicuik, Midlothian, Scotland, EH26 0PZ, U.K.

JOURNAL OF VIROLOGY, May 2002, p. 5131–5139 Vol. 76, No. 10
0022-538X/02/$04.00+0 DOI: 10.1128/JVI.76.10.5131–5139.2002

Temporary Blockade of the Tumor Necrosis Factor Receptor Signaling Pathway Impedes the Spread of Scrapie to the Brain

Neil A. Mabbott,[1]* Gillian McGovern,[2] Martin Jeffrey,[2] and Moira E. Bruce[1]

Neuropathogenesis Unit, Institute for Animal Health, Edinburgh EH9 3JF,[1] and Veterinary Laboratories Agency—Lasswade, Pentlands Science Park, Midlothian EH26 0PZ,[2] Scotland, United Kingdom

Received 3 December 2001/Accepted 12 February 2002

Although the transmissible spongiform encephalopathies (TSEs) are neurodegenerative diseases, their agents usually replicate and accumulate in lymphoid tissues long before infection spreads to the central nervous system (CNS). Studies of a mouse scrapie model have shown that mature follicular dendritic cells (FDCs), which express the host prion protein (PrP^c), are critical for replication of infection in lymphoid tissues. In the absence of mature FDCs, the spread of infection to the CNS is significantly impaired. Tumor necrosis factor alpha (TNF-α) secretion by lymphocytes is important for maintaining FDC networks, and signaling is mediated through TNF receptor 1 (TNFR-1) expressed on FDCs and/or their precursors. A treatment that blocks TNFR signaling leads to the temporary dedifferentiation of mature FDCs, raising the hypothesis that a similar treatment would significantly delay the peripheral pathogenesis of scrapie. Here, specific neutralization of the TNFR signaling pathway was achieved through treatment with a fusion protein consisting of two soluble human TNFR (huTNFR) (p80) domains linked to the Fc portion of human immunoglobulin G1 (huTNFR:Fc). A single treatment of mice with huTNFR:Fc before or shortly after intraperitoneal injection with the ME7 scrapie strain significantly delayed the onset of disease in the CNS and reduced the early accumulation of disease-specific PrP in the spleen. These effects coincided with a temporary dedifferentiation of mature FDCs within 5 days of huTNFR:Fc treatment. We conclude that treatments that specifically inhibit the TNFR signaling pathway may present an opportunity for early intervention in peripherally transmitted TSEs.

The transmissible spongiform encephalopathies (TSEs), or "prion diseases," are infectious neurodegenerative diseases that affect humans and both wild and domestic animals. The host prion protein (PrP^c) is critical for TSE agent replication (8) and accumulates in diseased tissues as an abnormal, detergent-insoluble, relatively proteinase-resistant isoform, PrP^{Sc} (4). Although the precise nature of the TSE agent is uncertain (13), PrP^{Sc} copurifies with infectivity and is considered to be a major component of the infectious agent (41).

Natural TSEs, including sheep scrapie, bovine spongiform encephalopathy (BSE), chronic wasting disease in mule deer and elk, and variant Creutzfeldt-Jakob disease (vCJD) in humans, are considered to be acquired peripherally. For example, the emergence of vCJD in the United Kingdom population is almost certainly due to consumption of BSE-contaminated tissues (7). Following peripheral exposure, TSE agents usually accumulate in lymphoid tissues long before infection spreads to the central nervous system (CNS). For example, after intragastric or oral challenge of rodents with scrapie, the infectious agent first accumulates in Peyer's patches and gut-associated lymphoid tissues (2, 24). The detection of PrP^{Sc} in Peyer's patches and gut-associated lymphoid tissues of sheep with natural scrapie (1, 20) prior to detection in other lymphoid tissues and the CNS (46) implies that this disease is also acquired orally. Lymphoid tissues play an important role in transmission in some TSE models (17), but this tissue tropism may be agent strain dependent. Although acquired peripherally, BSE in cattle (43) and iatrogenic Creutzfeldt-Jakob disease in humans (21) appear to be confined to nervous tissues. However, within the lymphoid tissues of patients with vCJD (21) and most sheep with natural scrapie (45) or following experimental peripheral infection of rodents with scrapie (5, 29, 30, 33), early PrP^{Sc} accumulation takes place on follicular dendritic cells (FDCs). Studies of mouse scrapie models have shown that mature FDCs are critical for replication in lymphoid tissues and that in their absence, neuroinvasion following peripheral challenge is significantly impaired (5, 29, 30, 35). From the lymphoid tissues, infectious agents spread to the CNS via peripheral nerves (19).

The FDC therefore presents a potential target for therapeutic intervention in peripherally acquired TSEs such as natural sheep scrapie and vCJD. Indeed, recent studies have demonstrated that treatments that temporarily interfere with the integrity (29, 35) or function (28) of FDCs also interfere with TSE pathogenesis. Signaling through lymphocyte-derived tumor necrosis factor alpha (TNF-α) is critical for FDC development, as mice deficient in TNF-α ($TNF\text{-}\alpha^{-/-}$ mice) lack mature FDCs in lymphoid tissues (38). The effects of TNF-α on FDC development are mediated via signaling through TNF receptor 1 (TNFR-1) expressed on FDCs and/or their precursors (44). Specific neutralization of the TNF-α signaling pathway leads to the temporary inactivation of FDCs (31), suggesting that FDCs require constant stimulation from this cytokine to maintain their differentiated state. It has previously been shown that in the absence of mature FDCs in the lymphoid tissues of $TNF\text{-}\alpha^{-/-}$ mice, susceptibility to peripheral challenge with scrapie is reduced (30). Therefore, in this study we sought to determine whether a treatment that temporarily

* Corresponding author. Mailing address: Institute for Animal Health, Neuropathogenesis Unit, Ogston Building, West Mains Rd., Edinburgh EH9 3JF, Scotland, United Kingdom. Phone: 44 131 667 5204. Fax: 44 131 668 3872. E-mail: neil.mabbott@bbsrc.ac.uk.

blocks the TNF-α signaling pathway would delay the spread of scrapie to the CNS.

MATERIALS AND METHODS

huTNFR:Fc treatment. At the times indicated, C57BL mice (8 to 12 weeks old) were given a single intraperitoneal (i.p.) injection of 100 μg of a dimeric fusion protein containing the soluble human TNFR (huTNFR) (p80) domain linked to the Fc portion of human immunoglobulin G1 (huTNFR:Fc; Immunex Corp., Seattle, Wash.) (34) or 100 μg of polyclonal human immunoglobulin G (hu-Ig) (Sandoglobulin; provided by J. Browning, Biogen Inc., Cambridge, Mass.) as a control. To monitor the effects of treatment on FDC status, at the times indicated following treatment, two spleens were taken from each group and halved. One half was fixed in periodate-lysine-paraformaldehyde and embedded in paraffin wax for immunocytochemical detection of PrP (33) with the PrP-specific antiserum 1B3 (15). The other half was snap-frozen at the temperature of liquid nitrogen, and 6-μm-thick sections were cut on a cryostat. FDCs were visualized by staining with the FDC-specific monoclonal antiserum FDC-M2 (27) or 8C12 monoclonal antiserum to detect CD35 (Pharmingen, San Diego, Calif.). Immunolabeling was carried out with alkaline phosphatase coupled to the avidin-biotin complex (Vector Laboratories Inc., Burlingame, Calif.). Vector Red (Vector Laboratories) was used as a substrate.

Scrapie infection. At the times indicated relative to treatment, mice were injected intracerebrally (i.c.) or i.p. with 20 μl of a 1.0, 0.1, or 0.01% (wt/vol) dilution of unspun brain homogenate from C57BL mice terminally affected with ME7 scrapie (20 μl of a 1.0% homogenate represents a dose of approximately $1 \times 10^{4.5}$ i.c. 50% infectious dose [ID_{50}] units). Following challenge, animals were coded and assessed weekly for signs of clinical disease and killed at a standard clinical end point (16). Scrapie diagnosis was confirmed by histopathological assessment of vacuolation in the brain. Where indicated, some mice were sacrificed 70 days postchallenge, and their spleens were taken for further analysis. For the bioassay of scrapie infectivity, individual half spleens were prepared as 10% (wt/vol) homogenates in physiological saline and 20 μl was injected i.c. into groups of 12 C57BL indicator mice. The scrapie titer in each spleen was determined from the mean incubation period for the assay mice with reference to established dose-incubation period response curves for scrapie-infected spleen tissue (11).

Immunoblot detection of PrP^{Sc}. The remaining half of each spleen collected 70 days postchallenge was prepared as previously described (12, 28, 30). In brief, before immunoblot analysis, spleen tissue homogenates were treated with 20 μg of proteinase K (to confirm the presence of PrP^{Sc}) and subsequently partially purified by treatment with 2% (wt/vol) *N*-lauroylsarcosine (in 0.1 M Tris [pH 7.4]), allowing sedimentation of only the proteinase-K-resistant, detergent-insoluble fraction of PrP (PrP^{Sc}). Samples were subjected to electrophoresis through sodium dodecyl sulfate–12% polyacrylamide gels (Bio-Rad, Hemel Hempstead, United Kingdom) and transferred to polyvinylidene difluoride membranes (Bio-Rad) by semidry blotting. PrP was detected with the PrP-specific rabbit polyclonal antiserum 1B3 (15) followed by alkaline phosphatase-conjugated goat anti-rabbit antiserum (Jackson ImmunoResearch Laboratories Inc., West Grove, Pa.), and bound alkaline phosphatase activity was detected with SigmaFast NBT/BCIP solution (Sigma, Poole, Dorset, United Kingdom).

Ultrastructural immunohistochemistry. Spleen fragments were immersion fixed in 0.5% paraformaldehyde–0.5% glutaraldehyde for 24 h at 4°C, postfixed in osmium tetroxide, dehydrated, and embedded in araldite. Serial 65-nm-thick sections were then placed on 300-mesh nickel grids and prepared as previously described (23). Briefly, PrP was detected by staining with the PrP-specific rabbit polyclonal antiserum 1A8 (14) followed by Auroprobe 1-nm colloidal gold. Sections were then postfixed in 2.5% glutaraldehyde in phosphate-buffered saline, and staining was enhanced with immunogold silver stain. The grids were then counterstained with uranyl acetate and lead citrate.

Previous studies have shown that the combination of fixatives and pretreatments required for the preparation of tissue for electron microscopy by this method destroys PrP^{c} immunoreactivity and reveals only disease-specific PrP accumulations (23).

Statistical analysis. Incubation period data are expressed as means ± standard errors of the mean, and significant differences between incubation periods were sought by one-way analysis of variance with Minitab for Windows (Minitab Inc., State College, Pa.).

RESULTS

Effect of huTNFR:Fc treatment on FDC status. A blockade of the TNF-α signaling pathway was achieved by a single i.p. injection of 100 μg of huTNFR:Fc (34). This fusion protein binds TNF-α with high affinity and acts as an antagonist of TNF-α biological activity in in vivo assays in mice (34, 47). Here, within 2 days of treatment of mice with huTNFR:Fc, a significant reduction in staining for the FDC markers FDC-M2 and CD35 was observed in lymphoid follicles of the spleen (Fig. 1). Furthermore, FDC-M2 and CD35 expression was absent 5 (data not shown) and 7 (Fig. 1) days after treatment with huTNFR:Fc. The cellular isomer of the prion protein, PrP^{c}, is expressed by FDCs in uninfected mice (Fig. 1) (5, 29, 33). Likewise, PrP^{c} expression was also markedly reduced within 2 days of treatment and undetectable 5 (data not shown) and 7 (Fig. 1) days after treatment with huTNFR:Fc. The effects of huTNFR:Fc treatment on FDC status were temporary, as PrP-expressing FDC networks were detected in the spleen 14 days after treatment (Fig. 1). Treatment of mice with 100 μg of polyclonal hu-Ig as a control had no adverse effect on FDC status (Fig. 1). In some follicles from hu-Ig-treated mice, there appeared to be increases in the size of the FDC network and the level of PrP^{c} expression 14 days after treatment compared to values for follicles analyzed 2 and 7 days after treatment (Fig. 1). This may be indicative of a germinal-center response to hu-Ig.

Ultrastructural analysis of the effect of huTNFR:Fc treatment on FDC status. Mice were treated with huTNFR:Fc or hu-Ig 38 days after i.p. injection with scrapie, and PrP deposition in the spleen was analyzed 7 days later by light-microscopical and ultrastructural immunohistochemical methods. As expected, in spleens of control-treated mice, abundant disease-specific PrP staining in association with FDCs was detected by light microscopy (Fig. 2a and c). Immunoelectron microscopic analysis confirmed that these PrP accumulations were disease specific and were found in association with electron-dense material at the surface of highly convoluted FDC dendrites (Fig. 2e and f), as previously reported (23). In some follicles, individual fibrils consistent with the dimensions of amyloid fibrils were present in association with FDCs (data not shown). Disease-specific PrP accumulations were also detected within secondary lysosomes of tingible body macrophages (Fig. 2e).

Mice were treated with huTNFR:Fc 38 days after scrapie injection, and abundant PrP labeling was still apparent in the spleen 7 days after treatment (Fig. 2d) despite a temporary absence of mature FDCs (Fig. 2b). Ultrastructural analysis revealed that the centers of secondary lymphoid follicles in spleens from huTNFR:Fc-treated mice showed marked degenerative changes compared with those from hu-Ig-treated control mice. Severe and extensive lymphocyte apoptosis was noted (Fig. 2g), and large numbers of highly reactive macrophages containing degenerative cellular material were also present in these sites (Fig. 2h). In many cases, whole apoptotic B lymphocytes could also be identified within these macrophages. At the ultrastructural level, FDC networks were identified but their processes appeared immature (Fig. 2i) and lacked the highly convoluted characteristics observed for those of hu-Ig-treated control mice (Fig. 2f). The immature nature of these FDC dendrites was consistent with the loss of expression of FDC-specific markers following huTNFR:Fc treatment (Fig. 1 and 2). Although a few mature FDC processes were identified at the ultrastructural level, it was not possible to

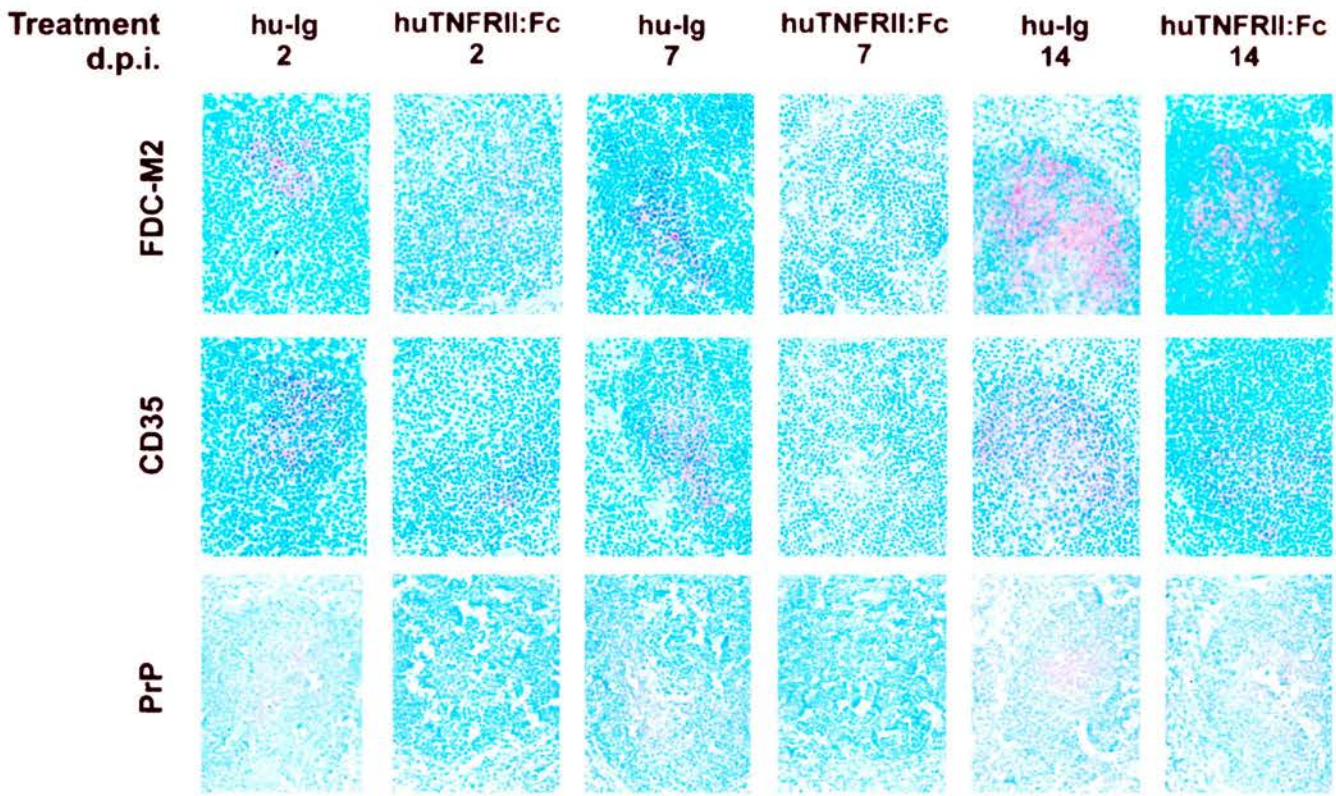

FIG. 1. Effect of huTNFR:Fc treatment on FDC status in spleens of uninfected mice. Tissues were taken on the indicated days postinjection (d.p.i.) with hu-Ig (control) or huTNFR:Fc, and adjacent frozen sections were stained with FDC-M2 monoclonal antiserum to detect FDCs (upper row; red) or with 8C12 monoclonal antiserum to detect CD35 (middle row; red). PrP was detected on paraffin-embedded sections with the PrP-specific polyclonal antiserum 1B3 (bottom row; red). Expression of FDC-M2, CD35, and PrP in the spleen was undetectable 7 days after treatment with huTNFR:Fc. Original magnification, ×400.

determine whether these were regenerating FDCs or mature FDCs unaffected by the TNFR signaling blockade (31).

Effect of huTNFR:Fc treatment on scrapie pathogenesis. Mice were given a single i.p. injection of huTNFR:Fc (or hu-Ig as a control) at one of three different times relative to scrapie challenge: 5 days before scrapie injection, so mature FDCs would be absent in lymphoid tissues at the time of scrapie injection; 14 days after scrapie injection, soon after the onset of scrapie replication in lymphoid tissues; or 38 days after scrapie injection, when high levels of scrapie infectivity are present in lymphoid tissues (5, 30). When groups of six mice were challenged with the ME7 scrapie strain by direct i.c. injection into the CNS, treatment with huTNFR:Fc 5 days before or 14 days after scrapie challenge had no effect on the incubation period of the disease (~164 to 172 days; Fig. 3a) or pathology within the brain (data not shown) compared with those of controls. These findings demonstrate that the blockade of the TNFR signaling pathway did not affect scrapie pathogenesis once disease was established in the CNS.

When treated with huTNFR:Fc before or shortly after peripheral (i.p.) injection with scrapie, mice developed neurological disease much later than did the hu-Ig-treated controls. The most significant effect was observed when mice were treated 5 days before i.p. scrapie injection (Fig. 3b). For example, following injection with a moderate dose of scrapie (20 μl of a 1.0% scrapie brain homogenate), all control-treated mice succumbed to disease, with a mean incubation period of 255 ± 15 days ($n = 8$), whereas those treated with huTNFR:Fc developed disease 47 days later, with a mean incubation period of 302 ± 7 days ($P < 0.01$; $n = 8$; Fig. 3b). Likewise, when treated with huTNFR:Fc before injection with a 10-fold-lower scrapie dose (20 μl of a 0.1% scrapie brain homogenate), mice developed neurological disease with a mean incubation period of 353 ± 4 days ($n = 9$), which was 38 days longer than the mean incubation period of the hu-Ig-treated controls (315 ± 7 days; $P < 0.001$; $n = 9$; Fig. 3b). Despite these highly significant prolongations of the incubation period, little effect on disease susceptibility was observed following treatment with huTNFR:Fc prior to injection with a low dose of scrapie (20 μl of a 0.01% scrapie brain homogenate): 7 of 9 huTNFR:Fc-treated mice remained free of scrapie disease 500 days after inoculation, compared to 5 of 9 control mice (Fig. 3b).

An increase in survival time was also observed when treatment with huTNFR:Fc was delayed until 14 days after i.p. injection with a moderate dose of scrapie (Fig. 3c). In this instance, mice developed neurological disease with a mean incubation period of 281 ± 7 days ($n = 8$), which was 19 days longer than the mean incubation period of the hu-Ig-treated controls (262 ± 8.0 days; $n = 8$). However, treatment with huTNFR:Fc 38 days after injection, a time when high levels of infectivity agents have already accumulated in the spleen (5,

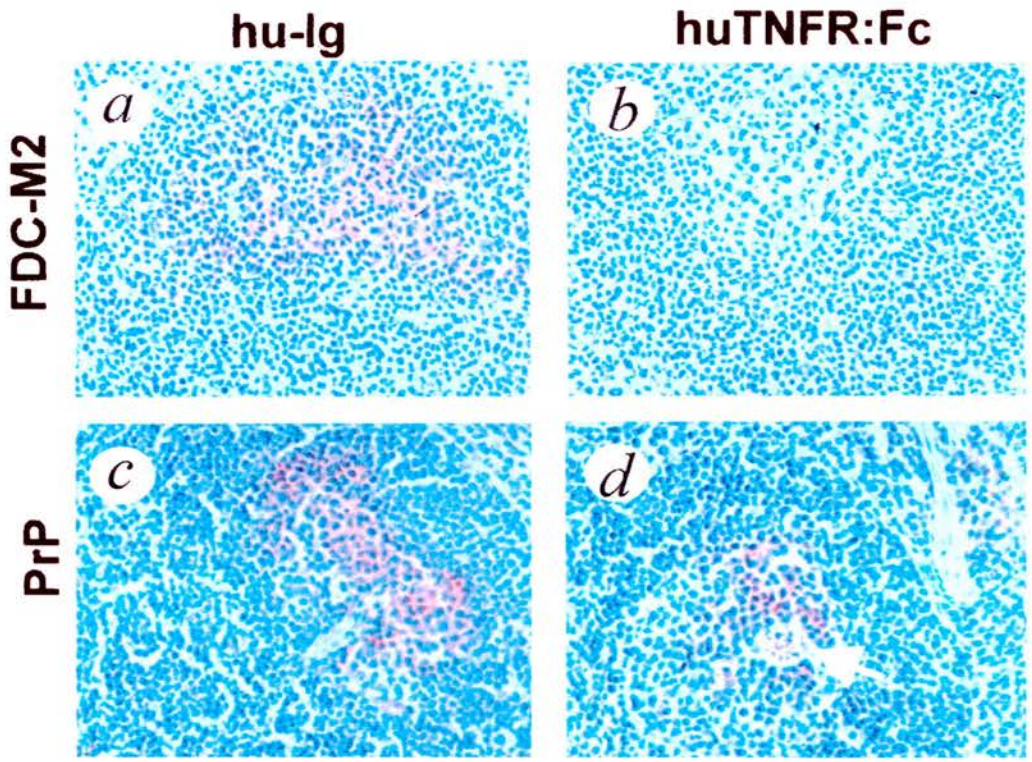

FIG. 2. Immunohistological analysis of the effects of huTNFR:Fc treatment on FDC status and PrP labeling in spleens of mice already incubating scrapie. (a to d) Light-microscopical analysis. Mice were injected i.p. with scrapie and 38 days later given a single i.p. injection of huTNFR:Fc (b and d) or hu-Ig as a control (a and c). Spleens were obtained 7 days later; frozen sections were stained for FDCs with FDC-M2 monoclonal antiserum (a and b; red), and PrP was detected on paraffin-embedded sections with the PrP-specific polyclonal antiserum 1B3 (c and d; red). Abundant abnormal PrP was detected in association with FDCs in the spleens of control mice 45 days after scrapie injection. However, when mice were treated with huTNFR:Fc 38 days after scrapie injection, heavy PrP labeling was still apparent in the spleen 7 days after treatment despite a temporary absence of FDC-M2 expression. The arrow in panel D indicates a tingible body macrophage containing apoptotic B lymphocytes. Magnification, ×400. (e to i) Ultrastructural analysis. Mice were injected i.p. with scrapie and 38 days later given a single i.p. injection of huTNFR:Fc (g to i) or hu-Ig as a control (e and f). Spleens were obtained 7 days later, and araldite sections were immunostained with the PrP-specific polyclonal antiserum 1A8. (e) An area of immunogold reactivity (indicated with an asterisk) is present between lymphocytes in the germinal center of a scrapie-injected, hu-Ig-treated control mouse. This focal immunoreaction is associated with a complex knot of mature FDC processes. Part of a tingible body macrophage is present at the bottom left (arrow). Bar = 1.76 μm. (f) High magnification of the FDC complex indicated with an asterisk in panel e. Highly convoluted FDC processes are associated with the immunogold reaction. Many short linear and curvilinear structures are immunolabeled. Bar = 0.35 μm. (g) Edge of a germinal center showing marked apoptosis (black arrows) in the spleen of a scrapie-injected, huTNFR:Fc-treated mouse. Immature FDC dendritic processes surround the germinal center (white arrows). Bar = 1.87 μm. (h) Tingible body macrophage (arrow) in the spleen of a scrapie-injected, huTNFR:Fc-treated mouse showing intralysosomal PrP accumulation. Moderately reactive FDC dendrites lie adjacent to the macrophage. Bar = 1.31 μm. (i) Foci of immunoreactivity associated with immature FDC dendritic processes in the spleen of a scrapie-injected, huTNFR:Fc-treated mouse. The immunogold reaction is associated with electron-dense material in the extracellular space surrounding FDC dendrites. Bar = 0.56 μm.

30), had no effect on the incubation period compared with that of control-treated mice (Fig. 3c).

Scrapie infectivity and PrP^{Sc} accumulation in the spleen. Within 70 days of a peripheral injection of untreated mice with the ME7 scrapie strain, high levels of infectivity and the disease-specific isomer of the prion protein, PrP^{Sc}, accumulate within lymphoid tissues (5, 12, 28, 30). In this study, spleens were taken from each control and huTNFR:Fc treatment group 70 days after i.p. injection with a moderate dose of scrapie and halved. PrP^{Sc} accumulation was determined in one half by immunoblot analysis, while the scrapie infectivity titer was estimated in the other half by bioassay in groups of indicator mice. As expected, all spleens from control mice treated with hu-Ig 5 days before or 14 or 38 days after scrapie challenge contained high infectivity titers (5.0 to 5.3 log i.c. ID_{50}/g, as estimated by incubation period assay; Fig. 4) and abundant detergent-insoluble, relatively proteinase-K-resistant PrP^{Sc} (Fig. 4). However, following treatment of mice with huTNFR:Fc 5 days before scrapie challenge, PrP^{Sc} was less abundant in the spleen 70 days postinfection (Fig. 4a, lanes 4 and 6). In contrast, the infectivity titers were as high as those detected in spleens from hu-Ig-treated controls, suggesting that the accumulation of PrP^{Sc} in the spleen lags behind replication of infectivity during the early stages of infection, as observed in previous studies (12, 28).

When treatment was delayed until 14 or 38 days after scrapie challenge, no differences in the accumulation of infectivity or abundance of PrP^{Sc} in the spleen were detected between control- and huTNFR:Fc-treated mice when measured 70 days after scrapie challenge (Fig. 4b and c).

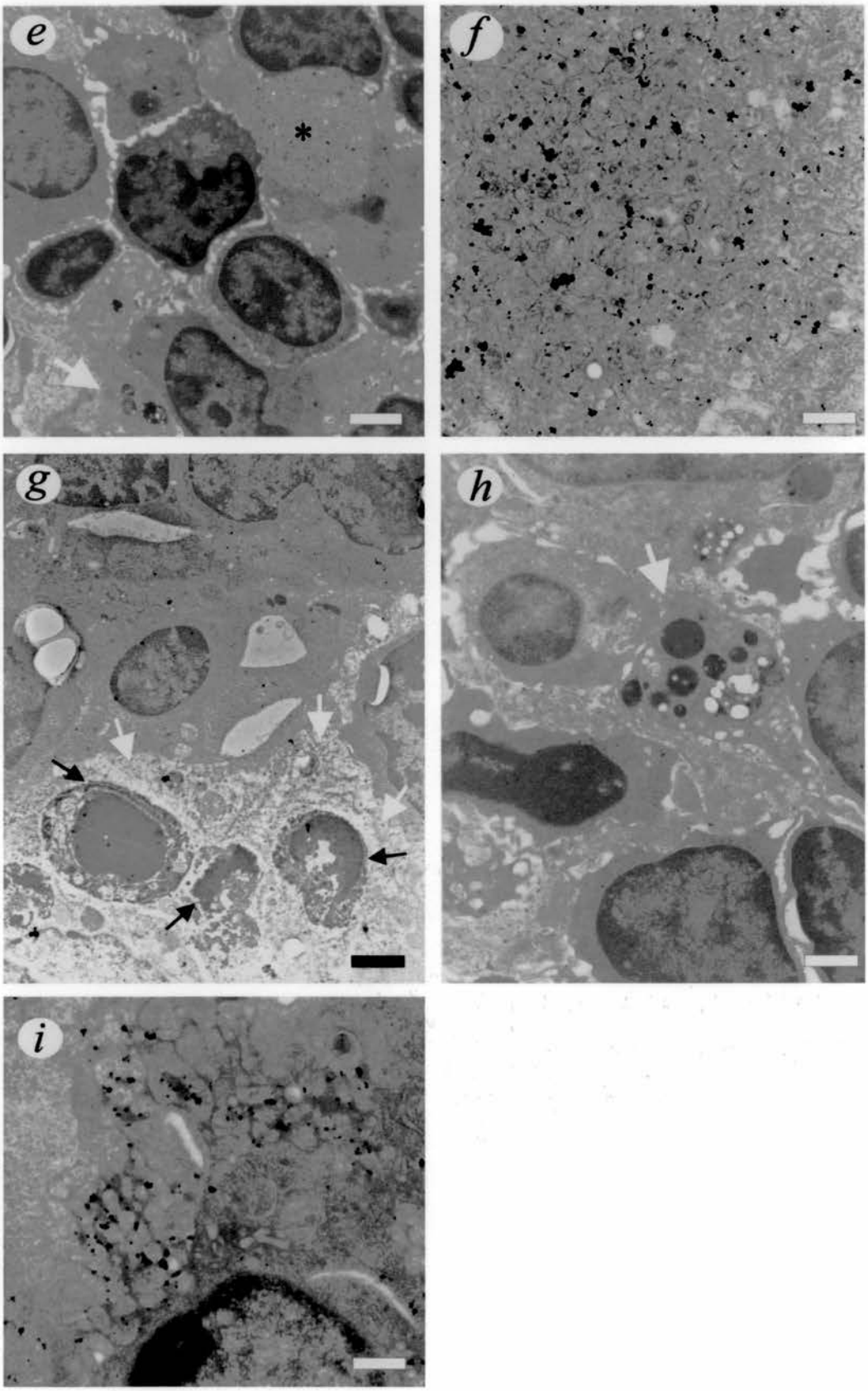

FIG. 2—*Continued.*

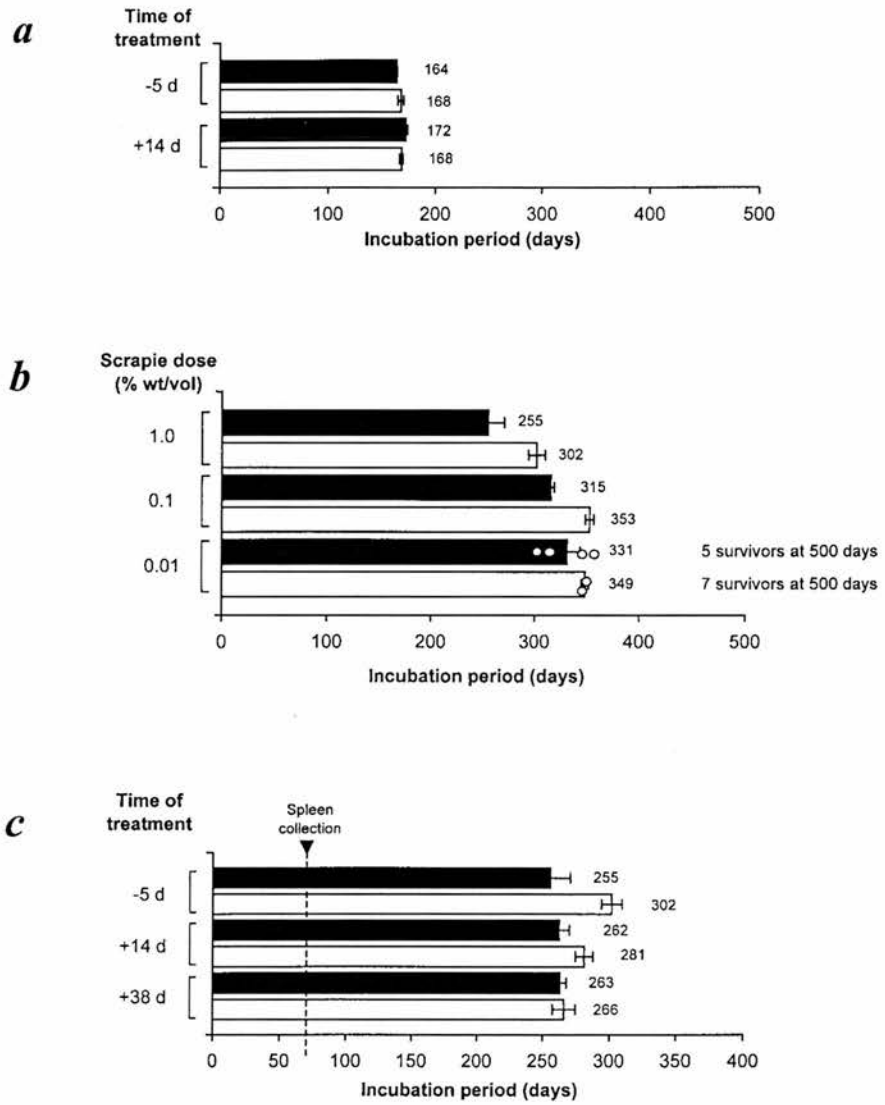

FIG. 3. Blockade of the TNFR signaling pathway significantly extends the incubation period of disease following peripheral injection with ME7 scrapie. (a) Mice were treated with huTNFR:Fc (□) or hu-Ig as a control (■) 5 days before or 14 days after i.c. injection with a moderate dose of scrapie (1.0% [wt/vol] scrapie brain homogenate). (b) Mice were treated with huTNFR:Fc (□) or hu-Ig as a control (■) 5 days before i.p. injection with a moderate (1.0%) or limiting (0.1% or 0.01%) dose of scrapie. ○, incubation periods for individual mice. (c) Mice were treated with huTNFR:Fc (□) or hu-Ig (■) 5 days before or 14 or 38 days after i.p. injection with a moderate dose of scrapie. Each bar represents a mean ± standard error of the mean for six to nine mice. The vertical broken line represents the time at which two spleens were taken from each treatment group for subsequent analysis of scrapie infectivity and PrP^{Sc} accumulation (see Fig. 4). d, days.

DISCUSSION

Here we have shown that a single treatment of mice with huTNFR:Fc before or shortly after a peripheral scrapie injection significantly extended survival time compared to that of control-treated mice. Our studies also demonstrated that treatment prior to peripheral exposure decreased the early accumulation of disease-specific PrP^{Sc} within the spleen. These effects coincided with a temporary dedifferentiation of mature PrP-expressing FDCs in the spleen following treatment with huTNFR:Fc. Taken together, these results are consistent with previous findings that in the absence of mature FDCs in lymphoid tissues, neuroinvasion following peripheral injection with scrapie is impaired (5, 29, 30). Surprisingly, a single treatment with huTNFR:Fc had little influence on disease susceptibility following low-dose scrapie challenge. Nevertheless, TNF-α blockade over longer periods may present a potential strategy for intervention in peripherally acquired TSEs.

Secretion of TNF-α has been implicated in the development of neuropathology in several human inflammatory, infectious, and autoimmune disorders (40). Although TNF-α expression has been reported to occur in the brains of mice showing clinical signs of scrapie (9), studies using TNF-$\alpha^{-/-}$ mice (30) and TNFR-1-deficient mice (25) suggest that this cytokine signaling pathway alone is not directly involved in the development of neuropathology in TSEs. Due to its high molecular weight, huTNFR:Fc would be unlikely to cross the blood-brain

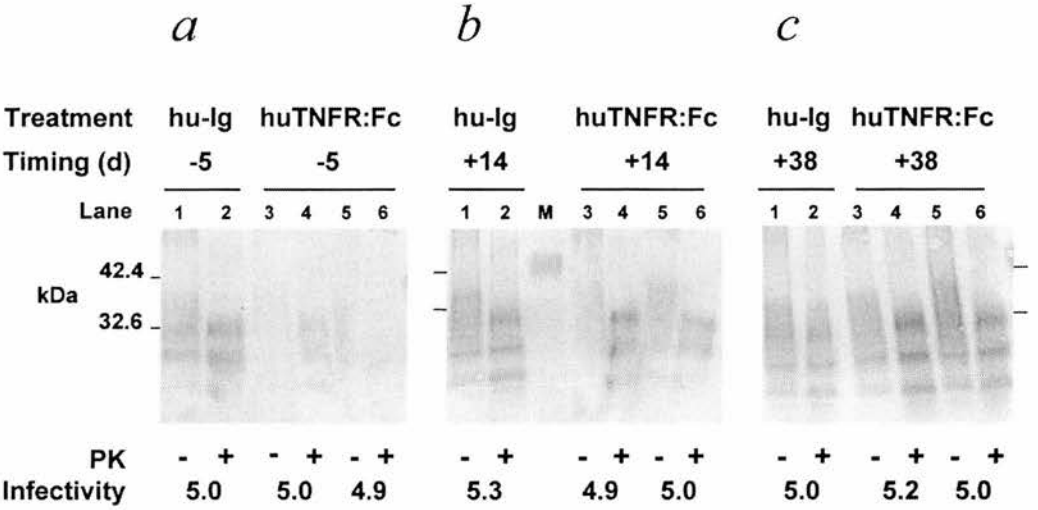

FIG. 4. PrP^{Sc} accumulation and infectivity titers in the spleen 70 days after i.p. injection with scrapie. Immunoblots show the accumulation of detergent-insoluble, relatively proteinase-K-resistant PrP^{Sc}. Treatment of tissue in the presence (+) or absence (−) of proteinase K before electrophoresis is indicated. Following proteinase K treatment, a typical three-band pattern was observed between molecular mass values of 20 and 30 kDa, representing unglycosylated, monoglycosylated, and diglycosylated isomers of PrP (in order of increasing molecular mass). Scrapie infectivity titers are expressed as log i.c. ID_{50} units per gram. Mice were treated with hu-Ig (control) or huTNFR:Fc 5 days before (a) or 14 (b) or 38 (c) days after scrapie injection. Lane M contained molecular mass markers. d, days; PK, proteinase K.

barrier and inhibit TNF-α signaling within the brain. Treatment with huTNFR:Fc in this study had no effect on survival time or neuropathology when mice were injected with scrapie directly into the CNS, confirming that the effects of treatment on TSE pathogenesis operate at a peripheral stage prior to neuroinvasion. Our studies suggest this is most likely due to a temporary interference with the integrity of FDCs, although effects of huTNFR:Fc treatment on other cell types in the spleen cannot be entirely excluded. However, the increased survival time following treatment with huTNFR:Fc 14 days after scrapie injection (Fig. 3b) and the recent demonstration that membrane lymphotoxin, not TNF-α, regulates the migration of dendritic cells in the spleen (48) suggest that it is unlikely that the effects of huTNFR:Fc treatment on scrapie pathogenesis are due to impaired cell trafficking from the site of scrapie challenge to the spleen.

Light-microscopical analysis demonstrated that mature PrP-expressing FDCs were temporarily absent in the spleen soon after treatment with huTNFR:Fc. Several hypotheses could explain the fate of FDCs following huTNFR:Fc treatment: (i) FDCs temporarily revert to an immature state that affects their function and phenotype; (ii) the chemokine gradients responsible for the organization of cell populations within the germinal center are altered (36), and as a consequence the FDCs disperse; or (iii) in the absence of stimulation from TNF-α, FDCs undergo apoptosis. We consider the first hypothesis most likely, as despite a temporary absence of FDC-M2, CD35, and PrP^{c} expression by FDCs, immature FDC processes were detected at the ultrastructural level, suggesting that these cells had reverted to a dedifferentiated state. Antigens are trapped and retained on the surface of FDCs through interactions between complement components and cellular complement receptors (37, 39). The loss of expression of complement receptor 1 (CD35; Fig. 1) and substantially decreased abundance of complement component C3 (data not shown) in lymphoid follicles of treated mice implied that these immature FDC processes had an impaired ability to retain antigens (31). Recent studies have demonstrated that C1q, C3, and complement receptors play an important role in the localization of TSE infectious agents to FDCs (26, 28). Therefore, it is unlikely that during the period of dedifferentiation following treatment with huTNFR:Fc, these immature FDC processes would have the potential to acquire TSE infectivity. Occasionally a few mature FDC processes were detected in the spleen by ultrastructural analysis 7 days after treatment (data not shown). These may represent FDCs in the process of regeneration, but it is also plausible that these were FDCs that were participating in strong antigenic responses and whose state of differentiation was unaffected by treatments which inhibit the TNFR signaling pathway (31).

Ultrastructural analysis of secondary lymphoid follicles from huTNFR:Fc-treated mice revealed other associated degenerative changes. FDCs provide important costimulatory factors which prevent B lymphocytes from undergoing apoptosis (18). Therefore, the detection of severe and extensive lymphocyte apoptosis following treatment with huTNFR:Fc suggested that this was most likely due to a loss of mature FDCs. Many of these apoptotic B lymphocytes were identified whole within tingible body macrophages which scavenge apoptotic lymphocytes and are considered to regulate the germinal-center reaction (42). The increased survival time following treatment with huTNFR:Fc is unlikely to be directly related to a loss of B lymphocytes by apoptosis, as ME7 scrapie pathogenesis is unaffected in mice with impaired germinal-center B-lymphocyte development (30). However, the effects of treatment on disease susceptibility could be indirectly related to a loss of cytokine stimuli from B lymphocytes, which leads to FDC dedifferentiation.

Within 70 days of a peripheral injection of immunocompetent mice with the ME7 scrapie strain, high levels of infectivity

titers and abundant PrP^{Sc} are detected in the spleen (5, 12, 28, 30). Here, when mice were given huTNFR:Fc before scrapie challenge, low levels of PrP^{Sc} were detected in the spleen 70 days postinoculation, approximately 50 days after the expected reappearance of mature FDCs. In the absence of mature FDCs at the time of scrapie challenge, it is likely that PrP^{Sc} and infectivity from the inoculum persist in the spleen but that a significant proportion is destroyed, for example by macrophages (3, 10). This effect would significantly delay both the onset of replication when the FDCs reappear within 14 days of treatment and the subsequent transfer of infectivity via peripheral nerves (19) into the CNS. Interestingly, infectivity titers in spleens from huTNFR:Fc-treated mice were the same as those from hu-Ig-treated controls, implying that the accumulation of PrP^{Sc} in the spleen lags behind the replication of infectivity during the early stages of infection (28). These experiments also suggest that the time interval during which the FDCs were unable to acquire and replicate scrapie was insufficient to allow macrophages adequate time to destroy most of the infectious agents, as huTNFR:Fc treatment had little, if any, effect on disease susceptibility.

Further experiments will show whether it is possible to extend the period of FDC dedifferentiation beyond that described in this report through prolonged treatment with multiple doses of huTNFR:Fc. Such an approach may reduce the accumulation of scrapie infectivity in the spleen and further delay or prevent the development of disease in the CNS. However, a prolonged blockade of proinflammatory cytokines such as TNF-α may cause serious side effects, including increased susceptibility to other infectious microorganisms, increased incidence of malignancies, or induction of autoimmune disease. A therapeutic blockade of TNF-α has been used to successfully treat rheumatoid arthritis and Crohn's disease in humans, where this cytokine plays a critical role in mediating inflammation (22, 32). The experience of long-term treatment of human rheumatoid arthritis patients with TNF-α antagonists suggests that they are safe and well tolerated (22, 32).

The detection of infectivity in lymphoid tissues and of PrP^{Sc} in association with FDCs from patients with vCJD (6, 21) and sheep with natural scrapie (1, 20, 45) suggests that these TSEs also share a similar requirement for FDCs. Therefore, the experiments described in this report and those of others suggest that treatments which temporarily interfere with the integrity (29, 35) or immune complex trapping function (28) of FDCs offer a potential approach for early intervention in peripherally acquired TSEs.

ACKNOWLEDGMENTS

We thank Irene McConnell, Dawn Drummond, and Emma Murdoch (Institute for Animal Health, Neuropathogenesis Unit, Edinburgh, United Kingdom) for excellent technical support; Immunex Corp. (Seattle, Wash.) for provision of huTNFR:Fc; Christine Farquhar (Institute for Animal Health, Neuropathogenesis Unit) for helpful discussion and provision of 1A8 and 1B3 polyclonal antisera; Marie Kosco-Vilbois (Serono Pharmaceutical Research Institute, Geneva, Switzerland) for provision of FDC-M2 monoclonal antiserum; and Jeffrey Browning (Biogen Inc., Cambridge, Mass.) for provision of hu-Ig.

This work was supported by funding from the Medical Research Council and the Biotechnology and Biological Sciences Research Council.

REFERENCES

1. **Andreoletti, O., P. Berthon, D. Marc, P. Sarradin, J. Grosclaude, L. van Keulen, F. Schelcher, J.-M. Elsen, and F. Lantier.** 2000. Early accumulation of PrP^{Sc} in gut-associated lymphoid and nervous tissues of susceptible sheep from a Romanov flock with natural scrapie. J. Gen. Virol. **81**:3115–3126.
2. **Beekes, M., and P. A. McBride.** 2000. Early accumulation of pathological PrP in the enteric nervous system and gut-associated lymphoid tissue of hamsters orally infected with scrapie. Neurosci. Lett. **278**:181–184.
3. **Beringue, V., M. Demoy, C. I. Lasmezas, B. Gouritin, C. Weingarten, J.-P. Deslys, J.-P. Adreux, P. Couvreur, and D. Dormont.** 2000. Role of spleen macrophages in the clearance of scrapie agent early in pathogenesis. J. Pathol. **190**:495–502.
4. **Bolton, D. C., M. P. McKinley, and S. B. Prusiner.** 1982. Identification of a protein that purifies with the scrapie prion. Science **218**:1309–1311.
5. **Brown, K. L., K. Stewart, D. Ritchie, N. A. Mabbott, A. Williams, H. Fraser, W. I. Morrison, and M. E. Bruce.** 1999. Scrapie replication in lymphoid tissues depends on PrP-expressing follicular dendritic cells. Nature Med. **5**:1308–1312.
6. **Bruce, M. E., I. McConnell, R. G. Will, and J. W. Ironside.** 2001. Detection of variant Creutzfeldt-Jakob disease (vCJD) infectivity in extraneural tissues. Lancet **358**:208–209.
7. **Bruce, M. E., R. G. Will, J. W. Ironside, I. McConnell, D. Drummond, A. Suttie, L. McCardle, A. Chree, J. Hope, C. Birkett, S. Cousens, H. Fraser, and C. J. Bostock.** 1997. Transmissions to mice indicate that 'new variant' CJD is caused by the BSE agent. Nature **389**:498–501.
8. **Bueler, H., M. Fischer, Y. Lang, H. Bluethmann, H.-P. Lipp, S. J. DeArmond, S. B. Prusiner, M. Aguet, and C. Weissmann.** 1992. Normal development and behaviour of mice lacking the neuronal cell-surface PrP protein. Nature **356**:577–582.
9. **Campbell, I. L., M. Eddleston, P. Kemper, M. B. A. Oldstone, and M. V. Hobbs.** 1994. Activation of cerebral cytokine gene expression and its correlation with the onset of reactive and acute-phase response gene expression in scrapie. J. Virol. **68**:2383–2387.
10. **Carp, R. I., and S. M. Callahan.** 1982. Effect of mouse peritoneal macrophages on scrapie infectivity during extended in vitro incubation. Intervirology **17**:201–207.
11. **Dickinson, A. G., V. M. Meikle, and H. Fraser.** 1969. Genetical control of the concentration of ME7 scrapie agent in the brain of mice. J. Comp. Pathol. **79**:15–22.
12. **Farquhar, C. F., J. Dornan, R. A. Somerville, A. M. Tunstall, and J. Hope.** 1994. Effect of *Sinc* genotype, agent isolate and route of infection on the accumulation of protease-resistant PrP in non-central nervous system tissues during the development of murine scrapie. J. Gen. Virol. **75**:495–504.
13. **Farquhar, C. F., R. A. Somerville, and M. E. Bruce.** 1998. Straining the prion hypothesis. Nature **391**:345–346.
14. **Farquhar, C. F., R. A. Somerville, J. Dornan, D. Armstrong, C. Birkett, and J. Hope.** 1994. A review of the detection of PrP^{sc}, p. 301–313. *In* R. Bradley and B. Marchant (ed.), BSE update. Proceedings of a commission of the European Communities, 14–15 September 1993, Brussels. Working document for the EC Ref: FII.3-JC/003.
15. **Farquhar, C. F., R. A. Somerville, and L. A. Ritchie.** 1989. Post-mortem immunodiagnosis of scrapie and bovine spongiform encephalopathy. J. Virol. Methods **24**:215–222.
16. **Fraser, H., and A. G. Dickinson.** 1973. Agent-strain differences in the distribution and intensity of grey matter vacuolation. J. Comp. Pathol. **83**:29–40.
17. **Fraser, H., and A. G. Dickinson.** 1978. Studies on the lymphoreticular system in the pathogenesis of scrapie: the role of spleen and thymus. J. Comp. Pathol. **88**:563–573.
18. **Freedman, A. S., D. Wang, J. S. Phifer, and S. N. Manie.** 1995. Role of follicular dendritic cells in the regulation of B cell proliferation. Curr. Top. Microbiol. Immunol. **201**:83–104.
19. **Glatzel, M., F. L. Heppner, K. M. Albers, and A. Aguzzi.** 2001. Sympathetic innervation of lymphoreticular organs is rate limiting for prion neuroinvasion. Neuron **31**:25–34.
20. **Heggebo, R., C. M. Press, G. Gunnes, K. I. Lie, M. A. Tranulis, M. Ulvund, M. H. Groschup, and T. Landsverk.** 2000. Distribution of prion protein in the ileal Peyer's patch of scrapie-free lambs and lambs naturally and experimentally exposed to the scrapie agent. J. Gen. Virol. **81**:2327–2337.
21. **Hill, A. F., R. J. Butterworth, S. Joiner, G. Jackson, M. N. Rossor, D. J. Thomas, A. Frosh, N. Tolley, J. E. Bell, M. Spencer, A. King, S. Al-Sarraj, J. W. Ironside, P. L. Lantos, and J. Collinge.** 1999. Investigation of variant Creutzfeldt-Jakob disease and other prion diseases with tonsil biopsy samples. Lancet **353**:183–189.
22. **Illei, G. G., and P. E. Lipsky.** 2000. Novel, non-antigen-specific therapeutic approaches to autoimmune/inflammatory diseases. Curr. Opin. Immunol. **12**:712–718.
23. **Jeffrey, M., G. McGovern, C. M. Goodsir, K. L. Brown, and M. E. Bruce.** 2000. Sites of prion protein accumulation in scrapie-infected mouse spleen revealed by immuno-electron microscopy. J. Pathol. **190**:323–332.
24. **Kimberlin, R. H., and C. A. Walker.** 1989. Pathogenesis of scrapie in mice after intragastric infection. Virus Res. **12**:213–220.

25. **Klein, M. A., R. Frigg, E. Flechsig, A. J. Raeber, U. Kalinke, H. Bluethman, F. Bootz, M. Suter, R. M. Zinkernagel, and A. Aguzzi.** 1997. A crucial role for B cells in neuroinvasive scrapie. Nature **390:**687–691.
26. **Klein, M. A., P. S. Kaeser, P. Schwarz, H. Weyd, I. Xenarios, R. M. Zinkernagel, M. C. Carroll, J. S. Verbeek, M. Botto, M. J. Walport, H. Molina, U. Kalinke, H. Acha-Orbea, and A. Aguzzi.** 2001. Complement facilitates early prion pathogenesis. Nature Med. **7:**488–492.
27. **Kosco-Vilbois, M. H., H. Zentgraf, J. Gerdes, and J.-Y. Bonnefoy.** 1997. To "B" or not to "B" a germinal center? Immunol. Today **18:**225–230.
28. **Mabbott, N. A., M. E. Bruce, M. Botto, M. J. Walport, and M. B. Pepys.** 2001. Temporary depletion of complement component C3 or genetic deficiency of C1q significantly delays onset of scrapie. Nature Med. **7:**485–487.
29. **Mabbott, N. A., F. Mackay, F. Minns, and M. E. Bruce.** 2000. Temporary inactivation of follicular dendritic cells delays neuroinvasion of scrapie. Nature Med. **6:**719–720.
30. **Mabbott, N. A., A. Williams, C. F. Farquhar, M. Pasparakis, G. Kollias, and M. E. Bruce.** 2000. Tumor necrosis factor alpha-deficient, but not interleukin-6-deficient, mice resist peripheral infection with scrapie. J. Virol. **74:** 3338–3344.
31. **Mackay, F., and J. L. Browning.** 1998. Turning off follicular dendritic cells. Nature **395:**26–27.
32. **Maini, R. N., and P. C. Taylor.** 2000. Anti-cytokine therapy for rheumatoid arthritis. Annu. Rev. Med. **51:**207–229.
33. **McBride, P., P. Eikelenboom, G. Kraal, H. Fraser, and M. E. Bruce.** 1992. PrP protein is associated with follicular dendritic cells of spleens and lymph nodes in uninfected and scrapie-infected mice. J. Pathol. **168:**413–418.
34. **Mohler, K. M., D. S. Torrance, C. A. Smith, R. G. Goodwin, K. E. Stremler, V. P. Fung, H. Madani, and M. B. Widmer.** 1993. Soluble tumour necrosis factor (TNF) receptors are effective therapeutic agents in lethal endotoxemia and function simultaneously as both carriers and TNF antagonists. J. Immunol. **151:**1548–1561.
35. **Montrasio, F., R. Frigg, M. Glatzel, M. A. Klein, F. Mackay, A. Aguzzi, and C. Weissmann.** 2000. Impaired prion replication in spleens of mice lacking functional follicular dendritic cells. Science **288:**1257–1259.
36. **Ngo, V. N., H. Korner, M. D. Gunn, K. N. Schmidt, D. S. Riminton, M. D. Cooper, J. L. Browning, J. D. Sedgwick, and J. G. Cyster.** 1999. Lymphotoxin α/β and tumour necrosis factor are required for stromal cell expression of homing chemokines in B and T cell areas of the spleen. J. Exp. Med. **189:**403–412.
37. **Nielsen, C. H., E. M. Fischer, and R. G. Q. Leslie.** 2000. The role of complement in the acquired immune response. Immunology **100:**4–12.
38. **Pasparakis, M., L. Alexopoulo, V. Episkopou, and G. Kollias.** 1996. Immune and inflammatory responses in TNFα-deficient mice: a critical requirement for TNFα in the formation of primary B cell follicles, follicular dendritic cell networks and germinal centres, and in the maturation of the humoral immune response. J. Exp. Med. **184:**1397–1411.
39. **Pepys, M. B.** 1976. Role of complement in the induction of immunological responses. Transplant Rev. **32:**93–120.
40. **Probert, L., K. Akassoglou, G. Kassiotis, M. Pasparakis, L. Alexopoulou, and G. Kollias.** 1997. TNF-alpha transgenic and knockout models of CNS inflammation and degeneration. J. Neuroimmunol. **72:**137–141.
41. **Prusiner, S. B., D. C. Bolton, D. F. Groth, K. A. Bowman, S. P. Cochran, and M. P. McKinley.** 1982. Further purification and characterisation of scrapie prions. Biochemistry **21:**6942–6950.
42. **Smith, J. P., G. F. Burton, J. G. Tew, and A. K. Szakal.** 1998. Tingible body macrophages in regulation of germinal center reactions. Dev. Immunol. **6:**285–294.
43. **Somerville, R. A., C. R. Birkett, C. F. Farquhar, N. Hunter, W. Goldmann, J. Dornan, D. Grover, R. M. Hennion, C. Percy, J. Foster, and M. Jeffrey.** 1997. Immunodetection of PrP^{Sc} in spleens of some scrapie-infected sheep but not BSE-infected cows. J. Gen. Virol. **78:**2389–2396.
44. **Tkachuk, M., S. Bolliger, B. Ryffel, G. Pluschke, T. A. Banks, S. Herren, R. H. Gisler, and M. H. Kosco-Vilbois.** 1998. Crucial role of tumour necrosis factor receptor 1 expression on nonhematopoietic cells for B cell localization within the splenic white pulp. J. Exp. Med. **187:**469–477.
45. **van Keulen, L. J. M., B. E. C. Schreuder, R. H. Meloen, G. Mooij-Harkes, M. E. W. Vromans, and J. P. M. Langeveld.** 1996. Immunohistological detection of prion protein in lymphoid tissues of sheep with natural scrapie. J. Clin. Microbiol. **34:**1228–1231.
46. **van Keulen, L. J. M., B. E. C. Schreuder, M. E. W. Vromans, J. P. M. Langeveld, and M. A. Smits.** 1999. Scrapie-associated prion protein in the gastro-intestinal tract of sheep with scrapie. J. Comp. Pathol. **121:**55–63.
47. **Wooley, P. H., J. Dutcher, M. B. Widmer, and S. Gillis.** 1993. Influence of a recombinant human soluble tumour necrosis factor receptor FC fusion protein on type II collagen-induced arthritis in mice. J. Immunol. **151:**6602–6607.
48. **Wu, Q., Y. Wang, E. O. Hedgeman, J. L. Browning, and Y.-X. Fu.** 1999. The requirement of membrane lymphotoxin for the presence of dendritic cells in lymphoid tissues. J. Exp. Med. **190:**629–638.

J. Comp. Path. 2004, Vol. 130, 181–194

ELSEVIER
www.elsevier.com/locate/jcpa

Murine Scrapie Infection Causes an Abnormal Germinal Centre Reaction in the Spleen

G. McGovern, K. L. Brown*, M. E. Bruce* and M. Jeffrey

*Veterinary Laboratories Agency (VLA) Lasswade, Pentlands Science Park, Bush Loan, Penicuik, Midlothian EH26 0PZ, *Institute for Animal Health, Neuropathogenesis Unit, Ogston Building, West Mains Road, Edinburgh EH9 3JF, UK*

Summary

Follicular dendritic cells (FDCs) of the lymphoreticular system play a role in the peripheral replication of prion proteins in some transmissible spongiform encephalopathies (TSEs), including experimental murine scrapie models. Disease-specific PrP (PrP^d) accumulation occurs in association with the plasmalemma and extracellular space around FDC dendrites, but no specific immunological response has yet been reported in animals affected by TSEs. In the present study, morphology (light microscopical and ultrastructural) of secondary lymphoid follicles of the spleen were examined in mice infected with the ME7 strain of scrapie and in uninfected control mice, with or without immunological stimulation with sheep red blood cells (SRBCs), at 70 days post-inoculation or at the terminal stage of disease (268 days). Scrapie infection was associated with hypertrophy of FDC dendrites, increased retention of electron-dense material at the FDC plasma membrane, and increased maturation and numbers of B lymphocytes within secondary follicles. FDC hypertrophy was particularly conspicuous in immune-stimulated ME7-infected mice. The electron-dense material was associated with PrP^d accumulation, as determined by immunogold labelling. We hypothesize that immune system changes are associated with increased immune complex trapping by hypertrophic FDCs expressing PrP^d molecules at the plasmalemma of dendrites, and that this process is exaggerated by immune system stimulation. Contrary to previous dogma, these results show that a pathological response within the immune system follows scrapie infection.

Keywords: follicular dendritic cells; germinal centre; mouse; prion protein; scrapie; spleen

Introduction

Transmissible spongiform encephalopathies (TSEs) are a family of slowly progressive neurodegenerative disorders, consisting of infectious, familial and sporadic forms of disease in both animals and man. The TSEs include bovine spongiform encephalopathy (BSE) of cattle and exotic ungulates, scrapie of sheep and goats, and Creutzfeldt-Jakob disease (CJD), kuru and Gertsmann-Straüssler syndrome (GSS) of human beings. TSEs can be naturally, experimentally or iatrogenically transmitted to several mammalian species and are characterized by the accumulation of an abnormal disease-specific isoform of a host-encoded cell surface glycoprotein called prion protein (PrP^d). The normal PrP molecule (PrP^c) is expressed abundantly in the central nervous system (CNS) (Manson *et al.*, 1992; Ford *et al.*, 2002) and less abundantly in many other tissues (Oesch *et al.*, 1985), while PrP^d accumulates in the CNS in many of the TSEs and also in the peripheral nervous system and lymphoreticular tissues in most experimental animal models.

The role of the lymphoreticular system (LRS) in the pathogenesis of TSEs has been extensively studied (Fraser and Dickinson, 1970; Mabbott and Bruce, 2001). Initial investigations into which cells

Correspondence to: G. McGovern.

0021–9975/$ - see front matter
doi: 10.1016/j.jcpa.2003.11.001

within the LRS permit prion replication demonstrated that T-cell depletion by adult or neonatal thymectomy had no effect on scrapie pathogenesis, suggesting that T cells were not critical for scrapie pathogenesis. However, surgical or genetic splenectomy prolonged the incubation period in several scrapie models (Kimberlin and Walker, 1989), demonstrating the pathogenetic importance of the spleen and its cellular components. Further studies revealed that exposure of scrapie-infected mice to lethal doses of gamma irradiation had no effect on pathogenesis, or on prion replication in the spleen, suggesting that a long-lived radiation-resistant cell was important for neuroinvasion and replication of the infective agent (Fraser and Dickinson, 1978; Fraser and Farquhar, 1987).

Genetically immunodeficient (SCID) mice lack functional B and T lymphocytes, and follicular dendritic cells (FDCs) in such mice remain immature due to lack of stimulation from B cells (Bosma *et al.*, 1983; Kapasi *et al.*, 1993). SCID mice are also relatively resistant to peripheral (i.e., non-CNS) inoculation with scrapie (Kitamoto *et al.*, 1991; O'Rourke *et al.*, 1994; Brown *et al.*, 1997). The lymphocyte population in SCID mice can be restored with bone marrow from immunocompetent donors, enabling FDCs to mature (Kapasi *et al.*, 1993). Lymphocyte-reconstituted SCID mice infected peripherally with scrapie develop the disease after incubation periods comparable with those of immunocompetent mice, confirming that cells of the immune system play a significant role in the peripheral pathogenesis of the disease (Fraser *et al.*, 1996; Lasmezas *et al.*, 1996).

While studies with SCID mice produced strong evidence in favour of a critical role for FDCs in pathogenesis, the possible role of lymphoid cells could not be excluded. A more conclusive role for FDCs in scrapie replication was provided by studies in chimaeric mice, in which PrP was expressed on FDCs but not on lymphocytes, and vice versa. In these models, replication of infectivity and progression of infection to the CNS depended upon the presence of mature PrP-expressing FDCs, and were independent of the expression of PrP on lymphocytes (Brown *et al.*, 1999, 2000).

FDCs are accessory cells that occur only in lymphoid follicles, where they are tightly surrounded by lymphocytes (Tew *et al.*, 1982). During germinal centre reactions, the function and morphology of FDCs change markedly. On stimulation, FDC processes elongate and make contact with numerous lymphocytes, while their surface receptors allow them to trap immune complexes which can be retained for extended periods. The immune complexes are then presented to, and processed by, B lymphocytes. Within the spleen, FDCs, unstimulated B cells and some macrophage populations are contained in the primary follicle of the white pulp region. This region is characterized by closely packed lymphocytes and is divided into two zones, namely, the follicle itself and the surrounding periarteriolar lymphoid sheath (PALS), which contains the arteriole, T cells and macrophages. The marginal zone tightly surrounds the PALS and merges into the highly vascularized red pulp.

In previous morphological studies of spleens from mice terminally affected by scrapie, FDCs formed highly convoluted labyrinthine structures, with irregular, often abundant, electron-dense deposits associated with cell dendrites (Jeffrey *et al.*, 2000). These deposits occasionally contained PrP^d-associated amyloid fibrils, which were seen to a lesser extent in tissues obtained from mice at pre-clinical stages of disease. Immunogold labelling was associated with plasmablast emperipolesis by FDC dendrites (i.e., FDC dendrite-encircled plasmablasts), and with the extracellular space surrounding FDC dendritic processes. Coated pits were more abundant on the surface of FDCs from scrapie-infected animals than from normal control animals; PrP^d labelling, however, was not associated with these structures. In the spleens of pre-clinically and terminally affected animals, immunogold labelling was also associated with tingible body macrophage (TBM) lysosomes. Immunolabelling within these lysosomal compartments is predominantly associated with the more electron-dense areas. This lysosomal PrP^d is probably scavenged from the extracellular space or from FDC processes (Jeffrey *et al.*, 2000). In sheep TBMs, PrP^d lacks the N terminus of the PrP, which further supports the suggestion that TBMs internalize and digest extracellular PrP (Jeffrey *et al.*, 2000). The aims of the present study were (1) to characterize the morphological response of the secondary follicle to scrapie infection, and (2) to determine whether this response was normal as compared with other forms of exogenous antigenic stimulation.

Materials and Methods

Animals and Experimental Procedure

C57BL mice of either sex ($n = 16$) were inoculated intraperitoneally with a 10^{-2} dilution of either ME7 (Brown *et al.*, 1997) scrapie brain homogenate, or normal brain (NB) homogenate. At 42 and 63 days

post-inoculation (dpi), two of the ME7-infected mice received intraperitoneally 0.1 ml of a sheep red blood cell (SRBC) suspension (10^7 SRBCs), and a further two received 0.1 ml of saline; similar injections were given to four of the NB-treated mice. These eight mice were all killed by cervical dislocation at 70 dpi. At 240 and 261 dpi, the remaining four ME7-infected and four NB-treated mice received injections exactly as described above. These eight mice were killed by cervical dislocation at 268 dpi, at which time the ME7-infected animals were in the terminal stage of disease.

The spleens of all mice, obtained at necropsy, were fixed in a solution containing paraformaldehyde 0.5% and glutaraldehyde 0.5%. Between 25 and 30 cubes (1 mm^3) of tissue, taken from each spleen, were then post-fixed in osmium tetroxide, dehydrated and embedded in araldite (Hayat, 1989).

Light Microscopy

Thick (1 μm) sections were stained by toluidine blue or were 'etched' (deplasticized) with saturated sodium ethoxide for up to 30 min. Endogenous peroxidase was blocked and sections were 'de-osmicated' with hydrogen peroxide 6% in methanol for 10 min, followed by pre-treatment with neat formic acid for 5 min (Jeffrey and Goodsir, 1996). Normal serum was then applied for 1 h to block non-specific labelling. The avidin–biotin complex method was used for immunohistochemical labelling, with 1A8 anti-PrP serum (Farquhar *et al.*, 1993) at a dilution of 1 in 3000, or pre-immune serum. The primary antibody was applied to the etched and pre-treated sections and incubated at 4 °C for 15 h. All other treatments were undertaken at room temperature. Reaction product was developed with 3-3′diaminobenzidine. Blocks (4–7 per animal) with appropriate immunolabelled areas and large areas of white pulp were then selected for ultrastructural studies from ME7-infected and uninfected groups.

Ultrastructural Immunohistochemistry

Serial 55-nm sections were taken from blocks previously identified as containing secondary follicles, which in the case of ME7-infected mice were also immunolabelled for PrP^d. These sections were placed on 400-mesh gold grids and etched in sodium periodate for 60 min. Endogenous peroxidase was blocked and sections were de-osmicated with hydrogen peroxide 3% in methanol for 10 min, followed by enhancement of antigen expression with neat formic acid for 10 min. Residual aldehyde groups were quenched with 0.2 M glycine in phosphate-buffered saline (PBS), pH 7.4 for 3 min. Primary antibody (1A8) at a 1 in 500 dilution in incubation buffer or pre-immune serum was then applied for 15 h at 4 °C. After thorough rinsing, sections were incubated for 2 h with Auroprobe 1-nm colloidal gold (Amersham Ltd, Amersham, UK), diluted 1 in 50 in incubation buffer. Sections were then post-fixed with glutaraldehyde 2.5% in PBS and labelling was enhanced with immunogold silver stain (IGSS) (Amersham Ltd) for 4 min. Grids were counterstained with uranyl acetate and lead citrate, and examined with a Jeol 1200EX transmission electron microscope.

Results

Light Microscopy

At both 70 dpi and during terminal stages of disease (268 dpi), single or multiple reactive germinal centres were identified in all blocks of spleen tissue from ME7-infected mice. Approximately twice as many germinal centres were present in scrapie-infected spleens as in the corresponding uninfected spleens. The splenic germinal centres from scrapie-infected mice showed PrP^d labelling mainly within secondary follicles; some TBM labelling, however, was seen at the periphery of follicles. The intensity of immunolabelling in the spleens from terminally diseased animals was considerably greater than in those from mice killed at 70 dpi, with most follicles showing extensive PrP^d accumulations (Fig. 1).

Immunolabelling of PrP^d, provisionally identified as TBM labelling, was also detected in the red pulp, mantle zones and periarteriolar sheaths of ME7- infected mice. No immunolabelling of PrP^d was seen in the spleens of age-matched uninfected mice, inoculated with normal brain.

Electron Microscopy (EM)

Morphology and immunolabelling of uninfected splenic tissue. No morphological difference was seen between spleens from NB-treated mice and spleens from NB-treated mice that also were immunized with SRBCs. Electron microscopy showed that follicles of tissues from uninfected mice contained FDCs at various stages of maturation. Mature FDCs were confined to the secondary follicles, had highly irregular nuclei and were

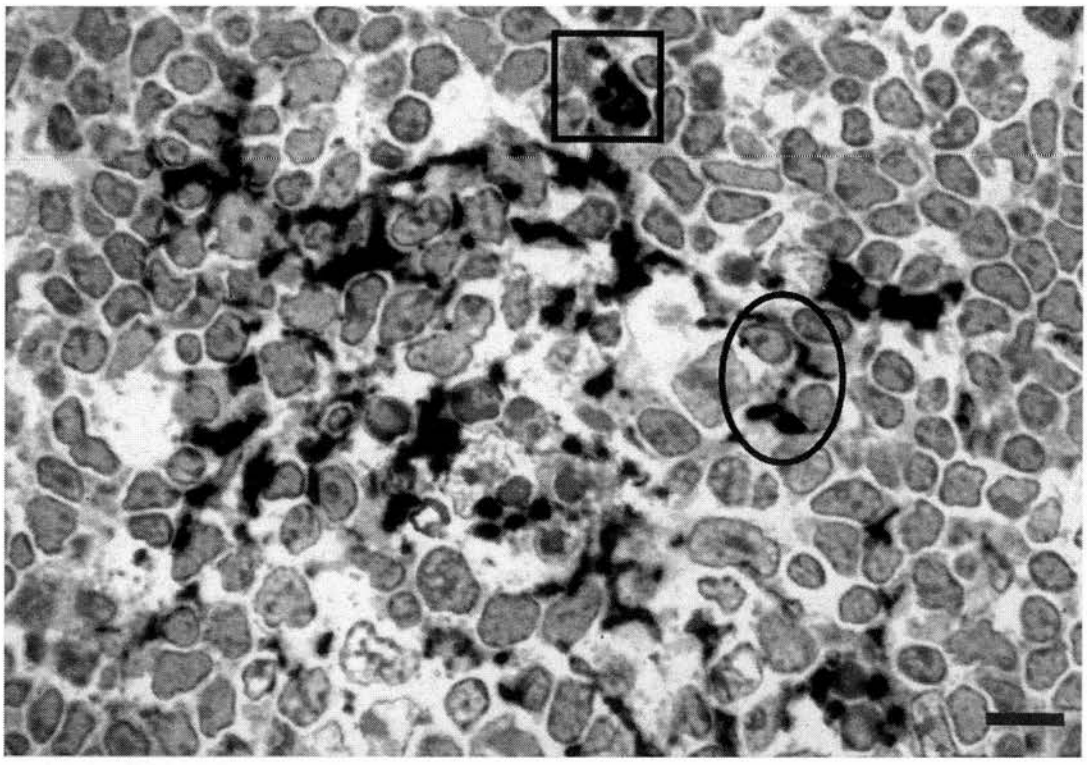

Fig. 1. Resin-embedded spleen (1 μm thick) from a terminally affected mouse. The germinal centre shows two types of PrP^d labelling. There is an interrupted linear pattern (oval) and condensed granular pattern (square). PrP^d immunolabelling. Bar, 17.36 μm.

often binucleate and occasionally multi-nucleate. The nucleus was clear, with abundant euchromatin and a distinctive band of heterochromatin adjacent to the nuclear membrane. The perikaryonal cytoplasm was relatively slight and contained moderate numbers of cell organelles. Dendritic processes of mature FDCs ran between the lymphoid cells of germinal centres. These processes were often extensive and sometimes formed small knots; occasionally more complex arrangements of dendrites (labyrinthine glomerular complexes) were present. Where several processes ran between cells they usually ran in parallel straight or curved lines. No visible structural features were present between the plasmalemmae of adjacent dendrites. Occasionally, two processes were joined by desmosomes. Where processes formed knots and labyrinthine glomerular complexes, curvilinear electron-dense material could be seen between the plasmalemmae of adjacent FDC dendrites (Fig. 2a). This electron-dense deposit formed a dense line (on average 0.18 μm in diameter), intermediate between dendrites and consistently located 0.15 μm from each dendritic process (Fig. 2b). FDCs of a similar size and complexity were present in all uninfected spleens, regardless of SRBC immune stimulation.

Within the secondary follicles, some FDCs appeared less mature, with more rounded, single nuclei and poorly developed processes. Unlike human or ovine secondary follicles, the murine secondary follicles showed little variation in lymphocyte nuclear size. As a result, dark and light zones could not be distinguished. Consequently, the location of the immature FDCs in relation to the dark and light zones was not determined.

Numerous TBMs, with phagocytosed nuclear remnants and abundant lysosomes in their cytoplasm, were present within the secondary follicle. Occasionally whole degenerate cells (presumed to be apoptotic lymphocytes) were found within the cytoplasm of these macrophages. Most lymphocytes showed little or no evidence of differentiation within the light zone of the secondary follicle. Rarely, some lymphocytes showed evidence of early B cell differentiation. These cells had dilated, oval or rough endoplasmic reticulum (RER) containing floccular material. In the mantle and PALS, occasional lymphocytes showed even more recognizable differentiation towards plasma cells. Such cells had numerous cisternae of widely dilated RER containing an amorphous electron-dense material (presumed to be globulins). No PrP^d immunolabelling was detected in these tissues.

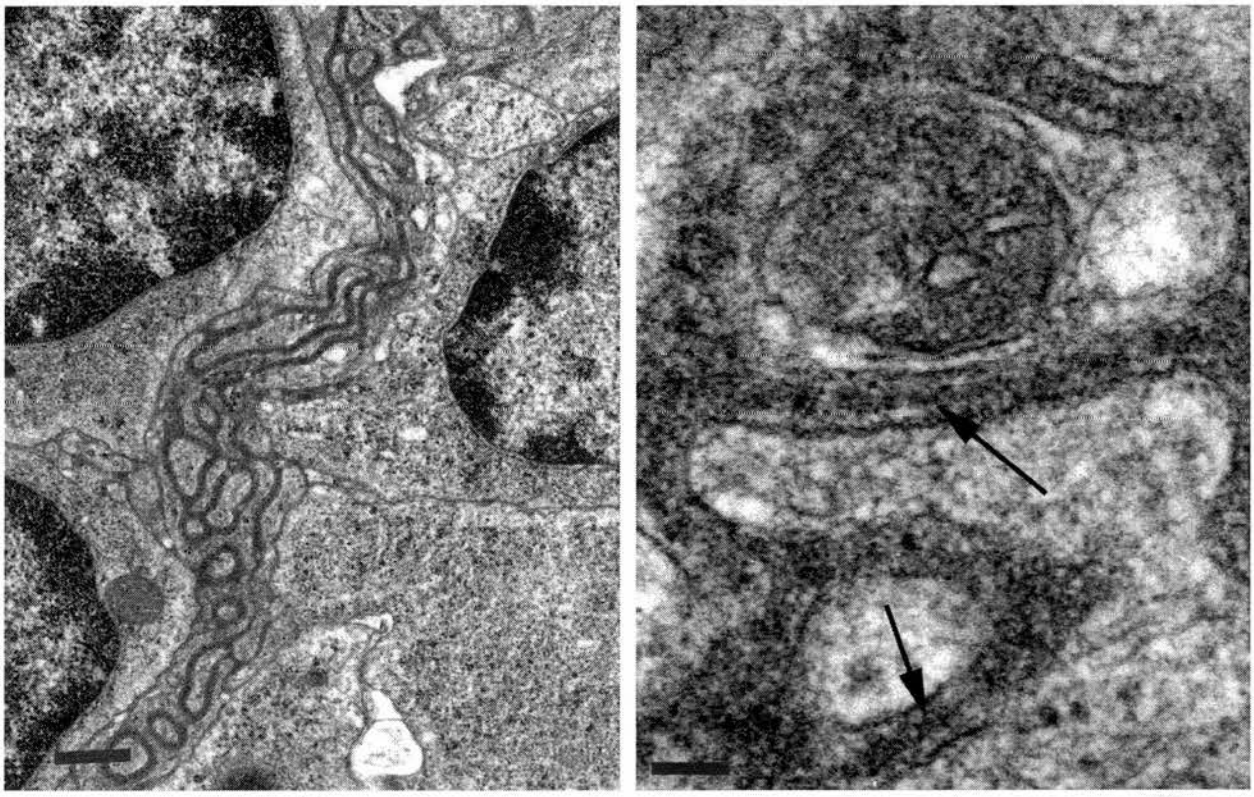

(a) (b)

Fig. 2a,b. (a) FDC dendrite processes from an uninfected mouse spleen. Simple FDC processes run between lymphocytes. The associated electron-dense deposit is uniform and linear. Ultrastructural counterstain. Bar, 1.22 μm. (b) Detail of labyrinthine glomerular complex from the spleen of an uninfected mouse treated with SRBC. The extracellular space surrounding dendritic process plasmalemmae consists of an intermediate dense lamina (arrows), bound on either side by two less electron-dense zones. This assembly is of a consistent width. Ultrastructural counterstain. Bar, 0.11 μm.

Morphology of infected splenic tissue. In tissues obtained from all terminally affected ME7-infected mice, regardless of SRBC immune stimulation, the majority of dendritic processes of FDCs within secondary follicles formed large labyrinthine glomerular structures. The area occupied by these structures was estimated to be 10–20 times larger in diameter than those of control tissues, with more elaborate branching and interweaving of dendritic processes. The space between the convoluted dendritic extensions within these glomerular structures was often markedly greater than in uninfected mice, and contained uniformly opaque, electron-dense material associated with the dendritic membrane. The intermediate electron-dense lamina, present in uninfected tissues, was absent. In other areas of hypertrophic labyrinthine glomerular complexes, the membrane-associated electron-dense deposit was sparse or absent. In these areas, the space between adjacent dendritic processes remained relatively constant, and an intermediate electron-dense line could clearly be seen. In yet other FDC dendritic complexes there was no abnormal accumulation of electron-dense deposit, and the size and frequency of occurrence of branching of dendrites was similar to that in uninfected mice. This pattern was seen with particular frequency in infected mice killed at 70 dpi. The complexity of branching of dendritic processes and the abundance of extracellular electron-dense material were directly related, i.e., the less complex the branching of dendrites, the less electron-dense material was seen. In some of the highly hypertrophic labyrinthine glomerular complexes there was a reduction in electron density of the material in the extracellular space around the dendrites. Within these areas were short, usually single, fibrillar structures; occasionally, however, small groups of randomly oriented fibrils were also seen (Fig. 3).

By comparison with unimmunized terminally diseased mice, SRBC-immunized terminally diseased mice showed larger hypertrophic labyrinthine glomerular complexes and greater amounts of extracellular material between them (Fig. 4).

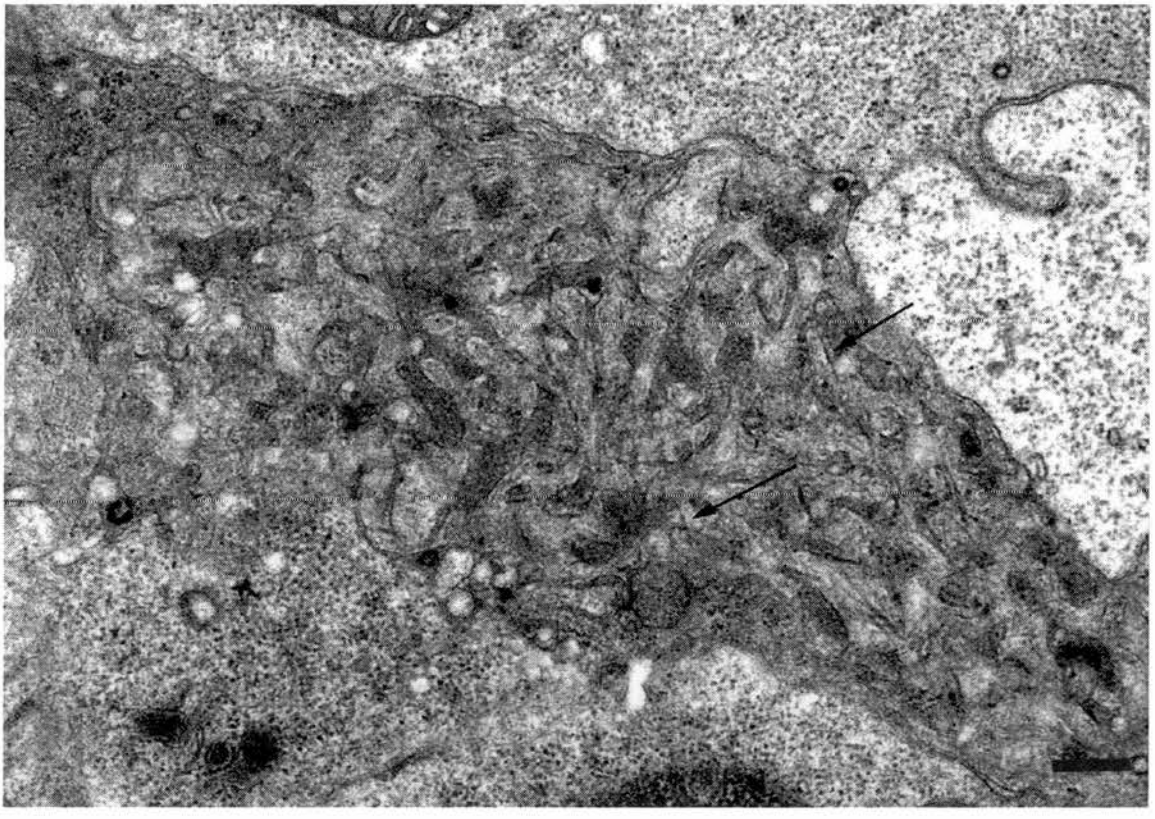

Fig. 3. Spleen from a terminally affected mouse treated with SRBC. Note fibrillar structures (arrows) in the expanded extracellular space surrounding mature FDC dendritic profiles. Ultrastructural counterstain. Bar, 0.34 μm.

In all terminally diseased animals, regardless of SRBC immunization, TBMs of secondary follicles contained abundant lysosomal compartments. Apoptotic cells were occasionally seen within these compartments, including B lymphocytes with dilated RER. Similarly sized TBMs were observed in mice killed at 70 dpi.

Well differentiated plasmablasts with distended RER, presumably containing globulins, were present in the secondary follicles of ME7-infected mice, regardless of SRBC stimulation. They were frequently surrounded (or emperipolesed) by FDC dendritic processes, as shown in Fig. 4. Less mature B cells, still with dilated RER, were found in the secondary follicles of both uninfected and infected animals; differentiated B cells were, however, generally more abundant in the latter.

Coated pits and vesicles were observed in all experimental groups, including the uninfected controls, but these structures were much more numerous in the infected mice. Increased numbers of coated pits were observed mainly at the plasmalemma of reactive FDC dendrites; less commonly they were observed at the cell surface of lymphocytes adjacent to FDCs of infected mice. The increased number of coated pits in infected mice killed at 70 dpi was similar to that in terminally diseased mice at 268 dpi.

Immunogold labelling of PrP^d in infected splenic tissue. In splenic tissue from both immune stimulated and unstimulated ME7-infected mice, this was associated with FDC dendritic plasmalemmae of both immature extended linear processes and mature labyrinthine glomerular complexes. The smaller particles of immunogold/silver reaction product demonstrated that labelling was generally associated with the plasma membrane itself. Only a small proportion of the reaction product was found within the electron-dense material of the extracellular space. This was conspicuous in the SRBC-stimulated animals, in which the extracellular electron-dense material was particularly abundant between separated FDC dendrites, making the distinction between plasmalemma-associated PrP^d and PrP^d accumulation in electron-dense material more readily apparent (Fig. 5). Within the extracellular space surrounding some FDC labyrinthine glomerular complexes, PrP^d-immunolabelled short fibrillar forms were observed.

Immunolabelling of hypertrophic labyrinthine glomerular complexes was indistinguishable in infected mice killed at 70 and 268 dpi. Subtle

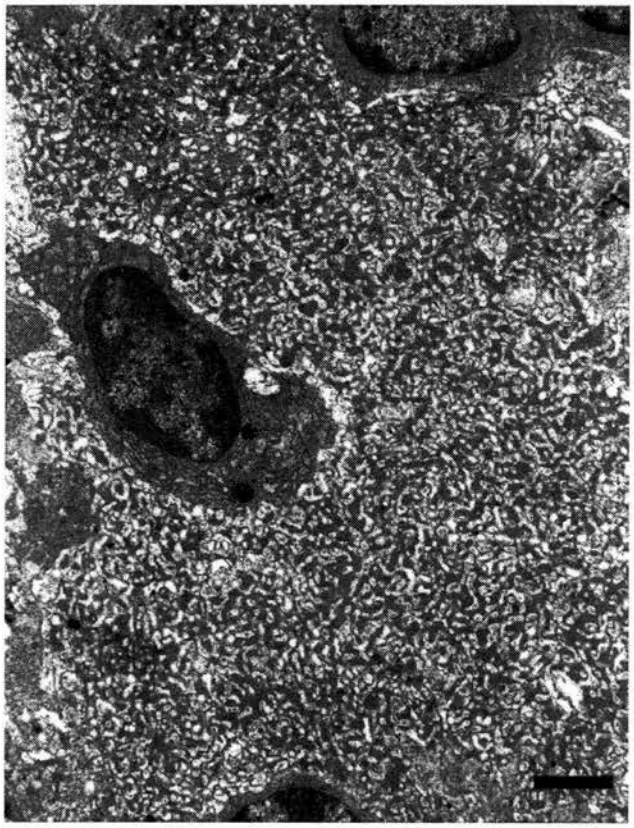

Fig. 4. Spleen from a terminally affected mouse treated with SRBC. A markedly hypertrophic FDC labyrinthine complex with highly convoluted dendrites and abundant associated electron-dense deposit is shown. Embedded within the hypertrophic dendrites is a differentiating plasmablast (asterisk), which is dwarfed by the hypertrophic FDC complex. Ultrastructural counterstain. Bar, 1.41 μm.

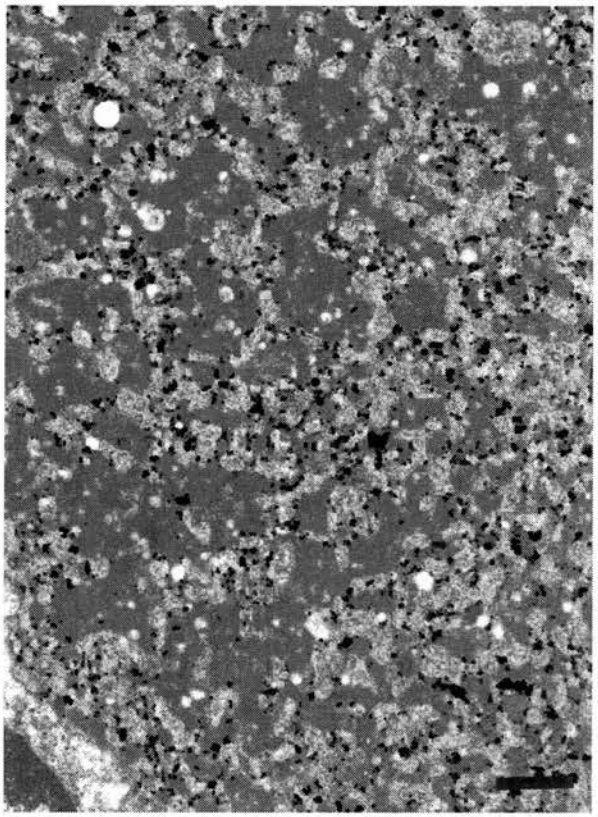

Fig. 5. Immunolabelled spleen from a terminally affected mouse treated with SRBC. Detail of a hypertrophic FDC complex. Immunogold PrP^d labelling is primarily associated with the plasmalemma of dendrites and not the adjacent electron-dense deposit. The abundant amorphous electron-dense material is unstructured and lacks an intermediate dense lamina. PrP^d immunogold labelling. Bar, 0.65 μm.

differences in the distribution of immunogold labelling occurred, however, in respect of immature FDCs and smaller groups of dendrites. At 70 dpi, all PrP^d accumulations were restricted to mature hypertrophic FDC glomeruli, no PrP^d accumulations being associated with smaller dendritic knots. Where labelling occurred, it was invariably associated with slight amounts of electron-dense material. At the terminal stage of disease, very few FDCs had not formed hypertrophic complexes. However, immunolabelling was found at the plasmalemma of dendrites of sparse, less mature FDC dendrites in which no intermediate dense lamina was present and no extracellular electron-dense material was formed (Fig. 6). These observations suggest a progression of events illustrated schematically in Fig. 7.

As described above, coated vesicles and pits were more abundant in infected than in uninfected groups. However, immunolabelling was not conspicuously associated with these structures (Fig. 8).

Large TBMs containing many apoptotic bodies were observed more frequently within the secondary follicles of infected groups than in the corresponding uninfected groups. In addition to TBM labelling of secondary follicles, intra-lysosomal PrP^d labelling of TBMs was seen in the red pulp, mantle zone and periarteriolar sheath of both SRBC-stimulated and unstimulated terminally diseased mice (Fig. 9). In some cases, PrP^d accumulations appeared to be associated with dense floccular material within lysosomes. Intralysosomal PrP^d labelling of TBMs was not seen outside the secondary follicles in infected mice killed at 70 dpi.

Immunolabelling demonstrated that the transformation of B lymphoblasts into plasmablasts and differentiated plasma cells was associated with FDC dendrites showing emperipolesis and PrP^d expression. An association between lymphocyte emperipolesis and PrP^d immunolabelling could also be seen within areas of the follicle in which labyrinthine glomerular complexes

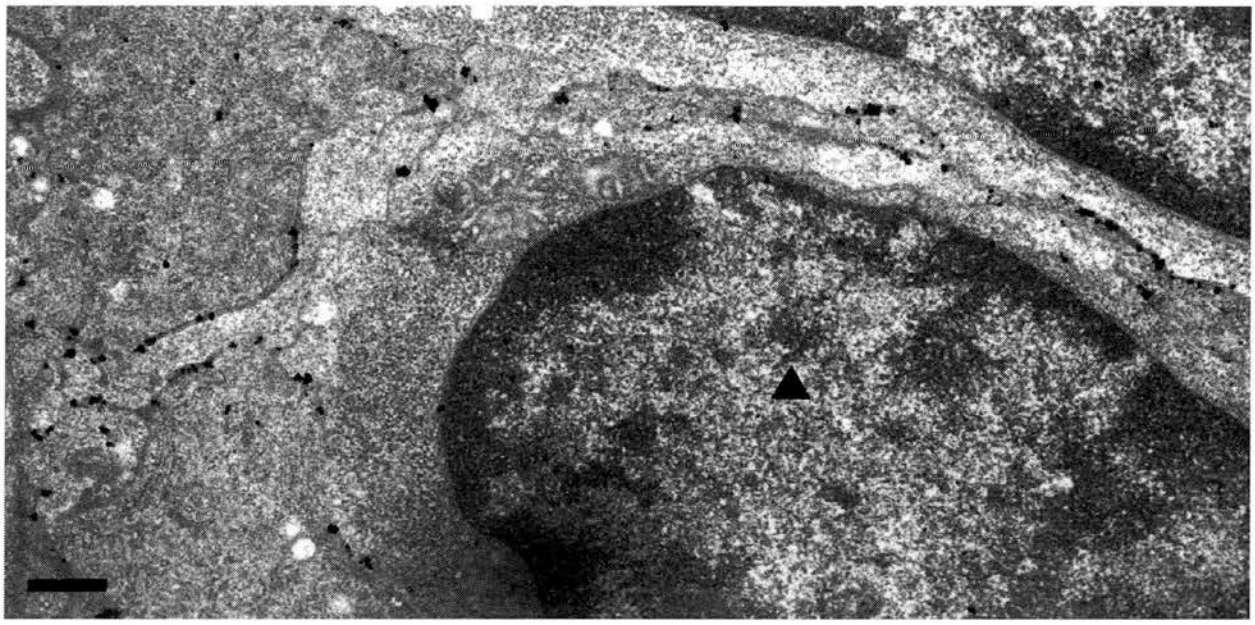

Fig. 6. Immunolabelled spleen from a terminally affected mouse treated with SRBC. A lymphocyte emperipolesed by FDC dendrites is shown (▲). Immunolabelling is associated with the plasmalemma of dendritic processes. There is no electron-dense material surrounding simple FDC dendrites. PrP^{d} immunogold labelling. Bar, 0.75 μm.

were not observed. A full range of differentiating B cells could be detected within the follicles of all infected groups, from undifferentiated lymphocytes (Fig. 10a) to fully mature plasma cells (Fig. 10b).

All the changes observed are summarized in Table 1.

Discussion

Following on from our initial investigations (Jeffrey *et al.*, 2000), this study further confirmed that PrP^{d} is associated with the plasmalemma and adjacent extracellular space of FDCs, and is localized intralysosomally within macrophages.

All scrapie-infected splenic tissue, whether or not from mice that subsequently received SRBC immune stimulation, showed an exaggerated or hypertrophic response of FDC dendrites within germinal centres. Cell processes were elongated and strikingly convoluted, forming large labyrinthine glomerular structures within the secondary follicle, while an electron-dense deposit accumulated around and between these processes. Both the accumulated electron-dense material and the hypertrophic FDC glomerular responses were more conspicuous in the SRBC-stimulated animals than in infected mice that did not receive such immune stimulation.

In splenic tissue from uninfected mice, an ordered electron-dense line or lamina, at a constant distance from the FDC dendritic process plasmalemmae, could be seen within the extracellular material. This line appeared as a tri-laminar assembly in conjunction with two FDC plasmalemmal membranes. A previous report of FDC antigen–antibody complex binding (Radoux *et al.*, 1985) described the binding of antibody/ferritin complexes as a line, equidistant between adjacent FDC membranes. The mechanism of antigen/antibody complex attachment was later shown to consist of fixation of the antigen in the extracellular space to the adjacent FDC membranes via the complexed antibody attaching to FDC C3b and Fc receptors (Bosseloir *et al.*, 1995). This would suggest that the electron-dense lamina seen in the detailed electron micrographs of the extracellular space surrounding normal FDC dendritic processes in uninfected mice is the site of normal antigen–antibody complex binding. The extracellular space around hypertrophic FDCs from mice inoculated with ME7 scrapie did not show the tri-laminar assembly indicative of antigen–antibody complex binding, but demonstrated abundant electron-dense material within the extracellular space. Because of its location and the similarity of its electron density to that of the intermediate dense line observed in association with normal FDCs, we suggest that this represented accumulated antigen–antibody complexes. Excessive trapping of antigen–antibody complex by FDC dendrites, with a subsequent breakdown of the normal binding and structural relationships

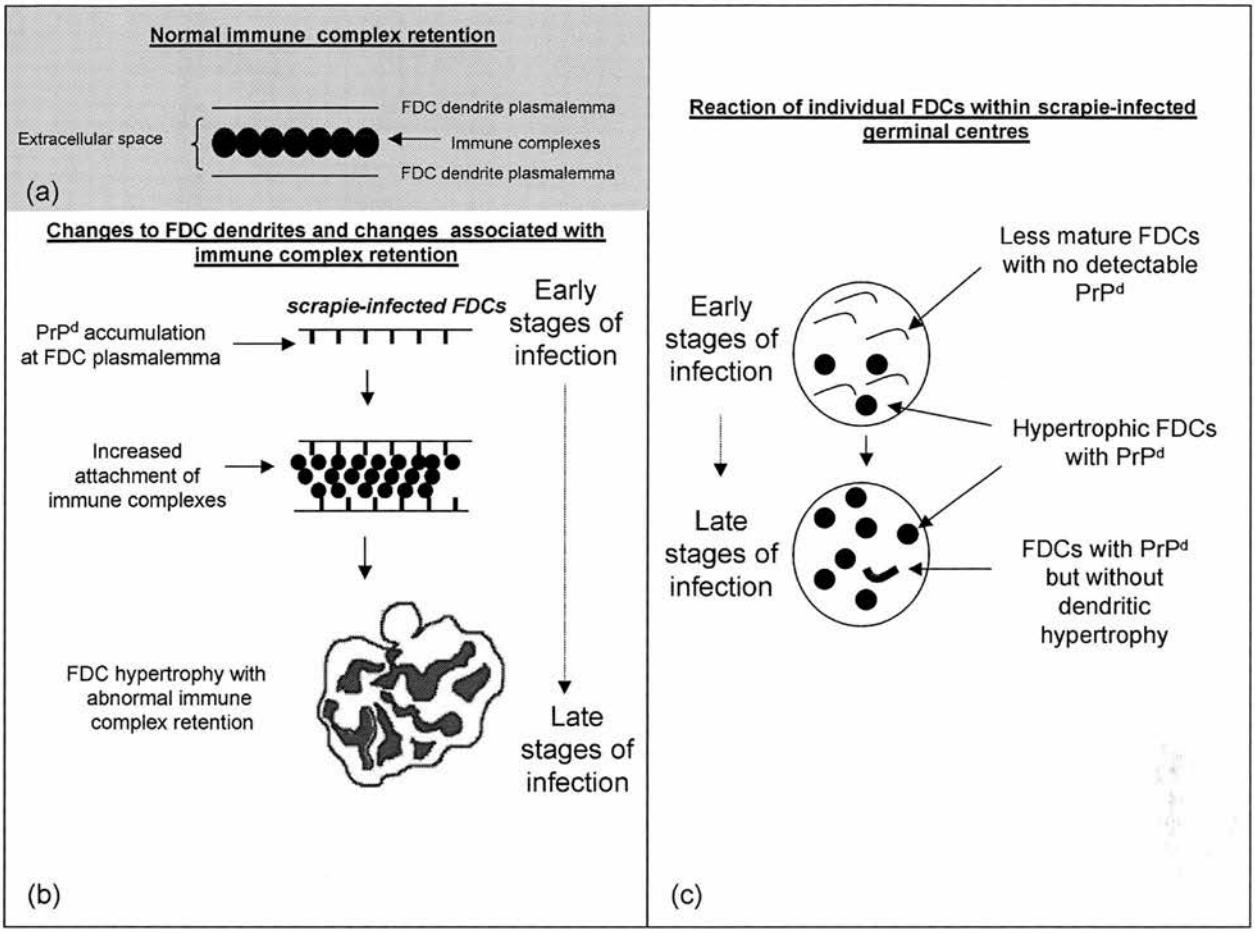

Fig. 7a–c. Schematic diagram showing relationship between immune complexes and FDCs in uninfected and scrapie-infected mice. (a) Antigen/antibody complexes (black circles) are held in the extracellular space at a regular interval between FDC dendrites. (b) After infection with scrapie, abnormal PrP (PrP^d) accumulates at the surface of FDC dendritic plasmalemma. This is associated with increased extracellular electron-dense material (presumed to be immune complexes) and FDC hypertrophy. (c) At early stages of infection, few FDCs within a germinal centre/secondary follicle show evidence of PrP^d accumulation. However, where PrP^d accumulation is found, evidence of hypertrophy is present. In contrast, at late stages of disease almost all FDCs show PrP^d accumulation. Most are hypertrophic, but occasionally PrP^d can be found at the plasmalemma of unreactive FDCs.

between antigen–antibody complex receptors, is therefore inferred by the presence of abnormal amounts of this extracellular electron- dense material.

The amount of FDC hypertrophy and extracellular electron-dense material was greater in infected animals that received SRBC immune stimulation than in those that did not. The triggers for FDC process extension are (1) an increased concentration of antigen–antibody complexes in the extracellular space surrounding FDC dendrites, and (2) the subsequent attachment of these complexes to FDC plasmalemmae (Terashima *et al.*, 1992; Heinen *et al.*, 1995). Therefore, the increase in FDC hypertrophy and the assumed immune complex attachment in spleens from SRBC-immunized scrapie-infected mice may simply have been due to an increase in available antigens and complexes.

The present study revealed changes suggesting that scrapie infection disturbs the processes of B-cell maturation and development. Normally, antigen–antibody complexes are retained at the FDC surface, and the presence of $CD4^+$T lymphocytes is an initial requirement for the formation of a germinal centre follicle (Steinman *et al.*, 1997; Tew *et al.*, 1997). Where primed circulating B cells recognize their cognate antigen held at the surface of FDCs, they cease their cycle of recirculation, proliferate and hypermutate. Many hypermutated B cells (centrocytes) are immediately abolished by apoptosis, but B cells with improved antigen binding affinity of their surface immunoglobulins survive. Interaction with $CD4^+$cells

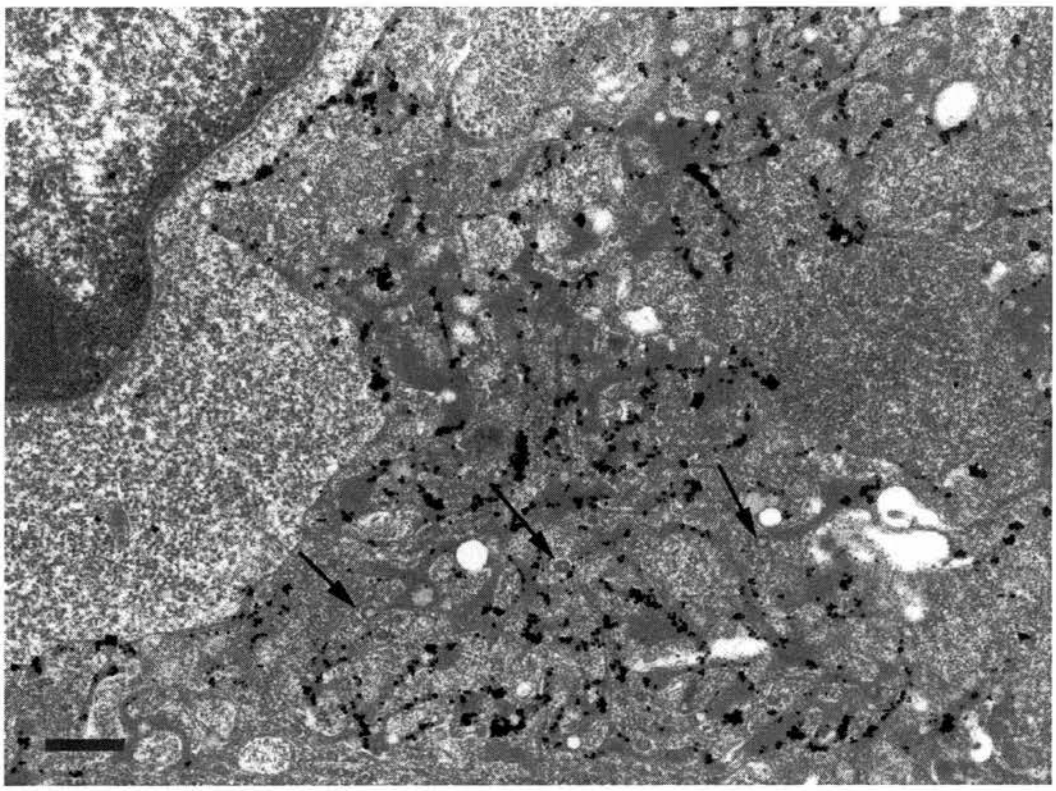

Fig. 8. Immunolabelled spleen from a terminally affected mouse treated with SRBC. Numerous coated pits are associated with FDC dendritic profiles (arrows), but are not associated with immunogold labelling. Immunogold plasmalemmal PrP^d labelling is present in areas with or without excess electron-dense deposit. PrP^d immunogold labelling. Bar, 0.52 μm.

results in affinity maturation of the immunoglobulin produced by centrocytes (Stockinger *et al.*, 1996). Some centrocytes become memory B cells, others join the pool of recirculating lymphocytes, while others migrate into body tissues where they further differentiate into long-lived antibody-secreting plasma cells (Takahashi *et al.*, 1998).

Greater numbers of plasmablasts and morphologically mature plasma cells were observed within the splenic germinal centres of scrapie-infected mice than in uninfected controls. In addition, there was an increase in the number of TBMs that contained large amounts of apoptotic debris (presumed apoptotic B cells). We suggest therefore that scrapie infection leads to an increase in the number of B cells that are selected for hypermutation. Although many of these will undergo apoptosis, many continue to survive and are retained beyond the stage at which they would normally migrate from the germinal centre. If scrapie infection induces FDC hypertrophy and subsequent abnormal antigen–antibody trapping, either by facilitating C3b or Fc receptor binding or by impairing the release of transiently attached immune complexes, the presentation of these immune complexes to B cells may also occur abnormally or in excess. Either this excess antigen complex or PrP^d itself may then induce a prolonged retention of B cells within the secondary follicle. Whether these morphologically mature B cells are

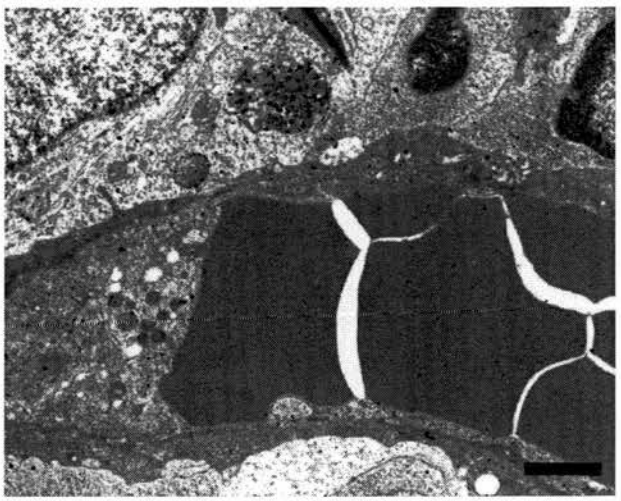

Fig. 9. Immunolabelled spleen from a terminally affected mouse treated with SRBC. Lysosomal TBM labelling is seen in the red pulp adjacent to a capillary containing erythrocytes. PrP^d immunogold labelling. Bar, 0.98 μm.

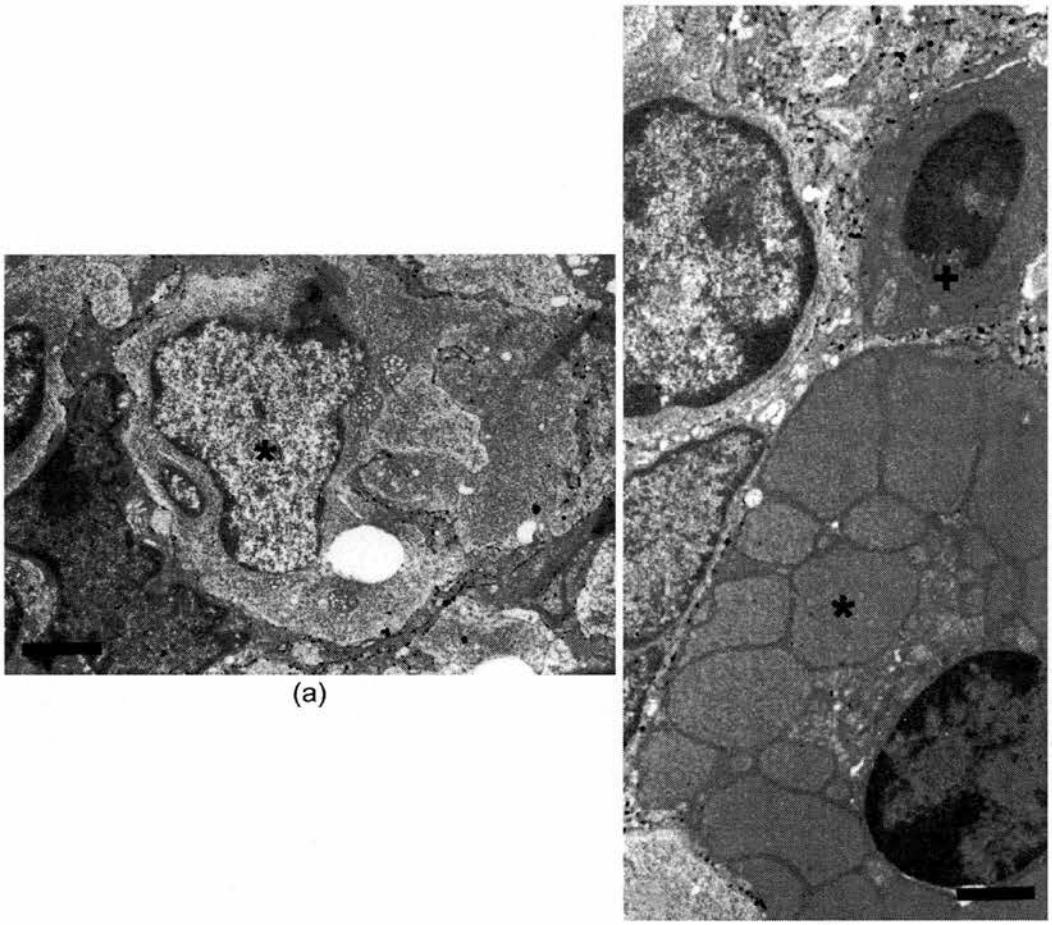

Fig. 10a,b. Immunolabelled spleen from a terminally affected mouse treated with SRBC. (a) PrP^d-labelled FDC dendritic processes are emperipolesing a maturing B cell (asterisk). PrP^d immunogold labelling. Bar, 1.51 μm. (b) Two differentiated B cells emperipolesed by PrP^d-accumulating FDC dendrites are shown. The B cell (asterisk) is terminally differentiated and shows endoplasmic reticulum organized into globulin-producing compartments. The B cell (indicated by a cross) is less mature, with dilated rough endoplasmic reticulum. PrP^d immunogold labelling. Bar, 1.32 μm.

in fact secreting antibody was not tested in the present study.

In ME7-infected mice, at both 70 and 268 dpi and regardless of SRBC immune stimulation, increased numbers of coated pits and vesicles were found in association with FDC hypertrophy. The reason for this increase remains unclear. Although the coated pits do not appear to be directly associated with PrP^d, they may still have an indirect bearing on pathogenesis (Jeffrey *et al.*, 2000). Harris (1999) showed that in purified preparations of coated pits from the brain, PrP^c co-localizes with these structures. In diseased animals, normal PrP may be 'upregulated', resulting in increased endocytic trafficking. Alternatively, coated pits may have a role in the removal of, or response to, PrP^d from the cell surface or plasmalemma. Coated pits show an abnormal increase in ovine (Ersdal *et al.*, 2003) and murine (Jeffrey, personal observation) scrapie-infected brain tissue.

Immunogold labelling of PrP^d was found at the plasmalemma of FDC dendrites, in the adjacent extracellular space, on extracellular fibrils, and in lysosomes of TBMs. As in an earlier study (Jeffrey *et al.*, 2000), the intensity of immunolabelling was increased in proportion to the tortuosity of the dendritic processes, the complexity of branching of dendrites, and the amount of extracellular electron-dense material. In the present study, a smaller particle size of immunogold reaction product revealed that FDC-associated PrP^d was located on the plasmalemma of dendrites within labyrinthine glomerular complexes. That most immunogold-labelled PrP^d was associated with the plasmalemma of dendritic processes and not with electron-dense deposits suggests that PrP^d remains membrane

Table 1
Observed and subjectively assessed changes in the various experimental groups of mice

	*Degree (− to +++) of change in groups**							
	killed at 70 dpi				*killed at 268 dpi*			
Type of change	*U*	*U/S*	*I*	*I/S*	*U*	*U/S*	*I*	*I/S*
FDC Hypertrophy	−	−	++	++	−	−	+++	+++
Increased electron- dense deposit accumulation	−	−	++	++	−	−	++	+++
PrP^d labelling of immature FDCs	−	−	−	−	−	−	+++	+++
Coated pit activity	+	+	++	++	+	++	+++	+++
Lysosomal TBM labelling	−	−	++	++	−	−	+++	+++
Increased follicular B cell maturity	−	−	++	++	−	−	+++	+++

*U, uninfected; U/S, uninfected and SRBC-stimulated; I, ME7-infected; I/S, ME7-infected and SRBC-stimulated.

bound and is not released into the extracellular space. A small amount of extracellular PrP^d was located within the extracellular space around FDC dendrites, mainly on fibrils. These FDCs were made conspicuous, not only by the increased number of fibrils within the extracellular space, but also by the lack of membrane-associated electron-dense deposits and highly convoluted dendritic profiles. FDCs of this type were found in all scrapie-infected spleens at both 70 dpi and during the terminal stages of disease; they were also observed by Mabbott *et al.* (2002) at 42 dpi. The mechanism or sequence of events leading to PrP^d aggregation, complex release and increase in dendrite complexity remains unclear. However, these findings suggest that PrP^d is initially attached to the FDC membrane until released or otherwise stimulated to aggregate and form fibrils (Jeffrey *et al.*, 2000).

The amounts of extracellular electron-dense material and plasmalemmal PrP^d, and the degree of dendritic hypertrophy and tortuosity, were directly proportional to each other. However, in terminally diseased mice, some immature FDCs which lacked any intermediate dense line between FDC dendrites, or in some cases lacked any extracellular structure, showed PrP^d accumulation at the plasmalemma. As both the accumulation of electron-dense material and hypertrophy of FDCs are considered to be the sequel to increased immune complex trapping, we suggest that excess PrP^d retained at the FDC dendritic plasmalemma may enhance capacity to trap complexes via C3b or Fc receptors. PrP^d accumulation at the plasmalemma of immature FDCs suggests that PrP^d accumulation at the cell surface is the primary event in the chain of pathological events described above (Fig. 7).

In this and previous studies of sheep and mice infected with scrapie, we found that all, or virtually all, follicles at the terminal stage of disease were scrapie-infected, as shown by the accumulation of PrP^d (Fig. 7b). This further suggests that follicles do not regress but are stimulated to continue to produce antibody. The presence of excess numbers of mature plasma cells was also consistent with delayed or impeded B cell migration from the follicle and delayed involution of secondary follicles.

In terminally diseased animals, the presence of intralysosomal PrP^d labelling of macrophages outside the germinal centre suggests that these cells play an important role in the transportation of infectivity away from the secondary follicle.

In conclusion, several novel morphological changes were identified in the spleens of scrapie-infected mice. Taken together, the loss of the intermediate electron-dense line between FDC dendrites, FDC hypertrophy and increased plasma cell retention within the secondary follicle all suggest the occurrence of functional abnormalities within the spleen as a result of scrapie infection. The nature of these changes suggests that there is a change in immune complex binding mechanisms, and associated changes in the responses of FDCs and plasma cell maturation. We speculate that these changes are due to the presence of abnormal PrP^d at the surface of FDCs and that this PrP^d retains a functional role in facilitating immune complex trapping. The progression of events suggests that PrP^d accumulation precedes functional immunopathological changes; PrP^d may be transported from the germinal centre in macrophage lysosomal compartments. While the exact mechanisms for the delayed release of B cells from the secondary follicle and increase in coated pit expression are unknown, these changes are also scrapie-associated.

References

Bosma, G. C., Custer, R. P. and Bosma, M. J. (1983). A severe combined immunodeficiency mutation in the mouse. *Nature*, **301,** 527–530.

Bosseloir, A., Bouzahzah, F., Simar, L. and Heinen, E. (1995). B cells in contact with FDC. In: *Follicular Dendritic Cells in Normal and Pathological Conditions*, E. Heinen, Ed., Springer, Heidelberg, pp. 53–78.

Brown, K. L., Stewart, K., Bruce, M. E. and Fraser, H. (1997). Severely combined immunodeficient (SCID) mice resist infection with bovine spongiform encephalopathy. *Journal of General Virology*, **78,** 2707–2710.

Brown, K. L., Stewart, K., Ritchie, D., Fraser, H., Morrison, W. I. and Bruce, M. E. (2000). Follicular dendritic cells in scrapie pathogenesis. *Archives of Virology*, **16,** 13–21.

Brown, K. L., Stewart, K., Ritchie, D. L., Mabbott, N. A., Williams, A., Fraser, H., Morrison, W. I. and Bruce, M. E. (1999). Scrapie replication in lymphoid tissues depends on prion protein-expressing follicular dendritic cells. *Nature Medicine*, **5,** 1308–1312.

Ersdal, C., Simmons, M. M., Goodsir, C., Martin, S. and Jeffrey, M. (2003). Sub-cellular pathology of scrapie: coated pits are increased in PrP codon 136 alanine homozygous scrapie-affected sheep. *Acta Neuropathologica (Berlin)*, **106,** 17–26.

Farquhar, C. F., Somerville, R. A., Dornan, J., Armstrong, D., Birkett, C. and Hope, J. (1993). A review of the detection of PrP^{sc}. In: *Transmissible Spongiform Encephalopathies.* Proceedings of a Consultation on BSE with the Scientific Veterinary Committee of the Commission of the European Communities held in Brussels, 14–15 September 1993, R. Bradley and B. Marchant, Eds, pp. 301–313.

Ford, M. J., Burton, L. J., Li, H., Graham, C. H., Frobert, Y., Grassi, J., Hall, S. M. and Morris, R. J. (2002). A marked disparity between the expression of prion protein and its message by neurones of the CNS. *Neuroscience*, **111,** 533–551.

Fraser, H., Brown, K. L., Stewart, K., McConnell, I., McBride, P. and Williams, A. (1996). Replication of scrapie in spleens of SCID mice follows reconstitution with wild-type mouse bone marrow. *Journal of General Virology*, **77,** 1935–1940.

Fraser, H. and Dickinson, A. G. (1970). Pathogenesis of scrapie in the mouse: the role of the spleen. *Nature*, **226,** 462–463.

Fraser, H. and Dickinson, A. G. (1978). Studies of lymphoreticular system in the pathogenesis of scrapie. The role of spleen and thymus. *Journal of Comparative Pathology*, **88,** 563–573.

Fraser, H. and Farquhar, C. (1987). Ionising radiation has no influence on scrapie incubation period in mice. *Veterinary Microbiology*, **13,** 211–223.

Harris, D. A. (1999). Cell biological studies of the prion protein. In: *Prions: Molecular and Cellular Biology*, D. A. Harris, Ed., Horizon Scientific Press, Norfolk, pp. 53–66.

Hayat, M. A. (1989). *Principles and Techniques of Electron Microscopy: Biological Applications, Principles and Techniques*, Macmillan Press, Hampshire.

Heinen, E., Bosseloir, A. and Bouzahzah, F. (1995). Follicular dendritic cells: origin and function. *Current Topics in Microbiology and Immunology*, **201,** 15–47.

Jeffrey, M. and Goodsir, C. M. (1996). Immunohistochemistry of resinated tissues for light and electron microscopy. In: *Prion Diseases*, H. F. Baker and R. M. Ridley, Eds, Humana Press, New Jersey, pp. 301–312.

Jeffrey, M., McGovern, G., Goodsir, C. M., Brown, K. L. and Bruce, M. E. (2000). Sites of prion protein accumulation in scrapie-infected mouse spleen revealed by immuno-electron microscopy. *Journal of Pathology*, **191,** 323–332.

Kapasi, Z. F., Burton, G. F., Shultz, L. D., Tew, J. G. and Szakal, A. K. (1993). Induction of functional follicular dendritic cell development in severe combined immunodeficiency mice. Influence of B and T cells. *Journal of Immunology*, 150, 2648–2658.

Kimberlin, R. H. and Walker, C. A. (1989). The role of the spleen in the neuroinvasion of scrapie in mice. *Virus Research*, **12,** 201–212.

Kitamoto, T., Muramoto, T., Mohri, S., Doh-Ura, K. and Tateishi, J. (1991). Abnormal isoform of prion protein accumulates in follicular dendritic cells in mice with Creutzfeldt-Jakob disease. *Journal of Virology*, **65,** 6292–6295.

Lasmezas, C. I., Cesbron, J. Y., Deslys, J. P., Demaimay, R., Adjou, K. T., Rioux, R., Lemaire, C., Locht, C. and Dormont, D. (1996). Immune system-dependent and independent replication of the scrapie agent. *Journal of Virology*, **70,** 1292–1295.

Mabbott, N. A. and Bruce, M. E. (2001). The immunobiology of TSE diseases. *Journal of General Virology*, **82,** 2307–2318.

Mabbott, N. A., McGovern, G., Jeffrey, M. and Bruce, M. E. (2002). Temporary blockade of the tumor necrosis factor receptor signalling pathway impedes the spread of scrapie to the brain. *Journal of Virology*, **76,** 5131–5139.

Manson, J., McBride, P. and Hope, J. (1992). Expression of the PrP gene in the brain of sinc congenic mice and its relationship to the development of scrapie. *Neurodegeneration*, **1,** 45–52.

Oesch, B., Westaway, D., Walchi, M., McKinley, M. P., Kent, S. B. H., Aebersold, R., Barry, R. A., Teplow, D. B., Tempst, D. B., Hood, L. E., Prusiner, S. B. and Weissmann, C. (1985). A cellular gene encodes scrapie PrP 27-30 protein. *Cell*, **40,** 735–746.

O'Rourke, K., Huff, T., Leathers, C., Robinson, M. and Gorham, J. (1994). SCID mouse spleen does not support scrapie agent replication. *Journal of General Virology*, **75,** 1511–1514.

Radoux, D., Heinen, E., Kinet-Denoel, C. and Simar, L. J. (1985). Antigen/antibody retention by follicular dendritic cells (FDC). *Advances in Experimental Medical Biology*, **186,** 185–191.

Steinman, R. M., Pack, M. and Inaba, K. (1997). Dendritic cells in the T cell areas of lymphoid organs. *Immunology Review*, **156,** 25–37.

Stockinger, B., Zal, T., Zal, A. and Gray, D. (1996). B cells solicit their own help from T cells. *Journal of Experimental Medicine*, **183,** 891–899.

Takahashi, Y., Dutta, P. R., Cerasoli, D. M. and Kelsoe, D. (1998). In situ studies of the primary immune response to (4-hydroxy-3-nitrophenyl)acetyl. V. Affinity maturation develops in two stages of clonal selection. *Journal of Experimental Medicine*, **187,** 885–895.

Terashima, K., Dobashi, M., Maeda, K. and Imai, Y. (1992). Follicular dendritic cells and ICCOSOMES in germinal center reactions. *Seminars in Immunology*, **4,** 267–274.

Tew, J. G., Thorbecke, G. J. and Steinman, R. M. (1982). Dendritic cells in the immune response: characteristics and recommended nomenclature (A report from the Reticuloendothelial Society Committee on Nomenclature). *Journal of the Reticuloendothelial Society*, **31,** 371–380.

Tew, J. G., Wu, J., Qin, D., Helm, S., Burton, G. F. and Szakal, A. K. (1997). Follicular dendritic cells and presentation of antigen and co-stimulatory signals to B cells. *Immunology Review*, **156,** 39–52.

[*Received, July 21st, 2003*
Accepted, November 10th, 2003]